

eman ta zabal zazu



Universidad  
del País Vasco

Euskal Herriko  
Unibertsitatea

# DEVELOPMENT OF AN ELECTRICAL RESISTANCE-BASED CORROSION MONITORING SYSTEM FOR OFFSHORE APPLICATIONS



Iñigo Santos Pereda

PhD thesis  
2022

(c)2022 IÑIGO SANTOS PEREDA



## Preface

This thesis is submitted as a partial fulfilment of the requirements for the Industrial PhD degree. In addition to the thesis, four contributions were prepared during the project period. The papers are not specifically included in the present document, but its content is reflected throughout chapters 5 and 8 and they play an important contribution to this thesis. A complete list of these is given after the conclusions.

Leioa, 11<sup>th</sup> of February 2022

Iñigo Santos Pereda

# Index

|  |  |           |
|--|--|-----------|
| 1.1  | Background and objectives .....                                      | 1         |
| 1.2  | Overview of Thesis .....   | 1         |
| <b>Chapter 2: Offshore facilities and mooring lines.....</b> |  | <b>3</b>  |
| 2.1  | Current challenges in offshore facilities .....                      | 3         |
| 2.2  | Offshore Energy Production: Wind Turbines and Oil&Gas Platforms..... | 5         |
| 2.2.1  | Marine Zones and Forms of Corrosion .....                            | 5         |
| 2.2.2  | Offshore structure types .....                                       | 7         |
| 2.3  | Mooring Lines .....  | 17        |
| 2.3.1  | Introduction to Mooring Line Systems .....                           | 17        |
| 2.3.2  | Types of mooring systems .....                                       | 17        |
| 2.3.3  | Mooring System configurations.....                                   | 19        |
| 2.3.4  | Mooring line components.....   | 21        |
| 2.3.5  | Composition of Mooring Chains .....                                  | 25        |
| 2.3.6  | Anchoring .....  | 26        |
| 2.3.7  | Mooring Line Patterns .....  | 27        |
| 2.3.8  | Mooring line failure modes.....                                      | 28        |
| 2.3.9  | Failure economic point of view.....                                  | 30        |
| <b>Chapter 3: Corrosion in marine environment.....</b>       |  | <b>36</b> |
| 3.1  | Corrosion: A general overview .....                                  | 36        |
| 3.2  | Seawater .....   | 37        |
| 3.3  | Corrosion mechanisms .....   | 39        |
| 3.3.1  | General forms of corrosion .....                                     | 39        |
| 3.3.2  | Specific corrosion mechanisms of offshore structures .....           | 40        |
| 3.3.3  | Electrochemistry of steel in seawater .....                          | 50        |
| 3.3.4  | Corrosion models .....   | 51        |
| 3.3.5  | Steel corrosion products in seawater .....                           | 59        |
| 3.4  | Main influential factors in corrosion development .....              | 61        |
| 3.4.1  | Temperature.....   | 61        |
| 3.4.2  | pH.....  | 63        |
| 3.4.3  | Dissolved oxygen (DO).....   | 64        |
| 3.4.4  | Bacterial activity.....  | 66        |
| 3.4.5  | Water flow.....  | 68        |
| 3.4.6  | Surface roughness.....   | 69        |

|  |            |
|--|------------|
| <b>Chapter 4: Corrosion protection strategies against corrosion .....</b>              | <b>76</b>  |
| 4.1 Barrier Coatings (Passive Protection).....   | 76         |
| 4.1.1 Organic coatings.....  | 79         |
| 4.1.2 Metallic coatings .....  | 83         |
| 4.1.3 Inorganic coatings.....  | 88         |
| 4.2 Active Protection .....  | 90         |
| 4.2.1 Chemical active coatings .....   | 90         |
| 4.2.2 Cathodic corrosion protection .....  | 92         |
| 4.3 Material selection .....   | 95         |
| 4.3.1 Corrosion allowance .....  | 96         |
| 4.3.2 Corrosion Resistant Alloys.....  | 96         |
| <b>Chapter 5: SRB settlement and corrosion influence on coated mooring chains.....</b> | <b>104</b> |
| 5.1 Prevention and Control of Biocorrosion.....  | 105        |
| 5.1.1 Cathodic Protection .....  | 105        |
| 5.1.2 Antifouling Protective Coatings .....  | 105        |
| 5.2 Materials and Methods.....   | 106        |
| 5.2.1 Preparation of samples .....   | 106        |
| 5.2.2 SRB culture and numeration technique.....  | 107        |
| 5.2.3 Immersion test conditions.....   | 108        |
| 5.2.4 Surface analysis .....   | 109        |
| 5.3 Immersion test results.....  | 110        |
| 5.3.1 Visual Inspection .....  | 110        |
| 5.3.2 Surface Analysis and Evaluation .....  | 111        |
| 5.4 Proposed corrosion degradation mechanisms.....                                     | 118        |
| 5.4.1 TSA and TSA + Se samples.....  | 119        |
| 5.4.2 PU Samples.....  | 123        |
| 5.5 Experimental conclusions.....  | 123        |
| <b>Chapter 6:.....</b>   | <b>131</b> |
| 6.1 Corrosion Management.....  | 131        |
| 6.1.1 Maintenance strategies .....   | 131        |
| 6.1.2 Life-cycle asset management.....   | 133        |
| 6.2 Risk-Based Inspection (RBI) .....  | 135        |
| 6.3 Economic impact and market share .....   | 139        |
| 6.4 Corrosion Monitoring Techniques .....  | 141        |
| 6.4.1 Response Time .....  | 142        |
| 6.4.2 Classification of monitoring techniques .....                                    | 143        |

|   |            |
|---|------------|
| <b>Chapter 7: Materials and methods .....</b>   | <b>163</b> |
| 7.1 R5 grade HSLA characterization.....   | 163        |
| 7.1.1 Microstructural analysis and chemical characterization.....                                 | 163        |
| 7.1.2 Structure-properties relationship .....   | 174        |
| 7.1.3 Mechanical characterization.....  | 175        |
| 7.1.4 Electrochemical analysis.....   | 179        |
| 7.2 Analysis of R5 steel corrosion in seawater .....  | 187        |
| 7.2.1 Lab-scale artificial seawater immersion test.....   | 188        |
| 7.2.2 Field-exposure samples: Biological influence .....  | 191        |
| 7.2.3 Corrosion products .....  | 195        |
| <b>Chapter 8: .....</b>   | <b>200</b> |
| 8.1 Fundamentals of corrosion monitoring system.....  | 200        |
| 8.1.1 Low-resistivity measurements and temperature influence .....                                | 200        |
| 8.1.2 Sensor geometry.....  | 203        |
| 8.1.3 Influence of the environment conductivity in low-resistance measurements.....               | 211        |
| 8.2 Temperature gradient in low resistance measurements.....                                      | 226        |
| 8.2.1 Subsea corrosion sensor .....   | 226        |
| 8.2.2 Experimental method and set-up .....  | 228        |
| 8.2.3 Proposed mathematical thermal model.....  | 232        |
| 8.3 From voltage measurements to corrosion rate output.....                                       | 246        |
| 8.4 Lab-scale experimental results and monitoring systems .....                                   | 251        |
| 8.4.1 Experimental verification of Ohm's Law .....  | 251        |
| 8.4.2 Electrical resistance monitoring device. (1 <sup>st</sup> Generation corrosion sensor)..... | 254        |
| 8.4.3 Lab-scale pilot system (2 <sup>nd</sup> Generation System).....                             | 260        |
| 8.4.4 Laboratory-scale test results of the second-generation sensor. ....                         | 277        |
| 8.5 Upgraded field-testing sensors.....   | 281        |
| 8.5.1 Low-consumption sensor (3 <sup>rd</sup> Generation Sensor).....                             | 281        |
| 8.5.2 Actual prototype design.....  | 288        |
| 8.6 Open-field exposure test: Case study. ....  | 301        |
| <b>Chapter 9: Conclusions and future work.....</b>  | <b>308</b> |
| 9.1 Future work.....  | 311        |
| 9.2 Publications and further work resulting from the research.....                                | 311        |

# List of figures

|   |    |
|---|----|
| FIGURE 2-1. WORLD NATURAL GAS DEMAND BY SECTOR IN Tm <sup>3</sup> /YEAR (UPPER IMAGE), WHERE DEMAND PEAKS IN 2035 ALTHOUGH NEW SECTORS AS THE HYDROGEN PRODUCTION WILL ARISE AT THE SAME TIME. WORLD PRIMARY ENERGY SUPPLY BY SOURCE IS PRESENTED BELOW, WITH A CLEAR FOSSIL FUEL DOWNWARD TENDENCY IN OIL AND COAL PRODUCTION, AND A NEAR 12-FOLD AND 30-FOLD UPWARD PRODUCTION FOR WIND AND SOLAR SOURCES, RESPECTIVELY. SOURCE: DNV-GL ENERGY OUTLOOK 2020. <sup>3</sup> ..... | 4  |
| FIGURE 2-2. WORLD ELECTRICITY GENERATION IN PWh/YEAR (PICOWATT/HOUR PER YEAR).....  | 4  |
| FIGURE 2-3. MARINE ZONES AND MAIN OCCURRING EVENTS FOR OIL&GAS RIGS AND OFFSHORE WIND TURBINES. ....  | 6  |
| FIGURE 2-4. OFFSHORE FACILITIES FOR BOTH OIL&GAS INDUSTRY AND THE STRUCTURES CONCERNING OFFSHORE WIND FARMS. ....   | 8  |
| FIGURE 2-5. FPSO UNIT PIONEIRO DE LIBRA. SOURCE: BRAZILENERGYINSIGHT.COM .....  | 10 |
| FIGURE 2-6. FPSO MOORING SYSTEM. SOURCE: GCAPTAIN.COM.....  | 10 |
| FIGURE 2-7. EXAMPLE OF A SPAR STRUCTURE FOR OFFSHORE WIND TURBINES. SOURCE: WORLDOCEANREVIEW.COM .....  | 11 |
| FIGURE 2-8. GRAPHICALLY ILLUSTRATED CONFIGURATIONS FOR SPAR TYPE STRUCTURES. SOURCE: XCIXZIG.COM .....  | 12 |
| FIGURE 2-9. SHELL OLYMPUS TLP PROFILE FOR O&G PLATFORMS. SOURCE: BIZJOURNALS.COM AND OFFSHORE-TECHNOLOGY.COM ....   | 13 |
| FIGURE 2-10. CHEVRON USA TYPHOON SEASTAR-PROFILE TLP FOR OFFSHORE OIL&GAS PRODUCTION. SOURCE: MATTEN (2002) <sup>21</sup> ..  | 14 |
| FIGURE 2-11. EXXONMOBIL STENA DON SEMI-SUBMERSIBLE UNIT FOR OFFSHORE OIL&GAS EXTRACTION. SOURCE: OFFSHOREENERGYTODAY.COM .....  | 14 |
| FIGURE 2-12. DRILLING BARGE FOR SHALLOW WATERS (LEFT) AND WEST GEMINI DRILLINGSHIP (RIGHT), FOR OFFSHORE LOCATIONS. SOURCE: MEDIA.SUBSEA.ORG AND MARITIME-CONNECTOR.COM .....   | 15 |
| FIGURE 2-13. FLOATING WIND TURBINES FOR OFFSHORE INSTALLATION. SPAR (LEFT), TLP (CENTRE) AND BARGE (RIGHT). SOURCE: EDENHOFER (2012) <sup>28</sup> .....  | 16 |
| FIGURE 2-14. WINDWARD AND LEEWARD LINES EXAMPLE IN A SPAR BUOY WIND TURBINE. ....   | 17 |
| FIGURE 2-15. TURRET TYPE MOORING IN M3NERGY FSO UNIT EXPOSED (LEFT) AND THE SAME MOORING SYSTEM FROM A SUBMERGED POINT OF VIEW (RIGHT). SOURCE: 2B1STCONSULTING.COM AND NOV.COM .....   | 18 |
| FIGURE 2-16. CALM BUOY TYPE MOORING EXPOSED (LEFT) AND FROM A SUBMERGED POINT OF VIEW (RIGHT). SOURCE: OFFSHORE-TECHNOLOGY.COM.....   | 18 |
| FIGURE 2-17. SPREAD MOORING EXAMPLE IN AN OFFSHORE SEMI-SUBMERSIBLE STRUCTURE. SOURCE: OFFSHORE-MAG.COM .....   | 19 |
| FIGURE 2-18. CATENARY SYSTEM (LEFT) AND TAUT-LEG CONFIGURATION (RIGHT). SOURCE: FLORY (2016) <sup>36</sup> .....  | 19 |
| FIGURE 2-19. DIFFERENT MOORING SYSTEM METHODS FOR A SINGLE SPAR-BUOY OWS. ....  | 20 |
| FIGURE 2-20. GEOMETRICAL DIFFERENCES BETWEEN STUD AND STUDLESS CHAIN (LEFT) AND DIFFERENCES IN THE NOMINAL DIAMETER (RIGHT). SOURCE: ORCINA.COM.....  | 21 |
| FIGURE 2-21. COMPARISON OF THE STRESS-STRAIN BEHAVIOUR OF VARIOUS FIBERS. SOURCE: WELLER (2005) <sup>46</sup> .....   | 23 |
| FIGURE 2-22. SIX STRAND ROPE (LEFT), CONVENTIONAL SPIRAL STRAND (CENTRE), ENCAPSULATED SPIRAL STRAND (RIGHT). SOURCE: WIREROPE-SLING.COM, REDAELLI.COM, ARCHIXPO.COM .....  | 24 |
| FIGURE 2-23. TYPICAL MOORING POINTS FOR OFFSHORE ASSETS. SOURCE: VRYHOF.....  | 27 |
| FIGURE 2-24. OFFSHORE MOORING PATTERNS. SOURCE: KHALIFEH (2020) <sup>54</sup> .....   | 28 |
| FIGURE 2-25. PHENOMENA INFLUENCING THE SAFETY AND INTEGRITY OF THE ANCHOR LINES. ....   | 29 |
| FIGURE 2-26. OUT-OF-PLANE BENDING SCHEME. SOURCE: DAS (2016) <sup>60</sup> .....  | 30 |
| FIGURE 2-27. SINGLE MOORING FAILURE SCENARIO. ADAPTED FROM RR444 <sup>31</sup> . ....   | 31 |
| <br>  |    |
| FIGURE 3-1. OCEAN TEMPERATURE PROFILE WITHIN THE MID-LATITUDE REGIONS. IMAGE MODIFIED FROM NOAA <sup>11</sup> .....   | 38 |
| FIGURE 3-2. CO <sub>2</sub> EQUILIBRIUM SYSTEM IN SEAWATER. SOURCE: EGCSA.COM .....   | 39 |
| FIGURE 3-3. MARINE DEGRADATION OF METALS. ILLUSTRATIONS PARTLY ADAPTED FROM ROBERGE (2008) <sup>14</sup> CHAPTER 6. ....  | 40 |
| FIGURE 3-4. UNIFORM CORROSION IN A CARBON STEEL SAMPLE TESTED IN TECNALIA'S HARSHLAB FACILITY IN OPEN SEAWATER.....   | 41 |
| FIGURE 3-5. SACRIFICIAL ANODES PLACED IN SUBMERGED MONOPILES TO AVOID STRUCTURAL CORROSION. SOURCE: CATHWELL.COM. ..  | 42 |
| FIGURE 3-6. GALVANIC SERIES IN SEAWATER WITH SHE AND SCE REFERENCE ELECTRODES. SOURCE: ENGINEERINGCLICKS.COM.....   | 42 |
| FIGURE 3-7. EXPOSED PIT (BLACKISH AREA) COMPARED WITH THE ORANGE-COLOURED RUST ALL OVER THE SURFACE ON A LOW ALLOY STEEL SAMPLE. (COURTESY OF: TECNALIA). ....  | 43 |
| FIGURE 3-8. SCHEMATIZED CREVICE MECHANISM BETWEEN TWO STEEL COMPONENTS. ....  | 44 |
| FIGURE 3-9. BARNACLE DEPOSITION OVER A LOW ALLOY STEEL SURFACE AT TECNALIA'S FOULING TESTING FACILITIES IN PASAIA (LEFT) AND REMAINING CREVICE CORROSION ONCE BIO-ORGANISMS ARE REMOVED (RIGHT, COURTESY OF: BOATS.COM) .....   | 45 |
| FIGURE 3-10. MODELS FOR PIT INITIATION LEADING TO PASSIVE FILM BREAKDOWN. REPRODUCED FROM KAESCHE, H. ET. AL. (2011) <sup>23</sup> .....  | 46 |
| FIGURE 3-11. TYPICAL CROSS-SECTIONAL SHAPES OF CORROSION PITS. REPRODUCED FROM ROBERGE (2008) <sup>14</sup> . ....  | 46 |
| FIGURE 3-12. SCHEMA OF EAC CRACK GENERATION. THE CRACK TIP REPRESENT THE ANODIC SITE, WHICH IS DEPLETED IN OXYGEN AND CONCENTRATED MAINLY IN METAL CATIONS, PROTONS AND ANIONS. ADAPTATION FROM BLAND ET. AL. (2017) <sup>25</sup> . ....   | 48 |
| FIGURE 3-13. SCHEMATIC ILLUSTRATION OF CRACK TIP ACIDIFICATION, WHILE TENSILE FORCES PROMOTE CRACK GROWING. FIGURE MODIFIED FROM KING FAHD UNIVERSITY OF PETROLEUM AND MINERALS.....  | 48 |

|  |     |
|--|-----|
| FIGURE 3-14. WEAR IN MOORING CHAINS UNDER DRY CONDITIONS. COURTESY OF MELCHERS ET. AL. (2015) <sup>29</sup> .....  | 49  |
| FIGURE 3-15. MASS LOSS COMPARISON IN MOORING CHAINS UNDER DRY AND WET CONDITIONS. SOURCE: MELCHERS ET. AL. (2015) <sup>29</sup> .<br>.....   | 49  |
| FIGURE 3-16. SUMMARY OF ELECTROCHEMICAL REACTION OF IRON IN SEAWATER. ADAPTED FROM: ROBERGE (2008) <sup>14</sup> .....   | 51  |
| FIGURE 3-17. SOME OF THE REVIEWED MODEL OVERVIEWS. A) POWER LAW BY TAMMANN. B) SOUTHWELL ET. AL. TREND MODEL. C)<br>GUEDES SOARES MODEL D) PAIK MODEL. E) QIN AND CUI MODEL. F) MELCHERS MULTI-PHASE MODEL. FIGURE ADAPTED<br>FROM MELCHERS (2019) <sup>65</sup> ..... | 53  |
| FIGURE 3-18. MELCHERS DEVELOPED SEAWATER CORROSION MODEL SHOWING SEQUENTIAL PHASES AS FUNCTION OF EXPOSURE PERIOD.<br>SOURCE: MELCHERS (2012) <sup>76</sup> .....  | 55  |
| FIGURE 3-19. OXYGEN CONCENTRATION PROFILES (%SAT) THROUGH SEAWATER AND RUST LAYER. ADAPTED FROM MELCHERS AND<br>JEFFREY (2005) <sup>80</sup> .....   | 56  |
| FIGURE 3-20. CORROSION RATE AS A FUNCTION OF EXPOSURE TIME AND RUST LAYER THICKNESS. ADAPTED FROM MELCHERS AND JEFFREY<br>(2005) <sup>80</sup> .....   | 57  |
| FIGURE 3-21. MELCHERS CORROSION MODEL WITH HIGHLIGHTED PHASE 3 AND 4. SOURCE: MELCHERS (2010) <sup>85</sup> .....  | 58  |
| FIGURE 3-22. MELCHERS PROPOSED BACTERIA MECHANISMS THROUGH PHASES 0 TO 4, WHICH SUPPORTS LONG-TERM CORROSION<br>MODEL. ADAPTED FROM MELCHERS (2010) <sup>85</sup> .....  | 60  |
| FIGURE 3-23. CORROSION RATE AS FUNCTION OF TEMPERATURE IN (1) CLOSE SYSTEM AND (2) OPEN WATER SYSTEM. SOURCE:<br>MARCINIAK AND LOBODA (2010) <sup>100</sup> .....  | 62  |
| FIGURE 3-24. CORROSION LOSS TRENDS IN TWO STEEL ALLOYS (STEEL A AND STEEL B) AND VARIOUS LOCATIONS. NOTICE THE LOWER<br>CORROSION LOSS TREND IN BOTH ALLOYS IN THE COLDER ENVIRONMENT. SOURCE: MELCHERS, CHERNOV ET. AL. <sup>101</sup> .....                          | 62  |
| FIGURE 3-25. INCREASING TEMPERATURE AND REDUCING OXYGEN CONCENTRATION EFFECTS ON MELCHERS' DEVELOPED BIMODAL<br>CORROSION MODEL. SOURCE: PENG ET. AL. (2016) <sup>102</sup> .....  | 63  |
| FIGURE 3-26. SIMPLIFIED POURBAIX PREDOMINANCE DIAGRAM FOR IRON SYSTEM. SOURCE: RIVETTI (2018) <sup>104</sup> .....   | 63  |
| FIGURE 3-27. CORROSION BEHAVIOUR OF STEEL IN SEAWATER WITH VARIATION OF CHLORIDES CONCENTRATION AT FIXED SO <sub>4</sub> <sup>2-</sup><br>CONCENTRATION OF 2 G/L. FIGURE ADAPTED FROM PAUL SUBIR (2012) <sup>105</sup> .....   | 64  |
| FIGURE 3-28. AVERAGE CORROSION RATE AS FUNCTION OF OXYGEN CONCENTRATION AND FLUX VELOCITY. SOURCE: COX (1931) <sup>107</sup> .....   | 65  |
| FIGURE 3-29. MICROBIAL COMMUNITY INFLUENCE IN THE CORROSION OF IRON AND STEEL. SULPHATE-REDUCING BACTERIA MECHANISM IS<br>SHOWN HIGHLIGHTED. SOURCE: LITTLE ET. AL. (2000) <sup>115</sup> .....  | 66  |
| FIGURE 3-30. PROGRESSION OF BIOFILM DEPOSIT THICKNESS WITH CORRESPONDING DO PROFILES IN FUNCTION OF TIME. REPRODUCED<br>FROM LEE ET. AL. (1993) <sup>119</sup> .....   | 67  |
| FIGURE 3-31. WATER FLOW EFFECT ON EARLY (100 DAYS) CORROSION. REPRODUCED FROM MELCHERS. <sup>12</sup> .....  | 69  |
| FIGURE 3-32. OXIDE LAYER BREAKDOWN STEPS AND FURTHER RE-PASSIVATION OF THE PROTECTIVE LAYER. ....  | 70  |
| <br>   |     |
| FIGURE 4-1. SCHEME OF CORROSION PROTECTION STRATEGIES. ....  | 77  |
| FIGURE 4-2. SCHEME OF DIFFERENT COATING LAYERS AND THEIR MAIN FUNCTION. ....   | 78  |
| FIGURE 4-3. COATING CONSTITUENT PARTS AND THEIR MAIN FUNCTION (LEFT) AND MULTI-LAYER PAINT SYSTEM EXAMPLE (RIGHT).<br>SOURCE: STEELCONSTRUCTION.INFO/PAINT_COATINGS .....  | 79  |
| FIGURE 4-4. GALVANIZING PROCESS. SOURCE: TRAILERGUYS.COM.AU. ....  | 84  |
| FIGURE 4-5. SCHEMA OF CROSS-SECTIONS OF ZN-AL-MG ALLOYS PRODUCED BY HOT-DIP METALLIZING. SOURCE: SCHUERZ ET. AL.<br>(2009) <sup>39</sup> .....   | 85  |
| FIGURE 4-6. THERMAL SPRAYING PROCESSES ACCORDING TO THE ENERGY SOURCE. ADAPTED FROM VUORISTO ET. AL. (2014) <sup>42</sup> .....  | 86  |
| FIGURE 4-7. THERMAL SPRAYED COATING FORMATION. SOURCE: OSAKA-FUJI CORPORATION (OFIC.CO.JP). ....   | 87  |
| FIGURE 4-8. PHOTOMICROGRAPHS OF VARIOUS ZINC-IRON COATINGS THICKNESSES AND FINISHES. ADAPTED FROM: METALPLATE.COM. ....  | 88  |
| FIGURE 4-9. ANODIZING POROUS LAYER FROM INSIDE (UP) AND DYING ANODIZING SCHEME. SOURCE: KASHIMA-COAT.COM .....   | 89  |
| FIGURE 4-10. NITRIDING MICROSTRUCTURAL PROFILE, WITH MAIN COMPOUNDS ON EACH ZONE AND SUBSEQUENT HARDNESS<br>IMPROVEMENT. ADAPTED FROM SURFACE ENGINEERING COURSE FROM MISKOLC UNIVERSITY. ....   | 90  |
| FIGURE 4-11. SCHEMATIC ILLUSTRATION OF THE INTRINSIC SELF-HEALING MECHANISM. REPRODUCED FROM: HU (2018) <sup>65</sup> .....  | 92  |
| FIGURE 4-12. EXTRINSIC SELF-HEALING PROCESS. REPRODUCED FROM GOULD (2003) <sup>66</sup> .....  | 92  |
| FIGURE 4-13. IMPRESSED CURRENT CATHODIC PROTECTION OPERATION IN SEAWATER, SCHEMATIZED. SOURCE: MARINETHAI.NET .....  | 93  |
| FIGURE 4-14. STEEL MONOPILE WITH DISTRIBUTED SACRIFICIAL ANODES, WITH THE SUBSEQUENT GENERATED DRIVING POTENTIAL<br>BETWEEN BOTH. SOURCE: CORROSION MODULE - COMSOL® 5.2 .....   | 95  |
| FIGURE 4-15. CORROSION RESISTANCE FOR TITANIUM/PALLADIUM ALLOY (LEFT) COMPARED TO PURE TITANIUM (RIGHT) AND THE<br>INFLUENCE OF TEMPERATURE, CONCENTRATION AND pH ON CREVICE AND PITTING CORROSION IN SEAWATER AND SODIUM<br>CHLORIDE BRINES. SOURCE: AZOM.COM. ....   | 99  |
| <br>   |     |
| FIGURE 5-1. ON TOP, POLYURETHANE SAMPLE (PU) AND BOTH PU+DEFECT AND TSA+SEALANT+DEFECT REFERENCES BEFORE THE<br>IMMERSION TEST. IN THE BOTTOM, TSA, STEEL AND TSA+SEALANT REFERENCES APPEARANCE AS RECEIVED. ....  | 107 |
| FIGURE 5-2. SRB GROWING IN AGAR PLATES FORMED IN BLACK COLONIES BEFORE BEING TRANSFERRED TO THE TEST BEAKERS. ....   | 108 |



|   |     |
|---|-----|
| FIGURE 5-3. APPEARANCE OF THE BEAKERS ONCE THE SRB WERE INOCULATED ON THE LEFT AT TIME ZERO (T=0 DAYS) AND AFTER 4 DAYS OF IMMERSION TEST ON THE RIGHT. ....  | 108 |
| FIGURE 5-4. ASPECT OF BEAKER 3 REFERENCES PRIOR TO DEHYDRATION AND BIOFILM FIXATION PROCESS. ....   | 109 |
| FIGURE 5-5. STEEL REFERENCE APPEARANCE AFTER IMMERSION TEST, BOTH ORIGINAL AND MACHINED SIDES. ....   | 110 |
| FIGURE 5-6. TSA REFERENCE (LEFT GROUP) AND TSA + SE (RIGHT GROUP) APPEARANCE AFTER IMMERSION TEST, BOTH ORIGINAL AND MACHINED SIDES. ....   | 110 |
| FIGURE 5-7. POLYURETHANE REFERENCE APPEARANCE AFTER IMMERSION TEST, BOTH ORIGINAL AND MACHINED SIDES. ....  | 111 |
| FIGURE 5-8. POLYURETHANE REFERENCE APPEARANCE AFTER IMMERSION TEST WITH THE PU TOPCOAT REMOVED, UNVEILING THE INTACT STEEL SUBSTRATE. ....  | 111 |
| FIGURE 5-9. MICROGRAPHY AT X1000 MAGNIFICATION SHOWING ATTACHED BIOFILM IN THE ORIGINAL SURFACE OF STEEL SAMPLE, WITH ASSOCIATED EDS SPECTRA. ....  | 112 |
| FIGURE 5-10. MICROGRAPHY AT X1000 MAGNIFICATION SHOWING ATTACHED BIOFILM IN THE MACHINED SURFACE OF STEEL SAMPLE, AS WELL AS GRINDING MARKS. ....   | 112 |
| FIGURE 5-11. MICROGRAPHY AT X500 MAGNIFICATION SHOWING GENERATED PITTING IN THE MACHINED SURFACE OF STEEL SAMPLE, WITH ASSOCIATED EDS SPECTRA. ....   | 113 |
| FIGURE 5-12. MICROGRAPHY AT X500 MAGNIFICATION SHOWING ATTACHED BIOFILM IN THE ORIGINAL SURFACE OF TSA SAMPLE, WITH ASSOCIATED EDS SPECTRA FOR BOTH YELLOW AND WHITISH AREAS. ....  | 114 |
| FIGURE 5-13. MICROGRAPHY AT X1000 MAGNIFICATION SHOWING ATTACHED BIOFILM IN THE ORIGINAL SURFACE OF TSA+SE SAMPLE, WITH ASSOCIATED EDS SPECTRA FOR BOTH GREY AND WHITISH AREAS. ....  | 115 |
| FIGURE 5-14. MICROGRAPHY AT X5000 MAGNIFICATION SHOWING CLEARLY ATTACHED BIOFILM IN THE ORIGINAL SURFACE OF PU SAMPLE, WITH ASSOCIATED EDS SPECTRA. ....  | 115 |
| FIGURE 5-15. MICROGRAPHY AT X150 MAGNIFICATION SHOWING ATTACHED BIOFILM IN THE SCRIBE EDGE OF PU SAMPLE. ....   | 116 |
| FIGURE 5-16. MICROGRAPHICS AT X5000 MAGNIFICATION AND ASSOCIATED EDS SPECTRA SHOWING NOTICEABLE DIFFERENCES BETWEEN TESTED PU SAMPLE (LEFT) AND NON-TESTED PU SAMPLE (RIGHT). ....  | 116 |
| FIGURE 5-17. PROPOSED INTERACTION BETWEEN BACTERIA COLONIES AND METAL OR ORGANIC SURFACES FOR A) STEEL, B) TSA, C) TSA+SE, D) PU SYSTEMS. ....  | 117 |
| FIGURE 5-18. MECHANISM OF BIOFILM FORMATION RELATED TO SRB ACTIVITY AND CONCENTRATION. SOURCE: KAKOOEI (2012) <sup>31</sup> . ....  | 118 |
| FIGURE 5-19. PROPOSED DEGRADATION MECHANISM ON TSA AND TSA+SE SAMPLES. IN THIS CASE, THE DEGRADATION PROCESS IS THE SAME FOR BOTH SEALED AND UNSEALED SAMPLES. ....   | 120 |
| FIGURE 5-20. MOST STABLE SPECIES AS FUNCTION OF THE ESTABLISHED PH BETWEEN THE PIT TIP AND THE PIT MOUTH AND BOLD SURFACE. ....   | 121 |
| FIGURE 5-21. CERTIFICATE OF ORIGIN AND ANALYSIS OF DSMZ 1926 DESULFOVIBRIO DESULFURICANS CULTURE. ....  | 125 |
| FIGURE 5-22. MARINE DESULFOVIBRIO (POSTGATE) MEDIUM SPECIFICATIONS. ....  | 126 |
|   |     |
| FIGURE 6-1. MAINTENANCE STRATEGIES SUMMARY. ADAPTED FROM ROBERGE (2007) <sup>2</sup> . ....   | 132 |
| FIGURE 6-2. DECISION DIAGRAM FOR OFFSHORE STRUCTURES AND COMPONENTS MAINTENANCE. ADAPTED FROM: HORNER ET. AL. (1997) <sup>4</sup> . ....  | 134 |
| FIGURE 6-3. RISK-BASED INSPECTION METHODOLOGY ACTIVITIES. SOURCE: PERUMAL (2014) <sup>8</sup> . ....  | 136 |
| FIGURE 6-4. GENERAL APPROACH AND METHODOLOGY OF RISK-BASED INSPECTION. ....   | 136 |
| FIGURE 6-5. EXAMPLE OF THE DESCRIPTION OF A COLOURED RISK MATRIX. ADAPTED FROM KAMSU-FOGUEM (2016) <sup>9</sup> AND MAZIAH MUNIRAH (2019) <sup>10</sup> . ....  | 137 |
| FIGURE 6-6. INTERRELATION SCHEME BETWEEN FAULTS, FAILURES AND DEFECTS. ADAPTED FROM: ROBERGE <sup>14</sup> . ....   | 138 |
| FIGURE 6-7. MONITORING APPLICATIONS GRAPHED IN A SENSITIVITY - RESPONSE TIME PLOT. SOURCE: ROBERGE <sup>23</sup> . ....   | 142 |
| FIGURE 6-8. SELECTION GUIDE OF THE PROBE ELEMENTS AVAILABLE FOR ELECTRICAL RESISTANCE CORROSION MONITORING IN METAL SAMPLES. (ALSPI.COM) ....   | 143 |
| FIGURE 6-9. CLASSIFICATION OF MONITORING SYSTEMS ACCORDING TO NACE 3T199. ....  | 144 |
| FIGURE 6-10. EVOLUTION OF CORROSION MONITORING FROM OFFLINE TECHNIQUES TO ONLINE MEASUREMENTS. REPRODUCED FROM KANE (2007) <sup>26</sup> . ....   | 145 |
| FIGURE 6-11. EXAMPLE OF A SENSOR MODULE ARRAY WITH WIRELESS COMMUNICATION OF THE DATA. ADAPTED FROM WWW.OFFSHOREWIND.BIZ - VICINAY MARINE GRABS HYWIND MOORING CONTRACT. ....   | 146 |
| FIGURE 6-12. CONDITIONS DISPLAYED BETWEEN AN OFF-LINE AND ON-LINE PARAMETERS' CONTROL SYSTEM. REPRODUCED FROM AUTOMATION.COM. ....  | 147 |
| FIGURE 6-13. PERIODIC INSPECTION VERSUS CORROSION MONITORING APPROACHES GATHERED AS FUNCTION OF ENVIRONMENTAL MONITORING OR ASSET MONITORING. ....  | 147 |
| FIGURE 6-14. SUMMARY OF THE MOST RELEVANT TECHNIQUES FOR OFFSHORE CORROSION MONITORING APPLICATION. ....  | 148 |
| FIGURE 6-15. SOME EXAMPLES OF CLASSICAL MASS-LOSS COUPONS WITH ASTM G-31 RECOMMENDED DIMENSIONS OF 50-25-3 MM. IN THIS CASE, DIFFERENT SURFACE FINISHING WAS TESTED IN ORDER TO EVALUATE THE RUGOSITY PERFORMANCE AGAINST ARTIFICIAL SEAWATER. .... | 149 |

|  |     |
|--|-----|
| FIGURE 6-16. OUTPUT EXAMPLE OF AN ELECTRICAL RESISTANCE PROBE. CORROSION PENETRATION ON THE LEFT, AND CORROSION RATE ON THE RIGHT.....   | 150 |
| FIGURE 6-17. COMMERCIAL SENSOR ELEMENTS FOR ER MEASUREMENTS. (COURTESY OF METAL SAMPLES) .....   | 150 |
| FIGURE 6-18. ELECTROCHEMICAL CURRENT NOISE (LARGE BAND) AND POTENTIAL NOISE (LOWER SIGNAL) IN AN OVERHEAD PIPING. REPRODUCED FROM DUNCAN ET. AL. <sup>42</sup> .....   | 153 |
| FIGURE 6-19. INSTALLED TRANSDUCERS OVER A PIPE WALL AND GENERAL UT MECHANISMS (LEFT) AND AN ARRAY OF 16 TRANSDUCERS TO COVER A CERTAIN AREA OF INTEREST (RIGHT). REPRODUCED FROM BARSHINGER <sup>44</sup> .....  | 154 |
| FIGURE 6-20. SCHEME OF THICKNESS MEASUREMENT USING THE REBOUND ECHOES GENERATED WITH A PULSE-ECHO ULTRASONIC TRANSDUCER.....   | 154 |
| FIGURE 6-21. EMBEDDED ULTRASONIC TECHNIQUE FOR DAMAGE DETECTION WITH THE PITCH & CATCH METHOD. REPRODUCED FROM SHEN ET. AL <sup>45</sup> .....   | 155 |
| FIGURE 6-22. MFL BASICS WHEN AN EXTERNAL DEFECT IS DETECTED (LEFT) OR INTERNAL DEFECT IS DETECTED (RIGHT). SOURCE: ROSEN-GROUP.COM .....   | 155 |
| FIGURE 6-23. SCHEMATIC REPRESENTATION OF DIFFUSION OF EDDY CURRENTS IN THE STEEL. REPRODUCED FROM CROUZEN ET. AL <sup>48</sup> .   | 156 |
| FIGURE 6-24. EXAMPLE OF A FIXED PEC SENSOR (1) ATTACHED WITH A SPRING (4) TO A FRAME (3) PLACED IN A SPOT OF INTEREST WITH AN EXTERNAL CLAMP (5). REPRODUCED FROM CROUZEN ET. AL <sup>48</sup> .....   | 157 |
| FIGURE 6-25. SCHEME OF FIBRE BRAGG GRATING. SOURCE: TRITEK-AUTOMATION.COM. ....  | 158 |
| FIGURE 6-26. IN BLUE, BASELINE WAVELENGTH DETECTED BY THE SENSOR. AS SAMPLES OF DIFFERENT THICKNESSES ARE APPROACHED TO THE MAGNET, THE MAGNETIC FORCE VARIES, GENERATING DIFFERENT INPUT IN THE RECORDED WAVELENGTH. ....   | 159 |
|  |     |
| FIGURE 7-1. DEFECT/INCLUSION SHAPE AS FUNCTION OF THE CHOSEN PLANE TO ANALYSE. IN THE TRANSVERSE PLANE, INCLUSIONS MIGHT LOOK LIKE BUBBLES WHILE IN LONGITUDINAL PLANE DEFECTS ARE SIMILAR TO A STRETCHED ELLIPSE. SOURCE: DA COSTA (2019) <sup>1</sup> .....  | 164 |
| FIGURE 7-2. LONGITUDINAL (BLUE) AND TRANSVERSAL (ORANGE) SAMPLES MACHINED FROM THE ORIGINAL MOORING CHAIN PIECE. ....  | 164 |
| FIGURE 7-3. TRANSVERSE (LEFT, T) AND LONGITUDINAL (RIGHT, L) SAMPLES MOUNTED IN RESIN. NOTE THAT THE RED RESIN FLAKES REFER TO THE TRANSVERSAL SAMPLE, TO AVOID MISTAKES IN THE INTERPRETATION OF THE RESULTS. ....  | 165 |
| FIGURE 7-4. THE MOUNTED SAMPLES WERE INTRODUCED INTO THE GRINDING AND POLISHING BATCH. THE SAMPLES ARE ATTACHED TO THE MACHINE FACING DOWN THE DISC/CLOTH, BEING THE LATTER MAGNETICALLY POSITIONED TO THE MACHINE. ....   | 166 |
| FIGURE 7-5. POLISHED SIDE OF THE SAMPLE (ON THE LEFT, SIDE WITH LITTLE DOTS) AND 4% NITAL ETCHED SIDE OF THE SAMPLE (ON THE RIGHT, OPAQUE). ....   | 167 |
| FIGURE 7-6. NITAL 4 % REVEALED MICROSTRUCTURE CONSISTING IN A MIXTURE OF MARTENSITE AND BAINITE AT 400X MAGNIFICATION (LONGITUDINAL PLANE). ....   | 168 |
| FIGURE 7-7. NITAL 4 % REVEALED MICROSTRUCTURE CONSISTING IN A MIXTURE OF MARTENSITE AND BAINITE AT 400X MAGNIFICATION (TRANSVERSAL PLANE).....   | 168 |
| FIGURE 7-8. REVEALED MICROSTRUCTURE AFTER NITAL 4 % ETCHING FOR BOTH LONGITUDINAL (UPPER ROW) AND TRANSVERSAL (LOWER ROW) PLANES, SHOWN AT DIFFERENT MAGNIFICATIONS (50X, 200X AND 400X). ....   | 169 |
| FIGURE 7-9. REVEALED AUSTENITE GRAIN BOUNDARIES AFTER EXPOSITION TO PICRAL, BOTH IN TRANSVERSE AND LONGITUDINAL PLANES. IN THE UPPER PART, THE TRANSVERSE METALLOGRAPHS AT 200X AND 400X MAGNIFICATION, AND IN THE LOWER PART THOSE OBTAINED IN THE LONGITUDINAL DIRECTION AT THE SAME MAGNIFICATION. ....   | 170 |
| FIGURE 7-10. OVERLAPPED GRAIN SIZED ACCORDING TO ASTM E112 STANDARD IN REVEALED AUSTENITE GRAIN BOUNDARIES FOR TRANSVERSE AND LONGITUDINAL PLANES. ....  | 171 |
| FIGURE 7-11. HV10 MEASUREMENTS OF VICKERS HARDNESS BOTH IN LONGITUDINAL AND TRANSVERSE PLANES.....   | 171 |
| FIGURE 7-12. GOLD-PLATED MOUNTED MICROGRAPHIC SAMPLE. ....   | 172 |
| FIGURE 7-13. SEM MICROGRAPHS OF THE LONGITUDINAL SAMPLE. THE MICROGRAPH OF THE ETCHING WITH 4% NITAL IS SHOWN ABOVE, WHILE PICRIC ACID ETCHING IS SHOWN BELOW. ....  | 172 |
| FIGURE 7-14. EDS SPECTRA SHOWING PEAK INTENSITY OF MAIN ELEMENTS AND ALLOYANTS OF THE MOORING CHAIN SAMPLE. ....   | 173 |
| FIGURE 7-15. WELDABILITY AS A FUNCTION OF CARBON CONTENT AND CE. ZONES II OR III MAY NEED PREHEATING OR POST-WELD TREATMENTS. SOURCE: NAITO ET. AL. (2012) <sup>4</sup> .....  | 174 |
| FIGURE 7-16. EXAMPLE OF MACROSTRUCTURE OF A HYDROGEN-INDUCED ROOT CRACK IN THE HEAT AFFECTED ZONE OF A WELD (LEFT) AND MICROSTRUCTURE OF A CARBON STEEL WELD REVEALED USING KLEMM'S I REAGENT. ORIGINAL AT 50X (POLARIZED LIGHT PLUS SENSITIVE TINT). THE VARIATION IN GRAIN SIZE FROM THE WELD ACROSS THE HEAT-AFFECTED ZONE TO THE BASE METAL IS NOTICEABLE. SOURCE: GEORGEVANDERVOORT.COM. .... | 175 |
| FIGURE 7-17. EXAMPLE OF A STRESS-STRAIN CURVE OF A METALLIC ALLOY. A DETAILED PLOT OF THE ELASTIC ZONE IS ALSO SHOWN TO DETERMINE THE YIELD STRENGTH. SOURCE: CALLISTER (2015). ....   | 176 |
| FIGURE 7-18. STANDARD TENSILE SPECIMEN WITH CIRCULAR CROSS SECTION AND ILLUSTRATION OF A) SPECIMEN ELONGATION DUE TO PLASTIC DEFORMATION AND B) DIAMETER REDUCTION IN THE FAILURE POINT. SOURCE: NUSATEK.COM/MECHANICAL-TESTING .....  | 177 |

|  |     |
|--|-----|
| FIGURE 7-19. SPECIMEN POSITIONED IN THE TENSILE TESTING MACHINE WITH EXTENSOMETER (LEFT) AND FRACTURED SPECIMEN AT THE END OF THE TEST.....  | 178 |
| FIGURE 7-20. OBTAINED STRESS-STRAIN CURVES FOR R4 AND R5 GRADE STEELS. ....  | 178 |
| FIGURE 7-21. HYPOTHETICAL CATHODIC AND ANODIC POLARIZATION PLOT TO DETERMINE CORROSION BEHAVIOUR IN A GIVEN ENVIRONMENT. REPRODUCED FROM ASTM G3. ....   | 181 |
| FIGURE 7-22. CYCLIC POTENTIODYNAMIC POLARIZATION CURVES OF HASTELLOY C-276 AND 304 STAINLESS STEEL. REPRODUCED FROM ASTM G61. ....   | 181 |
| FIGURE 7-23. PERFORMED CORROSION POTENTIAL DETERMINATION BY A SMALL CPP OF $\pm 250$ mV OF DIFFERENT METALLIC ALLOYS COMMONLY FOUND IN SEAWATER AND OFFSHORE APPLICATIONS. EVERY TEST HAS BEEN CONDUCTED IN NaCl 3.5 wt % MEDIUM AND pH = 8..... | 183 |
| FIGURE 7-24. ARRANGEMENT OF THE COMPONENTS NECESSARY TO PERFORM AN ELECTROCHEMICAL TEST. NOTE THAT THE SAMPLE (WORKING ELECTRODE) IS PLACED BELOW THE CELL AND IS NOT VISIBLE IN THE IMAGE. ....   | 184 |
| FIGURE 7-25. SHORT ( $\pm 250$ mV) POTENTIODYNAMIC POLARIZATION CONDUCTED ON DUPLEX 22Cr STEEL, 316L STAINLESS STEEL AND R5 GRADE SAMPLES. NOTE THE LOGARITHMIC PLOT IN Y-AXIS. ....   | 185 |
| FIGURE 7-26. CYCLIC POTENTIODYNAMIC POLARIZATION CONDUCTED ON R5 HSLA AND N80 CARBON STEEL. ....   | 186 |
| FIGURE 7-27. CYCLIC POTENTIODYNAMIC POLARIZATION CONDUCTED ON R5 HSLA AND DC04 CARBON STEEL. ....  | 187 |
| FIGURE 7-28. RESULTS OF THE HALF A YEAR EXPOSURE OF TWELVE R5 GRADE SAMPLES UNDER ARTIFICIAL SEAWATER. ....  | 189 |
| FIGURE 7-29. THE TWELVE MASS LOSS SAMPLES IN THE FIRST DAYS OF THE ARTIFICIAL SEAWATER IMMERSION TEST, FROM A SIDE VIEW (LEFT) AND TOP VIEW (RIGHT). ....  | 189 |
| FIGURE 7-30. ILLUSTRATION OF EMPLOYED SAMPLES IN THE SECOND BATCH. NOTE THAT CYLINDRICAL SAMPLE IS NOT IN SCALE. ....  | 190 |
| FIGURE 7-31. EVOLUTION OF THE CORROSION RATE VS TIME IN THE FOUR TYPES OF SAMPLES STUDIED, TO ASSESS THE PERFORMANCE OF DIFFERENT ROUGHNESS AND GEOMETRY OF THE SAMPLES. ....  | 191 |
| FIGURE 7-32. TECNALIA'S FACILITIES UBICATION IN THE PORT OF PASAIA. ....   | 192 |
| FIGURE 7-33. IMAGE OF THE SAMPLES EMPLOYED IN THE FIELD IMMERSION TEST. NOTE THAT CYLINDRICAL AND CHAIN SURFACE SAMPLES ARE NOT IN SCALE. ....   | 193 |
| FIGURE 7-34. PICTURE OF THE SAMPLES IN THE RACK PREPARED TO START THE FIELD IMMERSION TEST. ....   | 194 |
| FIGURE 7-35. UP-TO-DATE RESULTS OF SAMPLES EXPOSED IN SEAWATER AT PASAIA PORT. ....  | 194 |
| FIGURE 7-36. ILLUSTRATION OF THE DEGREE OF FOULING COLONIZATION OF THE SAMPLES EXPOSED IN THE PORT OF PASAIA. ....   | 195 |
| FIGURE 7-37. XRD RESULTS OF THE CORROSION PRODUCTS FORMED ON THE COUPONS EXPOSED AT THE PASAIA FACILITY, WITH THE MAIN PHASES AND COMPOUND IDENTIFICATION. ....  | 196 |
| FIGURE 7-38. APPEARANCE OF THE MOORING CHAIN SAMPLE SURFACE AFTER 15 MONTHS OF EXPOSURE (LEFT) AND ONCE GOING THROUGH THE PICKLING PROCESS. ....   | 197 |
| FIGURE 7-39. SEM MICROGRAPH AND EDS SPECTRA OF THE MOORING CHAIN OUTER SCALE. ....   | 198 |
| FIGURE 7-40. SEM MICROGRAPH AND EDS SPECTRA OF THE MOORING CHAIN OUTER SCALE, FOCUSING ON THE CORROSION AFFECTED AREA IN FORM OF PITTING. ....   | 198 |
|  |     |
| FIGURE 8-1. RELATIONSHIP BETWEEN RESISTIVITY AND SPECIFIC RESISTANCE EXPLAINED BY MEASURING THE RESISTANCE OF A PIPE. (SOURCE: ELPROCUS.COM) .....   | 200 |
| FIGURE 8-2. ELECTRICAL CONDUCTIVITY (1/OHM·M) VERSUS THERMAL CONDUCTIVITY (W/eC·M) OF THE MOST COMMON METAL ALLOYS. (SOURCE: UNIVERSITY OF CAMBRIDGE, DOITPOMS.AC.UK). ....  | 201 |
| FIGURE 8-3. VOLTAGE MEASUREMENTS WITH POLARITY REVERSALS TO CANCEL THERMOELECTRIC EMF BY THE CURRENT-REVERSAL METHOD. NOTE THAT THE VOLTAGE VALUE IS THEN EASILY TRANSFORMED INTO RESISTANCE BY THE OHM'S LAW WITH THE KNOWN CURRENT VALUE. .... | 203 |
| FIGURE 8-4. SECTION OF A HOLLOW CYLINDER. ....   | 203 |
| FIGURE 8-5. RELATIONSHIP BETWEEN WALL THICKNESS AND SENSIBILITY OF THE SENSOR. ASSUMING A MEAN CORROSION RATE OF 0.3 MM/YEAR, THE LOWER THE THICKNESS, THE SHORTER THE LIFESPAN OF THE SENSING TUBE, BUT HIGHER IS THE SENSIBILITY. ....         | 204 |
| FIGURE 8-6. CORROSION PENETRATION AND REMAINING LIFETIME OF A TWO-SENSOR BATCH ASSUMING UNIFORM CORROSION WITH A CONSTANT CORROSION RATE OF 0.3 MM/YEAR. ....  | 204 |
| FIGURE 8-7. RELATIONSHIP BETWEEN THE MEASURED RESISTANCE AND THE DECREASE OF THE EXTERNAL RADIUS OF 1 AND 4 MM WALL THICKNESS TUBE WITH A CURRENT INPUT OF 100 mA. ....  | 205 |
| FIGURE 8-8. EXAMPLE OF A PROCESS TREE FOR SENSOR GEOMETRY DEFINITION WITH AN ACTUAL EXAMPLE OF THE FIRST SENSOR FOR THE CORROSION MONITORING SYSTEM IN OFFSHORE MOORING CHAINS. ....   | 207 |
| FIGURE 8-9. SENSOR SCHEME WITH DIFFERENT EXTERNAL RADIUS DEPICTED ONLY IN THE EXPOSED AREA OF THE SENSING TUBE. ....   | 208 |
| FIGURE 8-10. EXAMPLE OF A THREE-SENSOR ARRAY WITH DIFFERENT INITIAL WALL THICKNESS VALUES. ....  | 209 |
| FIGURE 8-11. PROCESS TREE FOR THE TRANSITION BETWEEN ONE SENSOR TO ANOTHER. ....   | 210 |
| FIGURE 8-12. RELATIVE VOLUME OF CORROSION PRODUCTS FORMED ON THE METAL SURFACE TAKING IRON (Fe) AS A UNIT REFERENCE. ....  | 211 |

|   |     |
|---|-----|
| FIGURE 8-13. ON THE LEFT, DIAGRAM OF AN ELECTROCHEMICAL CELL WITH A FOUR-POINT MEASUREMENT SETUP, AND ON THE RIGHT, VISUAL DIAGRAM OF THE POTENTIAL DROP BETWEEN THE COUNTER ELECTRODE (CE) AND THE WORKING ELECTRODE (WE).   | 212 |
| FIGURE 8-14. SCHEMES OF DIRECT AND REVERSE POTENTIAL MEASUREMENT.   | 213 |
| FIGURE 8-15. SCHEMATIC VIEW OF THE SENSING PROBE EMPLOYED, DISTINGUISHING BETWEEN THE PART EXPOSED TO THE TEST MEDIUM AND THE DISTANCE BETWEEN POTENTIAL MEASUREMENT PINS.  | 213 |
| FIGURE 8-16. MEASURED AND EXPECTED VALUES OF INTERNAL AND EXTERNAL RADIUS OF THE THREE SAMPLES.   | 214 |
| FIGURE 8-17. POTENTIAL DROP RESULTS DISPLAYED FOR EACH SPECIMEN IN THE THREE MEDIA. AS SHOWN, NONE OF THE SPECIMENS SUFFERS AN INCREASE IN THE POTENTIAL DROP WITH THE EXPOSURE TO DIFFERENT MEDIA.   | 224 |
| FIGURE 8-18. POTENTIAL DROP RESULT DISPLAYED FOR EACH MEDIA. AS SHOWN, AS THE INTERNAL RADIUS DIMINISHES, POTENTIAL DROP DOES SO, DUE TO A HIGHER EXPECTED RESISTANCE. COMPARISON BETWEEN EXPOSED MEDIA PROVE THAT THERE IS NO INFLUENCE IN THE POTENTIAL MEASUREMENTS. | 225 |
| FIGURE 8-19. MOST EXTENDED CONFIGURATION OF A RESISTIVE CORROSION SENSOR. THE SENSITIVE PROBE IS IMMERSSED IN SEAWATER AT CERTAIN TEMPERATURE AND THE REFERENCE PROBE IS KEPT AT THE SAME TEMPERATURE AS THE ENVIRONMENT.   | 226 |
| FIGURE 8-20. ELECTRICAL MODEL OF THE VOLTAGE MEASURED ON A LONG TUBE OF $R_{CORR}$ RESISTANCE WHEN A DIRECT CURRENT, $I_0$ , PASSES THROUGH IT, IN PRESENCE OF A TEMPERATURE GRADIENT THROUGH THE TUBE.   | 227 |
| FIGURE 8-21. VIEW OF THE THERMAL GRADIENT SETUP WITH THE MULTIMETER CONNECTED TO THE MEASURING TUBE TO QUANTIFY THE POTENTIAL GENERATED BY THE TEMPERATURE GRADIENT BETWEEN TWO POINTS.   | 228 |
| FIGURE 8-22. GRADIENT GENERATION ALONG THE TESTING TUBE REPLICA WITH HEATING AND COOLING PROFILES.  | 229 |
| FIGURE 8-23. TEMPERATURE PROFILES REGISTERED DURING TEST 1. A STEADY INCREASE OF MEASURED TEMPERATURE IN T <sub>COLD</sub> SIDE CAN BE OBSERVED, ALTHOUGH UNDESIRE.   | 229 |
| FIGURE 8-24. MEASURED POTENTIAL BETWEEN TWO TEST POINTS (BLUE CHART) AND THE ESTABLISHED GRADIENT BETWEEN THEM (ORANGE CHART).  | 230 |
| FIGURE 8-25. MEASURED THERMOELECTRIC EFFECT TREND IN TEST 1. NOTE THE EQUATION OF A LINE IS ALSO INCLUDED.  | 230 |
| FIGURE 8-26. MEASURED THERMOELECTRIC EFFECT TREND IN TEST 1 ONCE DATA PROCESSING IS . THE SOURCE OF REPRESENTED DATA IS TABLE 5. NOTE THE EQUATION OF A LINE IS ALSO INCLUDED.  | 231 |
| FIGURE 8-27. MEASURED THERMOELECTRIC EFFECT TREND IN TESTS 1, 2 AND 3. THE EQUATION OF A LINE ARE ALSO INCLUDED.  | 231 |
| FIGURE 8-28. DIAGRAM OF THE GENERATED FEM BETWEEN TWO DISSIMILAR MATERIALS, CAUSED A TEMPERATURE DIFFERENCE BETWEEN THE TWO ENDS.   | 232 |
| FIGURE 8-29. SCHEME OF THE OBSERVED Peltier effect in presence of an imposed thermal gradient.  | 233 |
| FIGURE 8-30. SCHEMATIC DRAWING OF THE MEASUREMENT OF THE THERMOELECTRIC EFFECT WHEN APPLYING CURRENT THROUGH THE SENSING TUBE.  | 237 |
| FIGURE 8-31. ALL VARIABLE CURRENT INPUT TEST REPRESENTED AS MEASURED POTENTIAL VERSUS THE GRADIENT SET IN °C.   | 239 |
| FIGURE 8-32. LOW CURRENT INPUT TESTS REPRESENTED AS MEASURED POTENTIAL VERSUS THE GRADIENT SET IN °C.   | 239 |
| FIGURE 8-33. MEAN VALUES OF THE GENERATED THERMOELECTRIC POTENTIALS AS A FUNCTION OF THE APPLIED CURRENT.   | 240 |
| FIGURE 8-34. BOX-AND-WHISKER PLOT FOR THE MEASURED THERMOELECTRIC EFFECT.   | 241 |
| FIGURE 8-35. VOLTAGE DEPENDENCE WITH $I_0$ MEASURED FOR FOUR DIFFERENT TEMPERATURE GRADIENTS BETWEEN BOTH ENDS OF THE TEST PROBE.   | 243 |
| FIGURE 8-36. VOLTAGE DEPENDENCE WITH $I_0$ MEASURED FOR FOUR DIFFERENT TEMPERATURE GRADIENTS BETWEEN BOTH ENDS OF THE TEST PROBE ONCE THE INFLUENCE OF THE $V_{SEEbeck}$ AND THE RESISTANCE IS REMOVED FROM THE PLOTTED DATA.   | 244 |
| FIGURE 8-37. DATA FROM FIGURE 8-36 EMPHASIZING LOW CURRENT MEASUREMENTS.  | 244 |
| FIGURE 8-38. DATA FROM FIGURE 8-36 EMPHASIZING HIGHER CURRENT MEASUREMENTS.   | 245 |
| FIGURE 8-39. RESISTIVITY VERSUS TEMPERATURE WITH THE LINEAL AND QUADRATIC REGRESSION PERFORMED.   | 248 |
| FIGURE 8-40. SUMMARY AND GRAPHICAL REPRESENTATION OF ALL THE MATHEMATICAL OPERATIONS THAT TAKE PLACE IN THE RESISTANCE VS TIME PLOT.  | 248 |
| FIGURE 8-41. SENSING PROBE WITH THE TWO DIFFERENTIATED MEASUREMENT POINTS.  | 249 |
| FIGURE 8-42. THEORETICAL REPRESENTATION OF RECORDABLE DATA IN A SENSOR.   | 250 |
| FIGURE 8-43. SCHEME OF THE MEASUREMENT OF A SUBJECT'S RESISTANCE BY AN OHMMETER IN A CLOSED CIRCUIT.  | 251 |
| FIGURE 8-44. FOUR-WIRE MEASUREMENT CIRCUIT WITH AN AMMETER AS A CURRENT SOURCE AND A VOLTMETER MEASURING THE POTENTIAL DROP ACROSS THE SUBJECT.   | 252 |
| FIGURE 8-45. FOUR-WIRE MEASUREMENT ASSUMING THAT BOTH THE AMMETER (IN SERIES) AND THE VOLTMETER (IN PARALLEL) ARE IN CLOSE CONTACT, E.G., IN A CONTROLLER CUPBOARD, WHILE THE SUBJECT (TESTING TUBE) IS EXPOSED IN A DETERMINATE HARSH ENVIRONMENT.                     | 252 |
| FIGURE 8-46. CURRENT FLOW PATH THROUGH A FOUR-WIRE RESISTANCE MEASUREMENT SYSTEM. THE HIGHER CURRENTS ALONG THE CIRCUIT ARE DEPICTED WITH LARGER ARROWS, WHILE THE CURRENTS IN THE VOLTMETER CIRCUIT ARE MUCH SMALLER AND ARE THUS DEPICTED WITH SMALLER ARROWS.        | 253 |
| FIGURE 8-47. A) DC04 SHEET MEASUREMENT IN ORDER TO PERFORM THE OHM'S LAW DEMONSTRATION. B) SUBSEQUENT IMAGES OF THE DEGRADATION PRODUCED BY THE NaCl 3.5 WT% SOLUTION OVERTIME.   | 253 |

|   |     |
|---|-----|
| FIGURE 8-48. POTENTIAL VALUES RECORDED OVERTIME WHILE THE TEST SPECIMEN IS IMMERSSED IN A NaCl 3.5 WT% SOLUTION, IN WHICH THE CHOSEN STEEL ALLOY TENDS TO CORRODE. ....   | 254 |
| FIGURE 8-49. BASIC SCHEMATIC OF A FOUR-WIRE MEASURING CORROSION SENSOR, WITH EXPERIMENTAL V (VOLTAGE) AND L (LENGTH) INDICATED ON THE EXPOSED PART OF THE SENSOR. ....  | 254 |
| FIGURE 8-50. PHOTOGRAPHY OF A SAMPLE TESTED, TRACKED WITH THE FOUR-WIRE MEASUREMENT TECHNIQUE.....  | 255 |
| FIGURE 8-51. AVERAGE OF MEASURED RESISTANCE AND CALCULATED REMAINING PROBE CROSS-SECTION OVERTIME IN HOURS. AS NOTICED, THE RESISTANCE VALUES INCREASE WITH TIME LINEARLY, AT LEAST DURING THE TIME THE SAMPLE WAS EXPOSED TO THE MEDIUM. AN INCREASING RESISTANCE INDICATES THAT THE CURRENT TRAVELS OVER A SMALLER CROSS-SECTION, AND THUS INDICATES THAT A CORROSION PHENOMENON IS HAPPENING. .... | 256 |
| FIGURE 8-52. MEASURED CORROSION PENETRATION EACH DAY (BLUE LINE) AND ACCUMULATED PENETRATION OVERTIME (ORANGE CHART) IN THE FIRST GENERATION SENSOR.....  | 257 |
| FIGURE 8-53. ACCUMULATED PENETRATION OVERTIME IN MM (RED CHART) AND REAL-TIME CORROSION RATE VALUE IN MM/YEAR (BLUE CHART). ....  | 257 |
| FIGURE 8-54. MEASURE AVERAGE RESISTANCE IN MOHMS (RED CHART) VERSUS CALCULATED CROSS-SECTION IN MM <sup>2</sup> (BLUE CHART), BOTH AS FUNCTION OF IMMERSION TIME IN DAYS. IN BOTH REPRESENTATIONS, A LINEAR FIT OF THE DATA HAS BEEN PERFORMED.....   | 258 |
| FIGURE 8-55. CALCULATED CROSS-SECTION VERSUS MEASURED AVERAGE RESISTANCE (BLUE CHART) AND ADJUSTED REGRESSION EQUATION (RED CHART). IN THE UPPER RIGHT PART OF THE IMAGE, THE EQUATION RESULTING FROM A FITTED LINE CAN BE FOUND.....   | 260 |
| FIGURE 8-56. BASIC ARCHITECTURE OF CORROSION MONITORING SENSORS .....   | 261 |
| FIGURE 8-57. SENSOR TUBE, WITH CYLINDRICAL SHAPE AND THE DIMENSIONS OF EACH PART DESCRIBED IN DETAIL.....   | 261 |
| FIGURE 8-58. SECTION CUT OF THE SENSOR TUBE AND SENSOR HOUSING, SHOWING THE FOUR-POINT MEASUREMENT CONNECTIONS EXITING FROM THE UPPER PART, WHILE THE LOWER PART IS PROTECTED FROM WATER FLOODING. A PICTURE OF THE GENERAL LOOK OF THE SENSOR IS ALSO PRESENTED, SHOWING ONLY THE EXPOSED LENGTH OF THE SENSOR TUBE.....   | 262 |
| FIGURE 8-59. 4-20 MA LOOPS PRESENT IN THE SENSOR TUBE.....  | 262 |
| FIGURE 8-60. LABORATORY SCALE MODULE. NOTE THAT THE SENSOR TUBE IS PROTECTED BY A THREADED PROTECTION. ....   | 263 |
| FIGURE 8-61. CIRCUIT INVERTOR SCHEME. THE PHYSICAL RELAYS ACT BY REVERSING THE CURRENT FLOW DIRECTION THROUGH THE CIRCUIT. (SOURCE: HOMOFACIENS.DE).....  | 263 |
| FIGURE 8-62. BASIC SCHEME OF THE NOISE FILTERING PROCESS USING AN ADC. ....   | 264 |
| FIGURE 8-63. DIRECT SENSOR CURRENT INPUT SCHEME FOR SENSOR 1. ....  | 265 |
| FIGURE 8-64. INVERSE CURRENT MEASUREMENT FOR SENSOR 1.....  | 266 |
| FIGURE 8-65. POTENTIAL CIRCUIT LOOP, WHICH IS DRIVEN BY THE EL 2798 RELAYS AND THEN DATA IS GATHERED THROUGH A 4-20 MA MODULE TO BE ABLE TO READ THE INFORMATION SENT BY THE SENSOR. ....   | 266 |
| FIGURE 8-66. SCHEMATIC ARRANGEMENT OF EVERY STEPS TAKEN IN THE SEQUENCE BY SENSOR DESCRIPTION. ....   | 268 |
| FIGURE 8-67. SHUNT IMAGE AND GRAPHICAL SCHEME WITH DIMENSIONS DETAILED (IN MM). SOURCE: CIRCUTOR.ES.....  | 269 |
| FIGURE 8-68. BECKHOFF CX8090 CPU CONTROLLER SCHEME. SOURCE: BECKHOFF.COM. ....  | 269 |
| FIGURE 8-69. 2-WIRE CONNECTION SSR MODULE. SOURCE: BECKHOFF.COM. ....   | 270 |
| FIGURE 8-70. BECKHOFF EL3602-0010 ANALOG MODULE FOR SHUNT CURRENT MEASUREMENT. SOURCE: BECKHOFF.COM. ....   | 270 |
| FIGURE 8-71. BECKHOFF EL3612 VOLTAGE DROP ANALOGIC MODULE. SOURCE: BECKHOFF.COM. ....   | 271 |
| FIGURE 8-72. 2-CHANNEL TEMPERATURE ANALOGIC MODULE COMPATIBLE WITH STANDARD PT100 SENSORS. SOURCE: BECKHOFF.COM. ....   | 271 |
| FIGURE 8-73. ANALOGIC 4-CHANNEL TEMPERATURE MODULE SIMILAR TO EL3202, BUT WITH A 2-WIRE CONFIGURATION. SOURCE: BECKHOFF.COM.....  | 272 |
| FIGURE 8-74. SENSOR CONTROLLER SCHEME. ....   | 273 |
| FIGURE 8-75. ACTUAL SCHEME OF THE ELECTRONIC ARRANGEMENT FOR THE SECOND GENERATION OF THE CORROSION MONITORING DEVICE.....  | 274 |
| FIGURE 8-76. MODBUS TCP/IP DATA SOURCE DEFINITION IN MANGODB M2M APP FOR CORROSION MONITORING MEASUREMENTS ANALYSIS.....  | 276 |
| FIGURE 8-77. WATCHLIST EXAMPLE FOR THE SENSOR 1 OF THE CORROSION MONITORING SYSTEM.....   | 276 |
| FIGURE 8-78. GRAPHICAL REPRESENTATION OF DATA POINTS LISTED IN THE WATCHLIST. ....  | 277 |
| FIGURE 8-79. SCHEME (LEFT) AND ACTUAL PICTURE (RIGHT) OF THE FABRICATED TESTBED FOR THE SECOND-GENERATION CORROSION MONITORING SYSTEM IN LABORATORY SCALE. ....   | 278 |
| FIGURE 8-80. TEMPERATURE AND RESISTANCE DATA DURING THE FIRST IMMERSION IN THE AQUARIUM.....  | 279 |
| FIGURE 8-81. CALCULATED CROSS-SECTION AND RESISTANCE DATA DURING THE FIRST IMMERSION IN THE AQUARIUM.....   | 279 |
| FIGURE 8-82. RESISTIVITY VALUES AS A FUNCTION OF TEMPERATURE COLLECTED BY THE CORROSION MONITORING SENSOR IN THE AQUARIUM.....  | 280 |
| FIGURE 8-83. CORRECTED SECTION OUTPUT FOR THE FIRST FOUR MONTHS OF EXPOSURE. EACH COLOUR PLOT REPRESENTS A DIFFERENT MONTH.....   | 280 |

|   |     |
|---|-----|
| <u>FIGURE 8-84. SENSING TUBE HOUSING UPGRADE, FROM FIRST VERSION (LEFT) TO A SECOND ONE MORE PROTECTED AGAINST COLLISIONS (RIGHT).</u> .....  | 281 |
| <u>FIGURE 8-85. EMBEDDED RTD TEMPERATURE SENSOR INTO THE DOWNSTREAM ELECTRONICS.</u> .....  | 281 |
| <u>FIGURE 8-86. A SECOND ENHANCED VERSION OF THE UPSTREAM ELECTRONIC DEVICES WHICH CONTROL AND GATHER THE DATA COMING FROM THE DOWNSTREAM CORROSION SENSOR.</u> .....   | 283 |
| <u>FIGURE 8-87. LOCATION OF THE OPEN FIELD TEST AT THE PASAJES PORT (TOP LEFT AND CENTER) AND INSTALLATION OF THE CONTROLLER AND SENSOR (BOTTOM RIGHT AND CENTER).</u> .....  | 284 |
| <u>FIGURE 8-88. RESULTS OF THE POTENTIAL (PLOTTED IN BLACK) AND TEMPERATURE (PLOTTED IN RED) MEASUREMENTS FOR THE FIRST MEASUREMENT CYCLES OF THE SENSOR.</u> .....   | 285 |
| <u>FIGURE 8-89. PHOTOGRAPHIC RECORDS OF SENSOR APPEARANCE AND CORROSION PROGRESS IN A REAL MARINE ENVIRONMENT.</u> .....  | 285 |
| <u>FIGURE 8-90. STORED VOLTAGE DATA, WHERE NO OR LITTLE VARIATION IS OBSERVED BETWEEN MEASUREMENTS.</u> .....   | 286 |
| <u>FIGURE 8-91. STORED TEMPERATURE DATA, WHERE UNEXPECTED MAXIMUM PEAKS ARE OBSERVED THAT DO NOT CORRESPOND TO A NORMAL TEMPERATURE MEASUREMENT ARE OBSERVED.</u> .....   | 286 |
| <u>FIGURE 8-92. TEMPERATURE DATA DIFFERENCE WHEN COINCIDING WITH THE POTENTIAL MEASUREMENT OF THE TEST PROBE OR WHEN PERFORMING A PASSIVE TEMPERATURE MEASUREMENT OUTSIDE THE CONTROLLER CYCLE.</u> .....   | 287 |
| <u>FIGURE 8-93. A) FINAL APPEARANCE OF THE TEST PROBE. B) CLOSE-UP DETAIL OF THE SURFACE, WHERE DIFFERENT CORROSION PATTERNS CAN BE APPRECIATED. C) ELECTRONIC COMPONENT VISIBLY CORRODED ON CONTACTS. D) TEMPERATURE CONTACT COMPLETELY CORRODED BELOW PLASTIC PROTECTION DUE TO SEVERE EXPOSURE CONDITIONS.</u> ..... | 287 |
| <u>FIGURE 8-94. ONE-SIDE INTERIOR VIEW OF THE SENSING TUBE OF THE SENSOR. CURRENT INPUT AND POTENTIAL DROP MEASUREMENT WELD ARE VISIBLE ON THE TOP PART OF THE TUBE, WHILE THE RTD DEVICE WHICH MEASURES THE TEMPERATURE IS ATTACHED IN THE LOWER PART. NOTE THAT COMPONENTS ARE NOT AT REAL SCALE.</u> .....           | 289 |
| <u>FIGURE 8-95. CORROSION RESISTANCE MEASUREMENT ELECTRONIC MAP. A RESISTANCE BRIDGE ALLOWS SMALL CHANGES IN RESISTANCE TO BE OBSERVED. THE SENSING TUBE RESISTANCE IS DEPICTED AS RX.</u> .....  | 290 |
| <u>FIGURE 8-96. THE RESISTANCE BRIDGE SIGNAL DEPICTED IN FIGURE 8-95 IS AMPLIFIED BY THE INA128 INSTRUMENT. THE AMPLIFIED SIGNAL IS CONVERTED TO 4-20 mA CURRENT, AMPLIFYING AT THE SAME TIME AND SENDING IT TO THE GROUND MONITORING</u> .....   | 290 |
| <u>FIGURE 8-97. ELECTRONICS DESIGN FOR THE CORROSION SENSOR.</u> .....  | 291 |
| <u>FIGURE 8-98. TWO-WAY MEASUREMENT SCHEME WITH AN ARDUINO NANO</u> .....   | 291 |
| <u>FIGURE 8-99. VOLTAGE MEASUREMENT AND RTD MEASUREMENT ARE SENT IN BITS FORMAT THROUGH RS485 MODULE TO THE UPSTREAM CONTROLLED, WHICH ALSO RECEIVES THE SIGNAL WITH A RS485 MODULE.</u> .....  | 293 |
| <u>FIGURE 8-100. ELECTRONICS ARRANGEMENT IN THE ABOVE-SEA HEAD CONTROLLER.</u> .....  | 294 |
| <u>FIGURE 8-101. HEAD-CONTROLLER ELECTRONICS ARRANGEMENT. SOLAR PANEL WAS OMITTED FOR SIZE DIFFERENCE REASONS.</u> .....  | 294 |
| <u>FIGURE 8-102. DOWNSTREAM ELECTRONIC ARRANGEMENT DESIGN.</u> .....  | 295 |
| <u>FIGURE 8-103. RAW ELECTRONICS WITH THE SENSING PART WIRE-ATTACHED (LEFT) AND ELECTRONICS MOUNTED IN THE SPECIFICALLY DESIGNED PROTECTION HOUSING (RIGHT).</u> .....  | 295 |
| <u>FIGURE 8-104. DATA PLOT OF MEASURED TEMPERATURE INSIDE THE CLIMATE CHAMBER OF BOTH TEST PROBE AND SENSOR BODY.</u> .....   | 297 |
| <u>FIGURE 8-105. EVOLUTION OF THE RESISTANCE (IN MOHM) WITH THE LOGGED PROBE TEMPERATURE. THE SLOPE OF THE RESULTING LINE IS SOLVED AS THE ALPHA COEFFICIENT.</u> .....   | 297 |
| <u>FIGURE 8-106. ACCELERATED CORROSION TEST SETUP.</u> .....  | 298 |
| <u>FIGURE 8-107. RESISTANCE AND TEMPERATURE DATA OF THE R5 GRADE HSLA STEEL TEST PROBE IN THE DILUTED AQUA REGIA SOLUTION.</u> .....  | 298 |
| <u>FIGURE 8-108. CALCULATED R<sub>CORR</sub> AND THE THREE IDENTIFIED BEHAVIOURS OBSERVED DURING THE ACCELERATED CORROSION TEST.</u> .....  | 299 |
| <u>FIGURE 8-109. SYSTEM HEAD PROTOTYPE FITTED IN THE RUGGED BOX.</u> .....  | 300 |
| <u>FIGURE 8-110. WATER-TIGHT SEALING OF THE SENSOR PROTOTYPE.</u> .....   | 300 |
| <u>FIGURE 8-111. DIAGRAM OF THE CORROSION MONITORING SYSTEM ACTUAL PROTOTYPE.</u> .....   | 301 |
| <u>FIGURE 8-112. HARSHLAB 1.0 SCHEME (LEFT) AND AN ACTUAL FOOTAGE OF THE TEST PLATFORM BEFORE DEPLOYMENT (RIGHT).</u> .....   | 302 |
| <u>FIGURE 8-113. CALM BUOY SCHEME CONFIGURATION IN HARSHLAB 1.0.</u> .....  | 302 |
| <u>FIGURE 8-114. MOORING LINES ORIENTATION IN HARSHLAB 1.0.</u> .....   | 303 |
| <u>FIGURE 8-115. STEVSHARK® REX ANCHOR ILLUSTRATION.</u> .....  | 303 |
| <u>FIGURE 8-116. PLAN OF THE HARSHLAB 1.0 MOORING LINE SYSTEM DEPLOYMENT.</u> .....   | 304 |

## List of tables

|   |     |
|---|-----|
| <u>TABLE 2-1. CORROSION CATEGORIES FOR ATMOSPHERIC (YELLOW) AND IMMERSION (BLUE, TABLE IN BLOD) AREAS. CORROSION VARIES ACCORDING TO THE AREA OF APPLICATION AND THE GIVEN CORROSION CATEGORY. SOURCE: ISO 12944.</u> ..... | 5   |
| <u>TABLE 2-2. MARINE EXPOSURE ZONE AND ASSOCIATED CORROSION RATE.</u> .....   | 7   |
| <u>TABLE 2-3. SUITABILITY OF STUD-LINK OF STUDLESS CHAINS DEPENDING ON THE CHOSEN REQUIREMENTS AND CRITERIA. SOURCE: RESEARCH REPORT 444<sup>31</sup>.</u> .....  | 22  |
| <u>TABLE 2-4. DURABILITY OF FIBRE ROPE MATERIALS FOR MOORING SYSTEMS. SOURCE: WELLER (2005)<sup>46</sup>.</u> .....   | 23  |
| <u>TABLE 2-5. RECOMMENDED ROPE IN FUNCTION OF DESIGN LIFE EXPECTANCY. SOURCE: ADAPTED FROM RR 444<sup>31</sup> AND SEFTON<sup>49</sup>.</u> .....   | 24  |
| <u>TABLE 2-6. SUMMARY OF MOORING LINE COMPONENTS</u> .....  | 24  |
| <u>TABLE 2-7. MOORING LINE CONFIGURATION MOST SUITABLE CHOICE DEPENDING ON THE INSTALLATION DEPTH.</u> .....  | 25  |
| <u>TABLE 2-8. SUMMARY OF OFFSHORE GRADE STEELS WITH UTS VALUES IN MPA AND BRINELL HARDNESS. SOURCE: VICINAY.</u> .....  | 25  |
| <u>TABLE 2-9. MAIN CHARACTERISTICS OF THE DIFFERENT ANCHOR TYPES. SOURCE: TOLEDO (2017)<sup>53</sup></u> .....  | 27  |
| <u>TABLE 2-10. VARIETY OF FAILURE MECHANISMS FOR CHAIN, WIRE ROPE, AND CONNECTORS. SOURCE: MA (2019)<sup>56</sup></u> .....   | 29  |
| <u>TABLE 2-11. SINGLE MOORING LINE FAILURE APPROXIMATE COST. SOURCE: TANDE (2010)<sup>64</sup></u> .....  | 31  |
| <u>TABLE 2-12. OPERATIVE YEARS UNTIL FAILURE OF DIFFERENT OFFSHORE ASSETS IN THE NORTH SEA (PERIOD: 1980-2001). SOURCE: TANDE (2010)<sup>64</sup></u> .....   | 31  |
| <br>  |     |
| <u>TABLE 3-1. AVERAGE COMPOSITION OF SEAWATER AT A SALT CONCENTRATION OF 3.5 WT%<sup>8</sup>.</u> .....   | 37  |
| <u>TABLE 3-2. SUMMARY OF CORROSION PHASES ACCORDING TO THE SEQUENCE MODEL, WITH INDICATION OF AEROBIC AND ANAEROBIC SCENARIOS.</u> .....  | 55  |
| <br>  |     |
| <u>TABLE 4-1. INVOLVED DEGRADATION PHENOMENA AS FUNCTION OF THE OFFSHORE ZONE. ADAPTED FROM MOMBET ET. AL. (2018)<sup>2</sup>.</u> .....  | 77  |
| <u>TABLE 4-2. APPLIED POTENTIAL IN THE CATHODIC PROTECTION DEPENDING ON THE METAL AND THE ENVIRONMENT.</u> .....  | 93  |
| <u>TABLE 4-3. PROPERTIES OF MAGNESIUM-BASED ALLOY, ZINC-BASED ALLOY, AND ALUMINIUM-BASED ALLOY EMPLOYED FOR SACRIFICIAL ANODES. SOURCE: HUANG (2018)<sup>70</sup> AND PRIYOTOMO, NURAINI (2017)<sup>77</sup>.</u> .....     | 94  |
| <u>TABLE 4-4. MAIN PROS AND CONS OF ICCP AND GACP SYSTEMS. SOURCE: MARCEPINC.COM</u> .....  | 95  |
| <u>TABLE 4-5. MINIMUM VALUES FOR DESIGN CORROSION RATE AS FUNCTION OF THE REGION. SOURCE: DNV-GL RP 0416.</u> .....   | 96  |
| <br>  |     |
| <u>TABLE 5-1. COATING SYSTEMS UNDER STUDY</u> .....   | 107 |
| <u>TABLE 5-2. SAMPLE NUMBER, CHARACTERISTICS AND SRB CONCENTRATION IN EACH BEAKER AT THE START AND END OF THE IMMERSION TESTS.</u> .....  | 109 |
| <u>TABLE 5-3. SUMMARY TABLE OF SEMI QUANTITATIVE EDS CHEMICAL ANALYSIS OF TESTED SAMPLES.</u> .....   | 127 |
| <br>  |     |
| <u>TABLE 6-1. COST OF CORROSION BY SECTOR AND TOTAL COST AS FUNCTION OF %GDP. SOURCE: NACE IMPACT.</u> .....  | 139 |
| <u>TABLE 6-2. SENSITIVITY AND RESPONSE TIME OF CORROSION MONITORING APPLICATIONS. ADAPTED FROM ROBERGE<sup>23</sup>.</u> .....  | 142 |
| <br>  |     |
| <u>TABLE 7-1. BALANCE OF THE MAIN ELEMENTS AND ALLOYANTS IN WEIGHT PERCENT.</u> .....   | 173 |
| <u>TABLE 7-2. CHEMICAL ANALYSIS BY SPARK OES SHOWING THE MAIN ELEMENTS AND ALLOYANTS IN WEIGHT PERCENT OF THE R5 TYPE HSLA.</u> .....   | 173 |
| <u>TABLE 7-3. ROLE OF THE ALLOYING ELEMENTS IN R5 GRADE HSLA STEEL.</u> .....   | 174 |
| <u>TABLE 7-4. AVERAGE EXPERIMENTAL MECHANICAL PROPERTIES OF CHAIN MATERIAL.</u> .....   | 178 |
| <u>TABLE 7-5. ELECTROCHEMICAL PARAMETERS OF 22Cr, 316L AND R5 STEELS OBTAINED FROM THE POTENTIODYNAMIC POLARIZATION EXPERIMENT.</u> .....   | 185 |
| <u>TABLE 7-6. EMPLOYED SAMPLES FOR THE CPP TEST IN ARTIFICIAL SEAWATER TO COMPARE CORROSION BEHAVIOUR.</u> .....  | 185 |
| <u>TABLE 7-7. ELECTROCHEMICAL PARAMETERS OF N80-1 AND R5 STEELS OBTAINED FROM THE POTENTIODYNAMIC POLARIZATION EXPERIMENT.</u> .....  | 186 |
| <u>TABLE 7-8. ELECTROCHEMICAL PARAMETERS OF DC04 AND R5 STEELS OBTAINED FROM THE POTENTIODYNAMIC POLARIZATION EXPERIMENT.</u> .....   | 187 |
| <u>TABLE 7-9. DESCRIPTION OF THE SAMPLES EMPLOYED IN THE SECOND IMMERSION TEST.</u> .....   | 190 |
| <u>TABLE 7-10. DESCRIPTION OF THE EMPLOYED SAMPLES, NAME, DIMENSIONS AND ROUGHNESS FOR THE FIELD IMMERSION TEST.</u> .....  | 192 |
| <u>TABLE 7-11. ROUGHNESS MEASUREMENT CONDITIONS FOR THE OPEN-FIELD IMMERSION TEST SAMPLES.</u> .....  | 193 |
| <br>  |     |
| <u>TABLE 8-1. PLANNED DIMENSION OF THE EXTERNAL RADIUS OF THE THREE MACHINED SPECIMENS FOR ENVIRONMENTAL CONDUCTIVITY ANALYSIS.</u> .....   | 212 |
| <u>TABLE 8-2. CONDUCTIVITY OF THE MEDIA USED FOR THE ELECTROCHEMICAL TEST IN S/M.</u> .....   | 212 |

|   |            |
|---|------------|
| <u>TABLE 8-3. CARRIED ON EXTRA DIMENSION MEASUREMENTS AND THE EXPECTED VALUES FOR EACH SPECIMEN.....</u>  | <u>214</u> |
| <u>TABLE 8-4. SUMMARY OF THE EXPECTED AND OBTAINED POTENTIAL DROP RESULTS IN THE DIFFERENT TESTED MEDIA (ATMOSPHERIC, ARTIFICIAL SEAWATER AND FeCl<sub>3</sub>) FOR THE THREE SPECIMENS. ....</u> | <u>214</u> |
| <u>TABLE 8-5. INFORMATION GATHERED FROM TEST 1 AFTER DATA PROCESSING. ....</u>  | <u>230</u> |
| <u>TABLE 8-6. MEASURED THERMOELECTRIC EFFECT IN TEST 1, WITH THE ASSOCIATED CONFIDENCE INTERVAL AT 95% AND THE R<sup>2</sup> COEFFICIENT OBTAINED IN THE EQUATION OF THE LINE.....</u>            | <u>231</u> |
| <u>TABLE 8-7. MEASURED THERMOELECTRIC EFFECT IN THE THREE REPLICATES, WITH THE ASSOCIATED 95% CONFIDENCE INTERVAL AND THE R<sup>2</sup> COEFFICIENT OBTAINED IN THE EQUATION OF THE LINE.....</u> | <u>232</u> |
| <u>TABLE 8-8. TESTS PERFORMED IN THE CALCULATION OF THE THERMOELECTRIC EFFECT DUE TO A CURRENT INPUT IN THE SYSTEM. ....</u>  | <u>238</u> |
| <u>TABLE 8-9. REGRESSION ANALYSIS FOR AVERAGE MEASURED THERMOELECTRIC EFFECT SHOWN IN FIGURE 8-34. ....</u>   | <u>241</u> |
| <u>TABLE 8-10. RESISTIVITY-TEMPERATURE PARAMETERS OBTAINED FROM THE DATA PLOTTED IN FIGURE 8-39.....</u>  | <u>248</u> |
| <u>TABLE 8-11. OBTAINED RESULTS FOR THE FIRST TEN DAYS OF THE IMMERSION TEST PRESENTED IN FIGURE 8-51. ....</u>   | <u>256</u> |
| <u>TABLE 8-12. REGRESSION ANALYSIS FOR THE AVERAGE MEASURED RESISTANCE SHOWN IN FIGURE 8-54. ....</u>   | <u>259</u> |
| <u>TABLE 8-13. REGRESSION ANALYSIS FOR SECTION CALCULATION SHOWN IN FIGURE 8-54. ....</u>   | <u>259</u> |
| <u>TABLE 8-14. REGRESSION ANALYSIS FOR AVERAGE MEASURED RESISTANCE VERSUS SECTION VARIATION SHOWN IN FIGURE 8-54. ....</u>  | <u>259</u> |
| <u>TABLE 8-15. FULL SCALE FOR TEMPERATURE AND POTENTIAL 4-20 MA LOOPS. ....</u>   | <u>262</u> |
| <u>TABLE 8-16. DETAILED STEPS AND ACTION COMMANDS IN THE CONTROLLER MEASUREMENT CYCLE. ....</u>   | <u>284</u> |



# 1

---

## INTRODUCTION

---

- Background and objectives
- Overview of the thesis



## 1.1 Background and objectives

In order to avoid corrosion-related major events, investment on integrity management and structural health monitoring is one of the best election that can be made. Periodical condition assessment is crucial to optimise the operation and maintenance of offshore assets and have been proven as an active alternative against corrosion.

The purpose of the present thesis is to provide a solid corrosion rate measurement device, based on electric resistance. This will allow a future development of a fully industrial-scale prototype, which provides on-site robust corrosion rate measurements and structural assessment of mooring chain conditions in, mainly, offshore floating assets. The thesis addresses the following objectives:

- **Development of a corrosion monitoring system based on electrical resistance measurement.**  
Perform a voltage measurement in a seawater-sensitive sensor which imitates the corrosion behaviour of an in-service mooring chain, with regard to measuring every detail: From temperature compensation of the resistance measurements to the corrosion rate data output is evaluated.
- **Effect of the sulphate-reducing bacteria in a R5-grade HSLA steel surface.**  
One of the long-term problems that immersion systems present is their behaviour against bacterial activity. A performance study of the alloy of interest is carried out in a controlled environment in the presence of high SRB concentration. In addition, current solutions against corrosion such as TSA and PU are evaluated.
- **Thermoelectric effect due to current imposition and temperature gradients.**  
Determination of the Peltier, Joule and Thompson effects on the measured potential drop and hence resistance measurement in a sensing tube. Propose of a thermal model for the thermoelectric effects that concern the sensor.

The development from a scratch resistance measurement system to a fully embedded and miniaturized corrosion monitoring system is presented. Conflicting explanations for the variations in the measured resistance values and therefore, corrosion rates, in the earlier prototypes, illustrate the need for an explanation in chronological order that highlights the necessary improvements in each case to reach a system with optimal results.

## 1.2 Overview of Thesis

The introductory Chapter 1 prefaces Chapter 2, where an introduction to the main offshore energy production units is given. Differences and similarities between Oil&Gas production units and floating offshore wind farms are highlighted. In addition, an introduction to mooring lines is also included, where their main characteristics, functions and materials are described.

Chapter 3 deals with a review of the main corrosion events in marine environment, especially emphasizing those degradation phenomena and influential factors that particularly concern immersed mooring lines. After that, the chapter makes a review of developed corrosion models in marine environment carried out up to date, while giving prominence to the model improved by Melchers.

Chapter 4 gathers corrosion control and mitigation strategies that exist nowadays, with specific detail in coating protection, describing pros and cons of the major types of coatings employed in offshore services, practically the central issue since coatings are usually the preferred solution

adopted for corrosion mitigation. Finally, a brief introduction to cathodic protection and material selection is made.

Chapter 5, and as a closing chapter of this first part of the thesis more focused on passive protection strategies, experimental activities in sulphate-reducing bacteria influence on coated and uncoated mooring chains is presented. The chapter is adapted from an actually submitted paper, focusing on protective properties of different proposed solutions against biocorrosion in mooring chains and components, bacterial settlement ability into the surface, and a mechanism is proposed for the degradation of Thermally Sprayed Aluminium in the presence of SRBs for environments with high bacterial concentration.

Chapter 6 deals with corrosion management and maintenance strategies at first, mentioning life-cycle asset management and risk-based inspection, but also highlighting corrosion actual economic impact and potential market share. This is followed by a review of current valid corrosion monitoring techniques for subsea applications, among which are the one used in the monitoring system: electrical resistance.

Chapter 7 describes the experimental activities in the present research project in terms of material characterization and employed techniques, incising in the chosen materials, manufacture of test specimens, conditioning and testing. The chapter is divided in two main sections. The first section describes materialographic experiments, where microstructural analysis, chemical and mechanical characterization are conducted. The second section investigates the behaviour against corrosion with electrochemical and immersion tests appraisal.

Chapter 8 details the fundamentals of the developed corrosion monitoring system, from the choice of the technique to the development from scratch, basic system to a more advanced and miniaturized corrosion monitoring device. In this chapter an in-detail discussion of low resistivity measurements for the detection of material loss, sensor geometry definition and the Ohm's Law application is done. Following this, the performed steps to translate from voltage measurements to corrosion rate output are presented. In addition, a detailed experimental procedure that evaluates the importance of the environment conductivity and the observed thermoelectric effects due to established temperature gradients along the sensing tube are also presented. Finally, the lab-scale full pilot system is reviewed, and the performance of all components working at the same time is evaluated.

Chapter 9 summarizes the main conclusions from the obtained results in the two previous chapters and where recommendations for further work are given. It also includes the work published as a result of the research carried out during the period of the doctoral thesis.

# 2

---

## OFFSHORE FACILITIES AND MOORING LINES

---

- Current challenges in offshore facilities
- Offshore Energy Production: Wind Turbines and Oil&Gas Platforms
- Mooring line systems



This chapter intends to highlight the relevance that offshore facilities will increasingly cope in years to come in both Oil&Gas and wind-power generation. On one hand, Oil&Gas demand will continue to rise, whose extraction will be carried out mainly in deepwater locations. On the other hand, despite the overwhelming monopoly of onshore wind, offshore wind is very promising as it is able to tap more consistent, less variable and higher wind speed; making offshore wind installations a more suitable option to meet the electricity demand profiles in the future.

The monitoring system is focused on a specific application: the structural control of mooring lines, permanently present in floating structures of different kinds. That is why, despite introducing fixed structures, a small review is also carried out of the structures that are suitable to be monitored by our system, the problems and different functions they have, and the challenges that should be tackled depending on the critical area that is desired to be monitored.

## 2.1 Current challenges in offshore facilities

Offshore Oil&Gas and wind turbines facilities are both linked to a general purpose: energy production. Despite sources are totally different, one accounting for gas and oil production while the other takes advantage of wind power to produce clean electricity, they compete between each other in a world tending to decarbonise. However, all offshore facilities share some of their mooring processes and designs, which are of interest in the present document. So, as we are approaching a future in which the world will demand more clean sourced energy, large energy-efficiency improvements in all sectors and accelerated electrification will gather all the attention, while global primary energy demand peaks in 2032. Technology advances to bring down the costs and maintenance of renewable energy resources will be important to cope demand requirements for green zero-emissions energy sources<sup>1</sup>.

Fossil-fuel share of the energy mix will decline steadily, falling from 81% of the share today to 54% by 2050. From that general output, today, offshore production accounts for more than a 25% of global oil and gas production<sup>1</sup>. Offshore facilities will become more and more important, as it is estimated that 84% of all non-renewable fuels in the earth are found under the ocean floor<sup>2</sup>. Moreover, DNV-GL most recent energy outlook establishes that natural gas demand will rise at least until 2035<sup>3</sup> (Figure 2-1).

It is important to highlight that natural gas is frequently considered as a bridge to a decarbonized future, as its CO<sub>2</sub> emissions per energy output are typically about half those of coal. What is more, carbon-free gas can be achieved by converting CH<sub>4</sub> (natural gas – methane) to hydrogen or to other carbon-free gases by capturing the CO<sub>2</sub>, keeping the interest in hydrocarbon resources strong<sup>4,5</sup>.

Wind-powered energy supply will rise from an actual 1% to a solid 11% in 2050<sup>3</sup>. The share of offshore wind in the total wind electricity generation will increase steadily, rising globally from 5.5% in 2018 to 28% in 2050, a fifth of which is floating offshore. As water has less surface roughness than land (especially deeper waters), offshore wind speeds are considerably higher than onshore, and thus, offshore wind facilities are characterised by higher load hours<sup>6</sup>. An analysis by the International Energy Agency (IEA)<sup>1</sup> offshore and no deeper than 60 m, 36.000

terawatt hours of renewable electricity a year could be generated. This would meet the actual global demand for electricity of more than 26.000 terawatt hours<sup>7</sup>.

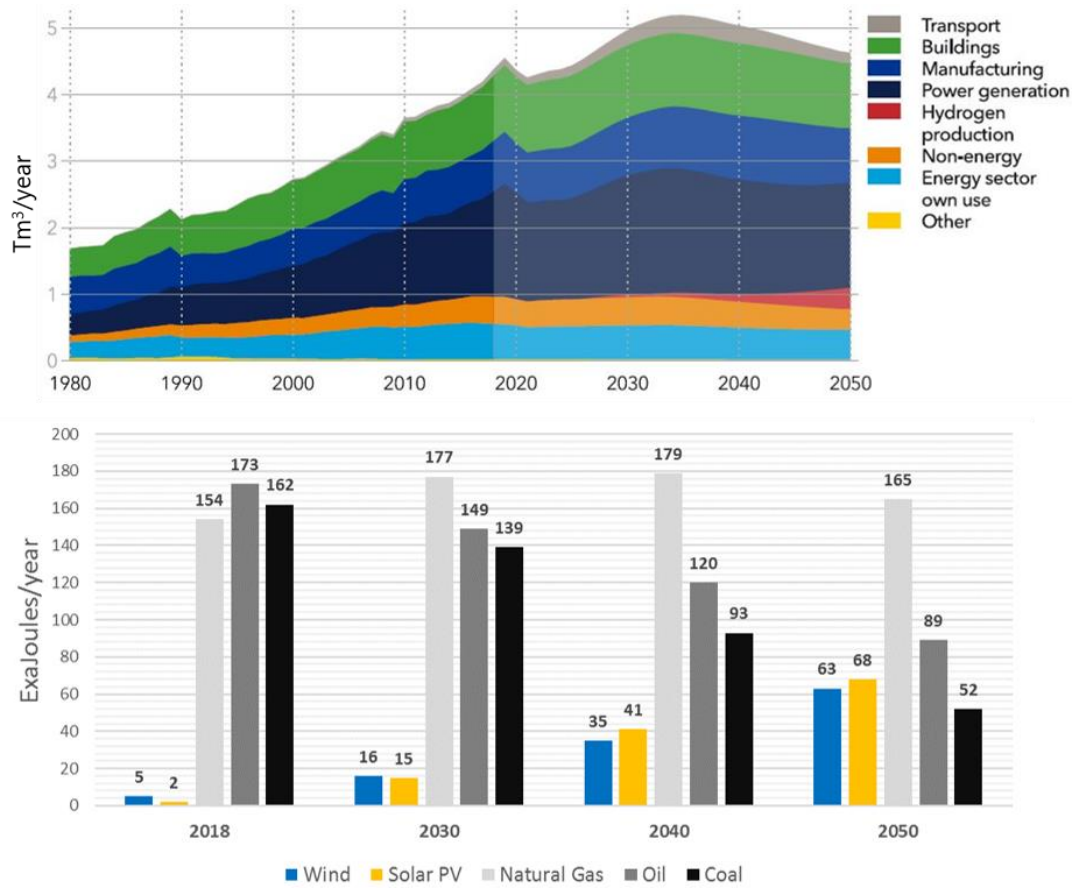


Figure 2-1. World natural gas demand by sector in Tm<sup>3</sup>/year (upper image), where demand peaks in 2035 although new sectors as the hydrogen production will arise at the same time. World primary energy supply by source is presented below, with a clear fossil fuel downward tendency in oil and coal production, and a near 12-fold and 30-fold upward production for wind and solar sources, respectively. Source: DNV-GL Energy Outlook 2020.<sup>3</sup>

As electricity demand will increase due to decarbonization and key-sector electrification, the transition in electricity generation from fossil fuels to renewables will accelerate. In 2018, only 26% of electricity was supplied from renewable sources. With continued declines in the costs of solar and wind technologies, by 2050 78% of the world's electricity is expected to be generated from renewable sources, from which the 31% will be wind-powered electricity (Figure 2-2).

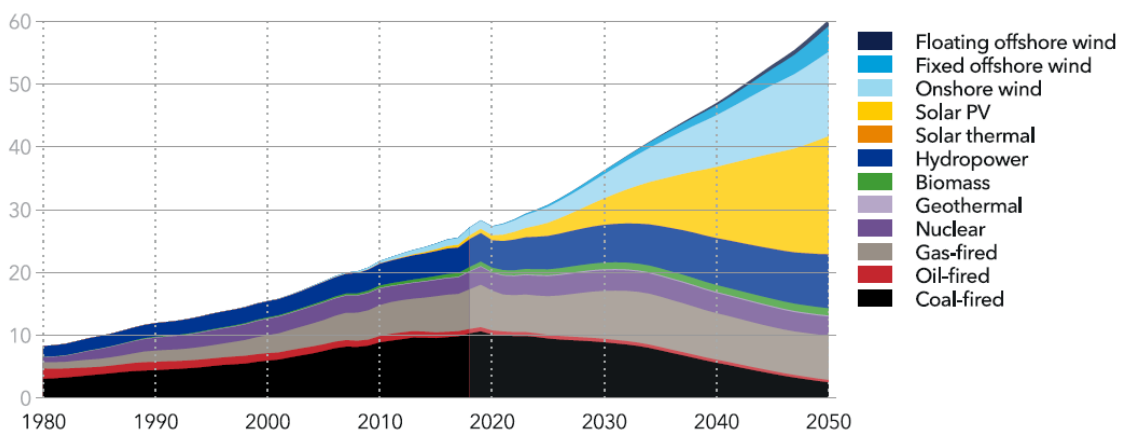


Figure 2-2. World electricity generation in PWh/year (picowatt/hour per year).

## 2.2 Offshore Energy Production: Wind Turbines and Oil&Gas Platforms

Marine locations are usually highly corrosive, and the corrosivity tends to be significantly dependent on many factors, which will be described in Chapter 3. Specifically speaking of atmospheric corrosion, the exposure zone also has critical consequences for the behaviour of a given material. It is important to contextualize the different marine zones, since the corrosion mechanisms in each of them is totally different, and in many cases practically impossible to predict.

Exposure zones are detailed later, along with the corrosivity categories found, for example, in standards as ISO 12944, where corrosion protection of steel structures by protective paint systems are evaluated. Despite mainly focusing on painted structures and apply exclusively to atmospheric environments, a section deals with purely immersed structures and classifies the corrosiveness of the environment in different categories. Hence, the classification helps to contextualize the severity of the environment and what life expectancy is given to each component depending on the area of exposure (Table 2-1), which is directly related to our monitoring system that is designed for evaluating immersed corrosion.

### 2.2.1 Marine Zones and Forms of Corrosion

Marine exposure can be divided into five main zones (Figure 2-3):

- Marine atmosphere
- Splash Zone
- Tidal or Intermediate Zone
- Immersion Zone
- Buried zone.

Table 2-1. Corrosion categories for atmospheric (yellow) and immersion (blue, table in bold) areas. Corrosivity varies according to the area of application and the given corrosion category. Source: ISO 12944.

| Suited area           | Category | Corrosivity                | Applies to  |
|-----------------------|----------|----------------------------|---|
| Atmospheric Corrosion | C1       | Very Low                   | Dry and low pollution   |
|                       | C2       | Low                        | Temperate low pollution                                       |
|                       | C3       | Medium                     | Temperate, medium pollution<br>Tropical low pollution         |
|                       | C4       | High                       | Temperate high pollution<br>Tropical moderate pollution       |
|                       | C5       | Very High                  | Temperate/subtropical with high pollution or chloride effects |
|                       | CX       | Extreme                    | Extreme industrial area<br>Offshore<br>Salt spray effect area |
| Immersed Structures   | IM1      | Fresh Water                | River installations   |
|                       | IM2      | Sea/Brackish water         | Immersion without CP  |
|                       | IM3      | Soil                       | Buried structures   |
|                       | IM4      | Sea/Brackish water with CP | Immersion with CP   |



Marine atmosphere is a particular form corrosion that, even if it does not involve exactly metal-seawater interaction, it occurs when a film of liquid or moisture deposits on the metal surface. The relatively high level of electrical resistance of the thin film of moisture is a major determinant of the corrosion rate, since oxygen access is practically unrestricted over the short diffusion pathways involved in corrosion process<sup>8</sup>. Moreover, the water film that condenses when the temperature drops or on relatively cold surfaces is usually saturated with oxygen.

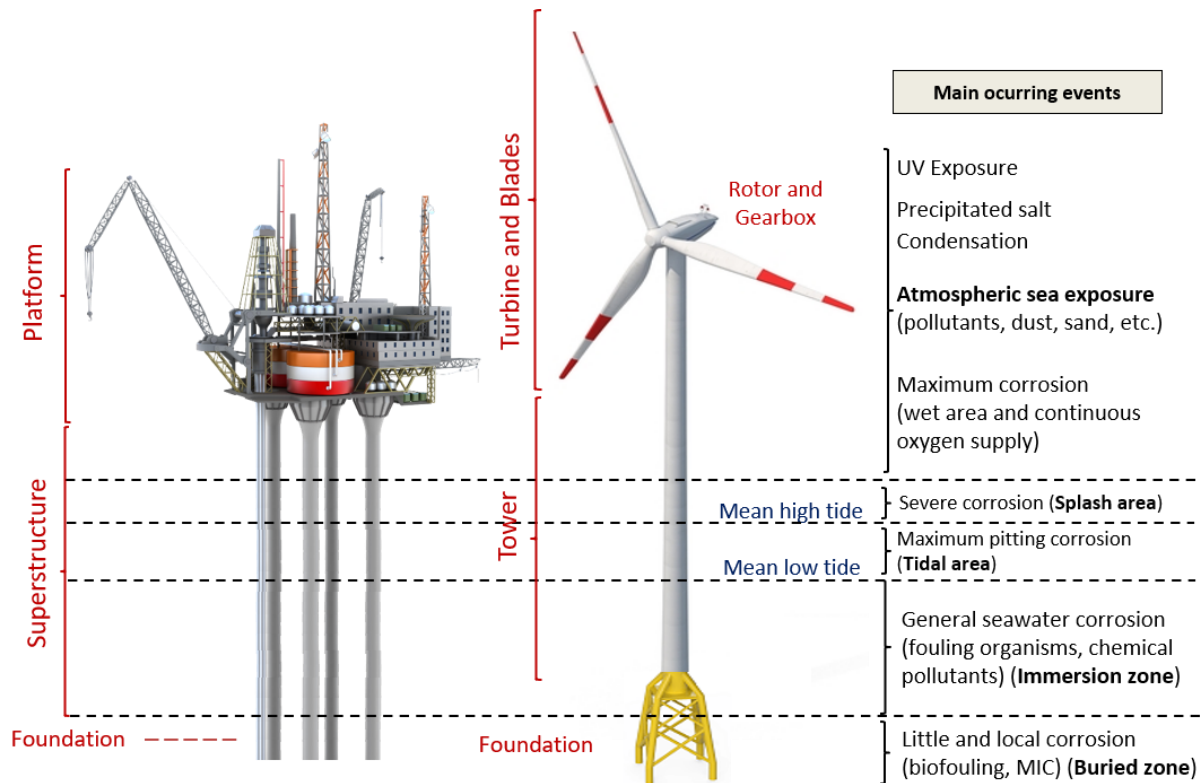


Figure 2-3. Marine zones and main occurring events for Oil&Gas rigs and offshore wind turbines.

Particularly in marine atmosphere, sea spray attaches salt particles to the steel surface, increasing the electrical conductivity of the electrolyte solution, and thus, the activity of the corroding elements, as chloride ions. Generally, the quantity of salt present decreases as a function of height distance from the mean tide. Heavy rains can reduce corrosion since they wash off salt particles, but they may also generate more pronounced corrosion on the lee side of structural elements, since the washout effect is missing.

Materials placed in the splash zone are intermittently under the influence of high moisture levels and high salt content levels due to tidal and/or waves action<sup>9</sup>. The height of the splash zone is variable and determined by the wave height and wind speed and direction. In this zone, corrosion becomes more severe as water evaporates, leaving remains of salts on the structure surface that enhance corrosion rate.

Tidal zone or intermediate zone has an unrestricted oxygen access to the moist surfaces in the low water phase that enhances corrosion, apart from being subjected to wetting and drying cycles. In this zone, fouling and wave action also have a considerable influence on corrosion processes.

In the **immersion zone**, the water is practically saturated with oxygen and permanently submerged. In addition to fouling, contaminants and water currents are additional factors to



be considered. In addition, some structural components as mooring lines, may suffer from EAC and wear throughout its entire length.

**Buried zone** includes any structural part buried in sea floor. Corrosion is extremely complex in the underground environment due to the variability of the local conditions, and also because the same steel structure may cross different types of soil in depth<sup>10</sup>. Even if it is considered that seabed zone has the least corrosiveness, diffusion of the oxygen is a main corrosion factor, determining corrosion rate of steel, but also corrosion caused by SRB activity, which is often manifested as localised corrosion<sup>11</sup>.

In Oil&Gas and offshore wind structures, corrosion rates are reported depending on the exposure area, since the difference between them can be several orders of magnitude (Table 2-2. Marine exposure zone and associated corrosion rate. Table 2-2).

Table 2-2. Marine exposure zone and associated corrosion rate.

| Marine exposure zone    | Corrosion Rate (mm/year) |
|-------------------------|--------------------------|
| Atmospheric Zone        | 0.050 - 0.075            |
| Splash Zone             | 0.20 - 0.40              |
| Tidal/Intermediate Zone | 0.05 - 0.25              |
| Immersion Zone          | 0.10 - 0.20              |
| Buried Zone             | 0.06 - 0.10              |

### 2.2.2 Offshore structure types

Offshore structures are installations and facilities in the deep ocean at strategic sites for the exploration, exploitation and large-scale production of, mainly, electricity and natural resources. Generally, all offshore platforms have:

- A superficial structure, mostly above the water level consisting of operations, machinery, accommodation, control systems, piping systems, etc.
- An intrinsic underlying system consisting of drilling equipment for the purpose of extraction of oil from the seabed in the case of Oil&Gas structures, and essentially marine foundations for those structures based on generating clean energy.

In the case of offshore drilling rigs, there are two types of structures:

- Movable from place-to-place structures, allowing for drilling in multiple locations.
- Permanently placed facilities.

Moveable rigs are often used for exploratory purposes because they are much cheaper to use than permanent platforms. Once large deposits of petroleum and natural gas have been found, a permanent platform is built to allow their extraction.

In general, for both cases, there are two main categories: fixed and floating (Figure 2-4). Each type has a few sub-categories, which are described below. In the present work, only the floating structures will be covered in depth, as the designed corrosion monitoring prototype is mainly designed for structures with mooring line-based clamping systems.

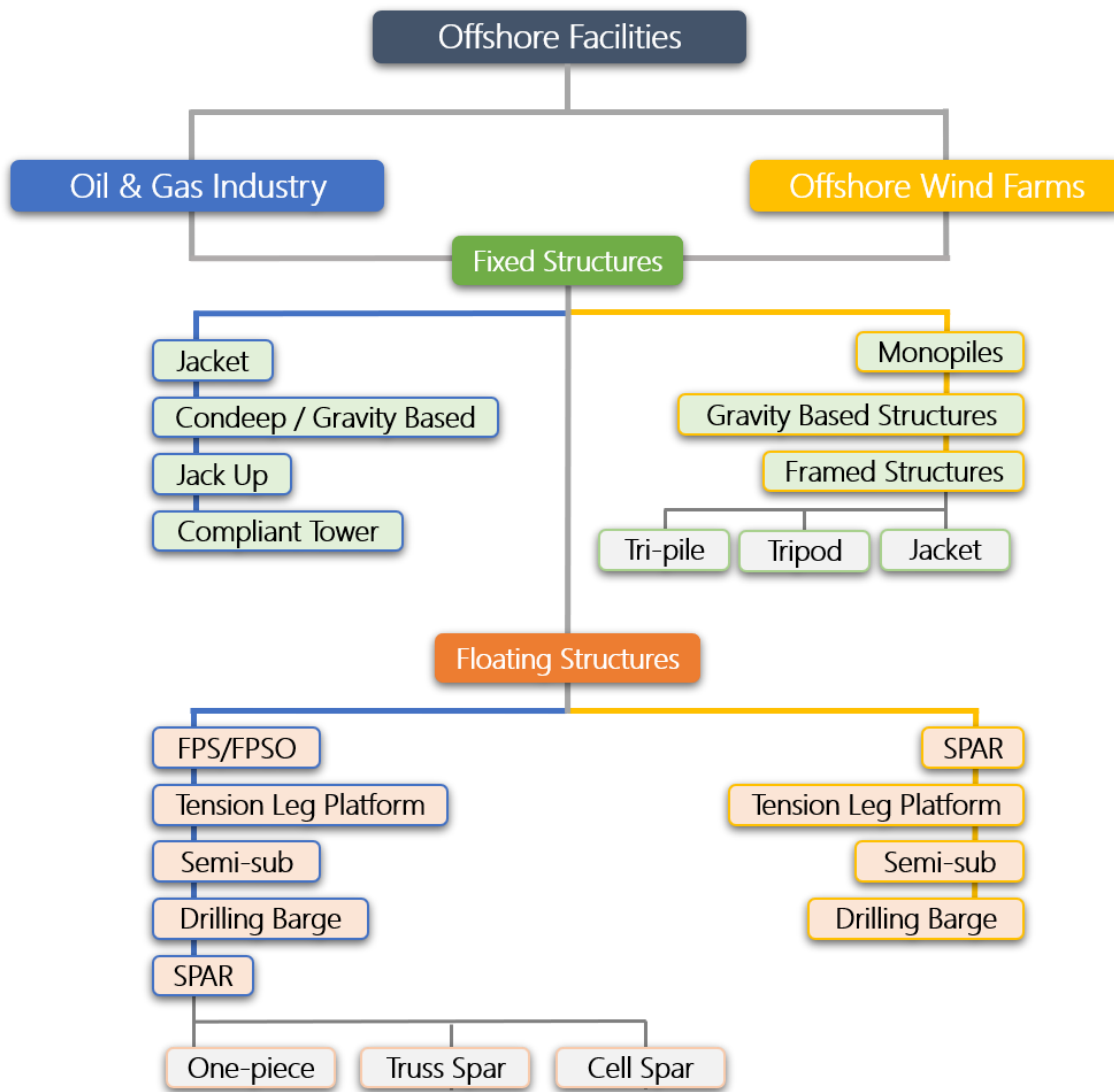


Figure 2-4. Offshore facilities for both Oil&Gas industry and the structures concerning offshore wind farms.

Briefly, marine foundations are necessary to transmit structural design loadings to the subsoil in fixed structures. The type of foundation element to be employed will depend on the nature of loading, the stiffness and strength of the surface sediments, and the depth of location<sup>12</sup>. They are characterized by being used at small depths, around 300 meters deep. The structures supported in the seabed, with the exception of those built-in concrete, are normally high strength steel tubular profiles that act as a framework that bear the weight of the entire structure and the forces due to wave action, ocean currents and wind.

As in the offshore oil industry, the first offshore wind farms were placed in shallow waters near the coast, for which they have been used fundamentally fixed structures. In this case, the different classes of foundations are generally classified by the maximum depth at which they can operate. At present, monopiles are by far the most widely adopted foundation system for modern offshore wind farms located in shallow water depths ( $\leq 40$  m), but mostly chosen for depths of less than 15 m.

### 2.2.2.1 *Similarities and differences between Oil&Gas and renewables structures*

As main assets in offshore energy production, there are fundamental differences between Oil&Gas platforms and wind turbines. Maybe the most noticeable difference is that turbines are unmanned structures with highly restricted access, while at any time you will find nearly 200 people living and working on a rig. Focusing on structure health monitoring, usually oil rigs have permanent corrosion protection and inspection tools installed, in addition to that the areas of deteriorated coating can be rapidly recognized and repaired. On the other hand, wind turbines' monitoring system is currently under development, and repairs and maintenance of deteriorated coating are not as feasible as in offshore rigs.

Regarding to mooring specification, design requirements are currently based on Oil&Gas mooring standards and practices. While there are similarities in some of their mooring processes and designs, when compared to oil and gas structures, many design and standards are unique to wind turbines<sup>13</sup>:

- Primary Goal – Offshore asset keeping without disturbing production or energy extraction.
- Mooring Equipment – Chain, wire, rope, anchoring, and associated components are required.
- Mooring Design Considerations – Installation requirements, weight of the asset, soil, meteorological and ocean conditions, dynamic analysis, mooring components' type and size are considered in a similar way.

Main differences between both energy source approaches can be summarized in the following list:

- Vessel Motions – Oil&Gas Industry Floating Production Units (FPUs) are single rigid body floating structures with motions better understood than the typical renewable's structure. These units may have several interacting moving parts that induce cyclic loads in different frequency ranges than those experienced by rigid floating bodies.
- Analysis – The mooring system for an Oil&Gas asset tends to minimize offsets. The opposite may be desirable for floating offshore wind turbines, as some required range of motion may be necessary for optimal power production.
- Environment – Harsh ocean conditions with strong wind, are a pre-requisite for floating OWSs to maximize energy production, whereas they are a term to avoid in Oil&Gas assets.
- Use of Synthetic Rope – While common in Oil&Gas, the use of polyester rope may be limited in the case of facilities in shallow water due to sunlight exposure or biological species growth, which affect severely to the rope performance.

### 2.2.2.2 *Floating Oil&Gas Platforms*

- Floating Production System (FPS) and Floating Production, Storage and Offloading System (FPSO)

A FPS is typically a large ship equipped with processing facilities and moored to a location for a long period (Figure 2-5). In use since the seventies, they are a more economical solution for bordering fields, as the vessel can be moved to another location and redeployed once the

original field has been depleted. Also, the FPSOs are an optimal choice for development when there are no existing pipelines or infrastructure to transfer production to shore<sup>14</sup>.



Figure 2-5. FPSO unit Pioneiro de Libra. Source: brazilenergyinsight.com

After processing, the system stores oil or gas before offloading periodically to shuttle tankers or transmitting processed product via pipelines. Commonly used in oil and gas processing at depths ranging from 180 to 1800 m, the vessel is moored in place by various mooring systems that allow the vessel to rotate freely to respond to weather conditions while keeping the riser tight in place (Figure 2-6).

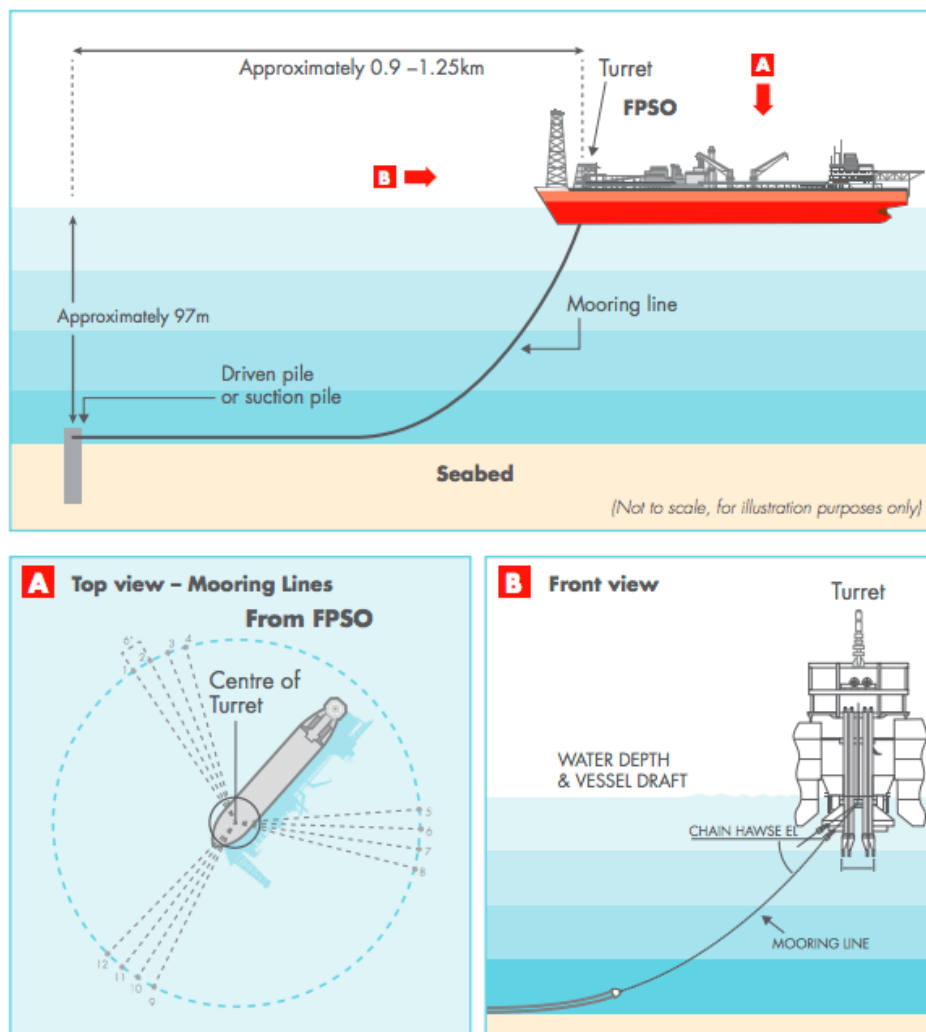


Figure 2-6. FPSO mooring system. Source: gcaptain.com

- SPAR Platform

The SPAR Platform (Single Point Anchor Reservoir) basically consists of a large-diameter single vertical cylinder supporting a deck where drilling, production and storage operations are supported (Figure 2-7).

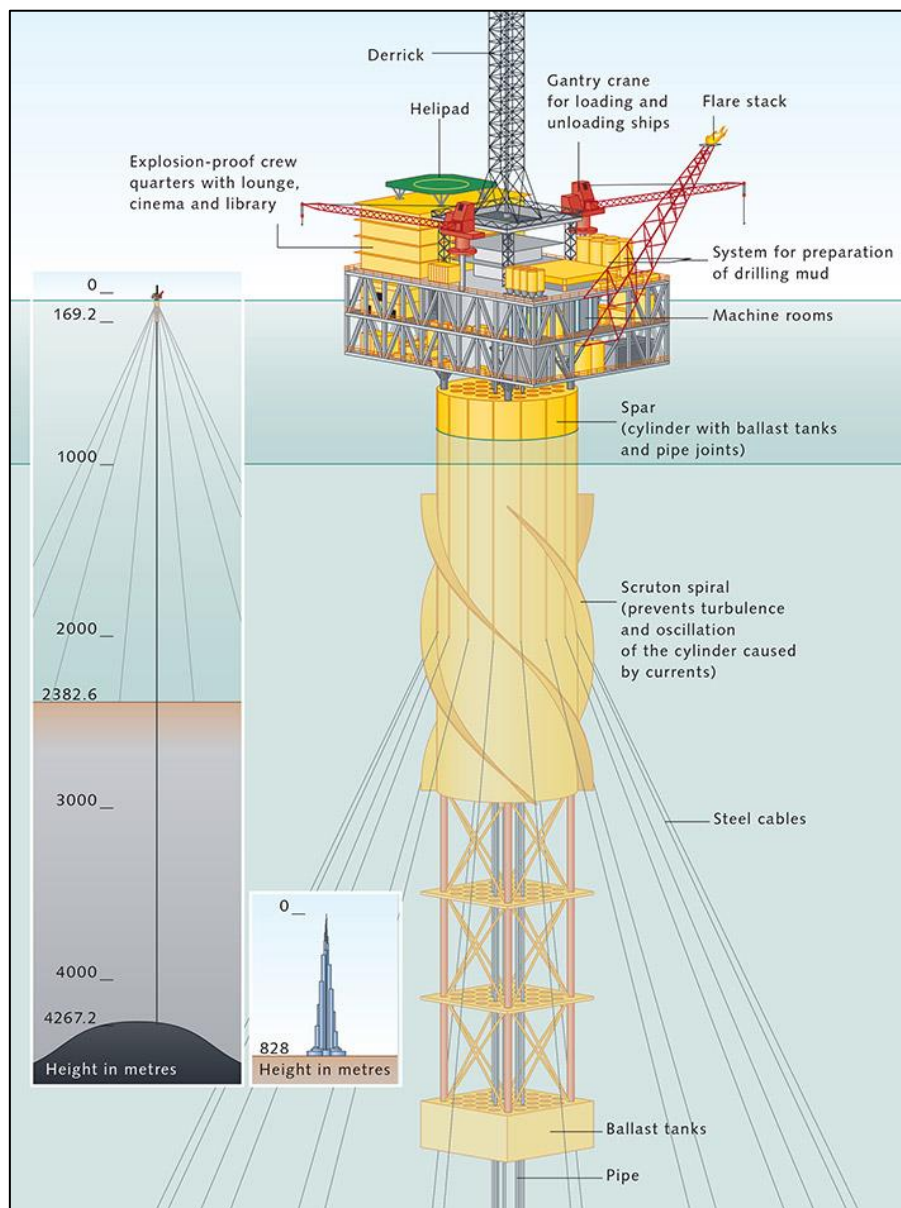


Figure 2-7. Example of a SPAR structure for offshore wind turbines. Source: worldoceanreview.com

Similar to an iceberg, the majority of a spar facility is located beneath the water surface, providing the facility an increased stability<sup>15</sup>. The structure floats so deep in water that the wave action at the surface is reduced by the counterbalance effect of the net buoyancy of the structure. Scruton spirals, attached helicoidally around the exterior of the cylinder, act to break the water flow against the structure (see Figure 2-7), further enhancing the stability<sup>15</sup>. Additionally, the bottom of the cylinder includes a ballasting section filled with heavy material, to ensure that the centre of gravity is located below the centre of buoyancy.

The whole SPAR facility is then moored to the seafloor with conventional systems of mooring lines, although the unique design of the spar ensures that the facility will not topple even if the moorings are not connected. It also has the ability, by adjusting the mooring

line tensions, lines), to move horizontally and to position itself over wells at some distance from the main platform location<sup>16</sup>.

SPAR platforms have been designed in three configurations (Figure 2-8): Conventional, Truss and Cell SPAR

**Conventional one-piece cylindrical hull.** Consists of a single cylindrical hull. The original design for spars was created in the mid '90s and firstly deployed in the Gulf of Mexico.

**Truss SPAR.** Differs in the midsection, which is composed of framework elements connecting the upper buoyant hull with the bottom permanent ballasts. Its design is advantageous because of the weight reduction from the original design, and as it requires less steel, fabrication and manufacturing costs drop down. Other of the main distinctions of the Truss SPAR type is that its centre of gravity is always lower than the centre of buoyancy, making it exceptionally stable<sup>12</sup>.

**Cell SPAR** is built from multiple vertical cylinders and divided into two basic sections. There is the hard tank section, which is made up of seven pressure vessels. Four cylindrical lengths stretch from the top of the hull and by regulating the pressure of air trapped inside these tubes, the operator can reduce or increase the hull's buoyancy. Cell Spar is then moored to the seabed with conventional mooring lines, made from cables with fixed lengths and single point mooring configuration.

Despite the exceptional performance and stability of the cell SPAR, mooring systems are used to connect the platforms to the seabed to maintain spar platforms in position at the production site. Any movement of the spar in environmental loads causes the mooring lines to increase in tension and produce a restoring force acting in the opposite direction. However, spar platforms use a variation of the catenary mooring system, designed to be lighter and cheaper than the conventional catenary systems<sup>17</sup>.

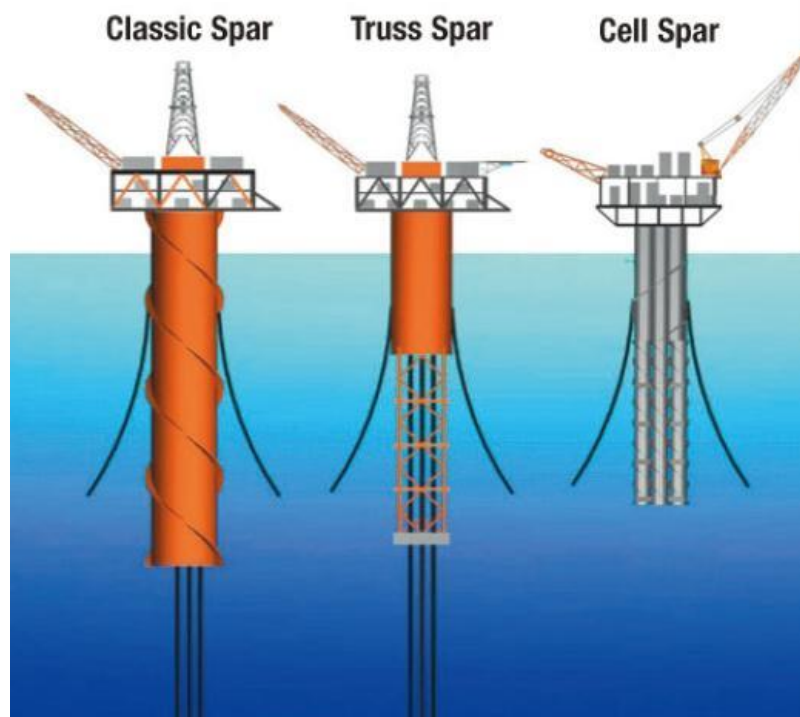


Figure 2-8. Graphically illustrated configurations for SPAR type structures. Source: xcjxjg.com



- Tension Leg Platform (TLP) and Mini-TLP (Sea Star)

A TLP refers to a platform that is held in place by vertical, tensioned tendons connected to the sea floor by pile-secured templates, tethered to the seabed in a manner that eliminates most vertical movement of the structure, but allows for horizontal movements. Plus, the platform is buoyant and held in place by a mooring system<sup>14</sup>. These structures have many operational advantages of the fixed platform while reducing the cost of production in water depths up to about 1500 m. Its production and maintenance operations are the same as in fixed platforms, but have limitations in accommodating heavy payloads<sup>18</sup>.

The typical TLP is a four-vessel design forming a square, which is supported and connected by pontoons. The hull supports the topside of the platform, and an intricate mooring system keeps the platform in place (Figure 2-9). The buoyancy of the hull of the platform offsets the weight of the platform, requiring tendons or tension legs, to secure the structure to the foundation on the seabed. Foundations secure the TLP to the seafloor by use of buried piles, which can be concrete or steel. Tendons are attached to the foundation and the platform is attached to the tendons<sup>19</sup>.

Apart from the classical TLP hull profile, several variations have been introduced. Conventional TLP has the characteristic four columns and a ring-shaped pontoon. An extended variant of this configuration is the SeaStar® TLP (Figure 2-10). It has a central column with three pontoons extending from the base column to the tendons attached at the extremities<sup>20</sup>. The platform stability against overturning is provided by tendons which run vertically from the extremities of each pontoon to piles driven in the seabed<sup>21</sup>. This enables to the tension-leg mooring system to suppress nearly all vertical motion.

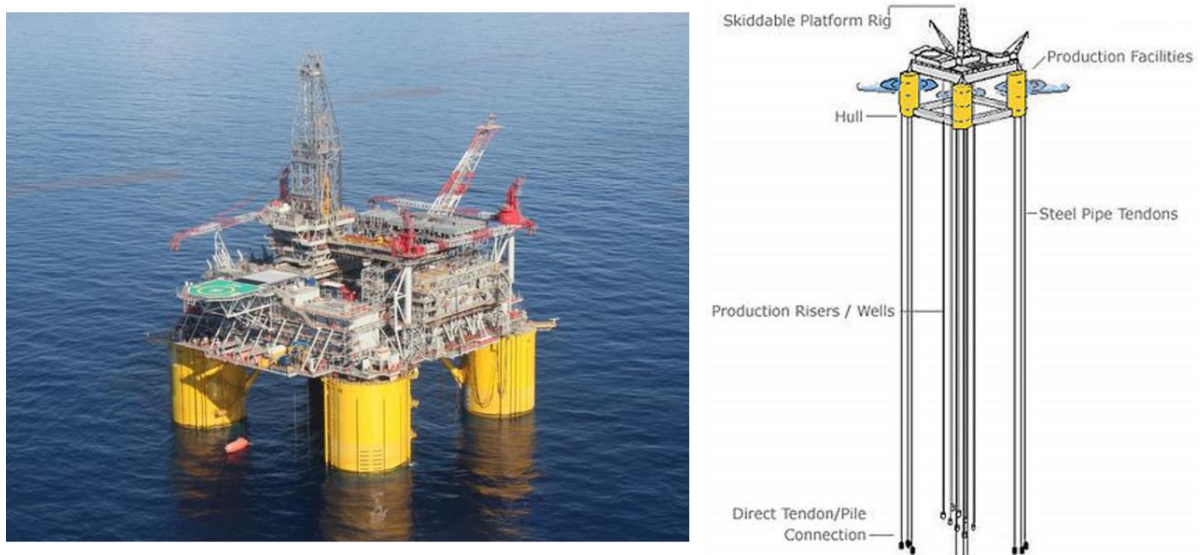


Figure 2-9. Shell Olympus TLP profile for O&G platforms. Source: bizjournals.com and offshore-technology.com

The SeaStar TLP family has been developed to unlock the economic potential of discovered, but as yet undeveloped, deepwater fields. Existing deepwater technology is available for fields with large reserves and many wells, but not for smaller fields with fewer completion targets, where the SeaStar's relatively small size and low cost are important advantages<sup>22</sup>.



Figure 2-10. Chevron USA Typhoon SeaStar-profile TLP for offshore Oil&Gas production. Source: Matten (2002)<sup>21</sup>

- Semi-submergible units

The semi-submersible rig is a floating platform that is supported primarily on large pontoon-like structures submerged below the sea surface, while operating decks are elevated 30 or more meters above the pontoons on large steel columns (Figure 2-11). Semi-submersible platforms offer a number of benefits, including large capacity, limited sensitivity to water depth and the ability to relocate the platform after field depletion<sup>14</sup>. It is also considered as the most stable of any floating rig, many times chosen for harsh conditions because of their ability to withstand rough waters. The rig offers exceptional stability for drilling operations, and rolling and pitching from waves and wind is greatly reduced<sup>23</sup>.



Figure 2-11. ExxonMobil Stena Don semi-submergible unit for offshore Oil&Gas extraction. Source: offshoreenergytoday.com

Most employed semi-subs design is the column-stabilized unit, as seen in Figure 2-11. Two horizontal columnar hulls are only submerged a few metres below the water line and are connected via cylindrical or rectangular columns to the drilling deck above the water<sup>24</sup>. Then the structure is moored to the seabed with mooring lines. Submerging this type of structure is achieved by partially filling the horizontal hulls with water until the rig has



submerged to the desired depth. Mooring lines anchor the rig above the well, and dynamic positioning can help to keep the semi-subergible on location, as well<sup>23</sup>.

- Drilling Barge and Drillships

A drilling barge is a large, floating platform, which must be towed by tugboat from location to location and are used mostly for shallow water drilling as canals, rivers and lakes (Figure 2-12)<sup>14</sup>.

Drillships are marine ships fitted with drilling equipment and a dynamic positioning system, which maintains their positions over oil well. They are primarily used for exploratory drilling and can operate in water depths up to 3.700 m. Because the drillship is also a vessel, it can be easily relocated to any desired location but due to the mobility, drillships are not as stable compared with semi-submersible platforms or other mentioned floating facilities. To maintain its position, drillships are highly dependent on their mooring system.



Figure 2-12. Drilling barge for shallow waters (left) and West Gemini Drillingship (right), for offshore locations. Source: media.subsea.org and maritime-connector.com

### 2.2.2.3 Floating Offshore Wind Structures

The floating technologies applied to the OWSs comes from the Oil&Gas industry and can be summarized in three main groups: SPAR (Spar-buoy), Tension Leg Platforms (TLP) and Semi-submersibles (semisubs and barges). The engineering behind these structures is remarkably similar to that of the Oil&Gas, but with certain peculiarities that it is important to highlight. Figure 2-13 shows a brief illustration of the differences between the three mentioned floating units.

- SPAR (Spar-buoy)

SPAR structure consists in a very large cylindrical buoy (usually between 70 and 120 m long) that stabilises the wind turbine using ballast<sup>25</sup>. The centre of gravity is much lower in the water than the centre of buoyancy. Whereas the lower parts of the structure are heavy, the upper parts are usually empty elements near the surface, raising the centre of buoyancy. Some loose mooring lines, usually three, keep the system on a given spot with some drift displacement freedom, although the catenary can tilt as a result of the wind and wave action<sup>26</sup>. Additionally, motion stabilizers can be used to reduce the overall tilt of the system. While these are simple structures having a low capex cost, it needs a deeper draft, i.e., deeper water and is not feasible in shallow waters<sup>27</sup>.

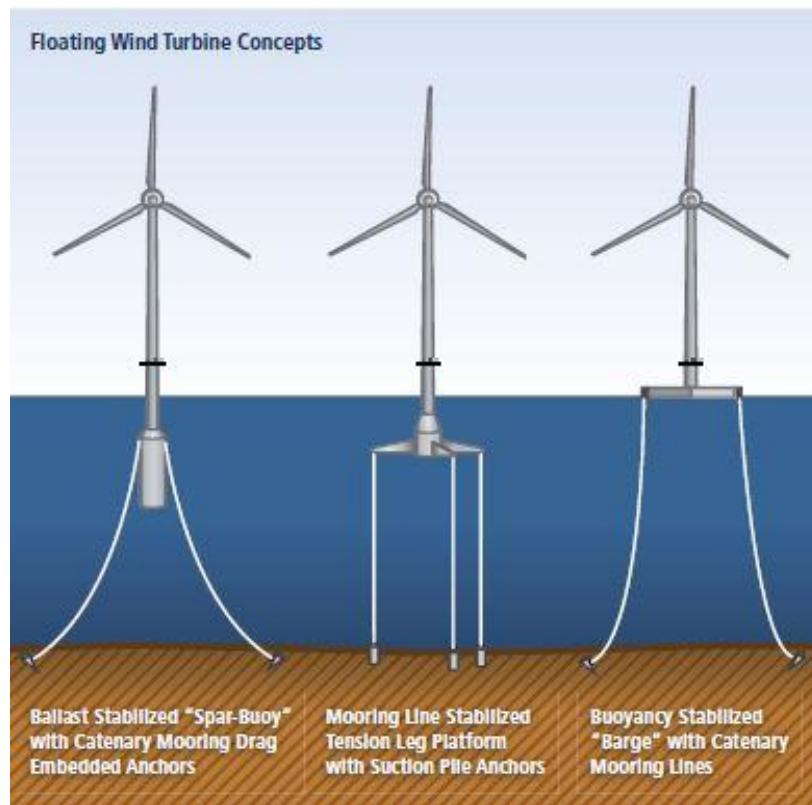


Figure 2-13. Floating wind turbines for offshore installation. Spar (left), TLP (centre) and Barge (right). Source: Edenhofer (2012)<sup>28</sup>

- Tension Leg Platform (TLP)

The TLP is connected to the seafloor by tensioned mooring lines, which are kept at a high enough tension following their connection to the wind turbine floater so that the system cannot tilt or rotate as a result of the effect of the wind and the waves<sup>29</sup>. In general, a TLP system could potentially be one of the most suitable platforms for offshore wind turbines, as the displacements can be the smallest, if compared to the other floating support structures. The major drawback is the high cost of the mooring system<sup>25</sup>, as it normally need between three to five tension lines to hold the wind turbine base submerged.

- Semi-sub:

This concept is a combination of ballasting and tensioning principle and consumes the largest amount of steel of the three options presented<sup>27</sup>. It is a three-legged, semi-submersible type, floating platform. This configuration is also called a 'Trifloater'. In this case, the static stability is achieved mainly through the three relatively large cylindrical columns of more than 10 m of diameter<sup>25</sup>. This allows the structure to have a relatively shallow draft, and, therefore, the possibility to be deployed in relatively shallow waters.

- Floating barge:

The barge-type floating wind turbine has a very large pontoon structure, and it achieves stability via distributed buoyancy and by taking advantage of the weighted water plane area. Usually concrete-filled and square shaped, the barge is considered to be ballasted with sea water to achieve reasonable draft and to avoid wave slamming<sup>30</sup>. The mooring for this type of wind turbine is done by conventional catenary anchor chains.

## 2.3 Mooring Lines

The mooring system performs the function of station-keeping and is particularly vital to the safe operation of offshore floating facilities, but also an important security device in fixed offshore units. Among other issues, mooring types, integrity management, failure modes and economic perspectives are going to be discussed in detail below.

### 2.3.1 Introduction to Mooring Line Systems

The primary purpose of a mooring system is to maintain a floating structure in place within a specified tolerance, typically based on an offset limit determined from the configuration of the risers in the case of Oil&Gas platforms. The mooring system provides a restoring force that acts against the environmental forces (wind, waves, and currents), which push the unit off station. The connection between the mooring system and the body of the vessel is where the restoring force of the mooring system acts (Figure 2-14).

When there is no external loading on the system the vessel will not move from its static equilibrium position, but when it does occur an imbalance in the system is generated. For going back to equilibrium, the mooring system restoring force must become equal to that of the environmental load. This is achieved through the vessel offsetting from its original position. As this occurs, the 'windward' lines will pick up tension and the 'leeward' lines will shed tension<sup>31</sup>, as seen in Figure 2-14.

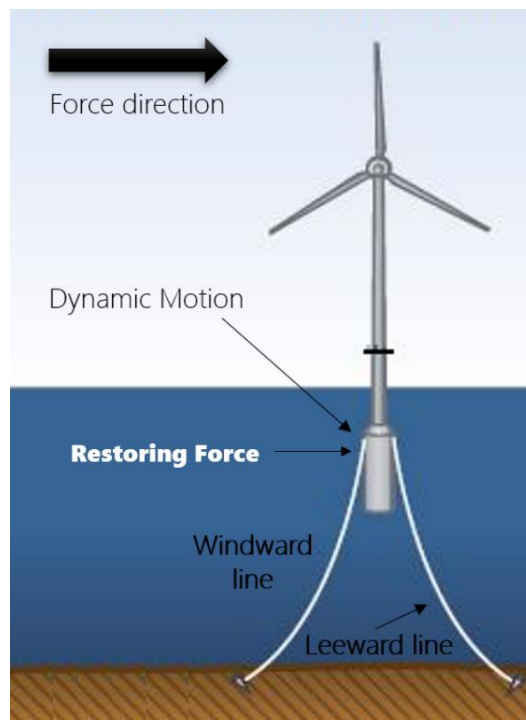


Figure 2-14. Windward and Leeward lines example in a Spar buoy wind turbine.

### 2.3.2 Types of mooring systems

There are many types of mooring systems to meet the performance requirements under various conditions, such as water depth, environment severity, type and duration of operation, type of the floating structure, etc. But in general, offshore mooring systems are classified as

either single-point moorings or multiple-point moorings (spread moorings). The key factors of these two types are going to be discussed hereinafter.

- **Single-Point Mooring**

Single point moorings are used primarily for ship-shaped vessels, as FPS and FPSO units. They allow the vessel to weathervane, necessary to minimize environmental loads. There is a wide variety in the design of SPMs, but they all perform essentially the same function. The most used are turret mooring and CALM buoys.

In **Turret mooring**, catenary mooring lines are attached to a turret, which is essentially part of the structure to be moored. The turret includes bearings to allow the structure to rotate independently of the mooring system<sup>32</sup>. The turret can be mounted externally from the structure's bow with appropriate reinforcements or internally, leaving it submerged (Figure 2-15).

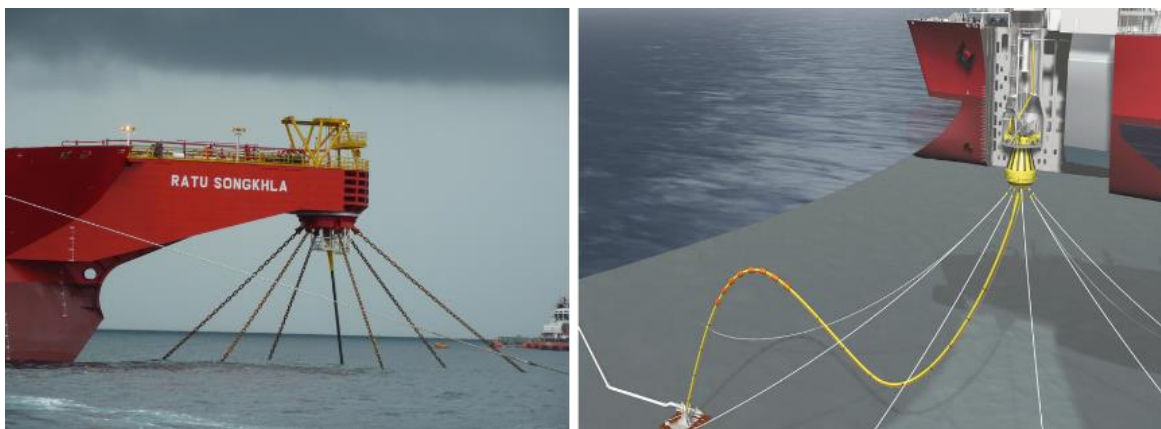


Figure 2-15. Turret type mooring in M3NERGY FSO unit exposed (left) and the same mooring system from a submerged point of view (right). Source: 2b1stconsulting.com and nov.com

**CALM Buoy** responds to the acronym for Catenary Anchor Leg Mooring. The CALM system consists of a large buoy, which supports a number of catenary legs anchored to the sea floor. An elastic mooring hawser is able to freely rotate so that the vessel can be positioned to offer the least resistance possible at all times (Figure 2-16). Only used in Oil&Gas facilities, riser systems or flow lines that emerge from the sea floor are attached to the underside of the CALM buoy. Then, fluid product is exchanged via the CALM to or from the tanker by the subsea pipe and hose systems<sup>33</sup>.

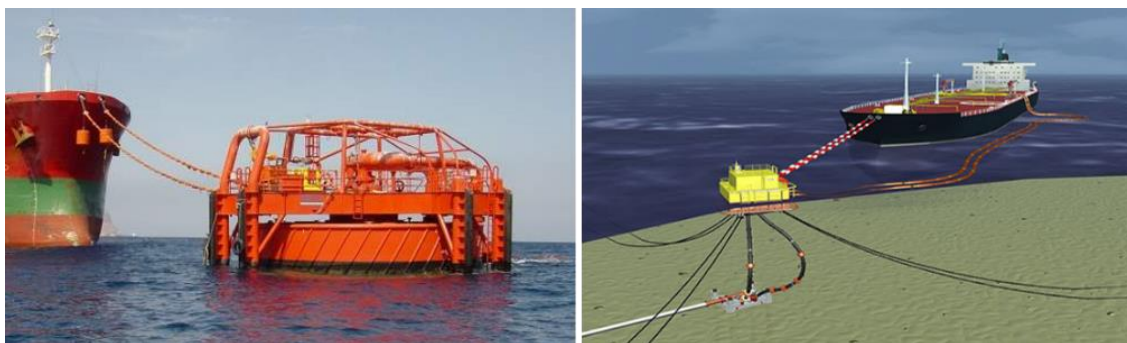


Figure 2-16. CALM Buoy type mooring exposed (left) and from a submerged point of view (right). Source: offshore-technology.com

- Spread Mooring

This type of mooring can be used indifferently in both OWS and Oil&Gas units, unlike the single-point mooring that is more exclusive of the latter one. Spread mooring systems are multi-point mooring systems that moor units to the seabed using multiple mooring lines<sup>34</sup>.

The mooring lines can be directly attached to the units as well as indirectly using buoys on the sea surface (Figure 2-17). When they are directly attached to the structure, strong points must be provided for the mooring lines. Spread mooring systems with buoys are called **Conventional Buoy Mooring (CBM)** systems.

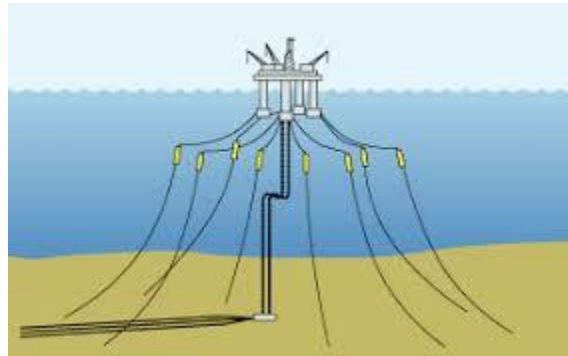


Figure 2-17. Spread mooring example in an offshore semi-submersible structure. Source: offshore-mag.com

Normally, spread mooring utilizes four groupings of anchor legs arranged in a symmetrical pattern maintaining the structure on location with a fixed course (Figure 2-17). Spread moorings can be used in applications requiring long service life, in any water depth, and on any size of floating structure. However, they are not so effective in harsh environments where changing wind, waves and currents may impose severe and multi-directional loads on the mooring system<sup>35</sup>.

### 2.3.3 Mooring System configurations

Regardless of the employed mooring system, there are two configurations with different mechanisms and scopes to withstand the applied forces. The two main types are called **catenary** and **taut-leg**. The main difference between these configurations are that where in a catenary system mooring lines arrives at the seabed horizontally, in the taut mooring arrives at an angle (Figure 2-18).

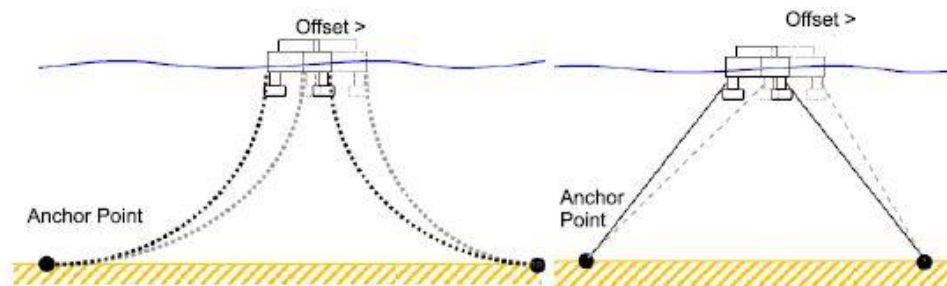


Figure 2-18. Catenary system (left) and taut-leg configuration (right). Source: Flory (2016)<sup>36</sup>

A **catenary** configuration generates restoring force by lifting and lowering the line onto the seabed, plus some amount of line stretch. Thus, the anchor point is only subjected to horizontal forces at the seabed, and the restoring force in catenary mooring is generated



by the weight of the components. This requires that the mooring lines be relatively long compared to the water depth, and as soon as it increases, the weight and the length of the mooring line start to increase rapidly.

On the other hand, **taut-leg configuration** suffers of both horizontal and vertical forces. The system uses the mechanical properties of the mooring line, especially elasticity, as the restoring forces are created through axial elastic stretching of the mooring line. Despite taut-legs are the best load sharing between adjacent mooring lines, which reduces fatigue, the mooring line must have sufficient elasticity to absorb the vessel wave motions without overloading.

Some researchers highlight some potential benefits of a taut system<sup>37</sup>, such as the potential for load reduction, smaller motion and smaller mooring footprint. But there are authors who claim that the best solution is a hybrid combination of both<sup>38</sup>, as **semi-taut** or **multicatenary** (Figure 2-19).

The **semi-taut system** is a combination of the taut mooring system and catenary mooring system, wherein some parts of the mooring system are taut and other parts are catenary<sup>38</sup>. The semi-taut system and taut system have shorter mooring lines and require less seafloor space or seafloor spread than the catenary system. The shorter mooring lines result in lighter designs and thus, in material saving<sup>39</sup>. To sum up, both semi-taut and taut systems are more recommended for deepwater application than catenary configuration.

**Multicatenary** mooring lines comprises various line types (as it will be discussed later) and include intermediate buoys to limit the vertical load on the structure. Lines can arrive at various angles to the seabed, to create a horizontal restoring force that come from the weights of line, as in catenary<sup>40</sup>.

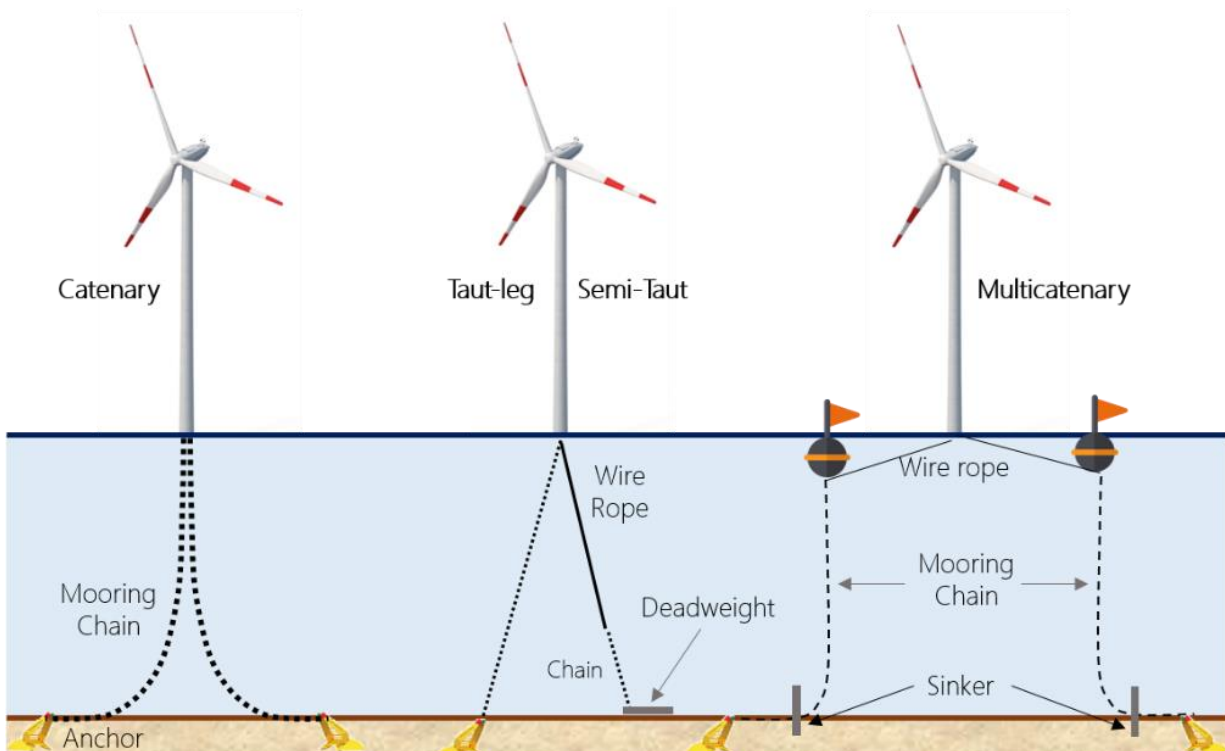


Figure 2-19. Different Mooring system methods for a single SPAR-buoy OWS.

Once determined the mooring line configuration, the next section will discuss the different materials available and their suitability according to the service to be performed.

### 2.3.4 Mooring line components

Mooring lines for floating structures may be made up of chain, wire rope, fibre rope, or multiple combination of these. There should be also considered the size of the sinkers and/or required buoys used to achieve the required mooring performance. Properties are given hereinafter, however, a good mooring system may use a hybrid mixture of the three types. For example, an idealized deepwater catenary line may consist of<sup>40</sup>:

- A **chain section** on the seabed floor providing deadweight, friction, and high abrasion resistance.
- A **synthetic section** starting just clear of the seabed floor providing reduction of weight and providing elasticity.
- A **steel wire rope** section starting just above the sea surface and providing high abrasion resistance.

**Chain:** There are two different branches of chains (Figure 2-20): Stud (or Stud-link) and studless. Stud chain is commonly used in anchoring systems where the mooring lines are often replaced, as in drilling units. On the other hand, studless chains are used for permanent moorings, as in floating units<sup>41</sup>.

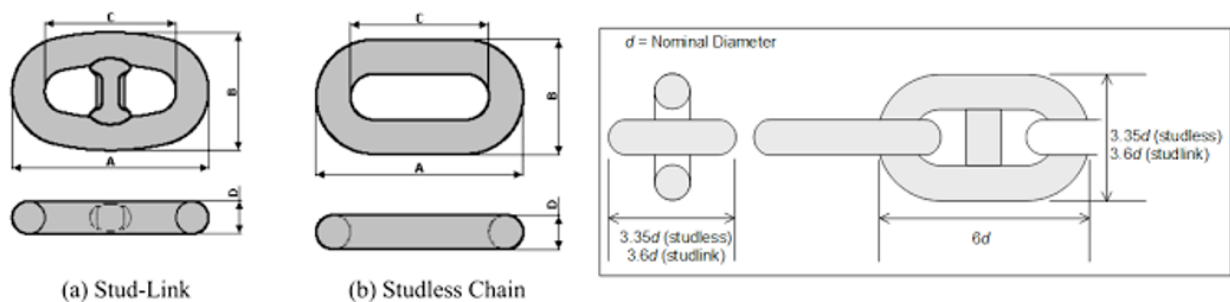


Figure 2-20. Geometrical differences between Stud and Studless chain (left) and differences in the nominal diameter (right). Source: orcina.com

A research<sup>42</sup> in long-term applications of chains in the moorings of floating systems conclude that the main difference between both types is the fatigue resistance, a crucial parameter as far as moorings are concerned. Maintenance, inspection costs and weight can be reduced with studless chain. However, the fatigue life can be as low as half compared to a studded chain. In general, stud-links are preferable in terms of ease handling and are considered to have a higher reliability than studless chains.

Table 2-3 summarises the suitability of studless and studded chain in terms of design, manufacturing, inspection and maintenance<sup>31</sup>. According to manufacturers, concerns over studlink chain have led many customers to opt for studless due to troubles with loose studs. This could generate tension in the weld area of the link, with a consequent reduction in the chains fatigue life, plus difficult and expensive repairs in service. To solve this trouble, link suppliers changed the manufacture process to ensure safer and more reliable studs, developing a dual solution involving the use of asymmetric studs fixed in place by a process of controlled stud expansion<sup>43</sup>.

Table 2-3. Suitability of stud-link of studless chains depending on the chosen requirements and criteria. Source: Research report 444<sup>31</sup>.

| Requirement                                      | Recommended Chain | Criteria  |
|--|-------------------|---|
| Lower weight in the whole catenary               | Studless          | Low weight per meter of mooring line                      |
| Versatility                                      | Studless          | Complete open link, with more interior link space         |
| Greater safety factor (strength to weight ratio) | Studless          | Larger possible diameter with less weight per meter       |
| Greater stiffness (rigidity) in the mooring line | Stud-link         | Higher elasticity modulus (Young's Modulus, E)            |
| Break load                                       | Both              | Same break load, but different proof loads                |
| Fatigue life                                     | Stud-link         | Researched conclusions <sup>42</sup>                      |
| General inspection of wear, corrosion, and welds | Studless          | Greater visual access due to lack of stud                 |
| Reduce repair costs                              | Studless          | No loose studs to repair                                  |
| Link oversize in the weld zone                   | Studless          | Removal of the material excess in the weld zone           |
| Reliability of chain                             | Stud-link         | Despite other requirements, fatigue performance is better |
| Handling and connectivity with other components  | Studless          | Better access through the pin. Minimal requirements.      |

Even though stud-link chain type is only recommended fewer times in the summary Table 2-3, those parameters in which is highlighted turn out to be crucial. According to Rämnas manufacturer, stud-link chain are more expensive, but is worthwhile investment to achieve longer life<sup>44</sup>. It is pointed out that studlink chain has numerous other advantages over studless, including:

- Higher proof load
- Increased fatigue life
- Reduced risk of stress corrosion in the weld
- Improved utilization of the base material ductility
- Increased peak loads without any deformation
- Easy installation, with no kinks or knots

The materials and grades to be used in this type of components will be discussed in the following section.

**Synthetic rope:** Fibre ropes are commonly used as segments in catenary or taut leg systems. It has great mechanical properties as high strength and high elastic modulus, it also offers certain advantages for offshore, as weight reduction, nonlinear stiffness, and minimum tension requirements<sup>31</sup>.

The fibres considered up to now for use in permanent or temporary deepwater moorings are grouped in two categories: fibres produced by melt spinning such as polyamides, polypropylenes, polyesters; and high-performance fibres produced by other techniques including aramid and high modulus polyethylene (HMPE).

Synthetic ropes do not suffer from corrosion problems and possess greater tension fatigue, out-of-plane loading and torsion performance than steel components. Additionally, Banfield et al<sup>45</sup>. tested experimentally that polyester ropes can have a fatigue life which is 50 times greater than steel wire rope. Nylon and polyester are the most commonly used materials for



mooring applications which require moderately high strength and ductility (Figure 2-21). Polyolefin ropes (polyethylene and polypropylene) are also used as mooring line components, and in fact possess similar stiffness characteristics to nylon and polyester, but have poor cyclic loading performance and are susceptible to ultraviolet (UV) light degradation<sup>46</sup>.

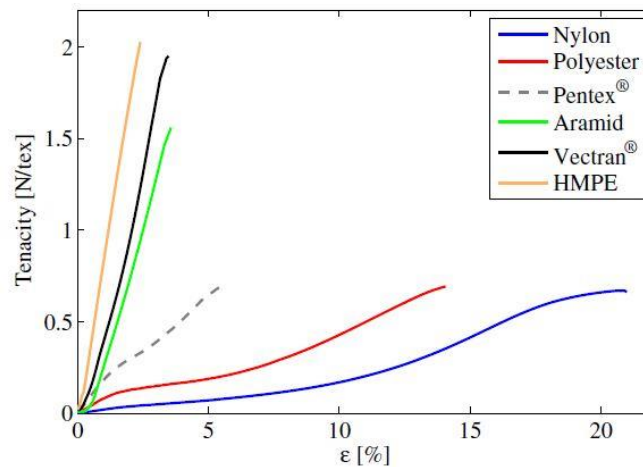


Figure 2-21. Comparison of the stress-strain behaviour of various fibers. Source: Weller (2005)<sup>46</sup>.

The behaviour of above-mentioned materials according to different parameters is listed in Table 2-4.

Table 2-4. Durability of fibre rope materials for mooring systems. Source: Weller (2005)<sup>46</sup>.

| Parameter       | Polyester | Nylon   | Aramid  | HMPE    |
|-----------------|-----------|---------|---------|---------|
| UV Light        | Good      | Good    | Average | Average |
| Temperature     | Good      | Good    | Average | Poor    |
| Abrasion        | Good      | Average | Average | Good    |
| Creep           | Good      | Average | Good    | Poor    |
| Tension fatigue | Good      | Good    | Good    | Good    |

Is worth to mention that hybrid materials have been also developed in the pursue of an excellence performance. As an example, the Lankhorst manufacturer’s synthetic fibre<sup>47</sup>, whose high modulus polyethylene core provides the strength and mechanical performance and the entire rope core is protected by a braided jacket and polyurethane coating to boost overall performance.

**Steel Wire Rope:** Steel wire rope has been used for mooring floating offshore production systems as they are very well understood and durable, but they exhibit limitations in their application to very deep water<sup>48</sup>. In the majority of systems, unless fully embedded in plastic, the life of the steel rope is less than that of the installation unit, so remaining lifetime predictions and replacement must be considered in this type of components. Wire rope moorings are normally installed in a multicatenary configuration. There are two main wire rope constructions used for offshore mooring purposes: spiral strand and stranded rope (Figure 2-22).

- The **spiral strand** is attractive for use with permanent moorings, since they do not generate significant torque with tension changes. It is made of layers of wires wounded in opposing directions to obtain spin resistance characteristics<sup>34</sup>.

- The **stranded rope** is made of several strands wound in the same rotational direction around a central core, generating a torque as it is braided. Core design and lay of strands are function of the required strength and bending fatigue parameters.

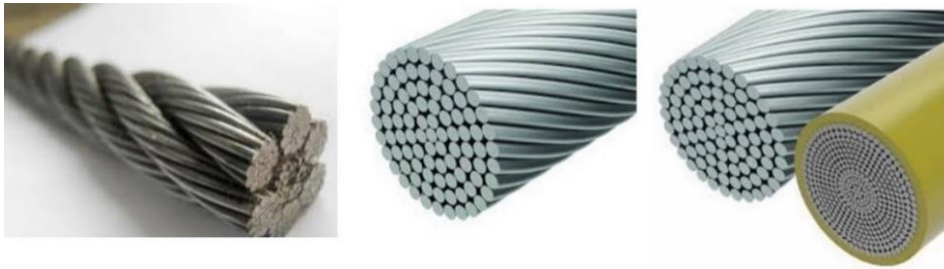


Figure 2-22. Six strand rope (left), conventional spiral strand (centre), encapsulated spiral strand (right). Source: wirerope-sling.com, redaelli.com, archiexpo.com

It is also included in Figure 2-22 an encapsulated spiral strand, which prevents from corrosion this type of wire ropes. For design lives of 20 years and above, spiral strand products are normally supplied with a polyethylene sheathed coating. The physical shield provided by the sheathing is essential to maintain the extended lifetime, as it provides the barrier against water ingress and subsequent corrosion. This solution also has been questioned, as a little break in the shelter could facilitate water ingress into the spiral, causing much more damage by localized corrosion. Typical service life expectancy of ropes is shown in Table 2-5

Table 2-5. Recommended rope in function of design life expectancy. Source: Adapted from RR 444<sup>31</sup> and Sefton<sup>49</sup>.

| Design Life    | Recommended Product                 |
|----------------|-------------------------------------|
| Up to 6 years  | Six Strand rope                     |
| Up to 8 years  | Six Strand rope (with anodes)       |
| Up to 10 years | Six Strand rope (galvanized)        |
| > 10 years     | Spiral Strand                       |
| > 15 years     | Spiral Strand (galvanized)          |
| > 20 years     | Spiral Strand (polyethylene jacket) |

A summary of features and main issues in mooring line components are gathered in Table 2-6.

Table 2-6. Summary of mooring line components

| Component    | Features  | Issues   |
|--------------|---|--|
| Chain        | Broad user experience<br>Good abrasion resistance<br>Long fatigue life          | Wear and corrosion susceptibility<br>Unsuitable for depths greater than 1000 m |
| Steel Rope   | Broad user experience   | Limited-service life   |
| Polyester    | High dry and wet strength<br>Lightweight<br>Most durable of all fibre materials | Moderate cost  |
| Nylon        | High stretch  | Low fatigue life<br>Moderate cost<br>Wet strength about 80% of dry strength    |
| Polyethylene | Lightweight<br>Moderate stretch<br>Low cost                                     | Low strength<br>Susceptible to creep   |
| HMPE         | High strength to weight ratio   | High cost  |

Once the components are chosen, mooring line setup must be decided in order to perform as expected in a given location. The most common setups as function of the mooring system configuration, are as follows:

1. Catenary system with an **all-chain** setup (best for very shallow waters).
2. Catenary system with a **chain-wire-chain** setup.
3. Taut (or semitaut) leg system with a **chain-wire-chain** setup.
4. Taut (or semitaut) leg system with a **chain-polyester rope-chain** setup (best for ultradeep waters).

Going a little deeper into the topic, it seems clear that the selection of a technically feasible mooring system type depends on water depth. Below is given a guide about which system to use depending on the situation (Table 2-7)<sup>50</sup>:

Table 2-7. Mooring line configuration most suitable choice depending on the installation depth.

| Depth                   | Suitable mooring setup   |
|-------------------------|--|
| Less than 500 m         | Catenary system. Both all-chain and chain-wire-chain setups, depending on the environment                            |
| Between 500 and 1000 m  | Every choice may be considered   |
| Between 1000 and 2000 m | Taut legs are the most suitable, with chain-wire chain setup feasible since we are not at significant maximum depths |
| Greater than 2000 m     | Taut leg system with polyester rope is likely the most cost-effective choice   |

### 2.3.5 Composition of Mooring Chains

Offshore mooring components are usually subjected to rigorous standards and end-user requirements that, among other conditions, establish mechanical properties such as tensile strength and toughness. This section will only focus on steel components in mooring systems with attention to chain material.

In general, chain and various connecting components such as shackles are made from low alloy steel, components that normally are not protected against corrosion through coating or anodes. Minimum values for strength and impact energy are defined for the existing different chain grades in Table 2-8. These grades are established based on the Oil Rig Quality (ORQ), dating from the beginning of the 1970s with 641 MPa issued by API.

Table 2-8. Summary of offshore grade steels with UTS values in MPa and Brinell Hardness. Source: Vicinay.

| Chain Grade | UTS Ultimate Tensile Strength (MPa) | Surface Hardness (Brinell HB) |
|-------------|-------------------------------------|-------------------------------|
| ORQ         | 641                                 | -                             |
| R3          | 690 (ORQ + 10%)                     | 235-260                       |
| R3S         | 770 (ORQ + 20%)                     | 250-275                       |
| R4          | 860 (ORQ + 35%)                     | 275-305                       |
| R4S         | 950 (R4 + 10%)                      | 305-325                       |
| R5          | 1000                                | > 325                         |
| R5S         | 1100 (R5 + 10%)                     | 350                           |
| R6          | 1200 (R5 + 20%)                     | > 350                         |

According to DNVGL-OS-E302 standard<sup>51</sup>, which rules the technical requirements, principles and acceptance criteria related to classification of offshore units, there are some further requirements involving chain composition. The steel used in mooring system components fall under the definition of Low Alloy Steels that would broadly be defined as steel containing 1 – 5% of deliberately added alloying elements by weight.

Employed steel shall be killed (completely deoxidized by the addition of an agent before casting) and fine grain treated. The austenite grain size shall be 6 or finer in accordance with another standard in which we will not go deeper, ASTM E112.

Regarding chemical composition, the only main requirement is that Mo content should be greater than 0.20%wt for grades R4 and higher, and that there are certain minimum requirements for alloying elements that contribute to grain size control (Al, Nb, V or Ti). Apart from this the chemical composition shall be agreed between the manufacturer and the purchaser. As R5S and R6S are still under validation and development process, there are not considered as options in Classification Rules<sup>52</sup>.

Finally, it is important to mention the requirements derived from heat treatment. More demanding grades (higher grades) shall be supplied in the quenched and tempered condition and cooling after tempering shall be in water.

### 2.3.6 Anchoring

The final component of a mooring line is the anchor and the anchoring process. Nowadays, different types of anchors are presented in the offshore industry, but the most common ones are deadweight anchor, drag embedment anchor, anchor piles and vertical load anchor. Among others, the most typical mooring points are depicted in Figure 2-23.

**Deadweight anchor (1, 2):** Is the simplest anchor. It consists of a heavy object placed on the seafloor to resist vertical and/or horizontal loads, where the anchoring capacity comes from the weight itself and from the friction with the seabed.

**Drag embedment anchor (3):** Designed to penetrate in the seabed, the holding capacity is mainly generated by the resistance and friction with the soil. It has an excellent performance resisting horizontal loads, but it lacks in large vertical loads.

**Anchor pile (4, 5):** Consist in a cylindrical pile made of steel. Is commonly used for taut mooring systems and TLP since they can hold omnidirectional loads.

**Vertical load anchor (6):** Installed in a similar way than drag embedment anchors, it penetrates into the seabed with a horizontal load. They are designed to fulfil drag embedment anchors lack of vertical load resistance, as their disposition enables them to hold vertical and horizontal loads.

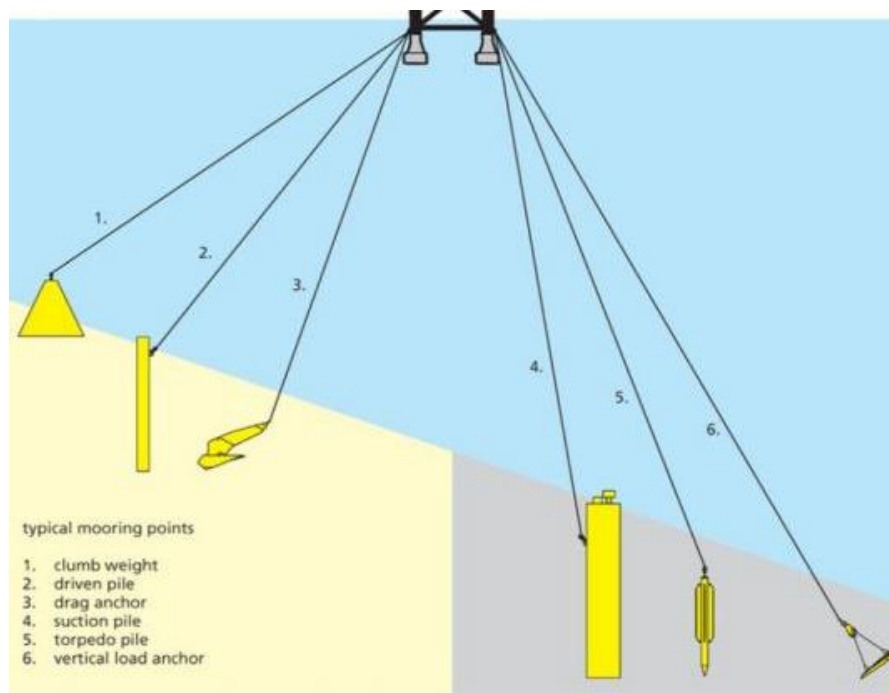


Figure 2-23. Typical mooring points for offshore assets. Source: Vryhof.

During the selection of anchor options and dimensions, required system performance and soil type and condition are considered key parameters. Table 2-9 summarises the main characteristics of the different anchor types presented as function of the soil and the bearing load.

Table 2-9. Main characteristics of the different anchor types. Source: Toledo (2017)<sup>53</sup>

|                      |                    | Deadweight | DEAs   | Anchor Piles | VLAs      |
|----------------------|--------------------|------------|--------|--------------|-----------|
| Soil Type            | Soft Clay          | Good       | Good   | Good         | Good      |
|                      | Medium Clay        | Good       | Good   | Good         | Good      |
|                      | Hard Clay          | Good       | Good   | Bad          | Bad       |
|                      | Sand               | Good       | Good   | Average      | Bad       |
|                      | Rock               | Good       | Bad    | Bad          | Bad       |
| Load Type            | Omnidirectional    | Good       | Bad    | Good         | Good      |
|                      | Horizontal         | Good       | Good   | Good         | Good      |
| Intrinsic Parameters | UHC*/Weight Ratio  | Highest    | Low    | High         | Low       |
|                      | Installation Costs | Expensive  | Lowest | Expensive    | Expensive |

\*UHC: Ultimate Holding Capacity (kN)

### 2.3.7 Mooring Line Patterns

The selection of a mooring system pattern is typically done by varying every section mentioned up to this point until a cost-effective system is found that suits functional requirements. Despite being one of the first tasks to be performed, it has been placed at the end of this section so that all the terms used are familiar. It is divided in two main steps:

- Determine the anchoring radius. For a deepwater taut leg system, a good starting point for line length is to have a R/D ratio at 1.4, that is, anchor radius is 1.4 times the water depth. For shallower water, more appropriate for catenary systems, the anchor radius is much larger, required to have sufficient chain length resting on the sea floor to ensure no uplift on the anchor.

- Estimate the correct number and size of lines. This is a crucial step that will provide a cost-effective mooring system. There exist multiple alternative mooring patterns with different numbers of lines and sizes for floating or fixed cases (Figure 2-24). Despite that, they can be arranged into four main types: grouped mooring, omni-directional mooring, asymmetric spread and symmetric spread.

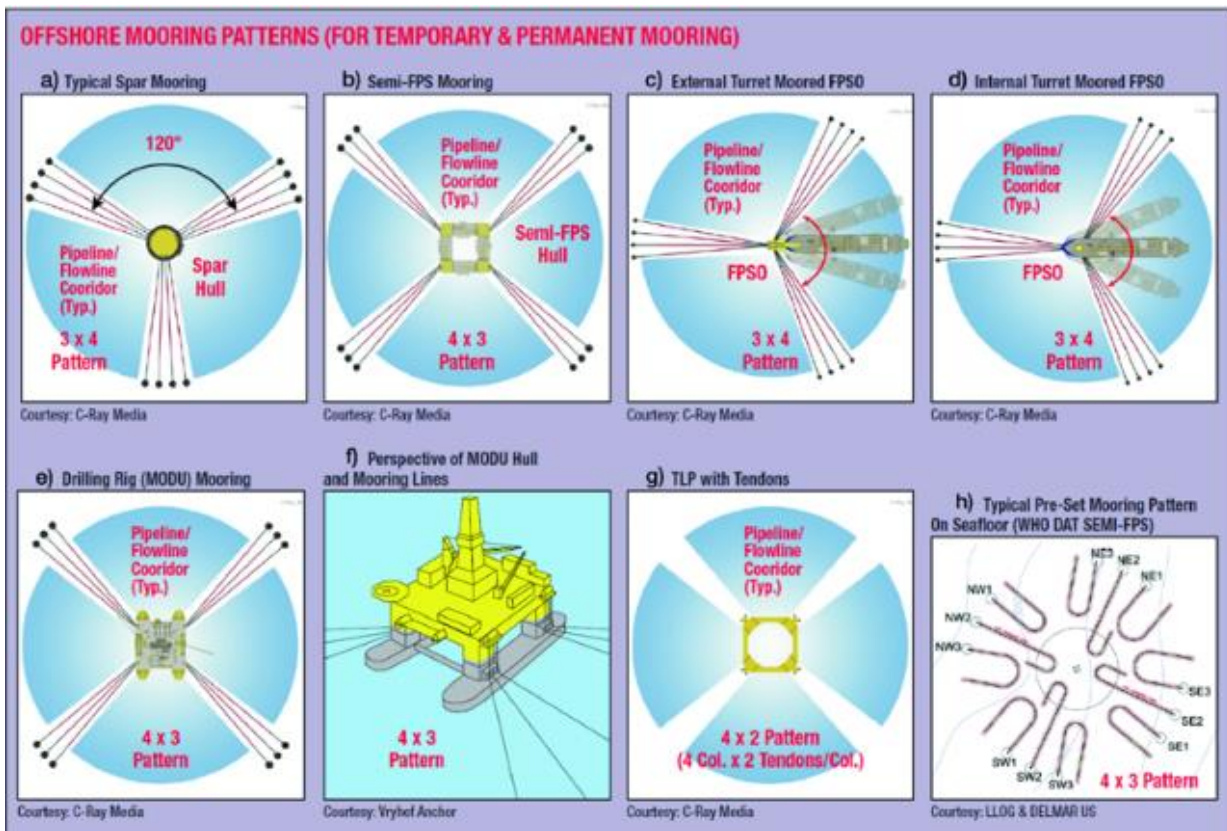


Figure 2-24. Offshore mooring patterns. Source: Khalifeh (2020)<sup>54</sup>

### 2.3.8 Mooring line failure modes

To ensure proper mooring design, mooring strength analysis is performed to predict extreme responses such as line tensions, anchor loads, and vessel offsets under the design environments and other external loads. Then, obtained values are compared against the minimum requirements by industry design standards dictated by various regulatory agents as DNV (Det Norske Veritas), BV (Bureau Veritas), API (American Petroleum Institute) and ISO (International Standards Organization), among others.

It is important to remark that the failure of a mooring line can be a quite dramatic incident. Even though most described units are designed to stand one single line failure, such failures could eventually develop into a multiple line failure, due to increased loads on the neighbour lines. What is more, it will also introduce considerable loss in costs and time due to repair and maintenance work.

A long-term mooring system is supposed to withstand the design load even at the end of its service life. Figure 2-25 illustrates some of the phenomena and degradation mechanisms that a mooring line should endure for at least 20 years. From an engineering point of view, there



are not many mechanical systems that can withstand 20 years of exhaustive use without diminishing any of their original specifications.

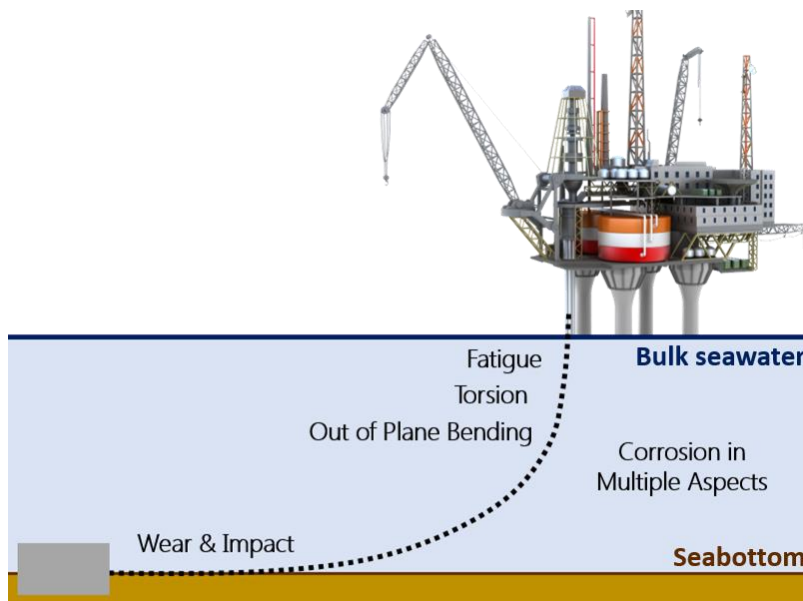


Figure 2-25. Phenomena influencing the safety and integrity of the anchor lines.

One of the most critical points of the mooring line is the part of the line that is in contact with the seabed at the end of the catenary. It is at this point where most cyclical movements occur and where the line suffers the greatest abrasion and impact. Studies carried out on semi-submersible oil platforms in the North Sea<sup>31</sup> reveal that after removing an anchor line due to service failure, a dimensional check revealed that after 16 years of service its nominal diameter had decreased by 10 mm, resulting in a corrosion rate of 0.625 mm/year, 50% higher than acceptable values<sup>55</sup>.

It was thought that the cause of every mooring failure is an environmentally assisted overload, leading to plastic deformations, yielding and ductile failure of the line. Parallely, associated cyclic axial load, cyclic bending and cyclic torsion can further accelerate plastic deformation, and thus, end up in geometrical changes causing irremediable failure or fracture<sup>56</sup>. Surprisingly, extensive studies in this topic, as the OTC 24025 review<sup>57</sup> show that most of the failures were not due to weather overload but due to many other failure mechanisms. These failure mechanisms included OPB fatigue, pitting corrosion, flawed flash welds, unauthorized chain repair, chain knotting (torsion) due to twist, and many others<sup>58</sup>.

Each failure mechanism affects differently to the multiple components of the mooring line, which are summarized below in Table 2-10:

Table 2-10. Variety of failure mechanisms for chain, wire rope, and connectors. Source: Ma (2019)<sup>56</sup>

| Chain Failure        | Rope Failure         | Component Failure |
|----------------------|----------------------|-------------------|
| Tension fatigue      | Corrosion (multiple) | Mis-installation  |
| OPB Fatigue          | Overload             | Fatigue           |
| Torsion              | Fatigue              | Brittle materials |
| Corrosion (multiple) |                      |                   |
| Weld failure         |                      |                   |
| Overload             |                      |                   |
| Mechanical damage    |                      |                   |

As corrosion related degradation, wear and fatigue phenomena will be extensively reviewed in Chapter 3. This section will be focused on **torsion** and **out-of-plane bending (OPB)** phenomena.

- **Out-of-plane bending:** Related to fatigue phenomena, OPB is a phenomenon where the chain link is bent out of its main plane (Figure 2-26), independently of the material employed, moored structure (fixed or floating) or the chain type (stud/studless). Generated friction between two links in that atypical position lead to OPB initiation, and if stresses are sufficient, crack propagation can occur at the first moving link leading to early failure<sup>59</sup>.

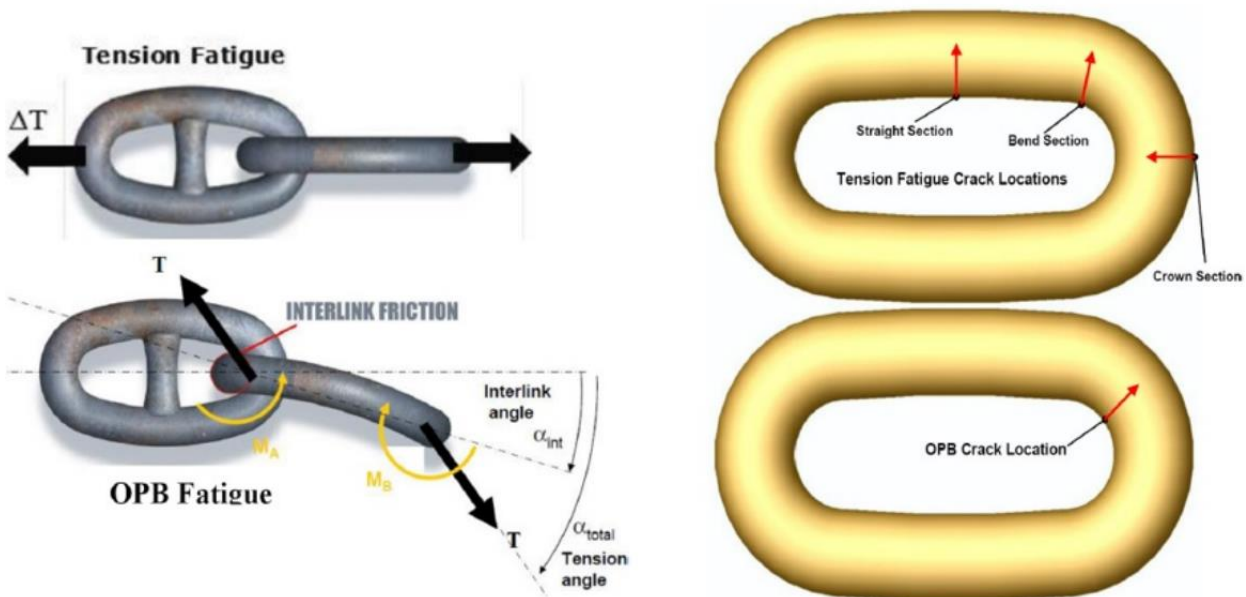


Figure 2-26. Out-of-plane bending scheme. Source: Das (2016)<sup>60</sup>

- **Torsion:** A chain subjected to a common axial load does not twist or generate any torque. However, if a chain is twisted while carrying axial load, it behaves in a highly non-linear manner<sup>61</sup>. This leads to a relatively high and potentially destructive stresses that may develop in a link that is highly twisted and at the same time subjected to moderate axial loads. At low levels of twist, the mooring line links remain axial to the centre, but as the level increases, and influenced by friction, the links start to displace from the centre, generating even more unpredictable stress.

These two quite common interactions between components generate a non-desired tension/torsion behaviour, whose effects have been extensively reviewed<sup>62,63</sup> as they seriously affect strength and fatigue endurance of the mooring line.

### 2.3.9 Failure economic point of view.

The consequences of a line failure are numerous, as mentioned before. A potential failure scenario is described below (Figure 2-27).



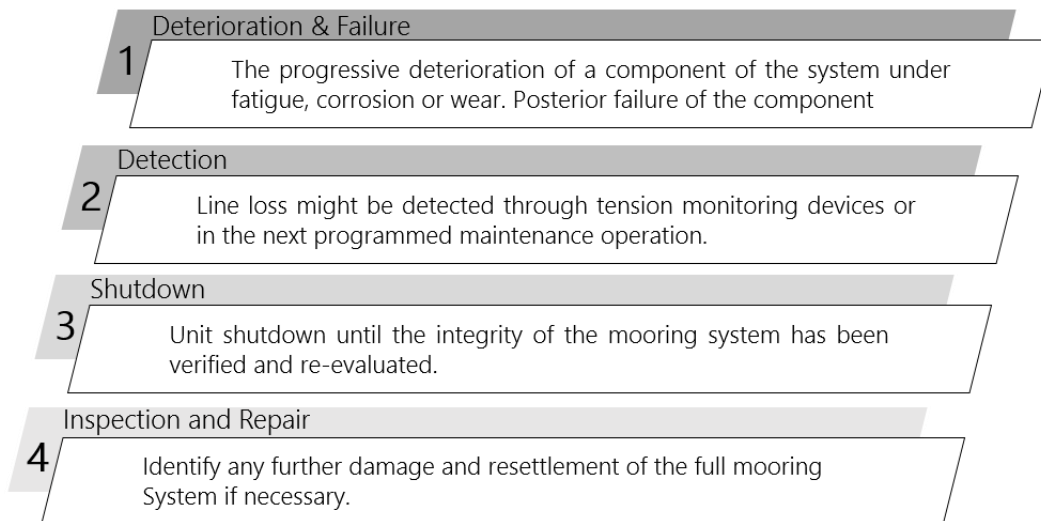


Figure 2-27. Single mooring failure scenario. Adapted from RR444<sup>31</sup>.

A further consequence is the unit downtime for repair, and the consequent loss of production, which affects directly to the related economic cost<sup>64</sup>. Two examples are represented in Table 2-11.

Table 2-11. Single mooring line failure approximate cost. Source: Tande (2010)<sup>64</sup>

| Description                       | Approximated cost of a single mooring line |
|-----------------------------------|--|
| North Sea – 50.000 barrels/day    | ~2 M£                                      |
| West Africa – 250.000 barrels/day | ~10.5 M£                                   |

The probabilities of failure in the anchor lines of the North Sea have historically been relatively high. In a research report published by SINTEF, the number of operational years for failure of the units installed in this geographical area was collected between the years 1980 and 2001 (Table 2-12).

Table 2-12. Operative years until failure of different offshore assets in the North Sea (Period: 1980-2001). Source: Tande (2010)<sup>64</sup>

| Unit type                | Operative years per failure |
|--------------------------|-----------------------------|
| Drilling unit            | 4.7                         |
| Oil&Gas semi-submersible | 9.0                         |
| Floating units           | 8.8                         |

The following conclusions were collected from the same report:

- 50% of units cannot adjust the length of their anchor lines.
- 33% of the units cannot determine the displacement suffered from their equilibrium or initial point.
- 50% of the units do not monitor the voltage in real time.
- 78% of the units do not have any type of fault alarm system installed.
- 67% of the units do not have a spare anchor line.
- 87% of the units do not have any type of repair procedure.

Therefore, the data support the importance of detecting a failure in the mooring line in order to avoid jeopardizing the rest of the anchor line and even the integrity of the operating station itself. Failures may go undetected due to a deficiency in monitoring equipment, and the broken anchor line cannot be detected in 78% of cases up to the date of the scheduled anchor line inspection. In 87% of the time, the inspection result rules in favour of the complete line replacement due to a lack of repair procedures.

Likewise, knowing the degradation pathway of the anchor line components subjected is a key aspect, since in addition to providing information for the design of the component and selection of materials, it can assist in the prevention of failures in structures or certain key components. This avoids unnecessary replacement, reduces the number of unnecessary stops and/or minimizes inspection times. Consequently, significant reducing maintenance costs are observed.

## Bibliography

---

1. Gould, T. *et al.* *World Energy Outlook: Offshore Energy Outlook 2019*. [www.iea.org/t&c/](http://www.iea.org/t&c/) (2018).
2. English, T. The Engineering and Construction of Offshore Oil Platforms. *Interesting Engineering* <https://interestingengineering.com/the-engineering-and-construction-of-offshore-oil-platforms> (2020).
3. DNV GL. *Energy transition outlook 2020. Global and Regional Forecast to 2050* (2019) doi:10.2307/j.ctv7xbrmk.21.
4. Malerød-Fjeld, H. *et al.* Thermo-electrochemical production of compressed hydrogen from methane with near-zero energy loss. *Nat. Energy* **2**, 923–931 (2017).
5. Antonini, C. *et al.* Hydrogen production from natural gas and biomethane with carbon capture and storage - A techno-environmental analysis. *Sustain. Energy Fuels* **4**, 2967–2986 (2020).
6. Uslu, A. & Kurfust, P. *Europe's onshore and offshore wind energy potential*. (2009).
7. *BP Statistical Review of World Energy 2019*. <https://www.bp.com/content/dam/bp/business-sites/en/global/corporate/pdfs/energy-economics/statistical-review/bp-stats-review-2019-full-report.pdf> (2019).
8. Drodten, P. Marine atmosphere, splash, tidal and immersion zones. in *Corrosion Handbook* (ed. Bender, R.) 263–332 (Wiley Online Library - DEHEMA, 2008).
9. DNV-GL-AS. Corrosion protection for wind turbines. *DNVGL-RP-0416 Standard* (2016).
10. Arriba-Rodriguez, L. De, Villanueva-Balsera, J., Ortega-Fernandez, F. & Rodriguez-Perez, F. Methods to evaluate corrosion in buried steel structures: A review. *Metals (Basel)*. **8**, (2018).
11. Wang, X. *et al.* Corrosion of steel structures in sea-bed sediment. *Bull. Mater. Sci.* **28**, 81–85 (2005).
12. Chaney, R. C. & Demars, K. R. Offshore Structure Foundations. in *Foundation Engineering Handbook* (ed. Fang, H. Y.) 679–730 (Springer Science+Business Media, 1991).
13. Mooring differences between Oil and Gas structures and Marine Energy Converters. *InterMoor* <https://intermoor.com/technical-articles/mooring-differences-oil-gas-renewables/> (2017).
14. Speight, J. G. Offshore Platforms. in *Handbook of Offshore Oil and Gas Operations* 71–106 (Gulf Professional Publishing, 2015). doi:10.1016/B978-1-85617-558-6/00003-9.
15. How Do Spars Work? [rigzone.com/training](http://rigzone.com/training) [https://www.rigzone.com/training/insight.asp?insight\\_id=307&c\\_id=](https://www.rigzone.com/training/insight.asp?insight_id=307&c_id=).
16. Spar. [2b1stconsulting.com/spar/](http://2b1stconsulting.com/spar/) <https://www.2b1stconsulting.com/spar/> (2012).
17. Dev, A. & Tan, T. D. N. Comparative Analysis on Mooring of SPAR Platforms. in *7th PAAMES and AMEC2016* 1–8 (2016).
18. Sadeghi, K. & Tozan, H. Tension leg platforms: an overview of planning, design, construction and installation. *Acad. Res. Int.* **9**, (2018).
19. Pike, J. Tension Leg Platform. [globalsecurity.org/military](http://globalsecurity.org/military) [www.globalsecurity.org/military/systems/ship/platform-tension-leg.htm](http://www.globalsecurity.org/military/systems/ship/platform-tension-leg.htm) (2011).
20. D'Souza, R. & Aggarwal, R. The tension leg platform technology - Historical and recent developments. in *Proceedings of the Annual Offshore Technology Conference* vol. 3 1899–1916 (Offshore Technology Conference, 2013).
21. Matten, R. B., Provost, M. J., Pastor, S. & Young, W. S. OTC 14123 Typhoon SeaStar TLP. in *Offshore Technology Conference* (Offshore Technology Conference, 2002).
22. Kibbee, S. TLP TECHNOLOGY SeaStar minimal platform for small deepwater reserves. [offshore-mag.com/deepwater](http://offshore-mag.com/deepwater) [offshore-mag.com/deepwater/article/16759274/tlp-technology-seastar-minimal-platform-for-small-deepwater-reserves](http://offshore-mag.com/deepwater/article/16759274/tlp-technology-seastar-minimal-platform-for-small-deepwater-reserves) (1996).
23. How Do Semisubmersibles Work? [rigzone.com/training](http://rigzone.com/training) [https://www.rigzone.com/training/insight.asp?insight\\_id=338&c\\_id=](https://www.rigzone.com/training/insight.asp?insight_id=338&c_id=).
24. Sadeghi, K. & Musa, M. K. Semisubmersible platforms: Design and Fabrication: An overview. *Acad. Res. Int.* **10**, 28–38 (2019).
25. Collu, M. & Borg, M. Design of floating offshore wind turbines. in *Offshore Wind Farms: Technologies, Design and Operation* (eds. Chong, N. G. & Ran, L.) 359–385 (Woodhead Publishing Limited, 2016). doi:10.1016/B978-0-08-100779-2.00011-8.
26. Arapogianni, A. & Genachte, A.-B. *Deep Water: The next step for offshore wind energy*. (2013).
27. Bhattacharya, S. Civil Engineering Aspects of a Wind Farm and Wind Turbine Structures. in *Wind Energy Engineering: A Handbook for Onshore and Offshore Wind Turbines* (ed. Letcher, T. M.) 221–242 (Academic

- Press, 2017). doi:10.1016/B978-0-12-809451-8.00012-6.
28. Edenhofer, O., Madrugá, R. P. & Sokona, Y. *Renewable Energy Sources and Climate Change Mitigation*. (2012).
  29. Sclavounos, P. Floating offshore wind turbines. *Mar. Technol. Soc. J.* **42**, 39–43 (2008).
  30. Vijay, K. G., Karmakar, D., Uzunoglu, E. & Guedes Soares, C. Performance of barge-type floaters for floating wind turbine. in *Progress in Renewable Energies Offshore* 637–646 (Taylor & Francis Group, 2016). doi:10.1201/9781315229256-76.
  31. Noble Denton Europe Limited. *RR444 - Floating production system: JIP FPS mooring integrity. Health and Safety Executive* <http://www.hse.gov.uk/research/rrpdf/rr444.pdf> (2006).
  32. Bidgoli, S. I., Shahriari, S. & Edalat, P. Sensitive Analysis of Different Types of Deep water Risers to Conventional Mooring Systems. *Int. J. Coast. Offshore Eng.* **5**, 45–55 (2017).
  33. SMB Offshore. *Calm Buoy*. (2012).
  34. Kwan, C.-T. T. Mooring systems. in *Encyclopedia of Maritime and Offshore Engineering* (eds. Carlton, J., Jukes, P. & Choo, Y.-S.) (John Wiley & Sons Ltd., 2018). doi:10.1016/b978-0-08-044381-2.50015-1.
  35. England, L. T., Duggal, A. S. & Queen, A. L. *A Comparison Between Turret and Spread Moored F(P)SOs for Deepwater Field Developments*. (2001).
  36. Flory, J. F. & Banfield, S. J. Mooring Systems for Marine Energy Converters. in *OCEANS MTS/IEEE Monterey 2016* 1–13 (2016).
  37. Alcorn, R., Bosma, B. & Thiebaut, F. *Comparison of a Catenary and Compliant Taut Mooring System for Marine Energy Systems. MARINET-TA1-GalwayBay PowerBuoy*. (2015).
  38. Chun-yan, J., Zhi-ming, Y. & Ming-Lu, C. Study on A New Mooring System Integrating Catenary with Taut Mooring. *Chinese Ocean Eng. Soc.* **25**, 427–440 (2011).
  39. Offshore Mooring Lines. *Offshore Consulting Engineering* (2006).
  40. Engineering, S. T. *Advanced Anchoring and Mooring Study*. (2009).
  41. Kulkarni, S. S. & Chhapkhane, N. K. Comparison Of Studless And Studed Chain Using Finite Element Analysis. *Int. J. Eng. Res. Technol.* **2**, 1619–1622 (2013).
  42. Arias, R. R., Ruiz, Á. R. & de Lena Alonso, V. G. Mooring and Anchoring. in *Floating Offshore Wind Farms* (eds. Castro-Santos, L. & Díaz-Casas, V.) (Springer International Publishing, 2016). doi:10.1007/978-3-319-27972-5.
  43. Chain reaction. *energy-oil-gas.com* <http://www.energy-oil-gas.com/2007/03/30/ramnas-bruk/> (2007).
  44. Stud solution aids mooring chain performance. *Offshore-mag.com* <https://www.offshore-mag.com/business-briefs/company-news/article/16762921/stud-solution-aids-mooring-chain-performance> (2005).
  45. Banfield, S. J., Casey, N. F. & Nataraja, R. Durability of polyester deepwater mooring rope. OTC 17510. in *Proceedings of the Annual Offshore Technology Conference* vols 2005-May 1532–1542 (Offshore Technology Conference, 2005).
  46. Weller, S. D., Johanning, L., Davies, P. & Banfield, S. J. Synthetic mooring ropes for marine renewable energy applications. *Renew. Energy* **83**, 1268–1278 (2015).
  47. Synthetic Tethers. *lankhorstoffshore.com* [lankhorstoffshore.com/markets/synthetic-tethers](http://lankhorstoffshore.com/markets/synthetic-tethers).
  48. Chaplin, R., Potts, A. & Curtis, A. Degradation of wire rope mooring lines in SE Asian waters. in *Offshore Asia 2008* (2008).
  49. Sefton, S. F., Firth, K. & Hallam, S. Installation and handling of steel permanent mooring cables. *offshore-mag.com* (1998).
  50. Ma, K.-T., Luo, Y., Kwan, T. & Wu, Y. Mooring design. in *Mooring System Engineering for Offshore Structures* 63–83 (Gulf Professional Publishing, 2019). doi:10.1016/B978-0-12-818551-3.00004-1.
  51. DNVGL-OS-E302 Standard. (2015).
  52. Albisu, B. et al. OTC-27024-MS. New grades of high strength steel for offshore mooring chains: R5S 1100 MPa and R6 1200 MPa. in *Proceedings of the Annual Offshore Technology Conference* vol. 2 1741–1751 (2016).
  53. Toledo Monfort, D. *Design optimization of the mooring system for a floating offshore wind turbine foundation*. (2017).
  54. Khalifeh, M. & Saasen, A. Different Categories of Working Units. in *Introduction to Permanent Plug and Abandonment of Wells* (eds. Dhanak, M. R. & Xiros, N. I.) 137–163 (2020). doi:10.1007/978-3-030-39970-2\_5.

55. DNVGL-OS-E301 Standard. (2015).
56. Ma, K.-T., Luo, Y., Kwan, T. & Wu, Y. Mooring Reliability. in *Mooring System Engineering for Offshore Structures* (Gulf Professional Publishing, 2019). doi:10.1016/B978-0-12-818551-3.00013-2.
57. Ma, K., Duggal, A., Smedley, P., L'Hostis, D. & Hongbo, S. OTC 24025 - A Historical Review on Integrity Issues of Permanent Mooring Systems. in *Offshore Technology Conference* (Offshore Technology Conference, 2013).
58. Seven mechanisms that contribute to mooring line failure. *intermoor.com/technical-articles*.
59. Izadparast, A., Heyl, C., Ma, K.-T., Vargas, P. & Zou, J. Guidance for Assessing Out-of-Plane Bending Fatigue on Chain used in Permanent Mooring System. in *23rd Offshore Symposium* (SNAME - Society of Naval Architects and Marine Engineers, 2018).
60. Das, N. Models to explain out-of-plane bending mechanism in mooring chain links. (TU Delft, 2016).
61. Ridge, I. M. L., Hobbs, R. E. & Fernandez, J. OTC 17789 - Predicting the Torsional Response of Large Mooring Chains. in *Offshore Technology Conference* (Offshore Technology Conference, 2006).
62. Hobbs, R. E. & Ridge, I. M. L. Torque in mooring chain. Part 1: Background and theory. *J. Strain Anal. Eng. Des.* **40**, 703–713 (2005).
63. Ridge, I. M. L. & Hobbs, R. E. Torque in mooring chain. Part 2: Experimental investigation. *J. Strain Anal. Eng. Des.* **40**, 715–728 (2005).
64. Tande, J. O. *Wind Power R&D seminar - Deep Sea Offshore Wind*. (2010).

# 3

---

## Corrosion in marine environment

---

- Corrosion: A general overview
- Seawater
- Corrosion mechanisms
- Main influential factors in corrosion development



In this chapter general issues related to the corrosion in marine environment are briefly discussed. The corrosion of offshore structures is somehow similar to the corrosion present in onshore facilities, except that the environment is more corrosive. Thus, an introduction to the seawater corrosivity and its most common forms of corrosion are presented initially in this chapter. Afterwards, seawater-related available corrosion models are reviewed, as well as the main influential factors affecting the corrosion rate of iron-based alloys in aqueous media. All this serves to contextualize the environment characteristics and the corrosion paths that we have to foresee in the corrosion monitoring system that is presented in this thesis.

### 3.1 Corrosion: A general overview

Corrosion can be defined in many ways. One common vision is to define it as the chemical degradation of materials, not only metals, but also semiconductors, insulators, and even polymers, due to the exposure to a non-inert environment<sup>1</sup>. More specifically, corrosion appears to be a physical-chemical interaction between a metal and its environment. This results in changes in the properties of the metal and can lead to significant disfunction of the system it is part of<sup>2</sup>.

On the theory, rust formation in iron-based alloys comes from iron diffusing in solution and hydrogen depletion in the presence of oxygen or other oxidizing agents. Each iron ion that appears at a certain spot demands the disappearance of one hydrogen ion in another in the form of a gas. Substances that acidify the medium by increasing the concentration of hydrogen ions, such as acids, enhance corrosion processes, while substances that promote the concentration of hydroxyl ions are said to inhibit it.

The basic requirement for steel corrosion to occur is to end up in a more stable situation, in a lower energy state. The different reactions involved in the degradation processes are related to a reduction potential. The anode (actively corroding part) must have a lower reduction potential than the corresponding cathodic reaction for corrosion to take place. The effective reduction potential of each half-reaction is strongly influenced by several factors including the composition and flow of the electrolyte (seawater), temperature, pH and surface conditions. Therefore, the corrosion tendency will depend on many factors and cannot be deduced from the standard redox potentials alone.

Regarding the specific material of this thesis, it could be said that plain-carbon steel is the most important metal in the marine service and has been widely used for many years in marine construction up to the recently developed low-alloy steels of higher strength (HSLA). These alloys have better general properties, finding more and more applications to the detriment of carbon steel. Above all, steels are selected for marine service because of factors such as availability, cost, ease of fabrication, design expertise, and advantageous physical and mechanical properties<sup>3</sup>. The behaviour of steel alloys tends to show outstanding differences depending on the exposure zones. Thus, the results, models and conclusions from exposure to atmospheric corrosion cannot be extrapolated to an environment involving tidal or fully immersed conditions, having to develop its own research and guidelines.

## 3.2 Seawater

Seawater is a complex chemical system that is affected by various environmental factors, being the most significant ones the pH, dissolved oxygen concentration, temperature and bacterial activity<sup>4</sup>. As an aqueous solution, it is composed roughly of 96.5% water, 3.5% salts and smaller amount of other substances, including dissolved inorganic and organic materials<sup>5</sup>. The average salt content in the major oceans is between 32 and 37 parts per thousand. High salt content levels result from high evaporation rates, while the low levels result when there is a constant source of fresh water that exceeds evaporation<sup>6</sup>.

The principal ionic constituents of seawater are outstandingly constant. It has been found that, regardless of the absolute concentration of the total solids, the ratios between the more abundant substances are virtually persistent with time. The uniformity of relative composition in the oceans is the result of circulation and mixing of ocean currents. These operations are continuous, and tend to eliminate regional differences in composition, whatever the cause<sup>7</sup>. The constancy of composition is, as already emphasized, of the greatest importance, since it is the basis of the salinity, chlorinity and density relationships. Main components are listed in Table 3-1<sup>8</sup>. Other elements and compounds are present in lower concentrations than those resumed in elements, such as oxygen and carbon dioxide in the form of dissolved gasses, or those elements causally linked to biological processes (e.g., nitrogen). These compounds exhibit highly variable concentration that will be discussed later, and they do not directly affect salinity values.

Table 3-1. Average composition of seawater at a salt concentration of 3.5 wt%<sup>8</sup>.

| Component   | Concentration (g/kg) | % of all salts in the sea |
|---|----------------------|---------------------------|
| Chloride (Cl <sup>-</sup> )                         | 18.98                | 55.04                     |
| Sodium (Na <sup>+</sup> )                           | 10.56                | 30.61                     |
| Sulphate (SO <sub>4</sub> <sup>2-</sup> )           | 2.65                 | 7.68                      |
| Magnesium (Mg <sup>2+</sup> )                       | 1.27                 | 3.69                      |
| Calcium (Ca <sup>2+</sup> )                         | 0.40                 | 1.16                      |
| Potassium (K <sup>+</sup> )                         | 0.38                 | 1.10                      |
| Hydrogen carbonate (HCO <sub>3</sub> <sup>-</sup> ) | 0.14                 | 0.41                      |
| Bromide (Br <sup>-</sup> )                          | 0.07                 | 0.19                      |
| Boron (B <sup>3+</sup> )                            | 0.03                 | 0.07                      |
| Strontium (Sr <sup>2+</sup> )                       | 0.01                 | 0.04                      |
| Fluoride (F <sup>-</sup> )                          | 0.001                | 0.007                     |

The seawater element most often associated with its effect on materials is salinity. Salinity term is used as a measure of the total salt content, and commonly employed units are either Siemens·cm<sup>-1</sup> or mΩ·cm<sup>-1</sup>, while chlorinity is related to chloride ion content, terms not to be confused. Ignoring the constituents that have no practical consequences in terms of corrosion degradation, salinity is often based on chloride and sodium ion content because they account for approximately the 85% of the salt content.

Temperatures of seawater range from -2 °C in the Antarctic Sea to 35 °C in the tropics<sup>9</sup>. The average incoming energy from the sun on the earth's surface is about four times higher at the



equator than at the poles<sup>10</sup>, establishing a heat exchange process that carries the heat from solar radiation to deeper levels by mixing. As a result, there is a net heat input to the earth's surface in tropical regions, where the warmest surface seawater is found. Heat is then transferred from low to high latitudes by winds near the surface and by currents in the deep ocean. Due to the high specific heat of the water, diurnal and seasonal temperature variations are relatively small compared to the variations on land, since ocean temperature variations are of the order of just few degrees.

Heat transfer mechanism establishes a mixed surface layer in the first 200 m of the sea. This first layer is important because remains in an exchange equilibrium with atmosphere, absorbing, for example, much of the CO<sub>2</sub> released through the water cycle. The transition to the deep ocean happens when water temperature drops and the density increases, defining a zone called the thermocline (Figure 3-1). The thermocline is a region where temperature decreases rapidly with increasing depth, a transition layer between the mixed layer at the surface and deeper water. The depth and strength vary from season to season and year to year. It is strongest in the tropics and decrease to non-existent in the polar winter season.

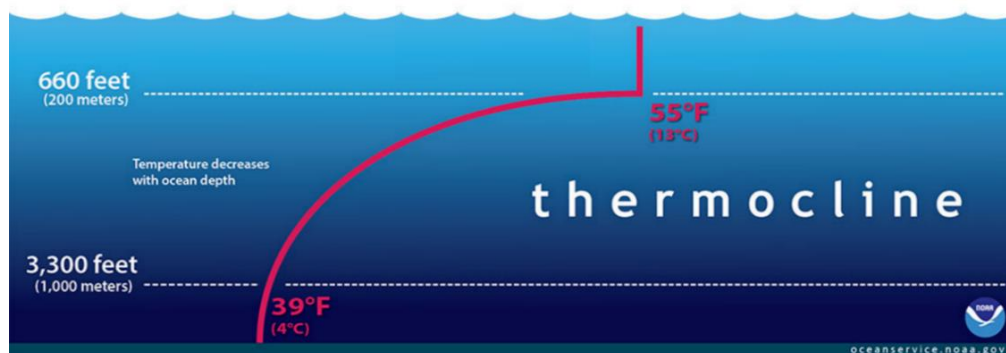


Figure 3-1. Ocean temperature profile within the mid-latitude regions. Image modified from NOAA<sup>11</sup>.

Deep ocean is considered all the water mass below 1000 meters. Here, the temperature is constant and normally never fluctuates far from 4 °C, due to the sinking of denser, nearly freezing water coming from the Earth's poles.

The depth itself has no influence on the corrosion of materials, but it affects other factors that have a direct and measurable influence, such as the dissolved oxygen (DO) concentration, the temperature, and the water velocity. The correlation with depth arises from the fact that, at least in both surface and thermocline zones, DO decreases linearly with depth, as does temperature<sup>12</sup>. Moreover, the water velocity in the deep zone is much lower than at the ocean surface. The latter arises from the wind pushing the water along the surface to form wind-driven currents, while the former is based on the sinking of cold water and the consequent displacement of warm water. Besides, marine organisms present in seawater in the form of micro or macrofouling have a great influence on the corrosion of metals, even if they are not steadily distributed throughout the oceans. Variations in the characteristics of the marine environment, such as DO, pH and temperature, create different habitats and influence the types of organisms that inhabit them. The availability of light, water depth, proximity to land, and topographic complexity also affect marine habitats<sup>13</sup>.

Causally related to the behaviour of materials, perhaps the most critical factor involving seawater and its composition is the established equilibrium between CO<sub>3</sub><sup>2-</sup> and CO<sub>2</sub>. When

carbon dioxide mixes with the water it is partially converted into carbonic acid, hydrogen ions ( $H^+$ ), bicarbonate ( $HCO_3^-$ ), and carbonate ions ( $CO_3^{2-}$ ), as seen in Figure 3-2. The equilibrium between these carbon species is a key aspect, as the acid-buffering capacity of seawater establishes a continuous pH between 7.5 and 8.4 due to the ability of the bicarbonate species to accept and donate protons. In absence of this equilibria, pH values would fluctuate greatly and corrosion in seawater would be unpredictable. Indeed, higher pH means there are fewer free hydrogen ions, and a change of one pH unit reflects a tenfold change in the concentrations of the hydrogen ion, which is the main source of corrosivity in aqueous media.

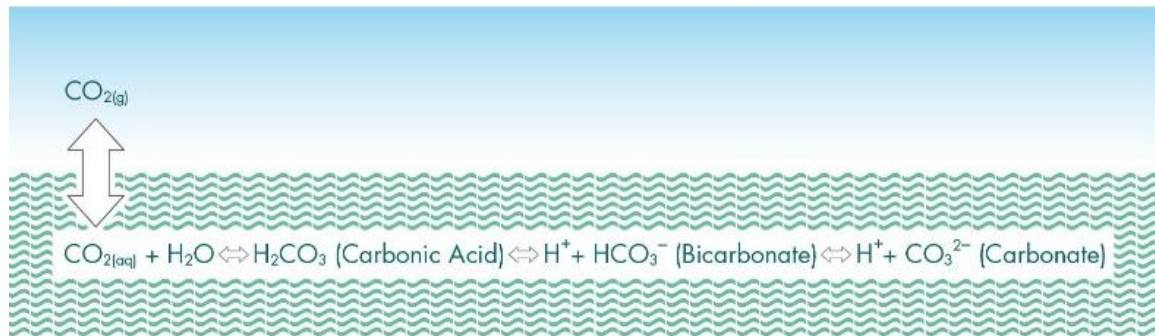


Figure 3-2.  $CO_2$  equilibrium system in seawater. Source: egcsa.com

In conclusion, seawater can be an aggressive and unpredictable medium, capable of causing degradation or corrosion in practically all metals and alloys, except the noble ones. As discussed above, corrosion behaviour of metals in seawater is mainly influenced by the oxygen content, pH, the temperature, and the marine organisms. Likewise, seawater is a good electrolyte, which facilitates many corrosion mechanisms from an electrochemical phenomena point of view, such as general thinning of the material or more localised penetration in a wide variety of degradation forms, which are reviewed in the following section.

### 3.3 Corrosion mechanisms

#### 3.3.1 General forms of corrosion

Traditionally, corrosion can be divided into two main lines of approach: electrolyte corrosion and high temperature corrosion. The most common classification of corrosion by electrolytes is based on the environment. Therefore, terms such as atmospheric corrosion, marine corrosion and soil corrosion arise as the three main branches of environmental degradation of metals. However, to avoid an uncorrelated and too extensive state of the art, the present thesis will focus on electrochemical phenomena and on high-strength low alloy corrosion in an aggressive wet environment, such as that found in marine offshore areas.

The mechanism and the electrochemical nature of marine corrosion define three requirements to take place:

- Electrolyte
- Oxygen
- Exposed metal surface

Corrosion of a metal, like steel, in aqueous medium is an electrochemical process where metallic atoms are oxidized, ending up as oxides or mixed salts. A normal corrosion pathway can be described as iron atoms oxidizing into positive cations ( $Fe^{2+}$ ) that are diffused into seawater where they react with other ions forming oxides and salts. As a rule, locations on the steel surface where ions are oxidized represent *anodic sites*, and the place where the spare electrons leave the metal are called *cathodic sites*.

### 3.3.2 Specific corrosion mechanisms of offshore structures

It is important to understand the nature, origin, and subsequent effects of all types of environmental degradation of metals and alloys in order to correctly classify and preventively act as soon as possible to ensure the reliability of the metallic components. Commonly, corrosion can be separated into general corrosion and localized corrosion and will also be considered mechanically assisted degradation (MAD) and environmentally assisted cracking (EAC).

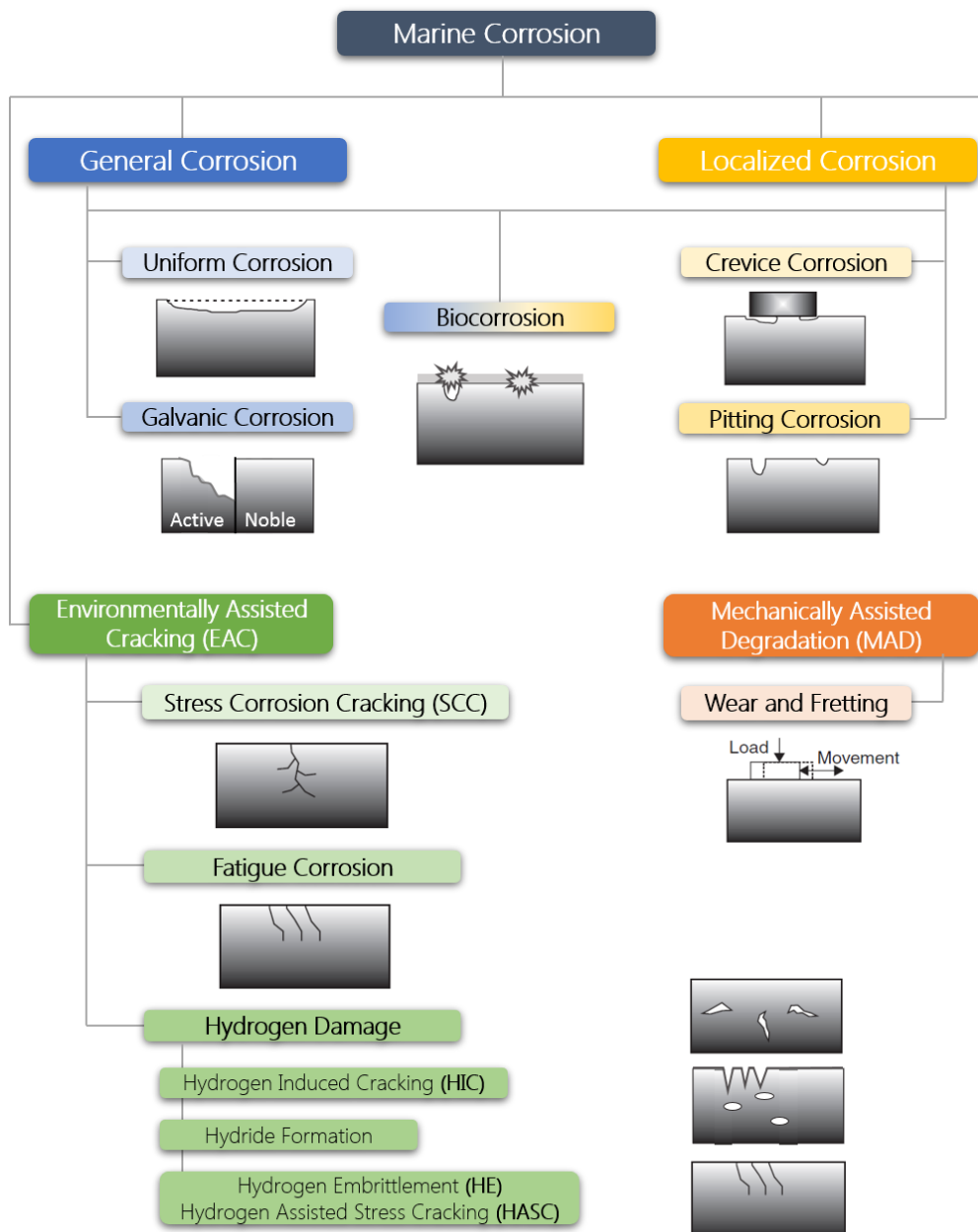


Figure 3-3. Marine degradation of metals. Illustrations partly adapted from Roberge (2008)<sup>14</sup> Chapter 6.

The general corrosion is distributed uniformly or without any preference for sites throughout the surface of the exposed steel. If protective measures are not taken, the steel thins down uniformly and eventually fails. However, in some alloys, corrosion tends to slow down as a protective film grows on the surface after the first stage of steel oxidation. Localized corrosion is spread over small areas, in form of pits or small cavities whose depth eventually increases, but with negligible reduction of material section. This type of corrosion is especially unpredictable. Differently, MAD is a form of corrosion that involves a mechanical component, such as velocity, abrasion and/or hydrodynamics, which has a significant effect on corrosion behaviour. Finally, EAC combines forms of cracking that are produced by corrosion in presence of static or dynamic stress<sup>6</sup>. A general scheme is presented in Figure 3-3.

### Uniform corrosion

Considered the most common corrosion type, it involves metal thinning in a uniform way, as the name points out (Figure 3-4). This corrosion is normally spread on the whole surface of the metal, resulting in a smooth appearance. It is not treated as the most serious form of corrosion because it is relatively easy to predict, and perhaps the most well-known corrosion type in existence, primarily caused by oxygen. Uniform corrosion is characterized and expressed as a mass loss per unit of time, e.g., mm/year.



Figure 3-4. Uniform corrosion in a carbon steel sample tested in Tecnia's HARSHLab facility in open seawater.

### Galvanic Corrosion

This type of corrosion results from a metal in contact with another conductive material in a corrosive medium. It is one of the most common types of corrosion<sup>15</sup>. It can be found at the junction when various components made of different metal alloys are immersed in water. So, if two components with different galvanic potentials are electrically connected in the same electrolyte, the metal with the lowest or most negative potential will preferentially oxidize the other metal, with the difference between both potentials establishing the degree of preferential corrosion. A typical example of galvanic corrosion can be found in the use of sacrificial anodes to protect certain structures from seawater corrosion. Sacrificial anodes are highly active metals that are used to prevent a less active material surface from corroding, as it will be consumed in place of the metal it is protecting, which is why it is referred to as a "sacrificial" anode (Figure 3-5).

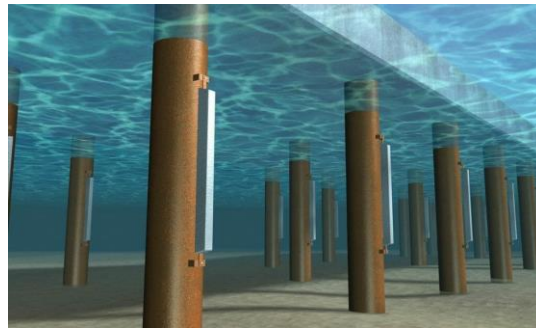


Figure 3-5. Sacrificial anodes placed in submerged monopiles to avoid structural corrosion. Source: cathwell.com.

It is important to note that potential values may change from one medium to another when influenced by temperature, dissolved oxygen and velocity of water mass. To avoid problems associated with this type of corrosion, it is especially important to pay attention to the location of the material in the electrochemical series, which establishes the activity or passivity of the material depending on the material with which it is compared (Figure 3-6).

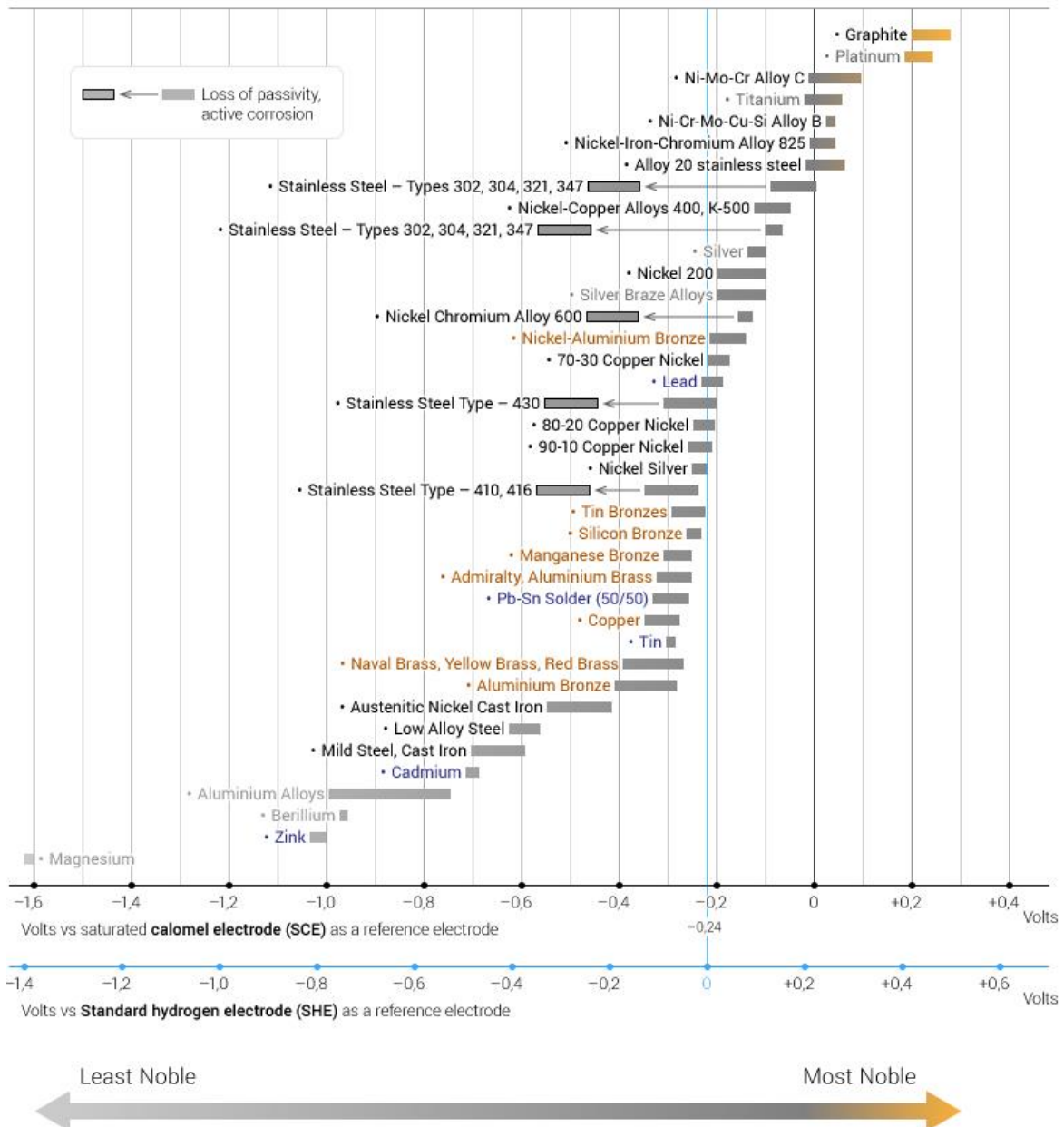


Figure 3-6. Galvanic series in seawater with SHE and SCE reference electrodes. Source: EngineeringClicks.com.



Attention should also be given to the area in contact between the two dissimilar alloys, or the ratio of cathodic to anodic area. Galvanic currents in many situations are proportional to the surface area of the cathode (i.e., most noble). The larger the cathode compared with the anode the more oxygen reduction, or other cathodic reaction, can occur and the greater the generated galvanic current<sup>14</sup>. From a surface condition point of view, attention should be paid to formed oxide films. If the formed oxide is continuous with good adherence, it can reduce the corrosion rate. However, oxide layers used to be brittle and can crack easily, exposing the bare steel directly to the environment (Figure 3-7).

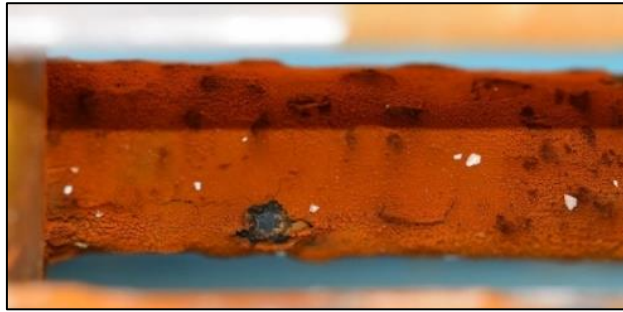


Figure 3-7. Exposed pit (blackish area) compared with the orange-coloured rust all over the surface on a low alloy steel sample. (Courtesy of: Tecnalia).

It is worth to mention that, in offshore facilities as mooring chains, there are two regions where galvanic effect can occur<sup>16</sup>:

- The inter-grip area, where wear tends to expose the fresh steel surfaces.
- The welds, where conditions during welding can induce changes that are not adequately corrected by heat treatment.

In the inter-grip area, galvanic effect between bare steel and oxide products can be established, as explained before. If an incorrect heat treatment is applied in the weld area, it can lead into compositional gradients and corresponding microgalvanic cells. Also, the slag that is still adhering to the weld deposit can result in crevices that can promote a localized concentration cell, resulting in crevice corrosion<sup>17</sup>.

### Biocorrosion or Microbiologically Influenced Corrosion

General corrosion is driven by the accessibility of oxygen to the bare metal surface. Therefore, the corrosion rate is controlled by any external agent that modifies the oxygen supply rate. Biological agents, present in the aqueous environments, can lower or enhance oxygen diffusion into the steel by biofilm formation into the surface, both in a uniform or localised way. Thus, the role of biofilms in enhancing corrosion of a biologically conditioned metallic surface may proceed through simultaneous or successive mechanisms. Those mechanisms include<sup>18</sup>:

- Alteration of the diffusion barrier for certain chemical species, for example, preventing the diffusion of oxygen to cathodic areas and promoting diffusion of chloride anions to anodic sites.
- Facilitating the removal of protection coatings where the biofilm deposits, by altering the structure of inorganic passive layers and increasing their dissolution and removal from the metal surface.

- Inducing differential aeration effects as a consequence of a non-uniform distribution of the biofilm, resulting in the formation of differential aeration cells, and consequently, promoting localized corrosion under the biofilm distribution.
- Changing oxidation–reduction conditions at the metal–solution interface, due to the close relation between metabolic activity of the biofouled surface and the redox conditions.

For example, the corrosive action of the sulphate-reducing bacteria (SRB) from the genera *Desulfovibrio desulfuricans* in anaerobic environments is evaluated as the main role in reducing sulphate ( $\text{SO}_4^{2-}$ ) to sulphide ( $\text{S}^{2-}$ ) and subsequently producing harmful  $\text{H}_2\text{S}$ . The  $\text{H}_2\text{S}$  reacts with the  $\text{Fe}^0$  present in the metal surface, forming  $\text{FeS}$  deposits that establish a galvanic couple with the steel surface<sup>19</sup>.

However, biofilms have demonstrated to contribute to corrosion not only by modifying the electrochemical conditions and increasing corrosion, but also sometimes by slowing it down. Iron-reducing bacteria (IRB) are a good example of the bacteria that can both accelerate and retard corrosion. These bacteria act by reducing the generally insoluble  $\text{Fe}^{3+}$  ions to the soluble  $\text{Fe}^{2+}$ , exposing the metal that is under a protective layer of ferric oxide to the corrosive environment<sup>20</sup>. Especially in anaerobic environments, IRB usually decreases the rate of corrosion, partly due to the high concentrations of soluble  $\text{Fe}^{2+}$  that prevent oxygen from attacking the steel surface<sup>21</sup>. Indeed, Duan et. al. found that sulphate-reducing bacteria and iron-reducing bacteria can be developed in the anaerobic biofilm under the rust layer of carbon steel: SRB grow in the inner rust layer, and IRB in the middle and outer layers<sup>22</sup>.

### Crevice Corrosion

Presence of narrow gaps between two components, either metals or nonmetal-metal, usually end in localized corrosion at these sites. Regardless of the material, a condition common to all types of crevice corrosion is the development of localized environments that differ greatly from the bulk environment. In its simplest form, crevice corrosion may result from the establishment of oxygen differential cells, when oxygen within the crevice area is consumed, while the rest of the exposed surface has easy access to oxygen and becomes cathodic relative to the crevice area<sup>4</sup>. Crevice corrosion can be divided into two categories: men-made and naturally materializing. The first one response to a failure in design and can be avoided (Figure 3-8).

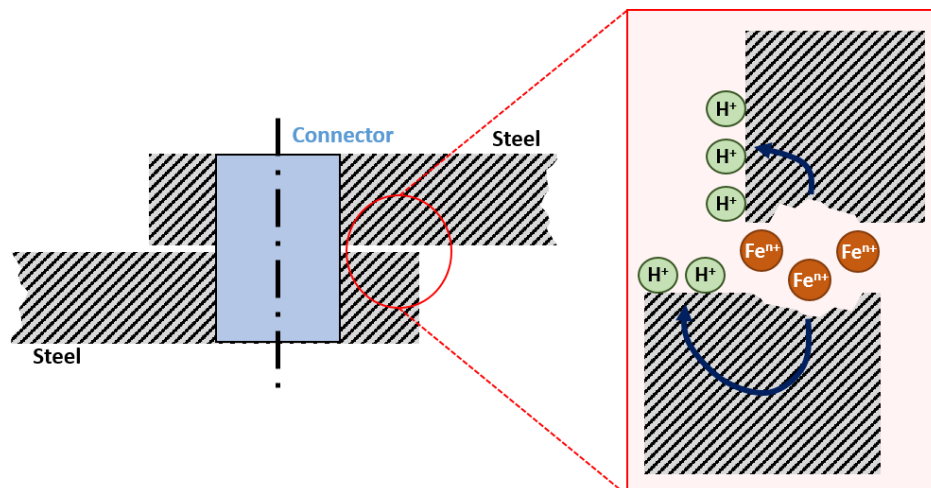


Figure 3-8. Schematized crevice mechanism between two steel components.

In this case, an improved design would minimize the crevice areas, for example, by avoiding overlapping welded parts. Welds are usually the most sensitive points to crevice, usually optimized using more alloyed filler metal and thermal treatments, to relieve the stress derivate from the fabrication process.

On the other hand, naturally occurring crevices, such as those formed by the attachment of biofouling, incurred in shallow crevice penetration beneath these organisms (Figure 3-9). This, usually, can only be minimized applying antifouling coatings or by cathodic protection. Those metals or alloys whose corrosion resistance rely on the formation of a superficial protection layer are very susceptible to suffer this form of localised corrosion.



Figure 3-9. Barnacle deposition over a low alloy steel surface at Tecnia's fouling testing facilities in Pasaia (left) and remaining crevice corrosion once bio-organisms are removed (right, courtesy of: boats.com)

### Pitting Corrosion

Pitting corrosion represents an important limitation of many alloys in industrial applications. It is a form of localized corrosion that generates small deep holes in the metal/steel surface. The driving force for pitting corrosion is based either on the breakdown processes of the passive film itself or on structural defects or heterogeneities such as dislocations, grain boundaries, precipitates, or inclusions that preferentially facilitate a path for corrosion progression. Theoretical models that describe the initiation process leading to passive film breakdown may be grouped into three classes (Figure 3-10)<sup>15</sup>:

- a) Ion migration and penetration models.
- b) Mechanical film breakdown theories.
- c) Adsorption-induced mechanisms, where the adsorption of aggressive ions like  $\text{Cl}^-$  present in the seawater is of major importance.

Regardless the pit initiation process, a common explanation for pitting corrosion is a metal oxidation that results in a local surface acidity (Figure 3-10a) that is maintained by a separation of cathodic and anodic areas, where the pit acts as anode and the metal surface acts as cathode. Inside the pit, the oxygen concentration is considered to be zero and metal dissolution is promoted, while cathodic oxygen reactions take place on the metal surface outside the pit.



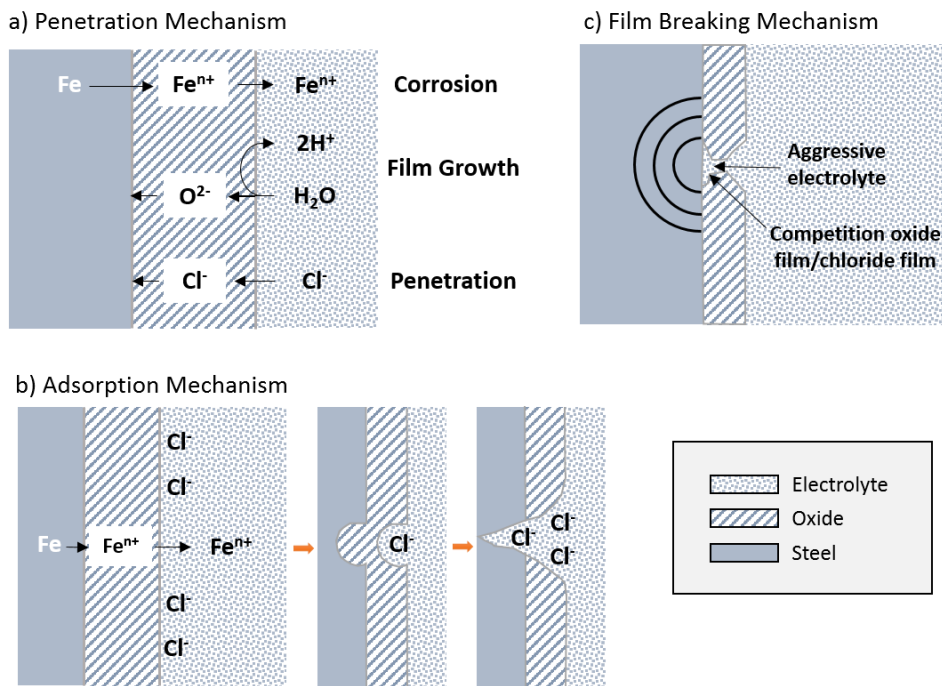


Figure 3-10. Models for pit initiation leading to passive film breakdown. Reproduced from Kaesche, H. et. al. (2011)<sup>23</sup>.

This type of corrosion is critical since it can become extremely harmful for susceptible steel structures. Indeed, it causes little loss of material with small or negligible effect on its surface but damaging the deep structures of the metal while the pits on the surface often remain covered by corrosion products. Some examples of pit shapes are shown in Figure 3-11.

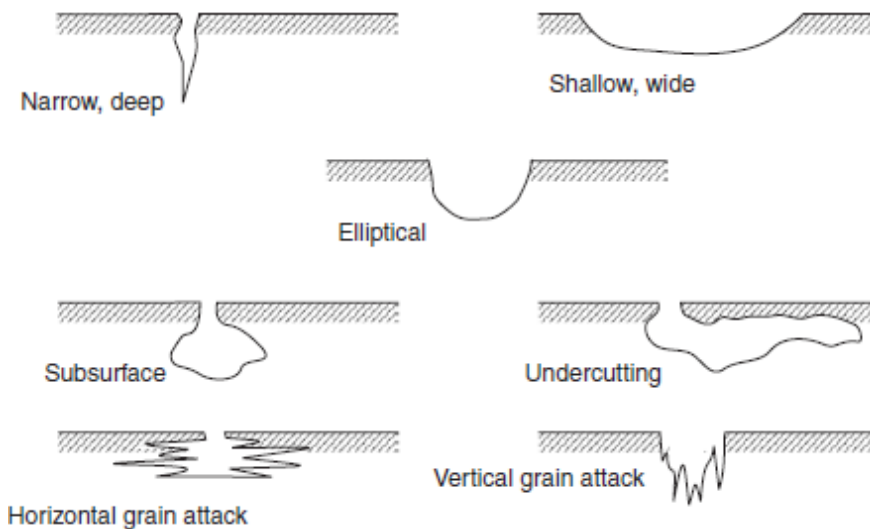


Figure 3-11. Typical cross-sectional shapes of corrosion pits. Reproduced from Roberge (2008)<sup>14</sup>.

### Environmentally Assisted Cracking (EAC)

When a component, such as mooring lines, must bear both a corrosive environment and high mechanical demands, it may be susceptible to premature failure due to environmental assisted cracking (EAC), when the load and environmental conditions are sufficiently aggressive. Although the mechanism by which EAC is driven is not yet standardised, two main mechanical

stress corrosion conditions are generated: Stress Corrosion Cracking (SCC), which occurs with continuous static loads, and Corrosion Fatigue (CF), in which loads tend to be cyclic.

Stress corrosion cracking (SCC) is a well-known corrosion mechanism normally associated with continuous high-load steel components whose chemical composition has tendency to suffer intergranular corrosion. This is a very localized corrosion, and even if the concentration of harmful ions present in seawater is quite small, and even in the absence of applied stress, the residual stresses in the structure due to poor heat treatment can often be high enough to cause SCC and failure in service.

In addition, when metals are exposed to the simultaneous actions of a corrosive environment and repeated stress, there is a significant decrease in fatigue strength compared to the behaviour in air. This phenomenon is called corrosion fatigue (CF). Although SCC is a phenomenon that occurs when metals encounter specific harmful environments, CF can take place at any time. CF cannot be avoided even for steels with passive surface films, in which rust is not necessarily visible on the fracture surfaces. CF should not be confused with the fatigue of corroded metals. The decrease in fatigue strength in corroded metals is caused by the notch effect of corrosion pits, but the decrease in fatigue strength is not as large as it is in CF<sup>24</sup>.

The fracture mechanism of CF is different from that of SCC, which takes place under a sustained load or residual stresses. In most cases, SCC causes intergranular cracking, whereas CF causes transgranular cracking.

When EAC occurs, two issues are generally accepted<sup>25</sup>:

- The chemical and electrochemical conditions of the bulk environment are not maintained along the generated crack; thus, a microenvironment is created through the surface defect.
- The stress state and chemical conditions of the local crack, and not the bulk environment, are the factors that control EAC, both for static and cyclic loading conditions.

Figure 3-12 provides a general schema describing the chemical and electrochemical conditions of the EAC. In general, the area nearest to the crack tip is expected to primarily support anodic reaction kinetics, while the bold surface and crack walls nearest to the crack mouth primarily support cathodic reaction kinetics.

Diffusion of O<sub>2</sub> into a crack is difficult and a growing crack due to accumulated tensions will quickly become depleted O<sub>2</sub> at the tip, which results in the separation of anode and cathode areas. The anodic dissolution that occurs primarily at the crack tip can result in high concentrations of metal ions leading to hydrolysis, and thus, higher acidity. In fact, the effect of hydrolysis on the crack tip chemical environment was noted in a study where the pH of the bulk solution was 6 and the pH near the crack tip for all steel alloys considered was ≈ 3.7 (Figure 3-13). The conclusions were the same for SCC tests in solutions between pH 1 and 10. The pH of the crack tip was independent of the pH of the bulk solution, where Fe<sup>2+</sup> and Fe<sup>3+</sup> were predominant cation species and Fe(OH)<sup>+</sup> and Fe(OH)<sup>2+</sup>/Fe(OH)<sub>2</sub><sup>+</sup> were the main products of the hydrolytic reaction<sup>26</sup>.

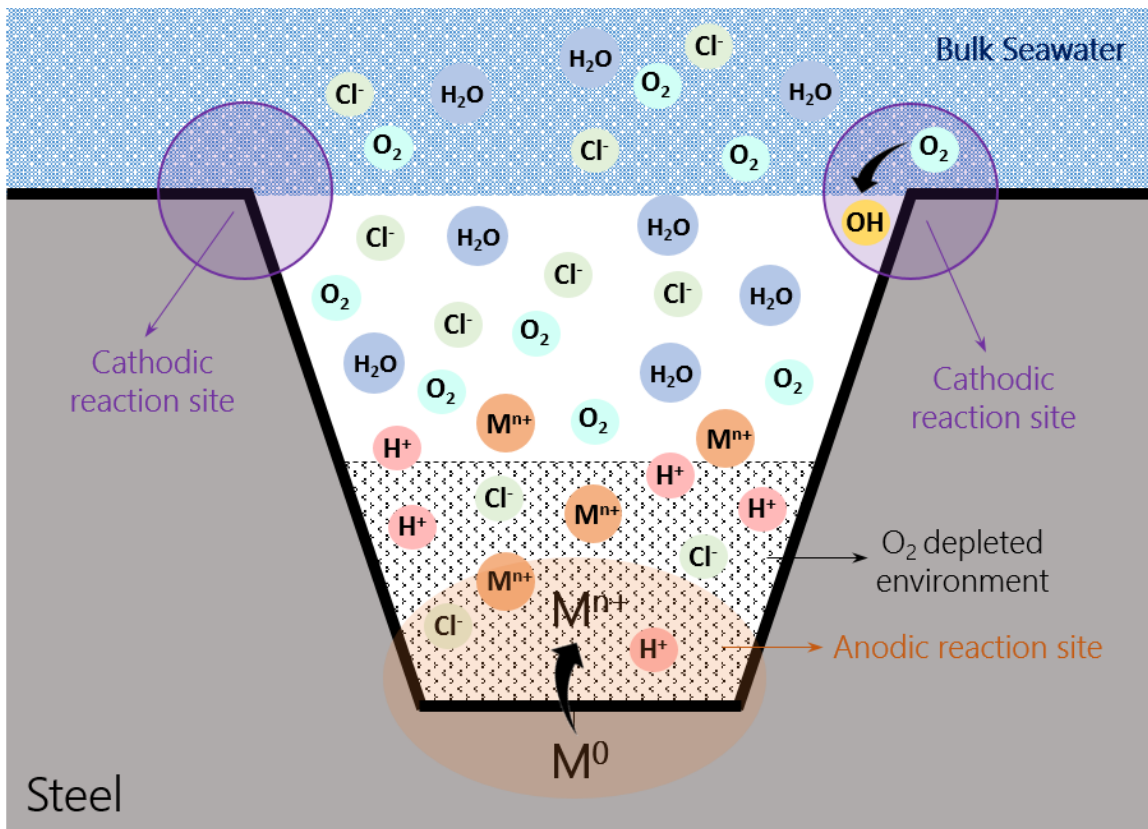


Figure 3-12. Schema of EAC crack generation. The crack tip represent the anodic site, which is depleted in oxygen and concentrated mainly in metal cations, protons and anions. Adaptation from Bland et. Al. (2017)<sup>25</sup>.

As a result of crack tip acidification and metal hydrolysis, phenomena such as hydrogen embrittlement or hydrogen induced stress cracking appear. The presence of hydrogen atoms on the surface of steel degrades some of its mechanical properties, especially its ductility, leading in some cases to embrittlement<sup>27</sup>. Hydrogen atoms are soluble in ferrite and can combine with each other to form hydrogen molecules. As hydrogen molecules are insoluble in the steel structure, high tensile stresses are produced when hydrogen gas molecules are created, which can initiate hydrogen cracking. When laminations are present in steel, hydrogen molecules form at the interface between them, creating blisters<sup>28</sup>.

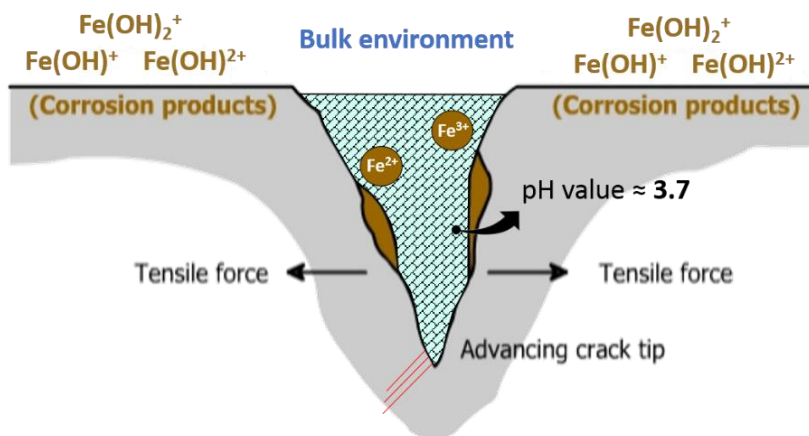


Figure 3-13. Schematic illustration of crack tip acidification, while tensile forces promote crack growing. Figure modified from King Fahd University of Petroleum and Minerals.

### Wear and Fretting

Steel normally presents a high surface hardness, a low friction coefficient and a high resistance to wear. But whenever two components in contact move, and thereby generate friction between them, wear is a potential problem, especially if the surrounding environment is potentially corrosive.

In a mooring line system, the main wear issue is observed in the intergrip between chain links or chains and other components such as shackles or ropes (Figure 3-14). The interaction between sliding metal surfaces, as those found in mooring chains, will cause both surface fatigue wear and corrosion wear, especially in environments such as seawater, where it is considered the main degradation mechanism.

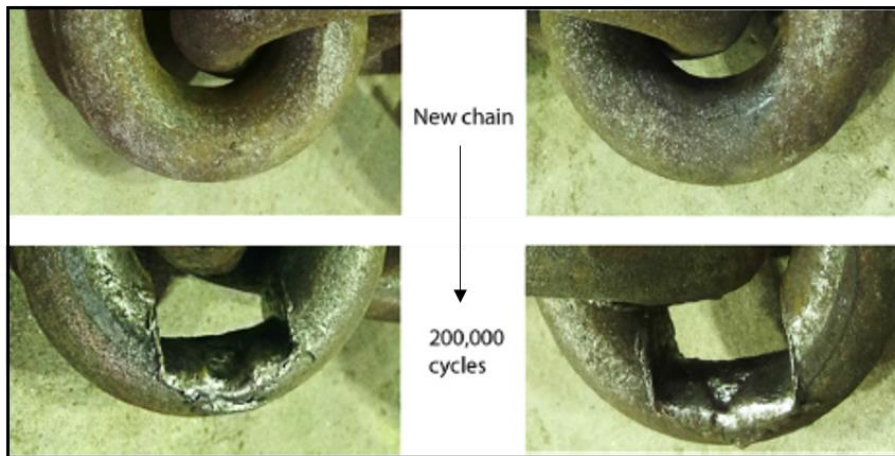


Figure 3-14. Wear in mooring chains under dry conditions. Courtesy of Melchers et. Al. (2015)<sup>29</sup>

The properties of the environment and the way it reacts with the wear surfaces have a huge influence. Per se, wear influence in corrosion rate, apart from the obvious material loss due to erosion, is due to the demands placed on the component. These prevent the protective oxide layers from being deposited on the surface of the metal, and therefore continuously exposing the bare metal to the aggressive environment. It is worth mentioning that, even in seawater, water in the interlink zones decreases the friction or wear coefficient, and thus, according to the results presented by Melchers et. al.<sup>29</sup>, the mass loss due to wear in dry conditions could be up to 6 times greater than in wet conditions (Figure 3-15).

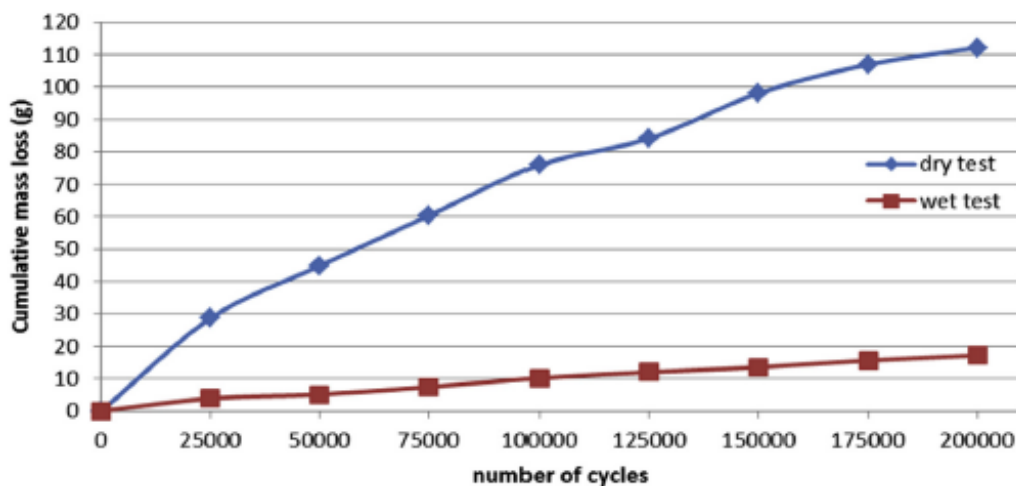


Figure 3-15. Mass loss comparison in mooring chains under dry and wet conditions. Source: Melchers et. Al. (2015)<sup>29</sup>.

Not only wear between chains and links must be considered, but also parallel abrasion phenomena coming from bottom sediments, sand and rocks. The work of Melchers et al.<sup>30</sup> in this field concludes that the phenomena of abrasion and wear must be treated separately from other influence parameters such as pH, temperature and DO content, among others.

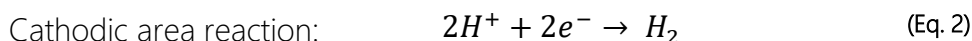
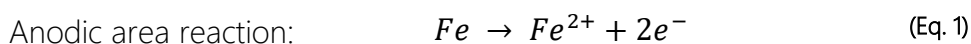
Wear is an effect that must be considered if the steel under consideration has very hard particles, such as large carbide inclusions, or if contact between the components results in the formation of large particles that can become trapped between the surface of interest and act in an abrasive manner<sup>16</sup>. The surface properties of the materials also play a key role in the susceptibility to wear. In fact, wear resistance increases with increasing hardness, as hardness is proportional to the ultimate tensile strength of the steel alloy.

The main effect of wear is the removal of protective oxide deposits from the surface, generating a metal-to-metal wear that exposes bare steel to seawater. As bare steel is more anodic than corrosion products, the dissolution of iron will be promoted and consequently the overall corrosion rate will be increased. Similarly, if deposits are only removed locally, it could cause severe pitting corrosion, worsening the corrosion resistance scenario of the structure.

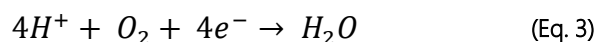
It is worth mentioning that in a tribocorrosion study performed in 2005 at Iwate University of Japan<sup>31</sup>, it was found that subtle  $\text{Cl}^-$  and  $\text{SO}_4^{2-}$  work as anti-wear additives under high load conditions. On the other hand,  $\text{SO}_3^-$  caused accelerated wear. Their results clearly show that the effect of dissolved ions in corrosive wear is clearly different from that of static corrosion, where  $\text{SO}_4^{2-}$  and  $\text{Cl}^-$  are normally considered as harmful elements. But in the field of tribology, it seems that S and Cl compounds act as extreme pressure additives, reducing wear and friction under severe wear sliding conditions by forming an antiwear protective film on the surfaces in contact<sup>32</sup>.

### 3.3.3 Electrochemistry of steel in seawater

Delving a little deeper into the mechanisms of degradation of steel in seawater, they are essentially electrochemical reactions involving electron transfer and oxidation-reduction processes. When iron-based alloys are exposed to seawater electrolytes, metal ions are released to the environment at anodic areas in a chemical equivalency with the reaction at cathodic areas.



This reaction proceeds rapidly in acidic media, but slows down in alkaline or neutral aqueous media, because the corrosion rate is usually controlled by the cathodic reaction<sup>33</sup>. In addition, the cathodic reaction can be promoted by the presence of dissolved oxygen, which reacts with hydrogen atoms adsorbed on the surface of the iron by the oxygen depolarization reaction:



The depolarization reaction removes the hydrogen surrounding the cathode and speeds up the corrosion process and, as a result, water that has a high content of dissolved oxygen is more corrosive than water with a low content of dissolved oxygen<sup>34</sup>. Thus, in aerobic conditions

the oxidation reaction progresses as fast as the oxygen reaches the metal surface. A simple scheme of electrochemical reactions occurring during the corrosion of iron in aerated water is presented in Figure 3-16. This topic will be discussed later in this chapter.

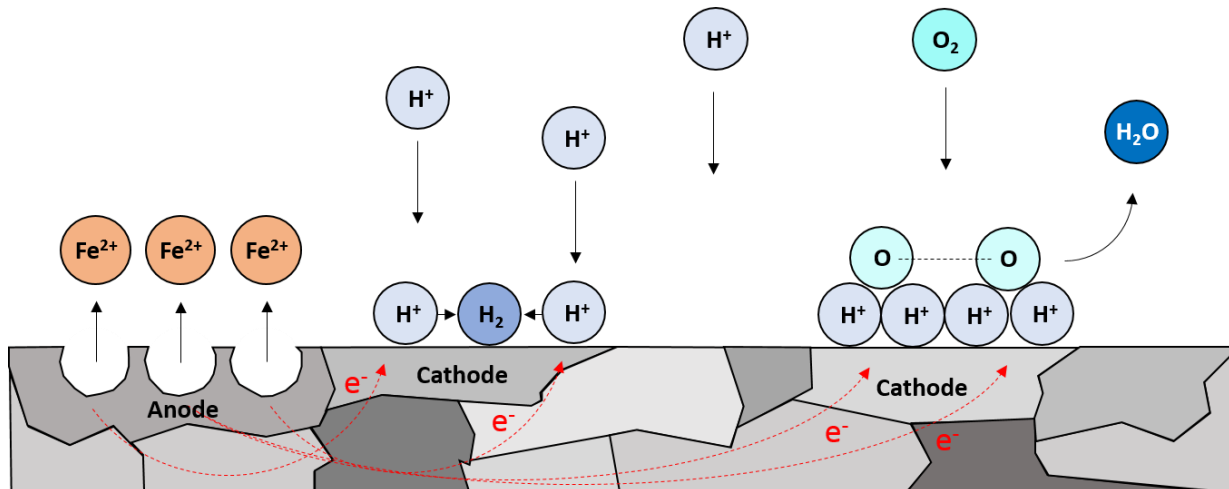


Figure 3-16. Summary of electrochemical reaction of iron in seawater. Adapted from: Roberge (2008)<sup>14</sup>

Corrosion in seawater may be initiated in the chemical concentration cells known as differential aeration cells. The concentration of dissolved oxygen (air) in the anodic region is lower than that in the cathodic regions. This occurs because oxygen is consumed at the metal surface by corrosion reactions, and the oxygen in the electrolyte migrates more rapidly to the exposed regions of the metal than to the less accessible damaged anodic regions. The cathodic reaction - oxygen reduction in this case - is stimulated by the presence of oxygen, so that in the low-oxygen region of the metal, the anodic reaction becomes dominant<sup>35</sup>.

As in any chemical reaction, thermodynamics and kinetic properties are important so that electrons can be transferred from one species to another. The thermodynamics of corrosion processes provide a tool to determine the theoretical tendency of metals to corrode, but cannot predict the corrosion rate<sup>36</sup>. Depending on the nature of the metal, the oxidation reaction may occur uniformly (as in the case of carbon, mild and low-alloy steel) or may be localized as in stainless steel.

### 3.3.4 Corrosion models

In general, environmental degradation is one of the main life-limiting aspects for any structure, and precisely corrosion in seawater is one of the most serious features of aging<sup>37</sup>. As will be discussed further in section 3.4, marine environments are subjected to many factors that influence corrosion, affecting equally every structure or component within the offshore energy production or storage. However, as reviewed in Chapter 2, floating or movable structures can often be repaired and maintained through scheduled conservation programs. Per contra, there are no such procedures for the maintenance of some fixed components at subsea, such as mooring lines or subsea pipelines<sup>38</sup>. Therefore, corrosion tolerance must be carefully considered in the initial design, and it is of great interest to control and model generated degradation over time.

Much research has been done on corrosion modelling throughout the last twenty years. The main purpose is, by means of statistical analysis of field corrosion data, to propose mathematical functions that define time-dependent corrosion models as a function of certain parameters. Depending on the data source, different field applied models can be developed. For example, studies have been conducted on pipeline corrosion, especially regarding to pitting corrosion, by Caley et al.<sup>39,40</sup>, Papavinasam et al.<sup>41</sup>, Heidary et al.<sup>42</sup> and Melchers<sup>43</sup>, as well as on corrosion wastage models for subsea pipelines<sup>38</sup>. Besides, Paik et al. developed an advanced method for the development of a mathematical model that provides statistical characteristics of corrosion waste as a function of time for floating production units and carrier structures<sup>44,45</sup>.

Interesting research has been conducted on modelling physical corrosion. The first physical models were proposed by Evans<sup>46</sup> and Tomashev<sup>47</sup> in the mid 60's. More recently, Chernov<sup>48</sup> and Chernov and Ponomarenko<sup>49</sup> proposed alternative physical models that consider the effect of the environment on corrosion, and suggested that phenomenon of corrosion on metallic surfaces is controlled by diffusion limitation of harmful ions through the layer of corrosion products. Melchers suggested a broader phenomenological model that takes into account kinetic processes, corrosion phases as well as diffusion of the species<sup>50</sup>.

When it comes to reviewing the empirical corrosion models, one of the earliest conducted studies was published by Southwell and Alexander. Their investigation details many controlled corrosion phenomena in tropical waters for stainless steel<sup>51</sup>, ferrous steels<sup>52</sup>, a number of commonly used structural steels<sup>53</sup>, and atmospheric corrosion<sup>54</sup>, among others. Reinhart and Jenkins<sup>55</sup> also reviewed an empirical corrosion model that employed 189 different alloys to dig into the effects of parameters such as water temperature, water depth and oxygen concentration in seawater. They even proposed a linear combination for the calculation of corrosion rate as function of O<sub>2</sub> concentration and temperature for average carbon and low alloy steels. However, this relationship was not adequate for prediction, because factors that were already known to influence corrosion, such as water velocity and sediments, were not considered.

By far, the most extensive empirical study of corrosion models in seawater exposure has been conducted by Robert Melchers. In addition to constantly updated physical corrosion models, Melchers et al. reviewed the effect of seawater parameters on metallic corrosion, such as temperature<sup>56</sup>, bacteriological influence<sup>57</sup>, carbon content<sup>58</sup>, surface profile<sup>59</sup>, water velocity<sup>60</sup>, immersion depth<sup>12</sup>, water pollution<sup>61</sup>, nutrient content<sup>62</sup> and tensile strength<sup>63</sup>.

#### *3.3.4.1 Marine corrosion phenomenological model*

It is important to understand how general corrosion occurs, which in the sea usually takes place in near-surface immersion, and how it varies over time in order to estimate the material loss and thereby the decrease in properties in a given component. General corrosion is the most important form of corrosion for mild and low-alloy steels<sup>50</sup>, which are the primary manufacturing materials for many structural steel applications such as offshore platforms, coastal facilities and mooring lines. It is important to point out that, in addition to general and



uniform corrosion, which reduces component thickness uniformly, pitting and other forms of localized corrosion may also be important.

Back in 1995, Robert Melchers presented a probabilistic model for seawater immersion corrosion of mild and low alloy steels based on fundamental physiochemical corrosion mechanics, showing that corrosion is a nonlinear function of time<sup>64</sup>. Before that, previous efforts to develop corrosion-time models were done, based either on totally empirical models applicable only to situations with similar conditions, or models with theoretical support. Some of those models are introduced in Figure 3-17. Models of Southwell et. al.<sup>52</sup> and Reinhart et al.<sup>55</sup> are limited as their time exposure is too short to validate long term data. In addition, the uncertainty associated with Southwell and Reinhart models is very large, suggesting that purely empirical models are not suitable for predictive purposes<sup>50,64</sup>.

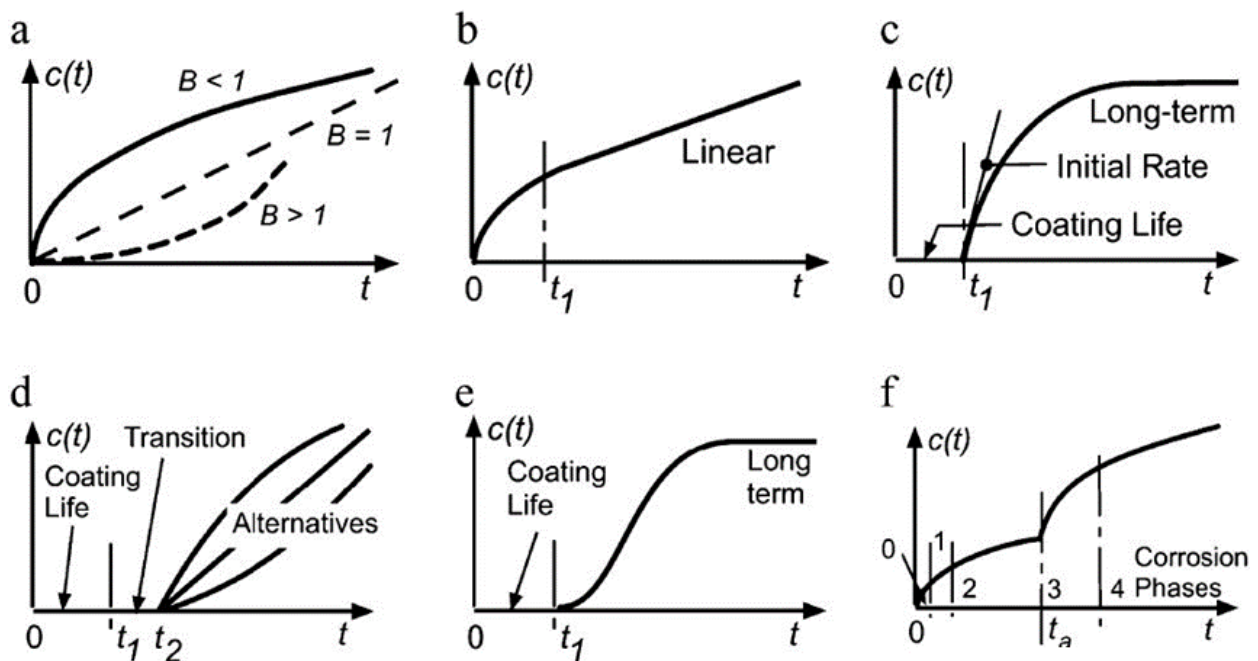


Figure 3-17. Some of the reviewed model overviews. a) Power Law by Tammann. b) Southwell et. al. trend model. c) Guedes Soares model d) Paik model. e) Qin and Cui model. f) Melchers multi-phase model. Figure adapted from Melchers (2019)<sup>65</sup>

Physical corrosion modelling proposed by other authors as Evans<sup>46</sup>, Tomashev<sup>47</sup> and Chernov<sup>48,49</sup> are based on two assumptions:

- Diffusion-controlled oxidation indefinitely rules the corrosion process over time.
- Diffusion-controlled phase starts from the first moment of immersion.

Guedes-Soares and Garbatov<sup>66</sup> proposed a non-linear time dependent corrosion model to account for the effects of salinity, temperature, dissolved oxygen, pH and flow velocity of water (Figure 3-17c). They identified these factors as the main issues affecting corrosion behaviour of steel plates in permanent contact with water. They described metal degradation by a non-linear function of time divided into three stages. At the beginning, it is assumed that there is no corrosion because a corrosion protection system is effective. Failure of the protection system will occur at some point and the corrosion degradation will start a non-linear trend with time.



On the same period, Paik et.al. also proposed a three stage corrosion model for coated/protected structures (Figure 3-17d)<sup>45</sup>. The first stage regards to the coating life, assuming no failures that lead to premature corrosion. The second is the transition when the coating breaks down and corrosion starts, but negligible in terms of corrosion rate. The third stage is a corrosion loss curve with a linear trend that may be subjected to alternative variations dependant of empirical data.

Alternatively, Qin and Cui proposed that the coating protection system deteriorates gradually (Figure 3-17e)<sup>67</sup>. They also assumed that after the coating breakdown, the first signs of corrosion are caused by pitting. In the long term, the corrosion loss is defined in relation to the volume of pitting corrosion and presents that the long-term instantaneous corrosion rate asymptotes to zero due to the accumulation of protective rusts.

Melchers departs from the attempt to model both the loss of protective coatings and the progression of corrosion with time. He states alternatively that long-term corrosion phenomena is composed by a multiphase model, in which each is involved by different factors and ruled by different influences (Figure 3-17f). The complexity of each of the two processes involved (coating deterioration and corrosion phenomena) cannot be summarized in a single model, since they belong to a completely different research domain and must be treated as such, despite the obvious interaction with corrosion when the coating begins to fail<sup>68</sup>.

The life expectancy of most offshore infrastructures is at least two or three decades; therefore, reliable corrosion prediction cannot be based on short-term field observations or laboratory data. The only way to make such predictions is a combination of mathematical models and empirical observations in field data.

Conclusions of the examination of Melchers work on long-term field data showed that in a longer-term trend of marine corrosion a bi-modal output is observed. Subsequent examination of the above influences permitted further development of the model with, for example, the effect of temperature increase<sup>50,56</sup>, the effect of reduced oxygen supply<sup>30</sup>, and the function of alloy composition at each corrosion stage<sup>58,69</sup>. The model has been expanded to include not only immersion conditions but also tidal and coastal marine atmospheric corrosion models, along with a variety of steels<sup>70,71</sup> and reinforced concrete<sup>72,73</sup>. A slight modification of the model is also able to work for materials whose main corrosion form is pitting corrosion<sup>74,75</sup>. Essentially, Melchers' base model is based on the idea that the corrosion process evolves as the layers of rust grow and thicken on the steel surface. This results in a model composed of four phases, from 0 to 4, mainly divided into two: aerobic corrosion-driven phases and anaerobic corrosion-driven phases (Figure 3-18).

The idea in this thesis is to use these corrosion models as a key aspect of the proposed system, since once the corrosion monitoring system starts working and retrieving data, it will be possible to predict the behaviour of the structure and estimate its useful life, without the need to perform unnecessary maintenance. Therefore, a detailed description of each phase has been considered necessary, in order to understand and gather the mechanisms and events associated with each phase.

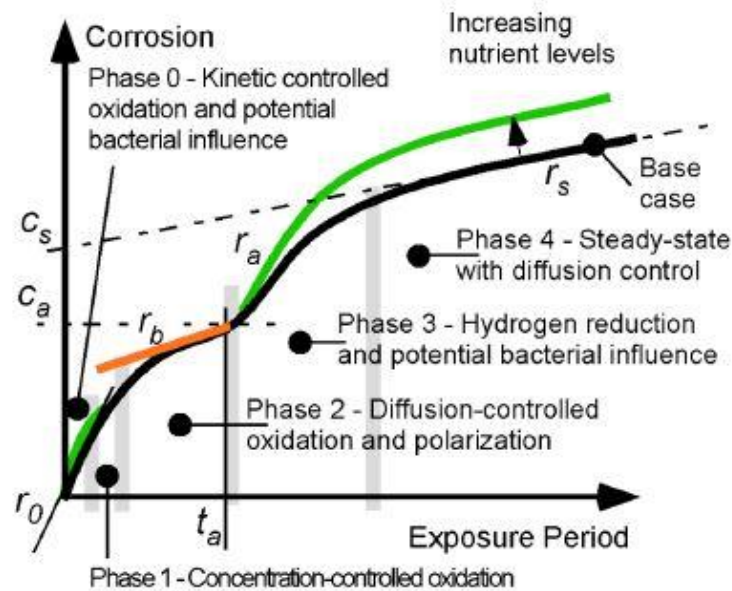


Figure 3-18. Melchers developed seawater corrosion model showing sequential phases as function of exposure period. Source: Melchers (2012)<sup>76</sup>

A summary of the phases is presented in Table 3-2. As stated above, Melchers divides the corrosion phases into two different scenarios, where in one of them the oxygen concentration is vital and in the other practically all the corrosion phenomena is originated in the absence of oxygen.

Table 3-2. Summary of corrosion phases according to the sequence model, with indication of aerobic and anaerobic scenarios.

| Scenario  | Phase | Description of the corrosion rate controlling process       |
|-----------|-------|---|
| Aerobic   | 0     | Electrochemical activity, activation polarization situation |
|           | 1     | Oxygen diffusion through surface surrounding water          |
|           | 2     | Oxygen diffusion through corrosion products                 |
| Anaerobic | 3     | Rapid growth of SRB and hydrogen reduction                  |
|           | 4     | Steady-state situation. SRB-nutrient level influence        |

### Phase 0

This phase is the shortest of all. It is of limited interest as it has little influence on long-term corrosion behaviour<sup>76</sup>. It results in a complex combination of high early abiotic electrochemical activity and polarization of corrosion kinetics driven by the first steps of oxygen diffusion from the bulk water to the steel surface, in a process called concentration polarization<sup>77</sup>. It seems clear, from all the empirical data gathered, that at this phase 0 there is a very high initial corrosion rate followed by a steady decline. The period immediately after immersion involves a rapid invasion of the surface by bio-organisms<sup>78</sup> and the rapid establishment of the anodic and cathodic regions on the surface being corroded<sup>79</sup>. From a theoretical perspective, this period is associated with a first activation control, and then a concentration control, driven by the limited diffusion of oxygen through the bulk water adjacent to the corroding surface<sup>80</sup>.

In this initial phase, the parameter  $r_0$  is defined, which responds to the initial corrosion rate. It is worth mentioning that temperature, nutrient levels and dissolved oxygen concentration play a key role in defining this initial corrosion rate. Immediately after immersion, the steel surface

at the seawater-metal interface is exposed to the full oxygen concentration of the bulk seawater, resulting in a remarkably high initial corrosion rate in a short time, which is not indicative of the long-term behaviour, often leading to misleading estimations of the corrosion rate.

## Phase 1

In this phase the initially formed corrosion product is considered to be uniform over the entire metal surface. This fact is not totally correct since rust tends to accumulate in different non-uniform layers along the surface and depth. Moreover, water velocity influences the settlement of sufficiently thick corrosion layer, since it constantly renews the surface due to erosion phenomena, exposing the bare steel substrate, and also because there is not enough time for anodic and cathodic reactions to take place at the water-metal interface of the surface<sup>81</sup>. On the other hand, angled and cornered structural designs may promote a much faster growth of corrosion products.

This phase 1 is governed by the transport of oxygen from the bulk seawater ( $C_{\text{bulk}}$ ) to the steel interface ( $C_{\text{rust}}$ ), which is consumed immediately on the steel surface and, thereby, defining the moment when  $C_{\text{steel}} = 0$  is reached as the start of the phase 1 (Figure 3-19).  $C_{\text{steel}}$  is defined as the concentration of dissolved oxygen at the corrosion interface between seawater and metal. The oxygen concentration in bulk seawater depends on many factors that will be discussed in section 2.4., but is mainly affected by temperature, depth and salinity<sup>82</sup>.

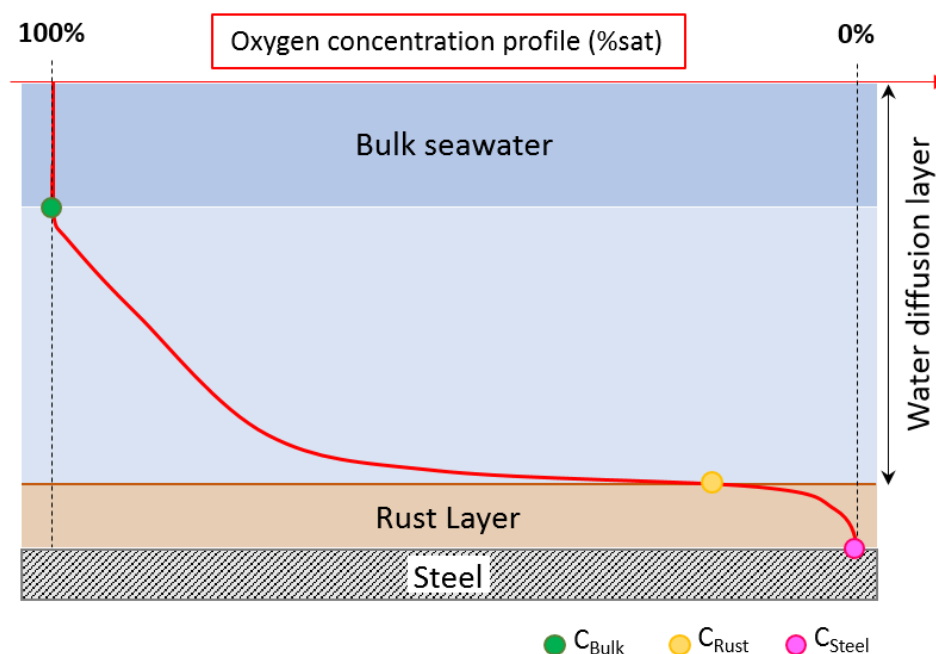


Figure 3-19. Oxygen concentration profiles (%sat) through seawater and rust layer. Adapted from Melchers and Jeffrey (2005)<sup>80</sup>.

In this phase limited by oxygen diffusion, the oxygen consumed at the steel interface will be replenished by transporting oxygen through the thickening rust layer. Initially, the rust layer can be considered negligible and thus,  $C_{\text{steel}} = 0$ , defining the corrosion rate as a linear function of temperature and dissolved oxygen concentration<sup>80</sup>. But as the corrosion product increases

in thickness, an oxygen concentration gradient is generated, and the net oxygen concentration, defined as  $C_{\text{bulk}} - C_{\text{rust}}$ , will be much lower. Eventually, the limiting condition of corrosion will be the rate at which oxygen can diffuse through the rust and fouling layer, diminishing the  $C_{\text{bulk}}$  in favour of the  $C_{\text{rust}}$ , reducing the net corrosion rate and defining the switch from phase 1 to phase 2 in time  $t_d$  (Figure 3-20). It is important to remind that the temperature of seawater plays a key role in the transition from phase 1 to 2, as the transition time from one to the other increases with temperature.

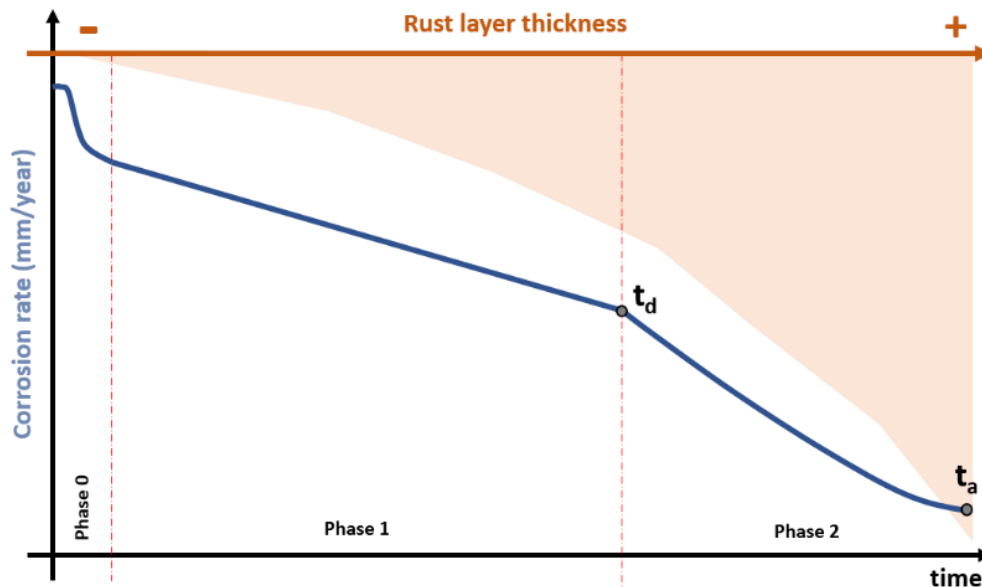


Figure 3-20. Corrosion rate as a function of exposure time and rust layer thickness. Adapted from Melchers and Jeffrey (2005)<sup>80</sup>

In summary, phase 1 (also known as the kinetic phase) is assumed to be a linear function of temperature and dissolved oxygen concentration, governed initially by the activation of the surface in zero phase and then by the oxygen concentration in the steel surface process<sup>50</sup>.

## Phase 2

As the metal surface corrodes further, the corrosion layer will continue to build up. As it can be observed in Figure 3-20, the corrosion rate at this stage is controlled by the slow decrease in the rate of oxygen diffusion through the thicker and thicker rust layers. At point  $t_a$ , shown in Figure 3-20, the rate of oxygen supply to the steel surface is virtually zero, and theoretical anaerobic conditions are reached. In practice, a uniform anaerobic condition is not expected over the entire surface. The non-uniformity of the oxide layer and the bacteria involved in the generation of anaerobic condition, will result in anaerobic conditions reached at different points of the surface at different times<sup>83</sup>. The time interval between  $t_a$  and  $t_d$ , which defines the duration of phase 2, is strongly influenced by the concentration of dissolved oxygen in the metallic surface.

## Phase 3

The increasing difficulty of oxygen diffusion through the rust layer produces anaerobic conditions, allowing the settlement of bacterial activity, such as the sulphate-reducing bacteria (SRB), whose influence will be discussed in chapter 5. The start of phase 3 is often related to a

significant increase in corrosion trend for a short period of time, followed by a gradual decrease in corrosion rate (Figure 3-21).

Wells and Melchers<sup>84</sup> reported that, regarding this first anaerobic phase of the degradation model, the observed corrosion behaviour is largely due to an accumulation of nutrients in the rust layer during phases 1 and 2 and their depletion over time during phase 3 as the stored nutrients migrate to the corrosion interface. Consequently, the rate of bacterial metabolism, which in this phase is directly proportional to the rate of corrosion, depends on the rate of availability of appropriate nutrients.

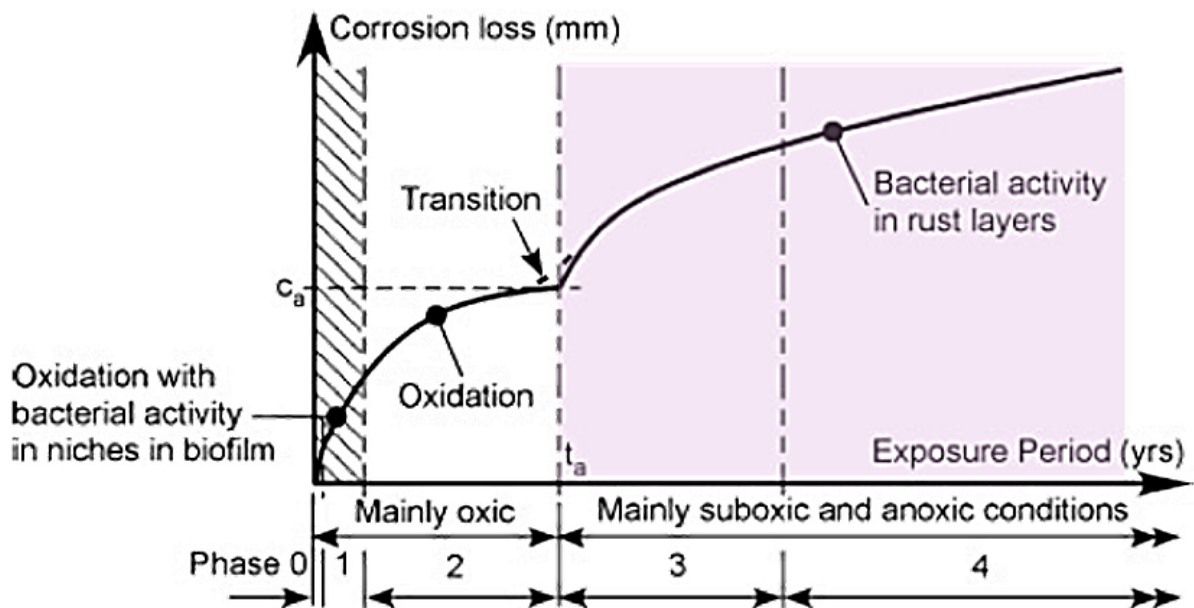


Figure 3-21. Melchers corrosion model with highlighted Phase 3 and 4. Source: Melchers (2010)<sup>85</sup>

The bacterial influence on the environment surrounding the corroding surface depends largely on the type of microorganisms active in the biofilm and their metabolic reactions. Back in phase 0, almost immediately upon exposure, the metal surface generates anoxic niches with bacteria that continue to grow over time. These bacteria proliferate particularly close to the corroding metal, providing suitable conditions for colonization, for example, by the well-known anaerobic sulphate-reducing bacteria (SRB)<sup>76</sup>. The difference in behaviour between phase 0 and phase 3-4 is that during the early phase there is little to impede the diffusion of nutrients to the bacteria from the external environment (supposedly nutrient-rich). This is not the case in phases 3 and 4, where a considerable rust layer is present between the bacteria and the external environment, hindering the diffusion process and, hence, slowing down the corrosion rate.

#### Phase 4

The phase 4 proposed by Melchers may be considered a quasi-steady-state situation, in which sufficient corrosion occurs to replace any loss of corrosion product due to physical erosion and bacterial activity. Moreover, corrosion under these conditions is likely to produce a slightly increased density of oxide layer and, therefore, a slight reduction in permeability over time<sup>84</sup>. Indeed, the presence of FeS in the rust layers, particularly in the region immediately adjacent to the corroding steel, is almost certainly evidence of microbial-induced corrosion resulting

from SRB activity. It has also been noticed that at this phase the hydrogen-reduction reaction produces black magnetite. Usually found at the base of older rusts, it is very adherent to the underlying metal, although it can be quite weak if hydrated, and is easily confused with FeS, which is typically soft and easily removed to reveal surface underneath<sup>76</sup>.

The consumption of nutrients at the corrosion interface will be assumed replenished through the transfer of nutrients from the bulk water to the corrosion surface, thus, controlling the rate of corrosion caused by the SRB metabolites. Nevertheless, SRBs do not attack steel directly but do so indirectly through their metabolites. The settled SRBs metabolize the sulphates present in seawater to produce hydrogen sulphide, which is harmful to steel. This will be discussed in chapter 5. It is worth mentioning that SRB, despite being one of the main biological species growing in such conditions, other bacteria such as ferrous oxidising bacteria (FeOB), are able to flourish and hence contribute to corrosion even before SRB activity<sup>86</sup>.

The transition between phase 3 and 4 is still based today on the assumption that nutrients can diffuse into SRBs to improve their metabolism under anaerobic conditions, although Melchers admits that there is no evidence to support this mechanism<sup>84</sup>.

In the following Figure 3-22 a schematic representation of the transition between the phases is resumed. Metabolites are embedded inside the biofilm every time, but it is only when an anoxic situation is reached that they become relevant and become the main source of corrosion.

### 3.3.5 Steel corrosion products in seawater

It is well known that corrosion products of iron come in a variety of forms. Generated corrosion products mainly rely on the pH and dissolved oxygen concentration of the steel surrounding media. Forrest, Roetheli and Brown reported an extensive review of the composition of corrosion products formed in oxygenated water<sup>87</sup>. They stated that, apart from the composition, the uniformity of oxide layers formed in the corrosion process of steel in aerated water are shown to be important factors in defining the rate of corrosion, as they are the responsible to provide resistance to oxygen diffusion.

For fundamental studies, it is useful to identify the iron oxide species present in the rust layers. Among those which have been extensively reported<sup>88,89,90,91,92</sup> to be present in both atmospheric and coastal corrosion on steel, seven oxide phases are the most common: amid most common oxyhydroxide precipitates, iron oxide-hydroxide (FeOOH) as lepidocrocite ( $\gamma$  polymorph) and goethite ( $\alpha$  polymorph), and the variably hydrated form  $\text{FeOOH}\cdot n\text{H}_2\text{O}$ , ferrihydrite, can be found. Under specific environmental conditions it is also known the formation of species such as Hematite and Maghemite ( $\alpha$  and  $\gamma$ - $\text{Fe}_2\text{O}_3$ ), and the ferrimagnetic  $\text{Fe}_3\text{O}_4$ .

At the beginning of the corrosion process, a thick film of water forms at the steel surface. The  $\text{O}_2$  and NaCl can dissolve in this water film producing an acid electrolyte in which Fe is anodically dissolved to  $\text{Fe}^{2+}$  by the action of the protons (Figure 3-16).



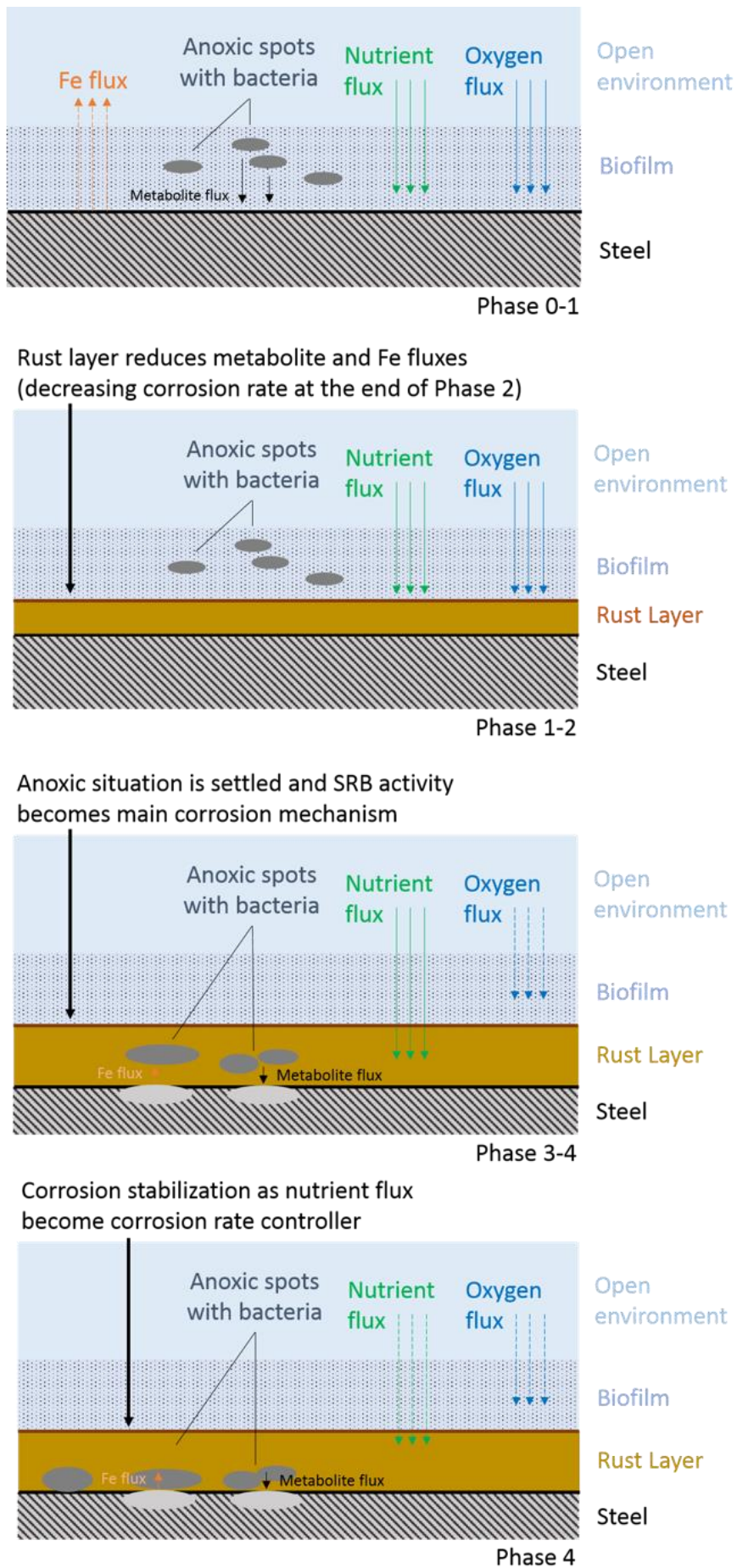


Figure 3-22. Melchers proposed bacteria mechanisms through phases 0 to 4, which supports long-term corrosion model. Adapted from Melchers (2010)<sup>85</sup>.

The  $\text{Fe}^{2+}$  formed is oxidized by the  $\text{O}_2$  of the electrolyte into  $\text{Fe}^{3+}$  which precipitates in the form of the different oxyhydroxides. Studies shown<sup>93</sup> that in the calculation of Fe(II) and Fe(III) percentage in an oxide film,  $\text{Fe}_3\text{O}_4$  is regarded as  $\text{FeO}\cdot\text{Fe}_2\text{O}_3$ . Fe(III) compounds are the primary iron oxidized species, and  $\text{Fe}^{2+}/\text{Fe}^{3+}$  relation increases with acidification due to dissolution of Fe(III), concluding that hydroxides are the primary components of the film in aggressive environments while oxides occupy the main position in less corrosive media<sup>94</sup>.

### 3.4 Main influential factors in corrosion development

Although Melchers further reviewed and developed the major influencing factors of immersion corrosion throughout his academic life, the first report covering the various factors governing corrosion specifically as it relates to metal compositions used in ocean environments was presented by Schumacher in 1979, in the *Seawater Corrosion Handbook*<sup>95</sup>. This section provides a brief abstract of each individual factor, to introduce the exceptional complexity of corrosion processes in open seawater conditions.

#### 3.4.1 Temperature

Water temperature affects corrosion in many ways and is a major influencing factor in the short and long term. It affects kinetic reaction rates, oxygen concentration and diffusion, and acts as a main facet in bacterial metabolism and biological activity. It also affects the solubility of key species such as carbonates and  $\text{CO}_2$ , and precipitation of carbonate species can significantly reduce the corrosion rate of the underlying steel<sup>96</sup>. Although it is difficult to evaluate each factor separately, seawater temperature has a strong influence on each corrosion phase in seawater, especially in the first kinetic phase, and also in the case of the second diffusion-controlled phase. As a general rule, it has been assumed that corrosion doubles for every 10 K increase in temperature in the kinetic phase and every 30 K increase in the diffusion-controlled phase<sup>50</sup>.

Recently, experimental work by Toloei et. al.<sup>97</sup> demonstrated that, as already reported in Melchers<sup>56</sup> and Melchers and Chernov<sup>98</sup>, the corrosion rate increases with increasing temperature in carbon steels. However, it is interesting to mention that as the temperature increases further, a different effect of temperature on the corrosion rate can be observed. Toloei reported that, unlike previous research, in stagnant conditions and as the temperature increases above 40 °C, corrosion rate is decreased (Figure 3-23). The reason given by Toloei et. al is that increasing the temperature to high level causes a decrease in the amount of oxygen concentration in solution and consequently a decrease in the cathodic reaction rate and total corrosion rate. This behaviour was also previously noticed by Mercer and Lumbard<sup>99</sup> in 1995, but they did not further investigate the origin of the phenomenon.



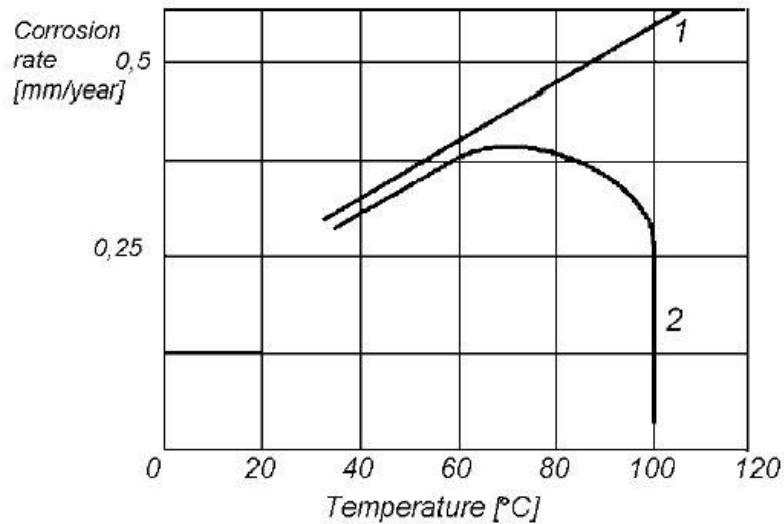


Figure 3-23. Corrosion rate as function of temperature in (1) close system and (2) open water system. Source: Marciniak and Loboda (2010)<sup>100</sup>

In another study conducted by Melchers, Chernov et. al.<sup>101</sup> the kinetic effect of temperature on the corrosion processes is evidenced. They exposed for a certain period of time carbon steel samples both in the temperate Pacific Ocean (Taylors Beach) and in the subarctic seawater (Vladivostok). Empirical results showed that the effect of temperature is noticed from the beginning of the sample immersion, as short-term corrosion losses are about 25 % less in subarctic water but increase up to 60 % less in long-term immersion test (Figure 3-24).

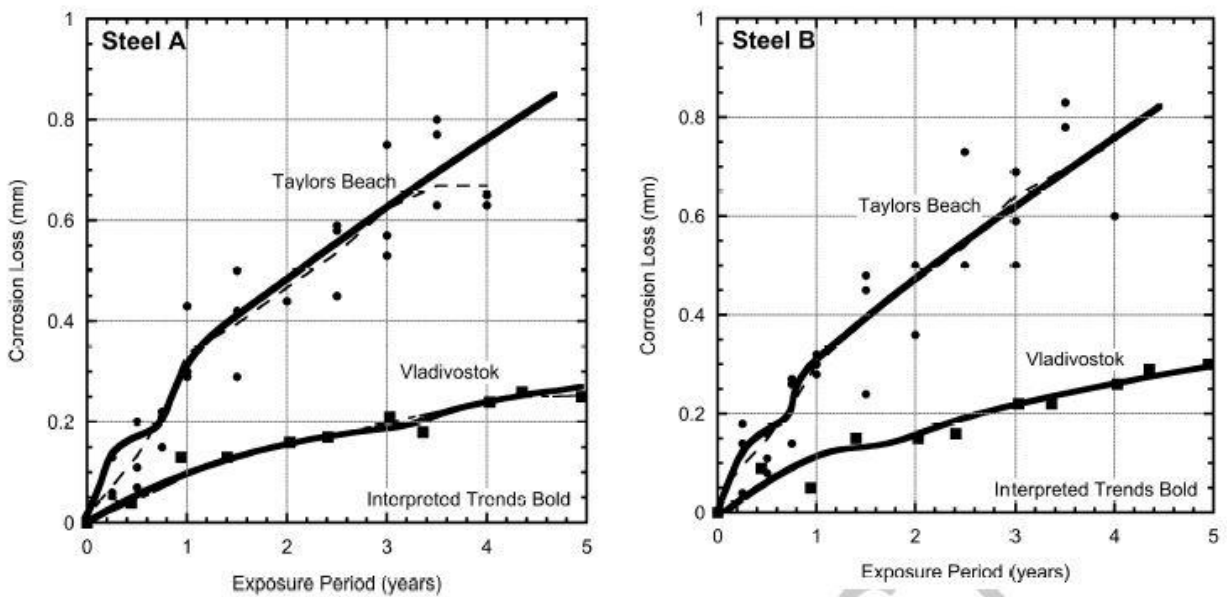


Figure 3-24. Corrosion loss trends in two steel alloys (Steel A and Steel B) and various locations. Notice the lower corrosion loss trend in both alloys in the colder environment. Source: Melchers, Chernov et. al.<sup>101</sup>

Notice in Figure 3-24 that the bimodal (aerobic-anaerobic) corrosion trend also diminishes, if not eliminated, when it comes to cold seawater corrosion, indicating that both the diffusion processes of phase 2 and the bacterial activity of phase 3 and 4 depend largely on the environment temperature. In the case of temperature increase, it appears that the whole model is affected, as reported by Melchers, Jeffrey<sup>74</sup>, and Peng et. al.<sup>102</sup> (Figure 3-25).

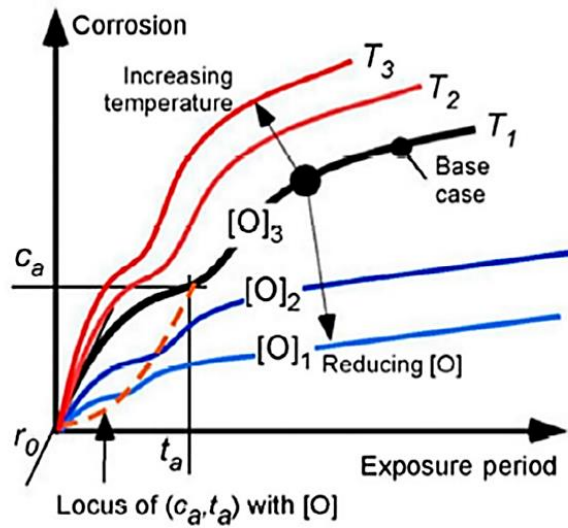


Figure 3-25. Increasing temperature and reducing oxygen concentration effects on Melchers' developed bimodal corrosion model. Source: Peng et. al. (2016)<sup>102</sup>

### 3.4.2 pH

The effect of pH on a given element that exists in seawater is summarized in the predominance diagrams or *Pourbaix* diagrams<sup>103</sup>. However, in the case of iron, knowing the pH of the environment is not enough to predict its state of oxidation. It is also critical to consider whether the surrounding is well aerated, and is therefore oxidizing, or if it is rich in organic waste and is therefore reducing.

Pourbaix diagrams play a fundamental role to understand the problems of steel corrosion in seawater. These diagrams indicate in which combinations of potential (of steel) and pH of the seawater corrosion takes place. The simple Pourbaix diagram (Figure 3-26) is useful for quickly understanding the key features on the diagram. Low potential (E) values represent a reducing environment, while high potential values represent an oxidizing environment. The potential versus Standard Hydrogen Electrode scale is intended to represent the concentration of a reducing agent (electrons) in an analogous way to the pH scale that represents the concentration of protons in the environment.

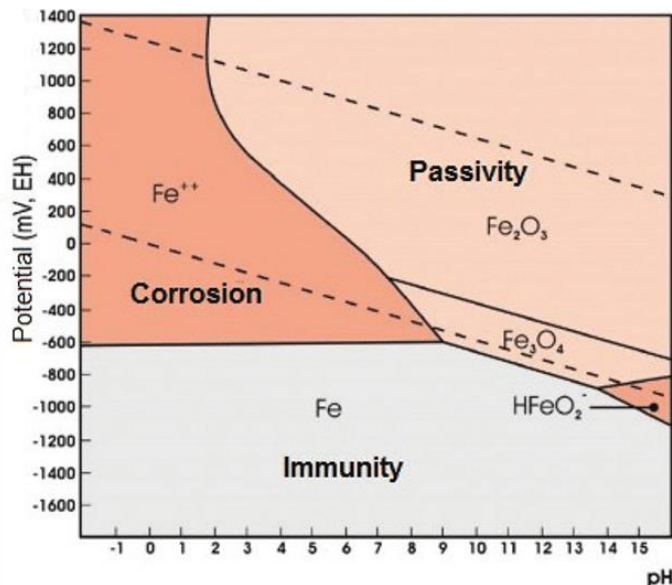


Figure 3-26. Simplified Pourbaix predominance diagram for iron system. Source: Rivetti (2018)<sup>104</sup>

From the Pourbaix predominance diagram the most thermodynamically stable form of iron can be obtained at any potential and pH condition. It allows an overall representation of the oxidising and reducing capacities of the main stable compounds of a given element to be obtained, allowing more accurate predictions of the forms in which the different elements will exist in aqueous media. The diagram also allows predicting the conditions in which corrosion, immunity and passivity are possible. As shown in the previous figure, the term *immunity* is reserved for non-corrosion and represents the case in which corrosion cannot occur for thermodynamic reasons. The term *corrosion* is reserved for the areas of the diagram in which the ionic species in their stable form react thermodynamically, while the *passivity* describes the area in which a solid product is formed, although it must be taken into account that the diagram is not sufficient to decide if a solid reaction product is also protective. Thus, it could be said that the term *passivation* applies to a region of the diagram in which thermodynamic corrosion is possible but might not occur due to the formation of a protective barrier<sup>15</sup>.

Although the pH of sea water is in the range of neutral to slightly alkaline, in corroded materials a local acidity can be developed due to the products of corrosion, lowering the pH up to 4. In general, the parameter pH has a variable effect on the corrosion depending on its value. The corrosion rate is high at lower pH due to acid corrosion, whereas at values of 8.5-12 it descends due to the formation of a passive layer. The sulphate ion present in seawater helps the formation of a corrosion resistant deposit with  $\text{Ca}^{2+}$  and  $\text{Mg}^{2+}$  ions, but at a lower pH this deposit breaks and corrosion rate increases again due to the exposure of the bare metal to the environment<sup>105</sup>. Despite this, the influence of the pH on the corrosion of seawater is best understood if it is explained together with the chloride concentration (Figure 3-27). At a higher chloride concentration, the variation of pH from 4 to 8 does not reflect much effect on the corrosion rate. At a lower level of  $\text{Cl}^-$  ions, the corrosion rate decreases at near neutral to alkaline region of the medium.

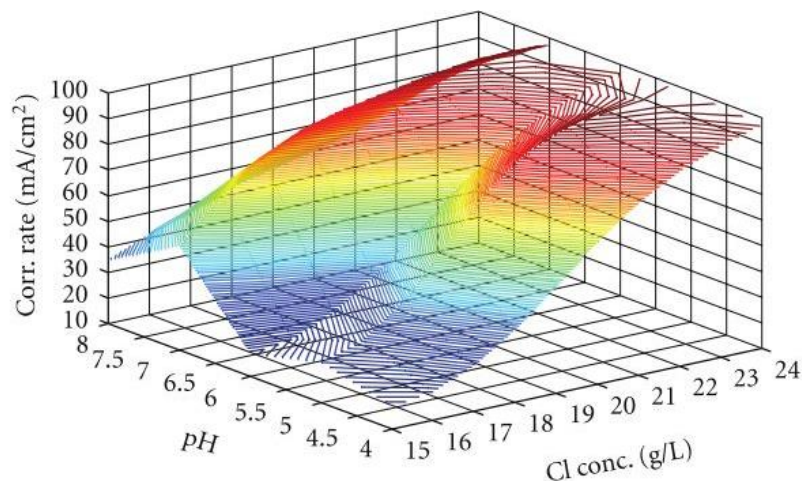


Figure 3-27. Corrosion behaviour of steel in seawater with variation of chlorides concentration at fixed  $\text{SO}_4^{2-}$  concentration of 2 g/L. Figure adapted from Paul Subir (2012)<sup>105</sup>.

### 3.4.3 Dissolved oxygen (DO)

Dissolved oxygen has been shown to increase corrosion rates at the very early stages of seawater exposure<sup>80</sup>, and is indirectly related to the long-term immersion corrosion of steels. The effect of the amount of oxygen as a control factor in the rate of dissolved gas diffusion

into the metal has been raised by Whitman and Russell, where corrosion rates were found to be proportional to the oxygen content over the tested iron specimens. Moreover, the rate of corrosion under natural waters is determined by the rate of oxygen diffusion to an effective cathodic surface and by the protection of the film formed on the metal. The composition and surface condition of the metal are trivial factors in the corrosion of ordinary steels and irons<sup>106</sup>.

Cox and Roetheli<sup>107</sup> studied the effect of oxygen concentration on the corrosion rates of steel and the subsequent corrosion products formed. Short-term studies of steel corrosion rates in water with varying amounts of dissolved oxygen concluded that corrosion rates were almost proportional to the oxygen concentration below 5.5 ppm, while at higher concentrations they were considerably lower, as they no longer follow a linear trend (Figure 3-28). In addition, the decrease in the differential corrosion rate as the oxygen concentrations are higher is due to the gradual formation of corrosion products of a type that exhibits a greater resistance to oxygen transfer to the steel surface. This conclusion was later ratified by Melchers and Jeffrey<sup>80</sup>.

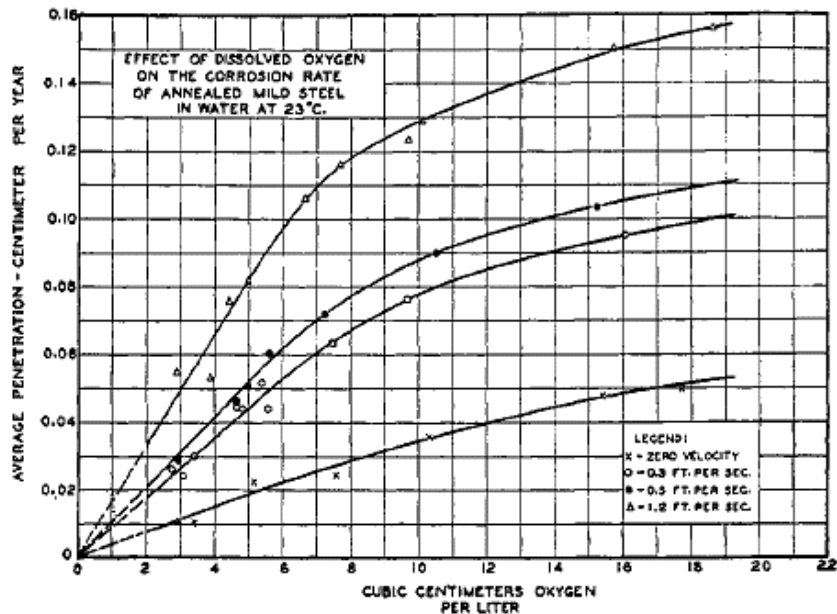
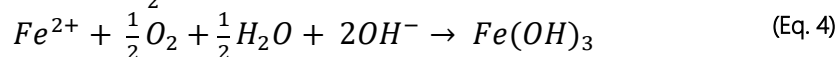
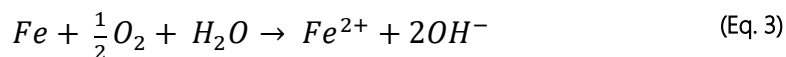
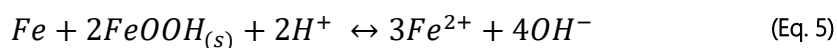


Figure 3-28. Average corrosion rate as function of oxygen concentration and flux velocity. Source: Cox (1931)<sup>107</sup>.

Dissolved oxygen has also demonstrated to increase corrosion rates by promoting bacterial activity and consuming metallic iron as an energy source, aggravating the localised corrosion<sup>108</sup>. Oxygen acts as an electron acceptor in the corrosion of iron, as well as in the oxidation of  $Fe^{2+}$ , according to the following reactions:



Kuch<sup>109</sup> reported that in the absence of oxygen, the ferric deposit  $\gamma$ - $FeOOH$  (lepidocrocite), previously formed in the metal surface as consequence of corrosion, may act as an electron acceptor, dissolving metallic iron into the electrolyte<sup>110</sup>:



This indicates that the corrosion process continues even after the oxygen concentration is depleted. Baek et. al.<sup>111</sup> also concluded that DO level facilitates the formation of different iron

oxide deposits in chloride media:  $\gamma\text{-Fe}_2\text{O}_3$  and  $\text{FeOOH}$  are formed at high DO concentrations while  $\alpha\text{-Fe}_2\text{O}_3$  is preferentially formed in deaerated solutions. In addition, DO helped the growth of the passive layer, and behaved as an oxidant promoting the conversion of divalent  $\text{Fe}_3\text{O}_4$  into the trivalent  $\gamma\text{-Fe}_2\text{O}_3$ . The latter is known to be responsible for the surface passivity of steels.

Oxygen concentration also severely affects the appearance of microbiologically influenced corrosion. Firstly, dissolved oxygen acts as an electron acceptor for cell respiration and bacterial growth, promoting corrosion, since the number of bacteria is directly related to the corrosion rate<sup>108</sup>. Secondly, dissolved oxygen also functions as a cathodic depolariser that affects the electrochemical corrosion process at the metal/seawater interface, and its uneven distribution easily leads to the generation of oxygen concentration cells. These oxygen concentration cells cause many corrosion problems in marine structures, as high oxygen concentration zones become cathodes and low oxygen concentration zones become anodic, setting a permanent oxygen flow to the cathode and thus enhancing localized corrosion<sup>112</sup>.

### 3.4.4 Bacterial activity

Microbiologically influenced corrosion (MIC) can be defined as a corrosion process led by bacteria that causes the degradation of materials, through the interaction of the three main components that constitute this system: the metallic component, the electrolyte and the mentioned biological organisms. The occurrence of MIC in seawater is common due to the very wide availability of microbes, adequate nutrients and corrosive products<sup>113</sup>, and they interact with diverse materials and surfaces in so many ways that make the complexity of the system is too high to be evaluated by standard corrosion model (Figure 3-29)<sup>114</sup>.

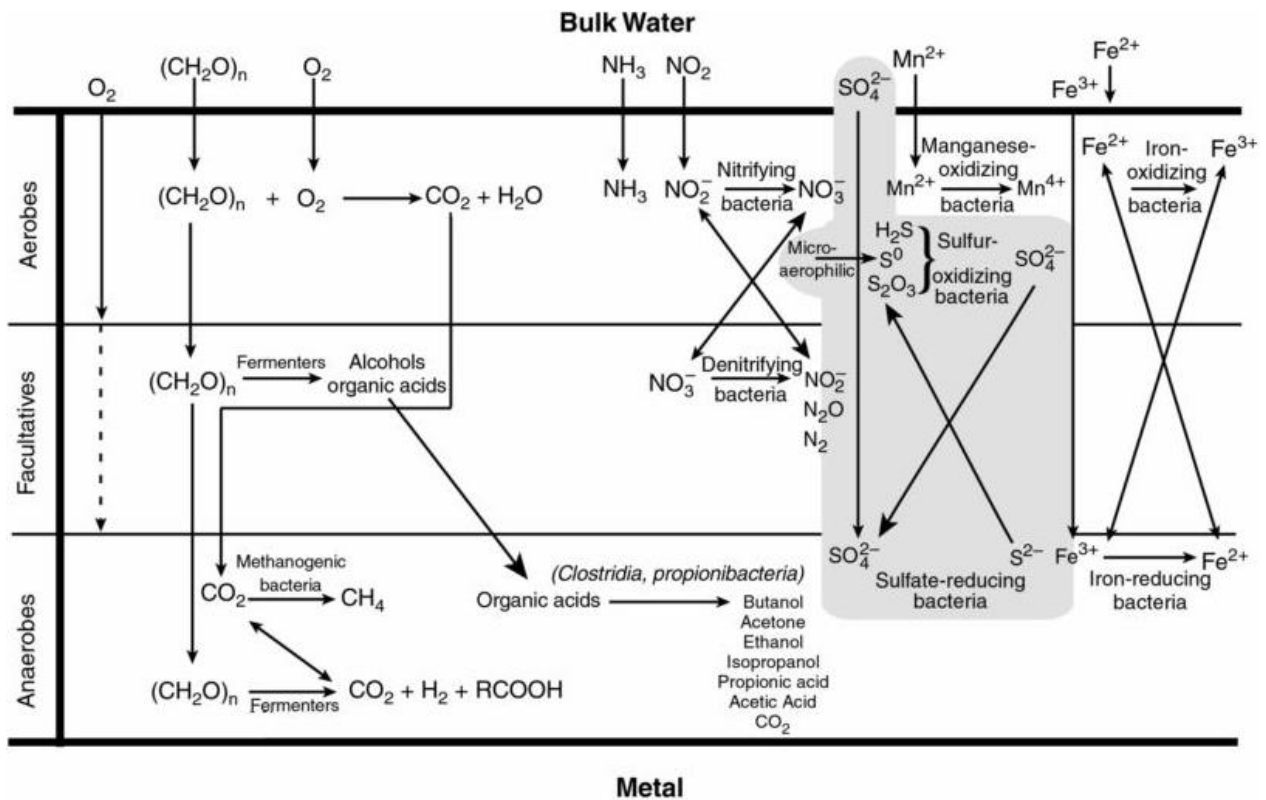


Figure 3-29. Microbial community influence in the corrosion of iron and steel. Sulphate-reducing bacteria mechanism is shown highlighted. Source: Little et. Al. (2000)<sup>115</sup>

The reduction of ferric iron ( $\text{Fe}^{3+}$ ) to ferrous iron ( $\text{Fe}^{2+}$ ) is one of the most important chemical reactions in anaerobic aquatic sediments due to its many consequences for the chemistry of these environments<sup>116</sup>. In marine environments, sulphate-reducing bacteria produce  $\text{H}_2\text{S}$ , which is extremely harmful to the metal surface, which can also reduce iron oxyhydroxides to form iron sulphides<sup>117</sup>. As example, the corrosive action of the sulphate-reducing bacteria (SRB) from the genera *Desulfovibrio desulfuricans* in anaerobic environments has been evaluated as the main role in reducing sulphate ( $\text{SO}_4^{2-}$ ) to sulfide ( $\text{S}^{2-}$ ) and subsequently producing  $\text{H}_2\text{S}$ . The  $\text{H}_2\text{S}$  reacts with the  $\text{Fe}^0$  present on the metal surface, forming  $\text{FeS}$  deposits, which establish a galvanic couple with the steel surface<sup>19</sup>, with the bare steel acting as the anode, and thus establishing an electrical contact by transfer of electrons through the iron sulphide. This mechanism of anaerobic oxidation of iron, also known as cathodic depolarization, is well known in carbon steels through the consumption of atomic hydrogen from the metal surface<sup>118</sup>.

The presence of sulphate-reducing bacteria (SRB) and other types of bacteria, such as iron oxidizing bacteria, has been identified as the main cause for multiple corrosion problems in seawater<sup>113</sup>. When they are found in aqueous solution, a fast surface colonization is produced forming a cover that attacks the metal surface, replicating and producing exopolymers (EPS). As a consequence, a cohesive structure called biofilm is formed, whose average thickness increases overtime, and also affecting the dissolved oxygen concentration in the metal surface (Figure 3-30). This biofilm can be considered as a gel containing more than 95% of water and EPS, in which microbial cells and inorganic detritus are suspended<sup>18</sup>.

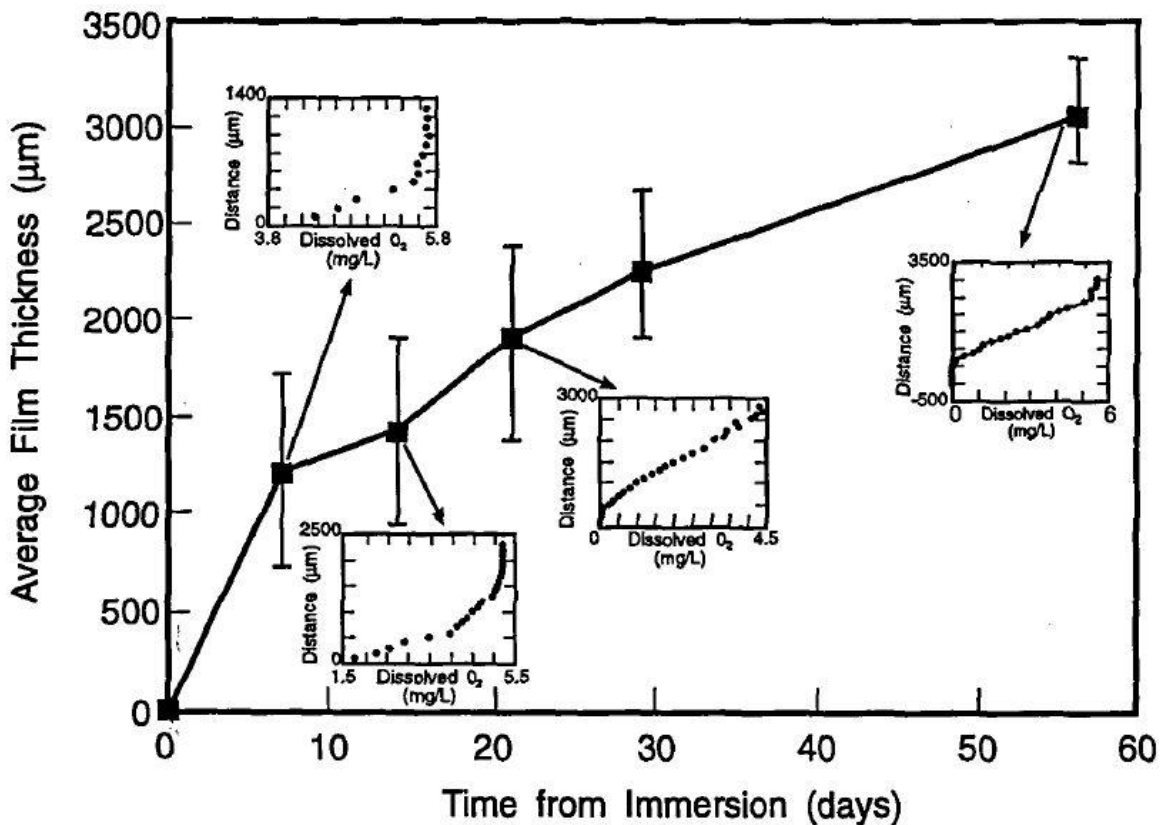


Figure 3-30. Progression of biofilm deposit thickness with corresponding DO profiles in function of time. Reproduced from Lee et. Al. (1993)<sup>119</sup>

The role of biofilms in enhancing corrosion in a metallic surface may proceed through simultaneous or successive mechanisms including<sup>18</sup>:

- Altering the diffusion barrier for certain chemical species, for example, preventing the diffusion of oxygen to cathodic areas and promoting diffusion of chloride anions to anodic sites.
- Facilitating the removal of protective coatings where biofilm is deposited, by altering the structure of inorganic passive layers and increasing their dissolution and removal from the metal surface.
- Inducing differential aeration effects because of a non-uniform distribution of the biofilm, resulting in the formation of differential aeration cells, and consequently, promoting localized corrosion under the biofilm distribution.
- Changing oxidation–reduction conditions at the metal–solution interface, due to the close relationship between the metabolic activity of the biofouled surface and the redox conditions. Indeed, SRB, which need a reducing environment to grow, can proliferate at the bottom of biofilms despite a measurable dissolved oxygen concentration in the bulk water.

Although sulphate reduction is thought to be an anaerobic process, microorganisms are known to be an important part of corrosion in aerobic environments if they can proliferate in aerated zones<sup>120</sup>. This becomes possible when aerobic organisms form a biofilm and then, through their metabolism, create an anaerobic microenvironment with the organic acids and nutrients necessary for the growth of the sulphate-reducing bacteria.

Corrosive biofilms generally include extensive mineral deposits of corrosion products (e.g., FeS, FeCO<sub>3</sub> and FeCl<sub>2</sub>). Moreover, most of the MIC phenomena are manifested as localized corrosion and can take the form of pitting, crevice corrosion, under-deposit corrosion, and de-alloying. Most organisms do not form a continuous film on the metal surface<sup>121</sup>, as they tend to settle on metal surfaces in the form of discrete colonies or in spotty areas, instead of continuous films. This enhances galvanic and erosion corrosion.

Indeed, it is well known that biological activity within the formed rust layer can consume oxygen and also produce it. As mentioned above, oxygen in the very early stages of corrosion can diffuse through the corrosion products and marine biofouling layers<sup>80</sup>. Then, a point is reached where there is no longer oxygen supply to the corroding surface and the generated rust layer plus bacterial and organic matter involved in the reaction generates an anaerobic driven degradation condition. In addition, anaerobic bacteria are known to prosper in conditions with some remaining aerobic bacteria as these keep providing energy sources coming from the sulphur cycle<sup>115</sup>.

### 3.4.5 Water flow

The influence of water velocity is very similar to the degradation mechanism observed in erosion processes, where the protective (or passive) oxide layer on the steel surface is dissolved due to the water mass movement. The underlying metal corrodes to re-create the protective oxide film, and thus the metal loss continues, enhancing corrosion of the steel if there is a strong dependence between the thickness of the oxide layer and the corrosion rate. Nevertheless, experimentally the protective film formed in the corrosion of steel in oxygenated water in a system permitting a low rate of stirring is considerably less protective than the film formed in a similar system in which the water is kept rapidly stirred<sup>107</sup>.

As mentioned before in section 2.2, surface ocean currents, strongly influenced by wind, appear to reach a peak of about 1 m/s at the equator, decreasing with increasing latitude and

reaching velocities of about 0.5 m/s<sup>122</sup>. On the contrary, deep ocean currents are slower, with a typical speed of 1 cm/s, but this flow extends to the seafloor and forms circulation patterns that envelop the global ocean<sup>123</sup>. Recent field tests conducted in near-surface conditions showed that water velocity has a particular effect on the corrosion time function plots. It is observed that as the seawater velocity increases, the overall corrosion increases. In the very early corrosion processes, the relationship appears to be linear, although it becomes progressively nonlinear as the water velocity increases<sup>12</sup>. Increasing time of exposure, the influence of the water velocity becomes gradually less significant, although the initial short-term influence is maintained (Figure 3-31).

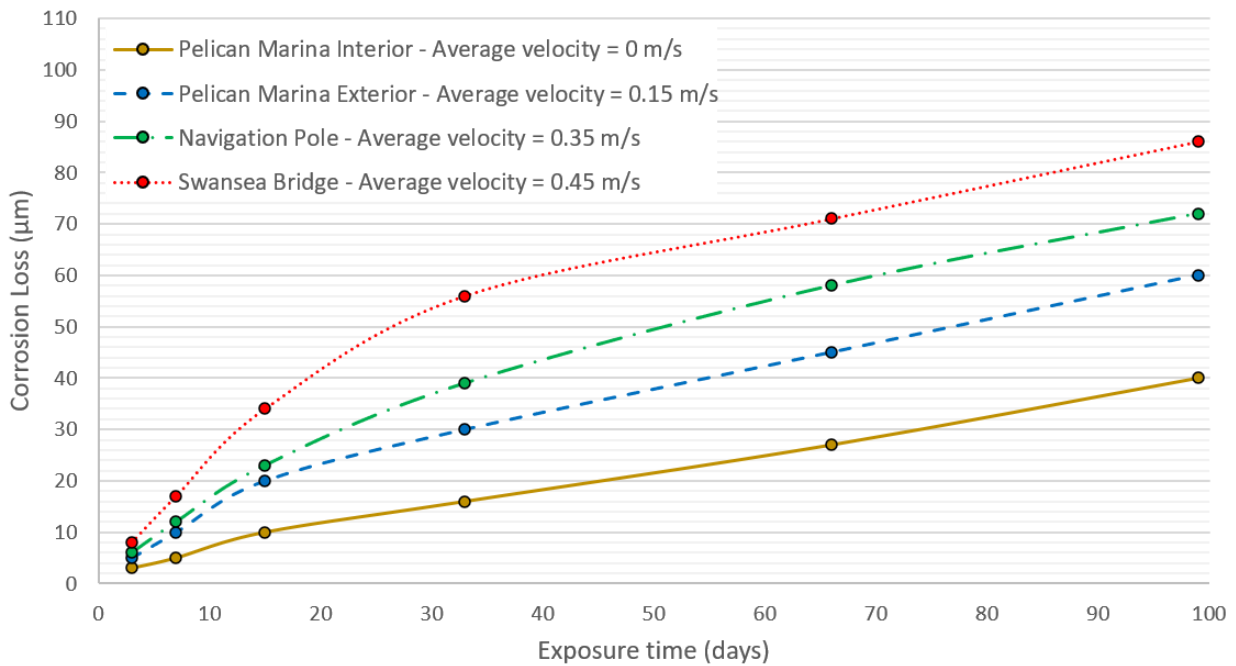


Figure 3-31. Water flow effect on early (100 days) corrosion. Reproduced from Melchers.<sup>12</sup>

Water flow and wave action are two factors whose consequences are normally considered in the same way, as they influence corrosion with similar mechanisms. The availability of oxygen on a steel surface will be promoted by the flow of water, which renews the water mass near the structure of interest. It is worth mentioning that high speed water action can damage biofilms, marine growth and corrosion deposits, thus influencing the corrosion mechanisms. Apart from facilitating the aeration of the metal surface, water flow will enhance nutrient replenishment, allowing more adhered and better adapted organisms to continue carrying out their metabolic cycle, and therefore, affecting the overall corrosion rate.

### 3.4.6 Surface roughness

The inherent vulnerability of steel to corrosion depends largely on the microstructural homogeneity of the material. This involves a fine structure for grains and inclusions, a homogeneous chemical composition and phase structure, and even an adequate and standardised heat treatment. On a surface with a high degree of homogeneity, there will exist short distances between the anodic and cathodic sites, so it is less likely that their location persists in the same spot avoiding, up to a limited degree, pitting corrosion. The precipitation of the oxides will also be homogeneous, ensuring a strong and adherent protective layer<sup>16</sup>. This fact is of special importance, as if the oxide films are continuous and with good adherence,



such as magnetite ( $\text{Fe(II,III)O}_4$ ) and haematite ( $\text{Fe}_2\text{O}_3$ ), corrosion can be reduced (Figure 3-32). However, if small areas of steel are exposed while large areas are covered by these oxides, since they are more noble than steel, localised corrosion will be promoted in those areas where the bare steel is shown.

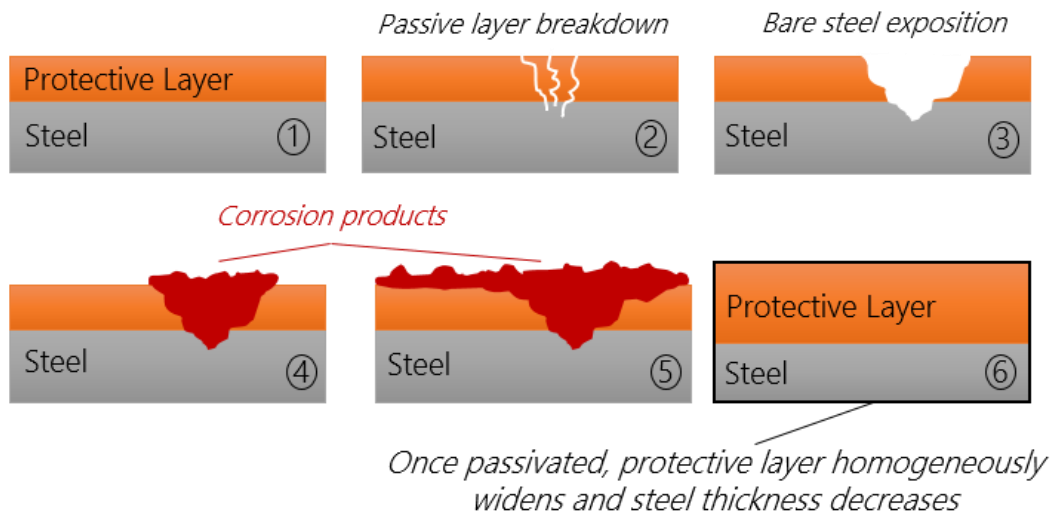


Figure 3-32. Oxide layer breakdown steps and further re-passivation of the protective layer.

## Bibliography

---

1. *Corrosion Books: Corrosion Mechanisms in Theory and Practice. Materials and Corrosion* vol. 54 (CRC Press, 2003).
2. *Hilti Corrosion Handbook*. (2015).
3. Boyd, W. K. & Fink, F. W. *Corrosion of Metals in Marine Environments*. (1977).
4. *ASM Metals Handbook Volume 13 - Corrosion*. (ASM International, 1992).
5. Mackenzie, F. T., Bryne, R. H. & Duxbury, A. C. Seawater. *Encyclopaedia Britannica* (2018).
6. *Corrosion Handbook Online*. (Wiley-VCH, 2008).
7. Sverdrup, H. U., Johnson, M. W. & Fleming, R. H. Chemistry of Seawater. in *The Oceans. Their Physics, Chemistry and General Biology*. 165–227 (Prentice-Hall, inc., 1942).
8. Lalli, C. & Parsons, T. The Abiotic Environment. in *Biological Oceanography: An Introduction* 16–38 (Butterworth-Heinemann, 1997). doi:10.1016/B978-075063384-0/50002-5.
9. aqua.nasa.gov.
10. Powell, C. *The corrosion performance of metals for the marine environment: a basic guide*. (Maney Publishing, European Federation of Corrosion, NACE International, 2012). doi:10.1201/9780429298387.
11. NOAA. What is a thermocline? <https://oceanservice.noaa.gov/facts/thermocline.html>.
12. Melchers, R. E. Effect on Immersion Depth on Marine Corrosion of Mild Steel. *Corrosion* **61**, 895–906 (2005).
13. Kingsford, M. J. Marine ecosystem. *Enciclopedia Britannica* (2018).
14. Roberge, P. R. *Corrosion Engineering: Principles and Practice*. (McGraw-Hill, 2008). doi:10.1177/0340035206070163.
15. *Uhlig's Corrosion Handbook*. (John Wiley & Sons, Inc., 2011).
16. Eriksen, M. & Brown, M. G. The effect of wear and corrosion of steel components on the integrity of mooring systems for floating offshore installations. (2017).
17. Basic Understanding of Weld Corrosion. in *Corrosion of Weldments* (ed. Davis, J. R.) 1–13 (ASM International, 2006). doi:10.1361/corw2006p001.
18. Videla, H. A. & Herrera, L. K. Microbiologically influenced corrosion: looking to the future. *Int. Microbiol.* **8**, 169–180 (2005).
19. Enning, D. & Garrelfs, J. Corrosion of Iron by Sulfate-Reducing Bacteria: New Views of an Old Problem. *Appl. Environ. Microbiol.* **80**, 1226–1236 (2014).
20. Javaherdashti, R. *Microbiologically Influenced Corrosion*. (Springer International Publishing, 2017).
21. Dubiel, M., Hsu, C. H., Chien, C. C., Mansfeld, F. & Newman, D. K. Microbial iron respiration can protect steel from corrosion. *Appl. Environ. Microbiol.* **68**, 1440–1445 (2002).
22. Duan, J. *et al.* Corrosion of carbon steel influenced by anaerobic biofilm in natural seawater. *Electrochim. Acta* **54**, 22–28 (2008).
23. Kaesche, H. *Die Korrosion der Metalle. Die Korrosion der Metalle* (Springer-Verlag Berlin, 2011). doi:10.1007/978-3-642-18428-4.
24. Komai, K. Corrosion Fatigue. in *Comprehensive Structural Integrity* (eds. Milne, I., Ritchie, R. O. & Karihaloo, B.) vol. 4 345–358 (Elsevier, 2003).
25. Bland, L. G. & Locke, J. S. Chemical and electrochemical conditions within stress corrosion and corrosion fatigue cracks. *Mater. Degrad.* **12**, 1–8 (2017).
26. Sandoz, G., Fujii, C. T. & Brown, B. F. Solution chemistry within stress-corrosion cracks in alloy steels. *Corros. Sci.* **10**, 839–845 (1970).
27. Gangloff, R. P. Hydrogen assisted cracking of high strength alloys. in *Comprehensive Structural Integrity* (eds. Milne, I., Ritchie, R. O. & Karihaloo, B.) vol. 6 31–101 (Elsevier Science, 2003).
28. Schofield, M. J. Corrosion. in *Plant Engineer's Reference Book* (ed. Snow, D.) 33–1, 33–25 (Butterworth-Heinemann, 2002). doi:10.1201/b11339-18.
29. Lotfollahi Yaghin, A. & Melchers, R. E. Long-term inter-link wear of model mooring chains. *Mar. Struct.* **44**, 61–84 (2015).
30. Melchers, R. E., Moan, T. & Gao, Z. Corrosion of working chains continuously immersed in seawater. *J. Mar. Sci. Technol.* **12**, 102–110 (2007).
31. Iwabuchi, A., Uchidate, M., Liu, H., Miura, T. & Shimizu, T. *The effect of dissolved ions on tribological properties in water. Tribology and Interface Engineering Series* vol. 48 (Elsevier Masson SAS, 2005).

32. Frêne, J., Nicolas, D., Degueurce, B., Berthe, D. & Godet, M. Lubricating oils. in *Tribology Series* (ed. Dowson, D.) vol. 33 27–46 (Elsevier, 1990).
33. Roberge, P. R. Aqueous Corrosion. in *Handbook of Corrosion Engineering* (eds. Esposito, R. & Fogarty, D.) 15 (McGraw-Hill, 2000).
34. Speight, J. G. Corrosion. in *Oil and Gas Corrosion Prevention. From Surface Facilities to Refineries* e1–e24 (Gulf Professional Publishing, 2014). doi:10.1016/B978-0-12-800346-6.00001-6.
35. Syrett, B. C. Corrosion, Crevice. in *Encyclopedia of Materials: Science and Technology* 1680–1681 (Pergamon, 2001).
36. Popoola, A., Olorunniwo, O. & Ige, O. Corrosion Resistance Through the Application of Anti- Corrosion Coatings. in *Developments in Corrosion Protection* (ed. Aliofkhazraei, M.) 241–270 (IntechOpen, 2014). doi:10.5772/57420.
37. Paik, J. K. & Thayamballi, A. K. Corrosion Assessment and Management. in *Ship-shaped offshore installations - design, building and operation*. 356–399 (Cambridge University Press, 2007).
38. Mohd, M. H., Kim, D. K., Kim, D. W. & Paik, J. K. A time-variant corrosion wastage model for subsea gas pipelines. *Ships Offshore Struct.* **9**, 1–15 (2013).
39. Caley, F., Velázquez, J. C., Valor, A. & Hallen, J. M. Probability distribution of pitting corrosion depth and rate in underground pipelines: A Monte Carlo study. *Corros. Sci.* **51**, 1925–1934 (2009).
40. Velázquez, J. C., Caley, F., Valor, A. & Hallen, J. M. Predictive model for pitting corrosion in buried oil and gas pipelines. *Corrosion* **65**, 332–342 (2009).
41. Papavinasam, S., Doiron, A. & Revie, R. W. Model to predict internal pitting corrosion of oil and gas pipelines. *Corrosion* **66**, 0350061–03500611 (2010).
42. Heidary, R., Gabriel, S. A., Modarres, M., Groth, K. M. & Vahdati, N. A review of data-driven oil and gas pipeline pitting corrosion growth models applicable for prognostic and health management. *Int. J. Progn. Heal. Manag.* **9**, 1–13 (2018).
43. Chaves, I. A. & Melchers, R. E. Pitting corrosion in pipeline steel weld zones. *Corros. Sci.* **53**, 4026–4032 (2011).
44. Paik, J. K., Lee, J. M., Hwang, J. S. & Park, Y. I. A time-dependant corrosion wastage model for structures of single/double hull tankers and FSOs/FPSOs. *Mar. Technol. Soc. J.* **40**, 201–217 (2003).
45. Paik, J. K., Thayamballi, A. K., Park, Y. I. & Hwang, J. S. A time-dependent corrosion wastage model for bulk carrier structures. *Int. J. Marit. Eng.* **145**, 61–87 (2003).
46. Evans, U. R. *The Corrosion and Oxidation of Metals: Scientific Principles and Practical Applications*. (Edward Arnold Publisher Ltd., 1966).
47. Tomashev, N. D. *Theory of Corrosion and Protection of Metals*. (The MacMillan Co., 1966).
48. Chernov, B. B. Predicting the corrosion of teels in seawater from its physiochemical characteristics. *Prot. Met.* **26**, 238–241 (1990).
49. Chernov, B. B. & Ponomarenko, S. A. Physiochemical modeling of metal corrosion in seawater. *Prot. Met.* **27**, 612–615 (1991).
50. Melchers, R. E. Modeling of Marine Immersion Corrosion for Mild and Low-Alloy Steels — Part 1: Phenomenological Model. *Corrosion* **59**, 319–334 (2003).
51. Alexander, A. L., Southwell, C. R. & Forgeson, B. W. Corrosion of metals in tropical environments. Part 5 - Stainless Steel. *Corrosion* **17**, 97–104 (1961).
52. Southwell, C. R. The corrosion rates of structural metals in sea-water, fresh water and tropical atmospheres. Summary of a sixteen-year exposure study. *Corros. Sci.* **9**, 179–183 (1969).
53. Southwell, C. R., Alexander, A. L. & Forgeson, B. W. Corrosion of metals in tropical environments. Part 3 - Underwater Corrosion of Ten Structural Steels. *Corrosion* **16**, 87–96 (1960).
54. Southwell, C. R., Alexander, A. L. & Forgeson, B. W. Corrosion of metals in tropical environments. Part 2 - Atmospheric Corrosion of Ten Structural Steels. *Corrosion* **14**, 55–57 (1958).
55. Reinhart, F. M. & Jenkins, J. F. *Corrosion of Materials in Surface Seawater after 12 and 18 Months of Exposure. Technical Note N-1213*. <https://apps.dtic.mil/docs/citations/AD0743872> (1972).
56. Melchers, R. E. Effect of temperature on the marine immersion corrosion of carbon steels. *Corrosion* **58**, 768–782 (2002).
57. Jeffrey, R. & Melchers, R. E. Bacteriological influence in the development of iron sulphide species in marine immersion environments. *Corros. Sci.* **45**, 693–714 (2003).
58. Melchers, R. E. Effect on marine immersion corrosion of carbon content of low alloy steels. *Corros. Sci.* **45**,

- 2609–2625 (2003).
59. Melchers, R. E. & Jeffrey, R. Surface “roughness” effect on marine immersion corrosion of mild steel. *Corrosion* **60**, 697–703 (2004).
  60. Melchers, R. E. & Jeffrey, R. Influence of Water Velocity on Marine Immersion Corrosion of Mild Steel. *Corrosion* **60**, 84–94 (2004).
  61. Melchers, R. E. The effects of water pollution on the immersion corrosion of mild and low alloy steels. *Corros. Sci.* **49**, 3149–3167 (2007).
  62. Melchers, R. E. Influence of seawater nutrient content on the early immersion corrosion of mild steel - Part 1: Empirical observations. *Corrosion* **63**, 318–329 (2007).
  63. Melchers, R. E. & Paik, J. K. Effect of tensile strain on the rate of marine corrosion of steel plates. *Corros. Sci.* **51**, 2298–2303 (2009).
  64. Melchers, R. E. Probabilistic Modeling of Marine Corrosion of Steel Specimens. in *5th International Offshore and Polar Engineering Conference* 205–210 (ASME International, 1995).
  65. Melchers, R. E. Predicting long-term corrosion of metal alloys in physical infrastructure. *Mater. Degrad.* **3**, 1–7 (2019).
  66. Soares, C. G., Garbatov, Y., Zayed, A. & Wang, G. Non-linear corrosion model for immersed steel plates accounting for environmental factors. in *2005 SNAME Maritime Technology Conference and Expo and Ship Production Symposium* (ed. Wang, G.) 193–212 (ABS Technical Papers, 2006).
  67. Qin, S. & Cui, W. Effect of corrosion models on the time-dependent reliability of steel plated elements. *Mar. Struct.* **16**, 15–34 (2003).
  68. Melchers, R. E. Development of new applied models for steel corrosion in marine applications including shipping. *Ships Offshore Struct.* **3**, 135–144 (2008).
  69. Melchers, R. E. Effect of small compositional changes on marine immersion corrosion of low alloy steels. *Corros. Sci.* **46**, 1669–1691 (2004).
  70. Melchers, R. E. Principles of Marine Corrosion. in *Springer Handbook of Ocean Engineering* 111–126 (2016). doi:10.1007/978-3-319-16649-0\_6.
  71. Melchers, R. E. Long-term corrosion of cast irons and steel in marine and atmospheric environments. *Corros. Sci.* **68**, 186–194 (2013).
  72. Melchers, R. E. Long-term durability of marine reinforced concrete structures. *J. Mar. Sci. Eng.* **8**, (2020).
  73. Melchers, R. E. & Chaves, I. A. A comparative study of chlorides and longer-term reinforcement corrosion. *Mater. Corros.* **68**, 613–621 (2017).
  74. Melchers, R. E. & Jeffrey, R. J. Probabilistic models for steel corrosion loss and pitting of marine infrastructure. *Reliab. Eng. Syst. Saf.* **93**, 423–432 (2008).
  75. Melchers, R. E. Pitting corrosion of mild steel under marine anaerobic conditions - Part 1: Experimental observations. *Corrosion* **62**, 981–988 (2006).
  76. Melchers, R. E. Modeling and prediction of long-term corrosion of steel in marine environments. *Int. J. Offshore Polar Eng.* **22**, 257–263 (2012).
  77. Melchers, R. E. Modelling long term corrosion of steel infrastructure in natural marine environments. in *Understanding Biocorrosion: Fundamentals and Applications* 213–241 (Woodhead Publishing Limited, 2014). doi:10.1533/9781782421252.2.213.
  78. Dang, H. & Lovell, C. R. Microbial Surface Colonization and Biofilm Development in Marine Environments. *Microbiol. Mol. Biol. Rev.* **80**, 91–138 (2016).
  79. Al-Moubaraki, A. H., Al-Judaibi, A. & Asiri, M. Corrosion of C-steel in the red sea: Effect of immersion time and inhibitor concentration. *Int. J. Electrochem. Sci.* **10**, 4252–4278 (2014).
  80. Melchers, R. E. & Jeffrey, R. Early corrosion of mild steel in seawater. *Corros. Sci.* **47**, 1678–1693 (2005).
  81. Shikshak, A. A. Al, Mansour, A. A. & Taher, A. Effect of Flow Velocity of Sea Water on Corrosion Rate of Low Carbon Steel. *Appl. Mech. Mater.* **799–800**, 232–236 (2015).
  82. Wetzel, R. G. Oxygen. in *Limnology* 151–168 (Academic Press, 2001). doi:10.1017/CBO9781107415324.004.
  83. Melchers, R. & Jeffrey, R. The critical involvement of anaerobic bacterial activity in modelling the corrosion behaviour of mild steel in marine environments. *Electrochim. Acta* **54**, 80–85 (2008).
  84. Melchers, R. E. & Wells, T. Models for the anaerobic phases of marine immersion corrosion. *Corros. Sci.* **48**, 1791–1811 (2006).
  85. Melchers, R. E. Transient early and longer term influence of bacteria on marine corrosion of steel. *Corros. Eng. Sci. Technol.* **45**, 257–261 (2010).

86. Emerson, D. The role of iron-oxidizing bacteria in biocorrosion: a review. *Biofouling* **34**, 989–1000 (2018).
87. Forrest, H. O., Roetheli, B. E. & Brown, R. H. Products of Corrosion of Steel. *Ind. Eng. Chem.* **23**, 650–653 (1931).
88. Antunes, R. A., Ichikawa, R. U., Martinez, L. G. & Costa, I. Characterization of corrosion products on carbon steel exposed to natural weathering and to accelerated corrosion tests. *Int. J. Corros.* **2014**, 419570 (2014).
89. de la Fuente, D. *et al.* Characterisation of rust surfaces formed on mild steel exposed to marine atmospheres using XRD and SEM/Micro-Raman techniques. *Corros. Sci.* **110**, 253–264 (2016).
90. Oh, S. J., Cook, D. C. & Townsend, H. E. Characterization of iron oxides commonly formed as corrosion products on steel. *Hyperfine Interactions* vol. 112 59–66 (1998).
91. García, K. E., Morales, A. L., Barrero, C. A. & Greneche, J. M. New contributions to the understanding of rust layer formation in steels exposed to a total immersion test. *Corros. Sci.* **48**, 2813–2830 (2006).
92. Zhang, X., Yang, S., Zhang, W., Guo, H. & He, X. Influence of outer rust layers on corrosion of carbon steel and weathering steel during wet-dry cycles. *Corros. Sci.* **82**, 165–172 (2014).
93. Cui, Z. *et al.* Passivation behavior and surface chemistry of 2507 super duplex stainless steel in artificial seawater: Influence of dissolved oxygen and pH. *Corros. Sci.* **150**, 218–234 (2019).
94. Liu, C. T. & Wu, J. K. Influence of pH on the passivation behavior of 254SMO stainless steel in 3.5% NaCl solution. *Corros. Sci.* **49**, 2198–2209 (2007).
95. Schumacher, M. M. *Seawater Corrosion Handbook*. (Noyes Data Corporation, 1979).
96. Sun, W., Nešić, S. & Woollam, R. C. The effect of temperature and ionic strength on iron carbonate (FeCO<sub>3</sub>) solubility limit. *Corros. Sci.* **51**, 1273–1276 (2009).
97. Toloei, A., Atashin, S. & Pakshir, M. Corrosion rate of carbon steel under synergistic effect of seawater parameters including pH, temperature, and salinity in turbulent condition. *Corros. Rev.* **31**, 135–144 (2013).
98. Melchers, R. E. & Chernov, B. B. Corrosion loss of mild steel in high temperature hard freshwater. *Corros. Sci.* **52**, 449–454 (2010).
99. Mercer, A. D. & Lombard, E. A. Corrosion of mild steel in water. *Br. Corros. J.* **30**, 43–55 (1995).
100. Marciniak, R. & Loboda, M. Influence of climatic conditions on corrosion of earth electrodes for lightning protection. in *30th International Conference on Lightning Protection, ICLP 2010* (IEEE, 2010). doi:10.1109/ICLP.2010.7845949.
101. Chernov, B. B., Chaves, I. A., Nugmanov, A. M. & Melchers, R. E. Corrosion performance of low alloy steels in sub-arctic natural seawater. *Corrosion*.
102. Peng, L., Stewart, M. G. & Melchers, R. E. Corrosion and capacity prediction of marine steel infrastructure under a changing environment environment. *Struct. Infrastruct. Eng.* 1–14 (2016) doi:10.1080/15732479.2016.1229798.
103. Courtney, A. *Chemistry Course Materials*. (1997).
104. Sousa Rivetti, M. L., Andrade Neto, J. da S., de Amorim Júnior, N. S. & Ribeiro, D. V. Corrosion Inhibitors for Reinforced Concrete. in *Corrosion Inhibitors for Reinforced Concrete* (ed. Aliofkhaezai, M.) 35–58 (IntechOpen, 2018). doi:10.5772/intechopen.72772.
105. Paul, S. Modeling to Study the Effect of Environmental Parameters on Corrosion of Mild Steel in Seawater Using Neural Network. *ISRN Metall.* **2012**, 1–6 (2012).
106. Whitman, W. G. & Russell, R. P. The submerged corrosion of iron. *J. Soc. Chem. Ind. Trans.* **XLIII**, 193T–199T (1924).
107. Cox, G. L. & Roetheli, B. E. Effect of Oxygen Concentration on Corrosion Rates of Steel and Composition of Corrosion Products Formed in Oxygenated Water. *Ind. Eng. Chem.* **23**, 1012–1016 (1931).
108. Qian, H. *et al.* Effect of dissolved oxygen concentration on the microbiologically influenced corrosion of Q235 carbon steel by Halophilic Archaeon *Natronorubrum Tibetense*. *Front. Microbiol.* **10**, 1–12 (2019).
109. Kuch, A. Investigations of the reduction and re-oxidation kinetics of iron(III) oxide scales formed in waters. *Corros. Sci.* **28**, 221–231 (1988).
110. Eyu, G. D., Will, G., Dekkers, W. & MacLeod, J. Effect of dissolved oxygen and immersion time on the corrosion behaviour of mild steel in bicarbonate/chloride solution. *Materials (Basel)*. **9**, (2016).
111. Baek, W. C., Kang, T., Sohn, H. J. & Kho, Y. T. In situ surface enhanced Raman spectroscopic study on the effect of dissolved oxygen on the corrosion film on low carbon steel in 0.01 M NaCl solution. *Electrochim. Acta* **46**, 2321–2325 (2001).
112. Schafer, G. J., Gabriel, J. R. & Foster, P. K. On the Role of the Oxygen Concentration Cell in Crevice Corrosion and Pitting. *J. Electrochem. Soc.* **107**, 1002–1004 (1960).

113. Loto, C. A. Microbiological corrosion: mechanism, control and impact—a review. *Int. J. Adv. Manuf. Technol.* **92**, 4241–4252 (2017).
114. Dall’Agnol, L. T. & Moura, J. J. G. Sulphate-reducing bacteria (SRB) and biocorrosion. in *Understanding Biocorrosion: Fundamentals and Applications* 77–106 (Woodhead Publishing Limited, 2014). doi:10.1533/9781782421252.1.77.
115. Little, B. J., Ray, R. I. & Pope, R. K. Relationship between corrosion and the biological sulfur cycle: A review. *Corrosion* **56**, 433–443 (2000).
116. Lovley, D. R., Holmes, D. E. & Nevin, K. P. Dissimilatory Fe (III) and Mn (IV) reduction. *Microbiol. Rev.* **55**, 259–287 (1991).
117. Coleman, M. L., Hedrick, D. B., Lovley, D. R., White, D. C. & Pye, K. Reduction of Fe(III) in sediments by sulphate-reducing bacteria. *Nature* **361**, 436–438 (1993).
118. Von Wolzogen Kühr, C. A. H. & Van der Vlugt, L. S. Graphitization of Cast Iron as an Electro-Biochemical process in anaerobic soils. *Water* **18**, 147–165 (1934).
119. Lee, W. *et al.* Corrosion of mild steel underneath aerobic biofilms containing sulfate-reducing bacteria part II: At high dissolved oxygen concentration. *Biofouling* **7**, 217–239 (1993).
120. Santegoeds, C. M. *et al.* Structural and Functional Dynamics of Sulfate-Reducing Populations in Bacterial Biofilms. *Appl. Environ. Microbiol.* **64**, 3731–3739 (1998).
121. Little, B. J. & Lee, J. S. *Microbiologically Influenced Corrosion*. (Wiley-Interscience, 2007).
122. Shirah, G. OSCAR Ocean Currents with Velocity. *NASA/Goddard Space Flight Center Scientific Visualization Studio* <https://svs.gsfc.nasa.gov/3958> (2012).
123. Cenedese, C. & Gordon, A. L. Ocean current. *Encyclopaedia Britannica* (2018).

# 4

---

## Corrosion protection, an overview

---

- Passive protection - Barrier coatings
- Active protection, ICCP and GACP
- Material selection



# I

As seen in the previous two chapters, corrosion is the main concern of metallic materials in terms of degradation. Although concrete and composite materials also suffer from degradation under the influence of environment, the present thesis is focused on metallic materials. This chapter aims to gather corrosion control and mitigation strategies existing nowadays, as well as to highlight the benefits and cost saving value of corrosion monitoring and integrity management. It will also be given an overview of the main commercially available solutions, as well as the most commonly adopted ones, as:

- Coating protection
- Cathodic Protection
- Structural Design and Material selection

The use of protection systems in a structure or in a key component is essential to ensure the expected life in service for which the structure was originally designed. Among protection systems, two approaches are differentiated: passive corrosion protection with barrier coatings pretends to isolate the metal from the corrosive environment; while an active approach focuses on reducing the corrosion rate by influencing the reactions that proceed during corrosion. Being an important part of the existing resources against corrosion, this section will quote and describe what corrosion protection is about and which strategies should be adopt depending on each scenario.

Essentially, coatings provide a barrier between the corrosive media and the metal substrate, providing resistance from physical, chemical, and biological degradation. Coating application is the most used form of corrosion protection strategy nowadays, but no system can be considered perfect or flawless. Since chemical and anti-ageing stability can be depleted over time<sup>1</sup>, the properties of a coating must remain constant under service conditions as long as possible without the need for repairs, providing long-term corrosion protection.

A coating is rated on the resistance it provides against corrosion in a specific environment, and due to many different scenarios in environment corrosivity, there is also a great variety of corrosion protective coatings. The different corrosion protection strategies are summarized in the following diagram (Figure 4-1). In order to choose the best protection strategy, it is necessary to analyse the different coating damages that may take place. A review of damages as function of the different zones in the offshore asset is presented in Table 4-1, independently of the protective mechanisms<sup>2</sup>.

## 4.1 Barrier Coatings (Passive Protection)

As mentioned before, passive corrosion protection with barrier coatings works by isolating the metal substrate from the corrosive media. In the scenario studied in this thesis the harmful media is seawater. Therefore, presented solutions are the ones used in offshore applications, named as marine coatings.



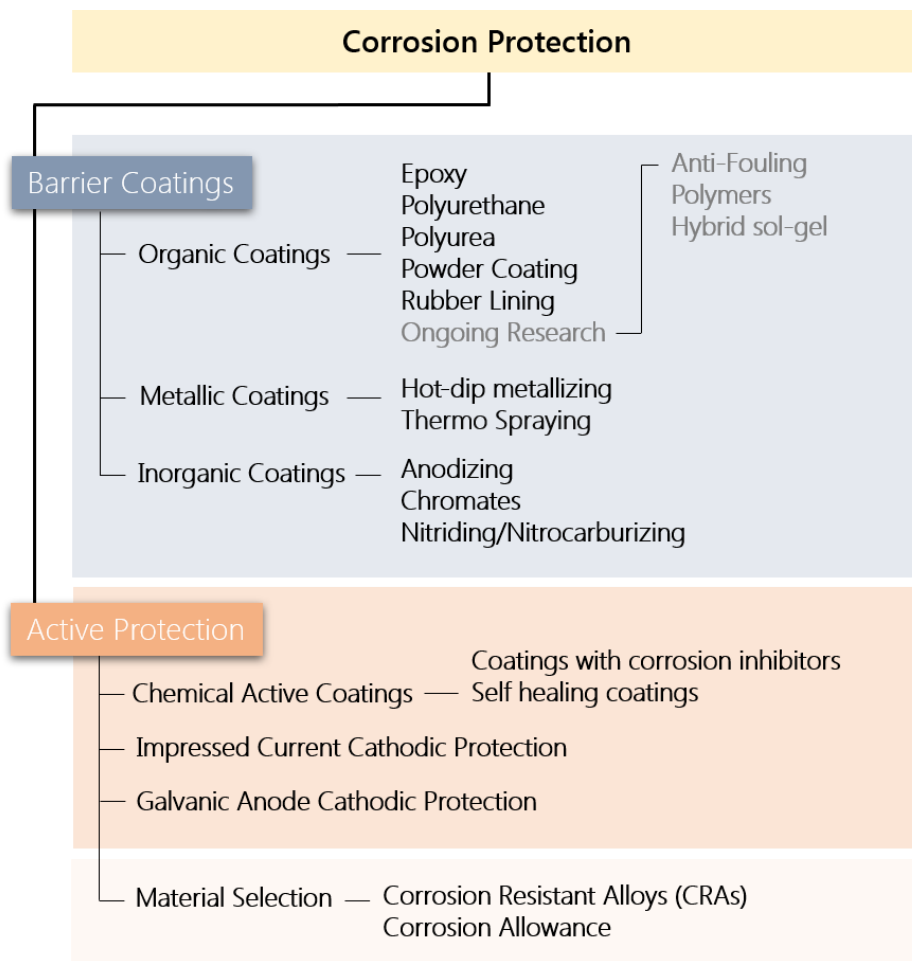


Figure 4-1. Scheme of corrosion protection strategies.

Marine coatings serve two main functions: Synergically, they prevent the deterioration of materials caused by the exposition to the marine environment and impart physical and chemical properties to surfaces that cannot be obtained in any other way<sup>3</sup>.

Table 4-1. Involved degradation phenomena as function of the offshore zone. Adapted from Momber et. al. (2018)<sup>2</sup>.

| Involved Phenomena   | Zone               |               |              |                  |               |                 |
|----------------------|--------------------|---------------|--------------|------------------|---------------|-----------------|
|                      | <i>Atmospheric</i> | <i>Splash</i> | <i>Tidal</i> | <i>Immersion</i> | <i>Buried</i> | <i>Internal</i> |
| Abrasion             |                    | X             | X            |                  | X             |                 |
| Cathodic disbondment |                    | X             | X            | X                |               | X               |
| Condensation         |                    |               |              |                  |               | X               |
| Colour loss          | X                  | X             | X            |                  |               |                 |
| Corrosion            | X                  | X             | X            | X                | X             | X               |
| Fouling              |                    | X             | X            | X                |               | X               |
| Gloss loss           | X                  | X             | X            |                  |               |                 |
| Icing                | X                  | X             | X            |                  |               |                 |
| Impacts              |                    | X             | X            |                  |               |                 |
| Microbial            |                    |               | X            | X                | X             | X               |
| <b>Total</b>         | <b>4</b>           | <b>8</b>      | <b>9</b>     | <b>4</b>         | <b>3</b>      | <b>5</b>        |

The main characteristic of the marine environment is constant moisture with variable salinity, ranging from high-salinity seawater to low-salinity rain and condensation. This, beside the constant spray and splash of water and constant wetting and drying cycles, causes materials

to be degraded much more rapidly offshore than onshore. Surface temperatures may range from below 0 °C to as high as 75 °C for a dark surface on a sunny day. The thermal shock caused by alternating exposure to hot sun, cold seawater, and rain severely stress materials used in the marine environment<sup>3</sup>.

One of the critical factors to be considered in applying a coating is the adhesion. Adhesion properties of the coating are not protection mechanisms in themselves, but they are vital for the longevity of the coating, as poor adhesion results in rapid failure of the coating<sup>4</sup>. Coatings normally consist of several layers of different types<sup>5</sup>, summarised in Figure 4-2.

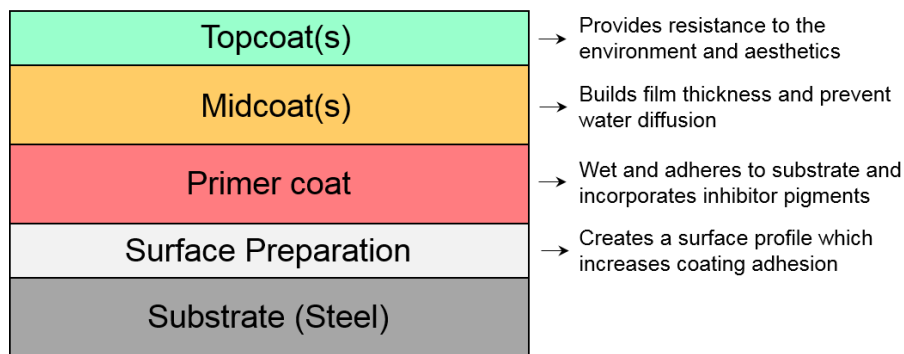


Figure 4-2. Scheme of different coating layers and their main function.

**Primer coat:** The primer is considered to be one of the most important elements of a protective system, whose main functions are:

- Strong adhesion to the substrate surface.
- Cohesion and internal strength.
- Inert to the environment.
- Strong bonding to the midcoat.
- Appropriate flexibility.

Primers for steel are usually classified according to the main corrosion inhibitive pigments used in their formulation, e.g., *zinc phosphate primers* and *metallic zinc primers*, etc. Each of these inhibitive pigments can be incorporated into a range of binder resins, giving for example *zinc phosphate epoxy primers*. These inhibitory pigments are composed of inorganic or organic compounds that are slightly soluble in water, and cause chemical reactions that prevent the corrosion reaction<sup>6</sup>.

**Midcoat:** Intermediate coats are employed in coating systems that benefit from thickness, building the total film thickness of the coating, normally with multiple paint layers. Midcoat is where, for example, pigments are added, giving coatings a heavy body that works well for the most demanding applications. The primary purposes of an intermediate coat are:

- Increase thickness of the protective coating.
- Give strong chemical resistance.
- Improve resistance to water diffusion.
- Increase cohesion and provide strong bonding to primer and topcoat.

**Topcoat:** Finishing coatings provide the sealing over the intermediate coats and the primer. The first topcoat may penetrate the intermediate coat, providing a waterproof topcoat. Whichever paint system is selected for exterior use, it is common to rate the system based on its ability to prevent filiform corrosion. The main functions of topcoats main functions are to provide:

- A resistant seal for the coating system.
- An initial barrier for the harsh environment.
- Toughness and wear resistance.
- Aesthetic purposes.

To a significant degree, the properties of a **topcoat** are usually designated by the type of material used as the main binder, in addition to the pigments, as both have a strong influence on the performance of the coating (Figure 4-3). To perform in a practical environment, a coating must become, after application, a dense, solid, and adherent layer. The binder is the material that makes this possible, providing uniformity and coherence to the coating system<sup>5</sup>. An overview of the most usually employed coatings for offshore applications is described in the following sections: organic, metallic and inorganic.

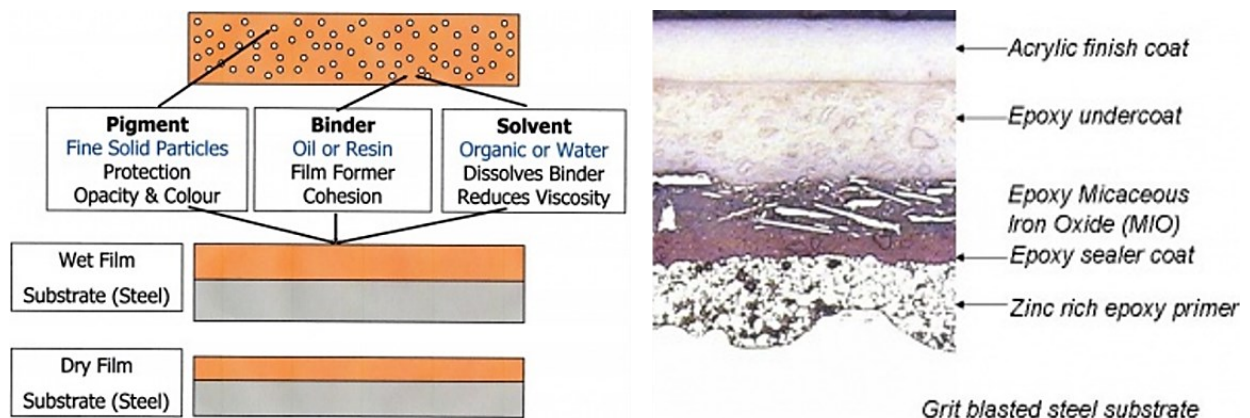


Figure 4-3. Coating constituent parts and their main function (left) and multi-layer paint system example (right). Source: [steelconstruction.info/Paint\\_coatings](http://steelconstruction.info/Paint_coatings)

#### 4.1.1 Organic coatings

Organic coatings have a high resistance to ionic conductivity, and thus offer good barrier properties and retard diffusion of chemical species (water, ions present in seawater or oxygen) to the metal surface<sup>4</sup>. Among many, most employed organic coatings systems are detailed below.

##### 4.1.1.1 Epoxy coating systems

Epoxy based paint systems are the most widely used anti-corrosion solution in offshore assets due to their superior properties, such as chemical resistance and adhesion. They are carbon chains with hydroxyl and high-reactive epoxide end-groups, which form highly cross-linked structures with high chemical resistance. Epoxy compounds are created through chemical

reactions between resins and co-reactants. It is typically applied in multilayer system, consisting of a primer, 2-3 intermediate coats and a topcoat. A higher total dry film thickness (DFT) of the coating system generally results in a longer protection life of the steel substrate<sup>7</sup>.

In general, epoxies have the following positive features:

- Strong mechanical properties.
- Very good adhesion to primers and between-layers.
- Excellent chemical resistance.

On the other hand, negative aspects of this type of coatings are:

- Susceptibility to UV degradation.
- Surface chalking.
- Insufficient performance at low temperatures in corrosion protection<sup>8</sup>.

The UV rays of the sun contain enough energy to break bonds in the polymeric structure of the cured epoxy binder. As the coat degrades, the breakdown of the binder begins to release pigment particles forming a fine powder consisting of pigment and binder fragments. This process is known as chalking, due to the similarity with chalk.

In offshore application, zinc phosphate epoxy primers are most commonly used as they provide the best durability within the epoxy group. Generally, it incorporates metallic zinc dust as a corrosion inhibitor for best performance.

The **resins** used in the epoxy reactions are available in a wide range of molecular weights. The lower the molecular weight, the lower the viscosity of the resin and more brittle the final cured system<sup>9</sup>, but with excellent penetrating properties into difficult surfaces. Due to their wide range of properties, there are many corrosion protective coatings based on epoxy systems, and most of them are typically used in midcoat applications. Besides, incorporation of laminar pigments and other additives in intermediate coats reduces moisture penetration and improves strength of the final product.

Other widely employed resin is coal tar epoxy resins. These systems are a combination of both substances. They are used on surfaces subjected to extremely corrosive environments, as they offer an excellent resistance to saltwater<sup>10</sup>. Besides, they can be applied in a single coat, providing a high dry film thickness.

#### 4.1.1.2 *Polyurethane and polyurea coating systems*

Polyurethane (PU) coatings are organic polymers created through chemical reactions between PU resins plus co-reactants and hardeners substances. They are very used in offshore industry. Although PU paints are more expensive than epoxies, generally PU has a better UV radiation resistance, which makes them an excellent option for topcoats in offshore environment with high UV exposure<sup>7</sup>.

Polyurethanes are obtained by reaction of precursors, as acrylics or polyesters containing hydroxyl groups (polyols), with organic isocyanates. The properties are highly limited by the

type of isocyanate and polyol employed in the composition. Precisely, aliphatic polyurethanes are considered the best performing coatings for applications that require UV durability, colour stability, high gloss, and exceptional chemical resistance<sup>11</sup>. Therefore, they are a great choice for submerged seawater applications<sup>12</sup>. Acrylic polyurethanes are widely used for atmospheric corrosion protection due to their outstanding UV resistance properties. However, they are not used on immersed seawater parts as they are not as stable as aliphatic ones<sup>13</sup>. Another type of PU are the aromatic PUs. They give more rigid PUs than aliphatic ones, but their oxidative and ultraviolet stabilities are much lower<sup>14</sup>.

In general, PUs have the following characteristics:

- Excellent chemical resistance to seawater.
- Good abrasion resistance.
- Good mechanical properties.
- Good UV resistance.

Independently of the employed isocyanate type in the PU formation, the curation process also affects its properties. As an example, moisture-cured urethanes are used as primers or midcoats as they can be applied to steel substrates with minimal surface preparation. The excellent adhesion that this type of systems present regardless of the surface finish on which they are applied make them very useful in any application where extreme resistance to abrasion is required, for areas that require good elongation to withstand expansion and contraction of substrate, and even on surfaces that still contain a thin layer of oxide<sup>15</sup>.

It is worth mentioning another coating class obtained by reaction of an isocyanate, but in this case with amine-functionalized polymers, creating **polyurea** (PUR) coatings. The quality of the coating is determined by the isocyanate nature, as in polyurethanes. In both systems the curation process can affect they hardness and they both exhibit similar chemical resistance properties. The most critical difference is that polyurea coatings exhibit much more flexibility than PU<sup>16</sup>. Apart from that, the polyurea reaction is much faster than the polyurethane one, and the systems can cure very fast, but they do not fully develop ultimate physical properties until 24 hours or more, depending on the urea precursor formulation<sup>17</sup>. This fact of curing speed does not offer significant advantages to protection, but it does to maintenance operations, since the sooner the finished surface is, the sooner subsequent layers or elements can be applied.

#### 4.1.1.3 Powder coating systems

Powder coating is the youngest coating technology, but also the fastest growing. In a powder coating all the constituents of the coating (binder, fillers, pigments, and additives) are present in a dry, solventless powder. This has several environmental benefits, as no volatile compounds are required in the mixture<sup>18</sup>. The powder is usually applied to the metal substrate by spraying processes, electrostatically deposited and then heat cured<sup>19</sup>.

In general, powder coatings have the following characteristics:

- Excellent temperature performance.

- Outstanding corrosion resistance.
- Good water tightness.

The most common powder coating in offshore applications is the fusion-bonded epoxy (FBE) coating, which is suitable for use alone or in a dual powder coating system. These FBE coatings provide external metal surfaces with extremely strong corrosion protection, with an average lifetime of 20 years<sup>20</sup>. This coating system is a dry powder, resulting in 400-600 microns coating layer on steel surfaces. The FBE coating forms a homogeneous surface that also provides:

- Mechanical resistance.
- Abrasion resistance.
- Flexibility.

Fusion-bonded epoxy is suitable for powder coating offshore structures, because it provides superior adhesion even in humid environments. High performance fusion-bonded epoxy powder can be obtained if a three-layer system is applied, which provides even better corrosion resistance than the FBE alone. This system consists of the following layers:

- FBE coating
- Co-polymer adhesive
- Polypropylene

The role of the copolymer is simply to increase the overall thickness of the coating, but it is the polypropylene topcoat the one that defines the total thickness of the coating. Indeed, polypropylene is the best choice when the temperatures are extreme and fluctuate, as it is suitable between -40 °C and 110 °C. It also provides additional mechanical and physical properties that can be beneficial for offshore pipelines, for example <sup>20</sup>.

Powder coating solutions have also been recently applied for protection of welded joints of steels, as they reduce surface heterogeneity and enhance the protective properties and resistance of welded joints to corrosion<sup>21</sup>.

#### 4.1.1.4 Rubber lining coating system

There is a huge variety of rubber lining coatings, depending on the technical requirements. They have arisen in the last years as a potential solution for offshore splash zone<sup>19</sup>. In offshore applications the most used class of rubbers are Chloroprene and Ethylene Propylene Diene (EPDM). Both have outstanding performance in seawater:

- Excellent chemical resistance.
- Flexibility.
- Extremely resistance to weather phenomena.

#### 4.1.1.5 *Ongoing research on organic systems*

Actually, ongoing research on organic systems are solely focused in enhance current solutions towards equipping them with antifouling properties. Blocking marine-immersed surfaces to reduce the attachment of biofouling organisms can be performed by employing biocides. However, the strategy has shifted towards a more respectful approach to the environment and thus, the most notable new developments are environment friendly **anti-fouling solutions**, **polymer materials**, and **hybrid sol-gel coatings**.

- **Environment friendly antifouling coatings:** Antifouling paints are used to prevent the attachment of living organisms to the submerged surfaces of ships, boats and aquatic structures, usually by the release of biocides<sup>22</sup>. Among all the different solutions proposed throughout the history of navigation, tributyltin self-polishing copolymer paints (TBT-SPC paints) have been the most successful in fouling and associated damage inhibition. Unfortunately, the TBT-SPC systems affect adversely the environment, and strong restrictions were applied, forcing to look for alternatives<sup>23</sup>. Nowadays, around eighteen compounds are used as antifouling paint biocides worldwide, reviewed by Thomas (2001)<sup>24</sup>. Currently, two eco-friendly strategies are typically followed in the design of novel, non-biocidal, non-fouling surfaces. The first one are Anti-Fouling coatings, in which the objective is to prevent the attachment stages of fouling organisms<sup>25</sup>. The second one are Fouling-Release coatings, which do not prevent organisms from attaching, but their interface is weakened so that attached organisms are more easily removed<sup>26</sup>.
- **Polymer materials:** Polymer brushes are molecular scale brush-like structures composed of surfaces covered with long-chain polymer molecules tethered at one end to the surface of the material<sup>25</sup>. The composite structure at the material interface (with hydrated polymer chains, hydrogen-bonded network structure of hydrated water and polymer chain dynamics) has been recognized as a key factor for biofouling and fouling release in wet conditions<sup>27</sup>. This combination of surface topography factors is proposed as a new concept for low adhesive, slippery surfaces.
- **Hybrid sol-gel coatings:** Hybrid organic/inorganic sol-gel coating technology provides a durable fouling-resistant surfaces on a variety of materials by applying thin ( $\geq 5 \mu\text{m}$ ) coatings<sup>25</sup>. The flexibility of sol-gel chemistry also allows fouling release functionality, as well as other applications based on low wetting and adhesion. In recent years, sol-gel derived coatings have been investigated as a potential corrosion-inhibiting barrier for use on metal surfaces<sup>28</sup>. It is possible to introduce additional components such as corrosion inhibitors into the formulation process in order to enhance its corrosion-inhibiting or self-healing properties.

#### 4.1.2 **Metallic coatings**

Metallic coatings provide an additional layer to the original substrate that positively modifies the surface properties of the structure or component on which it is applied. The protective efficacy of metallic coatings depends on its capacity to act as an isolating barrier between the surrounding atmosphere and the underlying metal, i.e. on its thickness, uniformity, adherence, porosity avoidance and ductility enhancement. This metallic coating has also the ability to provide electrolytic protection for the steel, acting as a sacrificial anode<sup>29</sup>.

The lifetime of metallic coatings generally depends on their thickness, but also the chemical composition is considered critical. Properties of a base material can be modified by the



composition of the metallic coating, providing a robust way to control its protection against corrosion. Another important function of metallic coatings is to provide wear resistance. The most technically demanding types of coatings are those grown in precisely defined multiple layers<sup>30</sup>. In general, metallic coatings for offshore applications can be divided into two groups: hot-dip metallizing (also known as galvanizing if a Zn coat is applied) and thermal spraying coatings.

#### 4.1.2.1 Hot-dip metallizing

Hot-dip galvanizing technique is the most common single coating process for substrate protection in offshore facilities. The process involves applying a zinc coat to the iron or steel surface by immersing the component in a molten zinc bath. The resulting coating varies depending on multiple factors such as the surface preparation, steel composition and others. For example, silicon concentration in steel plays a major role, as it influences the growth and microstructure of the zinc layer<sup>31</sup>. Steels containing small amounts of silicon (< 0.03%wt) have a compact and continuous zinc coating, while between 0.03-0.14% and above 0.3%, produce a coating with excessive thickness, grey appearance, and poor adherence<sup>32</sup>.

The advantage of hot dip galvanizing is that not only does a moisture impervious barrier, but the coating has the additional benefit of protecting steel by a sacrificial action. In fact, hot dip galvanizing protects steel from corrosion by providing a thick metallic zinc jacket, which is metallurgically bonded to the steel. As a result, galvanized steel has a great resistance to mechanical damage. Even if its damaged, or there is a minor discontinuity into the zinc cover, protection is maintained by the sacrificial action of the surrounding zinc coating<sup>33</sup>. The complete galvanizing process is being summarized in Figure 4-4, including the surface preparation steps.

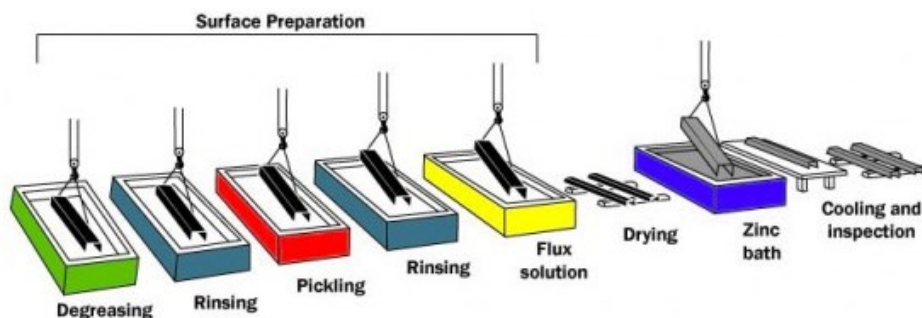


Figure 4-4. Galvanizing process. Source: trailerguys.com.au

When it comes to decide which is the optimum zinc thickness, requirements are mainly agreed by specification such as the DIN EN ISO 1461 standard, which applies to batch galvanizing. Depending on the base material thickness, an optimum galvanizing process requires coating thicknesses of at least 45 to 85  $\mu\text{m}$ . Also, depending on the kind and form of the component, the immersion time of the components in the zinc melt should be 30 s up to 1.5 min per millimetre of wall thickness<sup>34</sup>. Despite that, authors like Momber claim that the minimum Zn coating for constructions in offshore should have a minimum value of 85  $\mu\text{m}^2$ . Hot dip metallizing can also be performed with other metals, as magnesium or aluminium. Zn-Mg coatings are an innovation for continuous hot-dip galvanizing, which can be performed on existing continuous galvanizing lines. Due to the high corrosion resistance of Zn-Mg coatings,

it is possible to reduce the overall required coating thickness while maintaining corrosion protection<sup>35</sup>.

Al-Zn alloys evidence outstanding resistance to atmospheric corrosion. Al-Zn coatings' performance is similar to that of aluminium coatings because they form on the surface a dense oxide film (characteristic of aluminium) that protects the material. The composition of the alloy will define the behaviour of the coating: either passive (greater amount of aluminium) or galvanic (greater amount of zinc). Besides, Al-Zn alloy coated steel has extremely high corrosion resistance compared to that of the Zn-coated steel, particularly in a seaside<sup>29</sup>. The addition of aluminium to the coating composition improves ductility and adhesion, since the interface region between the coating and the substrate is composed of a heterogeneous fine phase mixture of zinc, aluminium and iron<sup>36</sup>.

Ternary mixtures of Zn-Al-Mg alloys deposited on steel have also been reported to hold promise for application to offshore structures. The formation of  $MgZn_2$  and other intermetallics on the top surface and through the cross-section of coating has been found to be the reason of a higher surface hardness than standard Zn coating layer<sup>37</sup>(Figure 4-5). Moreover, steel samples coated in Zn-Al-Mg show better corrosion resistance properties than the ones coated in pure zinc or Zn-Mg binary composition<sup>38</sup>

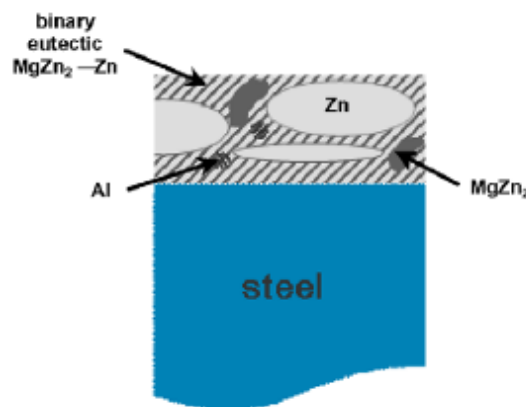


Figure 4-5. Schema of cross-sections of Zn-Al-Mg alloys produced by hot-dip metallizing. Source: Schuerz et. al. (2009)<sup>39</sup>

Although metal coatings have shown good performance in offshore conditions, when outstanding resistance to seawater attack is required, an organic based topcoat is recommended in addition to hot-dip galvanizing.

In line with galvanized steels, promising applications of hybrid sol-gel coatings have been developed in Tecnalia Research & Innovation specially driven for galvanized steel<sup>40</sup>. In the search of more extensive corrosion protection and as an alternative to classic chromate coatings, sol-gel processing is a promising route for barrier protection due to the ability to combine inorganic and organic precursors that can be chemically bonded. Resulting hybrid coatings show an excellent adhesion properties to the substrate, obtaining thicker, denser, more flexible, and further functionalised films with enhanced compatibility to different organic top-coatings. In this case, the addition of bi-functionalised organic precursor to silica and zirconia network permits to synthesise a coating with a high barrier effect.

#### 4.1.2.2 Thermal spraying (metallizing)

Thermal spray coating, sometimes referred to as metallizing, is the process of spraying a thin metallic coating to a substrate for the purpose of protecting it against corrosion and physical wear. Most commonly aluminium, zinc, magnesium and their alloys are employed.

Metallizing is similar to hot-dip galvanization, but has some distinct advantages<sup>40</sup>:

- Metallizing utilizes a spray application, making it a viable solution on any size structure and location. Hot-dip galvanization is strictly limited to what will fit in the kettle.
- The colour and appearance of metallizing is uniform and continuous.
- Metallizing results in a very uniform appearance as well as consistent performance with respect to adhesion. This facilitates topcoat application because a metallized surface is porous enough to coat and adheres as well as it would to a blasted substrate, while galvanizing is very difficult to apply a topcoat.

Metallizing materials range from the standard zinc, zinc/aluminium and aluminium, to the more unique such as tungsten carbide, copper, and other metallic alloys mostly Ni based<sup>41</sup>, and even ceramic composites. It can provide thick coatings depending on the process and the material. The most common thermal spraying methods for offshore applications are: combustion methods (HVOF, HVOF) and electrical methods (plasma, arc wire), among many other existing. A more detailed classification of thermal spraying processes is shown in Figure 4-6.

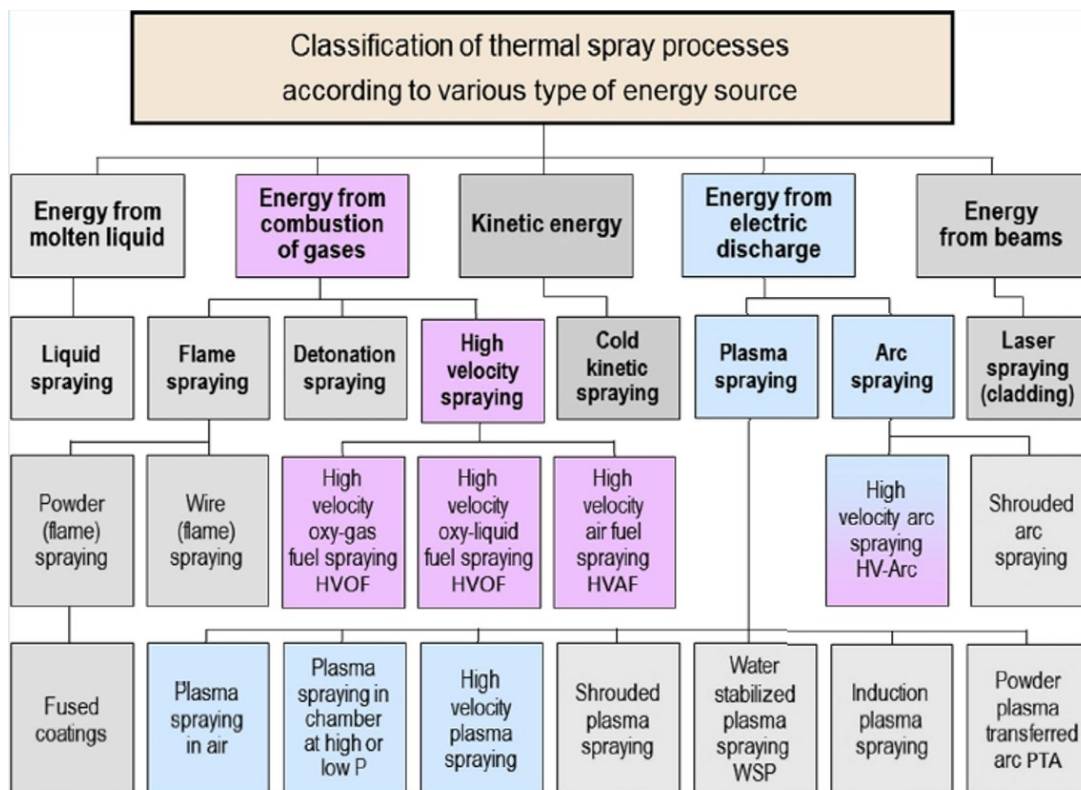


Figure 4-6. Thermal spraying processes according to the energy source. Adapted from Vuoristo et. al. (2014)<sup>42</sup>.

In order to meet the most demanding properties of offshore conditions, metal spraying protection is recommended<sup>2</sup>. Mooring lines, for instance, are usually subjected to severe corrosion erosion as consequence of the wear generated between components by waves, wind, and ocean currents<sup>43</sup>. Indeed, Thermally Sprayed Aluminium (TSA) coatings have been

broadly employed since the middle of the past century<sup>44</sup> to protect steel components from corrosion in marine environment<sup>45</sup>. In the marine environment, zinc or aluminium coatings offer high corrosion resistance, especially in the splash zone, but seems to be not protective enough in the tidal zone<sup>46</sup>, the most severe offshore zone according to Table 4-1.

Despite its proven efficiency and suitability in many cases and materials, TSA coating manufacturing process sometimes has small drawbacks, such as porosity (Figure 4-7). In the TSA coating process aluminium is atomized and propelled onto a substrate by compressed air. Due to the high speed of spraying and sudden cooling of melted metal droplets spread at the substrate, pore formations and high rated roughness of the surface are generated in Al-deposited coatings<sup>47</sup>. Even during solidification and diffusion of deposited metals towards substrate, some pores/defects in different sizes remain on coating, facilitating the diffusion of oxygen and other aggressive ions from the environment. To minimize the porosity of the coating and maintain the corrosion resistance, the application of topcoats to fill the pores is recommended, among other solutions.

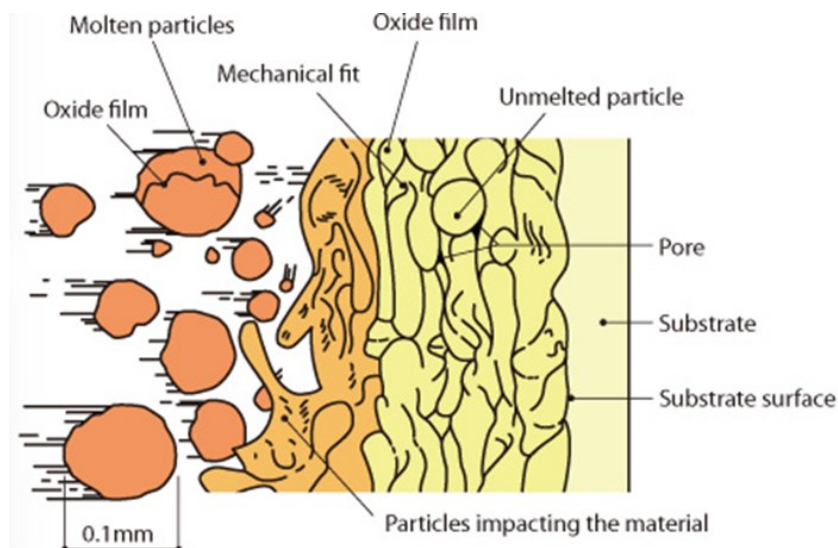


Figure 4-7. Thermal Sprayed coating formation. Source: Osaka-Fuji Corporation (ofic.co.jp).

The main differences between metallic coating methods over a steel are the density and the thickness of the coating (Figure 4-8):

- Thermal spraying is approximately 15% less dense than hot-dip method and, in fact, the black areas on the first photomicrograph in Figure 4-8 are voids in the coating, which are not observable in the second photomicrograph.
- In zinc paints applied zinc dust is bounded in organic or inorganic binders. The observable white particles in the photomicrograph are zinc oxides while the black areas are the binders.
- In galvanized sheets coating thickness is minimal compared to hot-dip galvanized coatings, but still provides corrosion protection.
- Lastly, in electroplated materials the zinc and iron layers are clearly differentiable, managing the finest thickness of all. However, chemical barrier and cathodic protection are still provided.

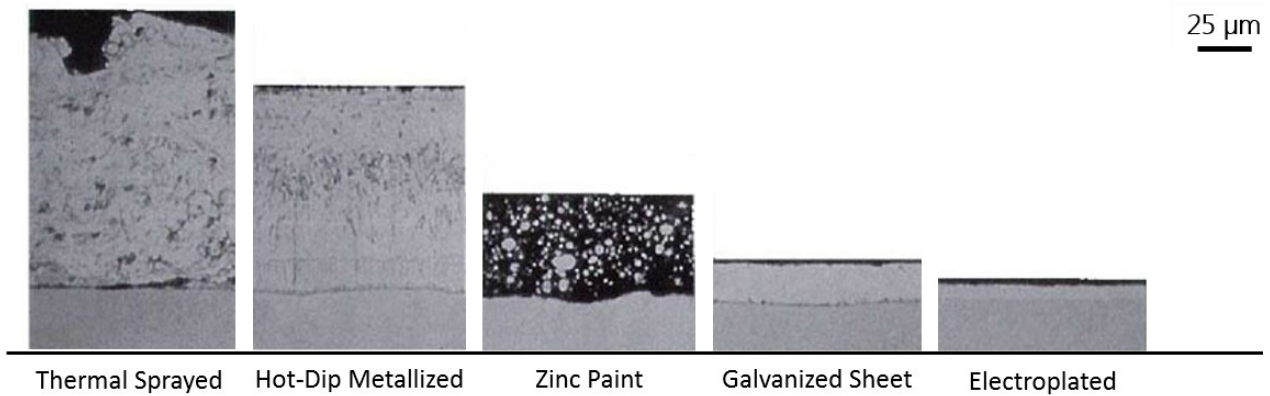


Figure 4-8. Photomicrographs of various zinc-iron coatings thicknesses and finishes. Adapted from: metalplate.com

### 4.1.3 Inorganic coatings

Inorganic coatings are chemical, electrochemical and thermal action-based coatings that change immediately the surface layer of the steel into a film of metallic oxide or compound that has better corrosion resistance than the natural oxide film. They may be used as either a standalone coating or as a surface pre-treatment for a subsequent organic topcoat finish. This section will focus on methods either to enhance the currently existing oxide, as **anodizing**, or on methods to apply an entirely new inorganic layer, as in **chromates** and **nitriding** process.

#### 4.1.3.1 Anodizing

Anodizing involves the electrolytic oxidation of a surface to produce a more adherent oxide scale which is thicker than the naturally occurring film, enhancing properties such as hardness and corrosion resistance. A number of metals including aluminium, magnesium, tantalum, titanium, vanadium, and zirconium can form such oxide films. However, only aluminium and its alloys and magnesium are anodized on a commercial scale for protection<sup>6</sup>. Resulting coating from anodizing is typically 2 μm to 25 μm thick and consists of an initial thin non-porous barrier layer with a porous outer layer (Figure 4-9). Depending on the anodizing conditions the outer pores distribution may be different. Thicker outer pores may be receptive to dyes, lubricants and paints, while tighter pore structures does not accept subsequent coats, but has excellent wear resistance<sup>48</sup>.

#### 4.1.3.1 Chromates

Chromate-based compounds are excellent corrosion inhibitors when deposited on the metal as a thin film, usually in the range of 0.5-5 μm. The major inhibitive compounds within chromate-based conversion coatings are those containing Cr<sup>6+</sup> species<sup>6</sup>. In metals that are more liable to corrode (e.g., magnesium and aluminium alloys), chromate films are used to provide a suitable surface for sealing resins or paints. It is worth to say that although the chromate coatings provide superior properties both for corrosion protection and for aesthetic point of view, their use in the EU is limited because the hexavalent chromium is carcinogenic. New types of coating procedures with trivalent chromium have been developed, introducing the term "chromium (VI)-free passivation". Nowadays, alternative coatings providing comparable corrosion resistance to chromate coatings are being researched. Coatings based



on Zr(IV) and Ti(IV) have already shown some success. Produced layers contain hydrated titanium and zirconium oxides and hydroxides, but do not reach the thickness of common chromate coating, the overall production process is more expensive, and the pre-coating surface treatment is more complicated<sup>49</sup>.

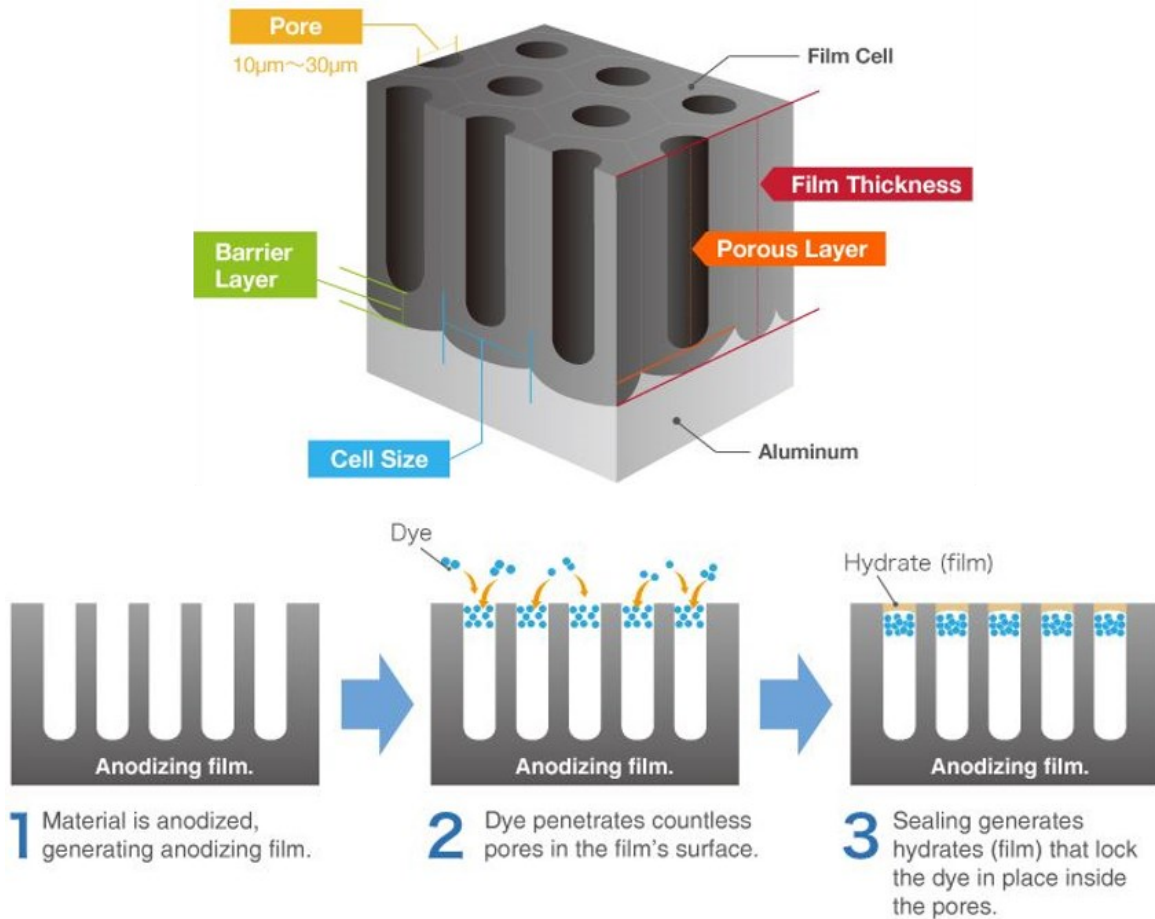


Figure 4-9. Anodizing porous layer from inside (up) and dyeing anodizing scheme. Source: kashima-coat.com

#### 4.1.3.2 Nitriding

Nitriding and nitrocarburizing are thermochemical treatments that diffuse nitrogen and carbon into the surface of metals (Figure 4-10). They both improve surface properties of metal components, corrosion resistance, and increase the fatigue strength<sup>50</sup>. Nitriding is commonly used in low-carbon and low-alloy steels alloys, in titanium, in aluminium and in molybdenum. Nitrocarburizing is only used on ferrous alloys, as it spreads nitride-alloyed elements into ferrite<sup>51</sup>.

The most efficient and well-known methods of both nitriding and nitrocarburizing are via plasma and gas. If an equally treatment of the complete item is required, gas methods should be used since the gas gets to the entire surface with no exception. If localized hardening is needed plasma methods are preferred, because non desired parts can be masked<sup>52</sup>. In overall, nitriding is considered an excellent method to mitigate corrosion, particularly when the corrosion is likely to be accompanied by mechanical damage, as in offshore locations. In Figure 4-10, the resulting microstructural profile of a nitrided steel sample is shown, remarking the

increasing hardness as it approaches the surface, where we find iron nitrides of different stoichiometry to those present in base steel.

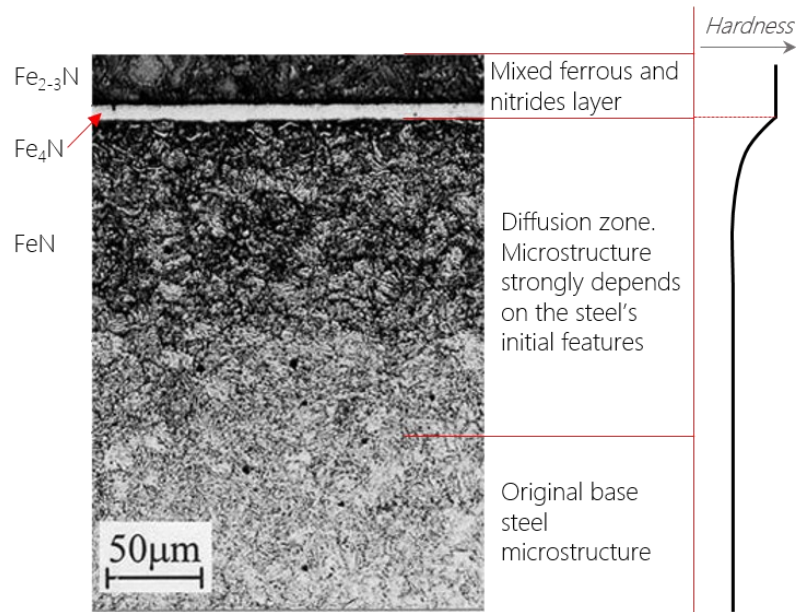


Figure 4-10. Nitriding microstructural profile, with main compounds on each zone and subsequent hardness improvement. Adapted from Surface Engineering course from MISKOLC University.

## 4.2 Active Protection

When it comes to face corrosion degradation by means of "active" protection, the employed strategies normally are Impressed Current Cathodic Protection (ICCP) and Galvanic Anode Cathodic Protection (GACP), but also Chemically Active Coatings (CAC).

Despite being essentially coatings, which have been considered part of passive protection strategy, some sort of coatings, as those who incorporate inhibitors and self-healing coating, fit best in active corrosion protection. Sacrificial coatings, as zinc and aluminium-based systems, have been described in the Metallic Coating section for a better understanding, even though they could also be considered as chemically active sacrificial coatings. The situation is repeated with the antifouling coatings, classified in ongoing research on organic coatings even if they could also fit in CACs. Lastly, alternative corrosion control measures are also mentioned, as Material Selection, Design and Detailing of a Structure and Wastage Allowance. Some authors claim that these, instead of corrosion control methods, should be classified as general precautions methods, as they are common concerns regardless the structure, industry, or environment.

### 4.2.1 Chemical active coatings

Chemically active surface-functional coatings use several different mechanisms. The active zone of the coating can be located either at the surface/air interface, or it can be in the near-interface layer, close to the metal surface. Reaction products can be removed from the surface either through natural action (wind, rainwater or ocean currents), or mechanically<sup>53</sup>.



#### 4.2.1.1 *Coatings with corrosion inhibitors*

Protective treatments with an active corrosion-inhibiting effect neutralise the harmful effect of corrosion-promoting media by acting on the coating and thus reducing the rate of an electrochemical reaction that causes corrosion. The technology of corrosion inhibition is very extensive and multidisciplinary. In fact, essentially an inhibitor is a chemical substance or a mixture that decreases corrosion when added to an environment (usually in small concentration), while a passivator, is an inhibitor which appreciably changes the potential of a metal to a more noble value (cathodic value), preventing it from being affected by corrosion<sup>54</sup>. It is very interesting to incorporate these type of inhibitors directly in the coating, although they can also be distributed from a solution or dispersion<sup>55</sup>. The passivators are the one of our interest, as they have been considered as an option in offshore application.

Inhibitive coatings are typically included in the primer of a coating system. They have to be in contact with the substrate to be effective. Through the use of pigments<sup>56</sup>, the corrosion inhibitor is released in response of changes in the coating integrity (cracks) or changes in the environment (pH, temperature)<sup>57</sup>. Good examples of corrosion inhibiting pigments are red lead pigments (PbO, Pb<sub>3</sub>O<sub>4</sub>) and lead soluble salts. These pigments promote passivation by strengthening the metal's oxide film until it becomes impermeable, impeding corrosion<sup>56</sup>. Other common examples are zinc phosphates, silicates and organic pigments as polyaniline or poly(aromatic amines)<sup>58</sup>. Solutions are currently being developed based on sol-gel coatings, which in addition to oxide nanoparticles as a reinforcement and reservoir for corrosion inhibitors, have been proven successful<sup>59</sup>. Other examples of ongoing research include rare-earth doped systems<sup>60</sup>, and even atomic thin layers of graphene as a protective coating that inhibits corrosion of underlying metals<sup>61</sup>.

#### 4.2.1.2 *Self-healing coatings*

Self-healing materials have the ability to partially repair themselves and recover functionality after degradation or punctual damage. Although many technologies can work as self-healing coatings, like for example different types of organic, hybrid and metallic systems, thin sol-gel based layers seem to be the most promising ones<sup>62</sup>. Self-healing coatings can be classified in two ways: intrinsic and extrinsic. Intrinsic method is based on hydrogen-bonding or covalent systems that do not require an external agent to heal. Extrinsic approach is based on healing agents added as a separated phase into the coating matrix and needs external stimulus to activate (UV light, temperature), for example encapsulated materials<sup>63</sup>.

In intrinsic self-healing method, commonly observed in polymers, the chemical structure of the polymer plays a key role as it can be designed to reconnect and repair after damage through the reformation of bonds (Figure 4-11)<sup>64</sup>.

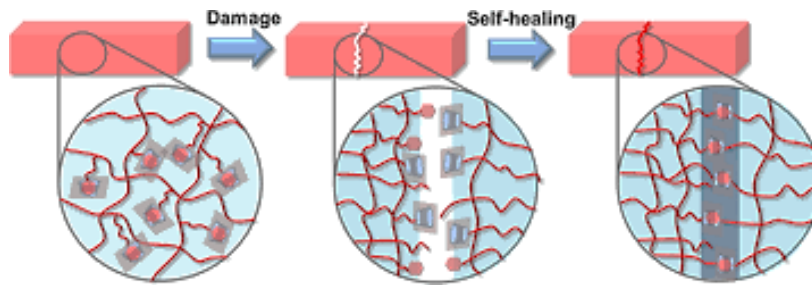


Figure 4-11. Schematic illustration of the intrinsic self-healing mechanism. Reproduced from: Hu (2018)<sup>65</sup>

The extrinsic self-healing concept can be explained in three steps (Figure 4-12). A microencapsulated healing agent is embedded in a structural composite matrix, which also contains a catalyst capable of cross-linking the healing agent. Once the damage occurs and the crack forms in the matrix, the microcapsules act releasing the healing agent into the crack space through capillarity. The healing agent also contacts the catalyst, enabling the polymerization that bonds the crack space<sup>66</sup>.

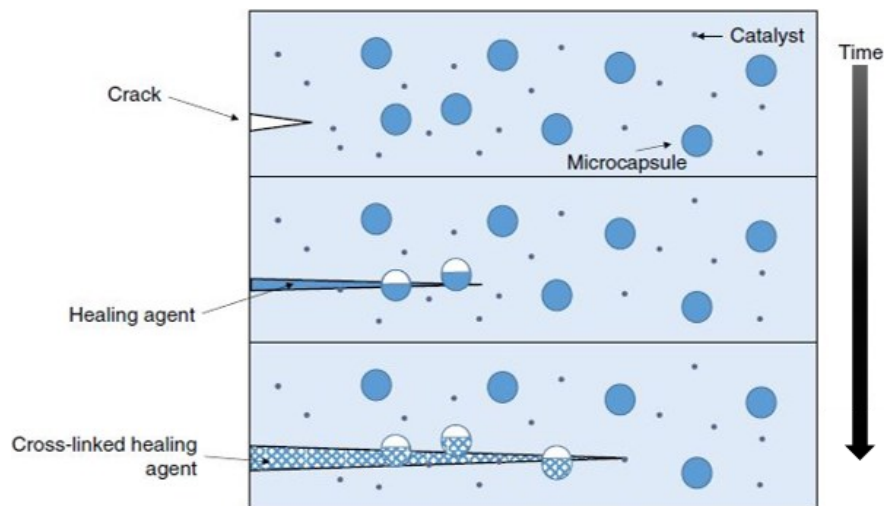


Figure 4-12. Extrinsic self-healing process. Reproduced from Gould (2003)<sup>66</sup>

#### 4.2.2 Cathodic corrosion protection

One of the primary methods of corrosion control is cathodic protection, extensively applied in offshore industries for submerged metal structures. Cathodic protection has been applied in two ways: **Impressed Current Cathodic Protection (ICCP)** and **Galvanic Anode Cathodic Protection (GACP)**. Overall, cathodic protection mainly induces a decrease of corrosion rate without drastic changes of the corrosion mechanisms<sup>67</sup>.

In impressed current systems a direct current is applied to the immersed structure or component through water from a source outside the structure (Figure 4-13). When the structure is placed under the control of a suitable cathodic protection, the anodic reactions take place in the impressed current anodes<sup>68</sup>, avoiding corrosion of the structure. In ICCP, auxiliary anodes are commonly non-consumable anodes with good electrical conduction, good mechanical properties and relatively low corrosion rate in seawater and low cost<sup>69</sup>. Examples of anode materials are high-silicon cast iron, graphite, lead-silver alloy and platinum.

Large areas of a structure can be protected with a single anode and it can be placed remote from the structure, employing high driving voltage<sup>70</sup>.

The applied current density required to achieve the minimum corrosion protection is called the minimum protection current density. The factors affecting the value of minimum protection current density include the amount of corrosion products and the sea creatures attached to the surface of the metal structure. In seawater steel structures are often covered by calcium and magnesium carbonates or hydroxides<sup>71</sup>. Whether it is the biofouling or the calcareous deposits, both would provide a certain protection to metal, making the minimum protection current density to decrease. Carbonate sediments may cause crevice corrosion under the calcareous layer, although they are considered of little effect.

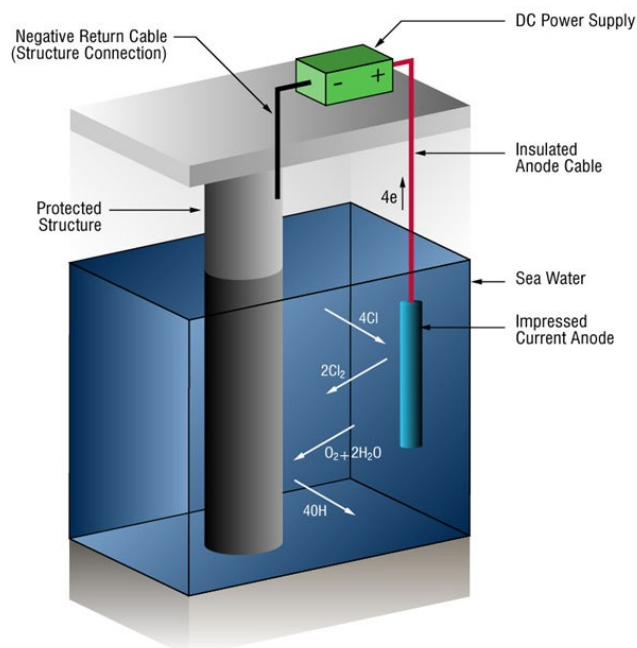


Figure 4-13. Impressed Current Cathodic Protection operation in seawater, schematized. Source: marinethai.net

In cathodic protection systems the steel structure is polarized to an electrical potential generally between -800 mV and -1100 mV, measured with a silver/silver chloride/seawater (Ag/AgCl/Seawater) reference electrode. This polarization can be adapted or modified throughout the life of the structure<sup>72</sup>. In Table 4-2 this changeable demand can be observed, as for example when corrosion takes place in presence of important bacterial activity, the current demand increases gradually. Polarization potential can also be subjected to changes when the metal is dissimilar to iron steel, as in case of aluminium.

Table 4-2. Applied potential in the cathodic protection depending on the metal and the environment.

| Metal or alloy          | Environment                   | Ag/AgCl/seawater reference |
|-------------------------|-------------------------------|----------------------------|
| Iron and Steel          | Aerated seawater              | -800 mV                    |
|                         | High conc. of SRB in seawater | -900 mV                    |
|                         | Structural yield < 550 MPa    | -1100 mV                   |
| Aluminium <sup>70</sup> | Seawater                      | -900 to 1150 mV            |

The yield strength of steel is a very important factor in determining how much protection current can be imposed during the cathodic reaction, while preventing the production of

atomic hydrogen that could cause hydrogen embrittlement or hydrogen induced stress cracking<sup>73</sup>, as previously seen in Chapter 2.

**Galvanic Anode Cathodic Protection (GACP)** method employs auxiliary anodes that are directly electrically connected to the steel to be protected. The difference in natural potential between the anode and the steel causes a current flow in the electrolyte from the anode to the steel. Thus, the whole surface of the steel becomes more negatively charged and becomes the cathode<sup>74</sup>. Commonly used materials as sacrificial anodes are based aluminium, or zinc or magnesium, normally alloyed to improve their long-term performance and dissolution characteristics, as exposed in Table 4-3.

The potential of the sacrificial anode should be negative enough to ensure the cathodic polarization of the steel to be protected. However, the potential should not be too negative, in order to avoid hydrogen formation in the cathode region<sup>75</sup>. This hydrogen may damage the applied coatings (cathodic disbondment<sup>76</sup>) or cause hydrogen embrittlement of the steel. The potential difference between the sacrificial anode and the steel to be protected is called driving potential, and is generally around 250 mV<sup>70</sup>.

Table 4-3. Properties of magnesium-based alloy, zinc-based alloy, and aluminium-based alloy employed for sacrificial anodes. Source: Huang (2018)<sup>70</sup> and Priyotomo, Nuraini (2017)<sup>77</sup>.

| Alloy           | Density (g/cm <sup>3</sup> ) | Ag/AgCl/seawater reference | Consumption rate (kg/(A-year)) | Current efficiency |
|-----------------|------------------------------|----------------------------|--------------------------------|--------------------|
| Zinc alloy      | 7,88                         | -1030 mV                   | 11,2                           | ≈ 90%              |
| Aluminium alloy | 2,77                         | -1100 mV                   | 3,3                            | ≈ 80%              |
| Magnesium alloy | 1,74                         | -1550 mV                   | 28,0                           | ≈ 50%              |

That means, for example, if we have a steel structure in seawater that requires an effective potential of 800 mV to be protected, with a zinc alloy anode the effective potential difference (the drive potential) of zinc and iron is small since it does not exceed the required 250 mV (1030 mV - 800 mV = 230 mV). In this example, another alloy such as aluminium would be more recommended.

When it comes to GACP, is difficult to over-protect the structure and generally a uniform electrode potential across the structure is achieved. The greatest limitation of the sacrificial anode is the small driving force achieved, which restricts its use to conductive environments or well-coated systems<sup>69</sup>. To protect a large structure with sacrificial anodes, for example a jacket foundation or a floating system, a large number of sacrificial anodes would need to be distributed along the structure, with the respective electrical connections (Figure 4-14).

In general, for offshore wind structures GACP is preferred, employing Zn-Al alloy sacrificial anodes. Mg is not considered a viable option in offshore structures due to its fast consumption in seawater<sup>19</sup>. ICCP systems are well known and strongly established in corrosion protection protocols, but are more susceptible to environmental and mechanical damage, and they require more inspections and maintenance. Therefore, ICCP systems have been widely deployed in Oil&Gas rigs since they are manned structures. Nevertheless, they offer several advantages over GACP. In Table 4-4 main advantages and disadvantages of ICCP are summarized.

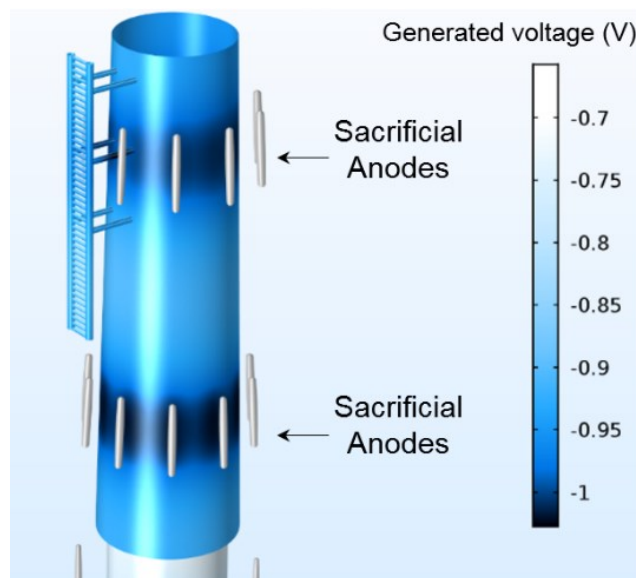


Figure 4-14. Steel monopile with distributed sacrificial anodes, with the subsequent generated driving potential between both. Source: Corrosion Module - COMSOL® 5.2

Table 4-4. Main pros and cons of ICCP and GACP systems. Source: marcepinc.com

| ICCP   |   |
|--|---|
| PROS   | CONS  |
| Unlimited power output capacity  | May allow considerable over-protection                        |
| Adjustable protection potential  | High maintenance costs  |
| Can protect a large, even uncoated, structure in high resistivity environments | May create stray current corrosion on other nearby structures |
| Few anodes needed compared to GACP   |   |
| GACP   |   |
| PROS   | CONS  |
| Simple to install  | Fixed protection potential                                    |
| Independent from electric power  | Current capacity based on the mass of the sacrificial anode   |
| Suitable for localised protection  | Scheduled replacements  |
| No interaction with neighbouring structures                                    |   |

The provision of a protective/insulating coating to the structure will greatly reduce the current demanded for cathodic protection of the metallic surface, increasing the effective spread of cathodic protection current. A combination of applying both a coating and cathodic protection will normally result in the most practical and economic protection system.

### 4.3 Material selection

The design and material selection of a given component or structure affects directly to the corrosion resistance and durability. As example, structures designed with many small components are more difficult to protect than those with large and flat surfaces. Although design remains a key factor, the main strategy to combat corrosion at sea is starting with a solid foundation: the use of corrosion resistant materials.

### 4.3.1 Corrosion allowance

Corrosion allowance is part of active corrosion protection strategies, usually determined by a simple multiplication: minimum years of operation, or years before replacement, by mean corrosion rate in a given environment. This implies that certain components can corrode without compromising the safety, stability and overall function of the structure. This approach is mainly considered when only general corrosion is expected, because it responds to uniform degradation of the whole component. In splash zone, where maintenance of coating systems is not practical, coating of primary structures shall therefore be combined with a corrosion allowance<sup>78</sup>. Despite the effectiveness corrosion allowance can be an additional cost of up to 9% in the severe environment of the North Sea<sup>79</sup>.

International standard guides as Norsok M-001 details specific formulae (Equation 3) in this topic:

$$\text{Corrosion allowance} = (\text{Design Life} - X \text{ years}) \cdot 0.4 \text{ mm/year} \quad (\text{Eq. 1})$$

where  $X = 5$  for thin film coating and  $X = 10$  for thick film coating, where thick film coating is understood as an abrasion resistant coating with thickness of minimum 1000 micron and applied in minimum two coats<sup>80</sup>. As an example, for submarine pipeline systems a maximum corrosion allowance of 10 mm is recommended as a general upper limit for carbon steel.

Regarding the corrosion rate, in the case of mooring lines, 0.4 mm/year for splash zone and 0.1 mm/year for fully submerged conditions shall be used as basis for corrosion allowance and lifetime estimates. Moreover, an evaluation of possible corrosion acceleration due to bacterial activity on the seabed is recommended. Indeed, as temperature promotes greatly corrosion, standards as DNV-GL RP 0416 detail the minimum values for design corrosion rate on primary structural parts as function of the region, summarised in Table 4-5.

Table 4-5. Minimum values for design corrosion rate as function of the region. Source: DNV-GL RP 0416.

| Region*                                       | Corrosion rate<br>(external components) | Corrosion rate<br>(internal components) |
|---|---|---|
| Annual mean $T^a < 12 \text{ }^\circ\text{C}$ | 0.30 mm/year                            | 0.10 mm/year                            |
| Subtropical and tropical climates             | 0.40 mm/year                            | 0.20 mm/year                            |

\*Note: More information available at: [ospo.noaa.gov/data/sst/contour/global\\_small.fc.gif](https://ospo.noaa.gov/data/sst/contour/global_small.fc.gif)

### 4.3.2 Corrosion Resistant Alloys

When choosing a material, in addition to paying attention to its corrosion resistance, it is necessary to consider the mechanical properties and performance throughout its entire life service. Among all the materials and alloys employed to avoid corrosion, only steel structural matters are considered in this section, which are the objective of the thesis. Moreover, a large variety of tasks are accomplished offshore, as Oil&Gas production and transportation, which employ different kind of alloys to deal with high pressures and temperatures and contain chlorides,  $\text{CO}_2$ , and  $\text{H}_2\text{S}$ , an additional source of corrosion in addition to the marine environment itself<sup>81</sup>.

High-strength and high-toughness materials with improved fatigue life are desirable, if not essential, to overcome the design challenges imposed by the offshore harsh environment<sup>82</sup>. There is no universal definition of what constitutes a high strength material, which depends on many factors including the alloy family, the application, and the dimensions or weight of the component. A common classification is made according to the yield strength, which is briefly described below.

### **Mild steel alloys**

At the beginning of offshore exploration, heavy structural materials with especially high ductility and high resistance were employed, as the S355 carbon-manganese steel that is still nowadays employed in offshore turbine monopiles as they offer good fatigue tolerance<sup>83</sup>. When the necessity of lowering the total weight of the structure gained importance, high-strength alloys like the S460 and S690 were also valued as options for offshore turbine monopiles. It has to be considered that mild carbon manganese and high strength steel have little resistance to corrosion in marine environment and must therefore be coated<sup>19</sup>.

### **High-Strength Low Alloy steels (HSLA)**

To fix mild steels' poor resistance to corrosion, special steels as low-alloyed structural steels have been developed. They contain small amounts of alloyants as copper, chromium and nickel, which increases corrosion resistance. The carbon content of HSLA steels is usually below 0.2%wt. Chromium addition provides improved oxidation and corrosion resistance, while molybdenum increases overall strength. Other advantages of HSLA steels over mild steels are:

- Improved yield strength
- Improved hydrogen resistance
- Lower temperature ductility

The fact that HSLA steels have microalloyed materials show that they have been developed for very precise applications and to address specific segments of engineering design<sup>84</sup>. In general, HSLA steels are designed to achieve their desired mechanical properties by the development of microstructures through controlled thermomechanical processing (TMP)<sup>85</sup>, without intended to meet a specific chemical composition but rather specific mechanical properties.

### **Stainless Steel (SS)**

Although material cost of stainless steel is much higher than low-alloyed steels, stainless steel is commonly used for structural and also for oil transport in the case of Oil&Gas applications. Higher chromium content (>12%) than previous classes is the main responsible for their corrosion resistance. However, most austenitic steels (like 304, 316 and their low-carbon equivalents) are highly susceptible to crevice and localized corrosion<sup>86</sup>. While efforts have been made to improve austenitic SS corrosion resistance<sup>87</sup>, steels with even higher chromium and molybdenum have been developed, as the 904L, to enhance all type of corrosion resistance in seawater<sup>88</sup>, but doubling or triplicating the purchase cost.

PREN numbers were designated to rank and compare between different grades of stainless steels. According to the British Stainless Steel Association (BSSA) specified range of concrete



compositions are used, involving chromium, molybdenum and nitrogen composition in the calculations, although tungsten also appears in some cases. In the Oil&Gas sector, chemical composition-related specifications may have tighter restrictions on the PREN for specific grades than the minimum composition of the grade defined in EN or ASTM Standards<sup>89</sup>.

The PREN is calculated from a formula and depends on the material considered. The higher the number is, the better the resistance to localized corrosion. However, the PREN must be used with special care since this number does not consider other particularly important parameters such as the metallurgical quality, the nickel content or the surface state. So, it is important to bear in mind that the value of PREN number cannot predict the localized corrosion phenomena.

The most used version of the formula is (equation 1):

$$\text{PREN} = \text{Cr} + 3.3\text{Mo} + 16\text{N} \quad (\text{Eq. 2})$$

For super-duplex stainless steel PREN calculations, tungsten is also included in the formula, defining equation 2:

$$\text{PREN} = \text{Cr} + 3.3(\text{Mo} + 0.5\text{W}) + 16\text{N} \quad (\text{Eq. 3})$$

Alloys with PREN above 38 are supposed to provide enough resistance to marine corrosion<sup>90</sup>. A list of the most common ferritic, austenitic and duplex steels and their associated PREN is reviewed in the BSSA webpage<sup>89</sup>.

Above standard austenitic stainless steel alloys, other more sophisticated grades have been developed to withstand offshore harsh environment. Examples of those steels are the aforementioned super-duplex, hyper-duplex and high-alloy austenitic stainless steels, which have further demonstrated an excellent microbiologically influenced corrosion resistance<sup>91</sup>.

### Titanium alloys

Another interesting material that is worth to mention is titanium alloy, which has increasing applications in marine structures since late 80's<sup>92</sup>. A very low corrosion rate in seawater (lower than 0.001 mm/year for Ti6Al4V alloy<sup>93</sup>) combined with a weight reduction compared to steel and excellent mechanical properties, make titanium alloys very useful for structural parts with high corrosive exposition (Figure 4-15). As example, hardenable alloys as Ti-3Al2.5V and Ti6Al4V are the most employed in this sector.

### Aluminium alloys

Finally, aluminium alloys are remarkable in this section as they can be used for offshore oil rigs and OWS to reduce the structure total weight<sup>19</sup>. As an example, an aluminium structure will weigh between 40-50% of an equivalent steel design. In today's offshore operations, where oil is drilled from increasingly deep waters, a 1 ton saving in the topsides weight delivers a multiple factor saving in the structure that supports that weight.

Besides, aluminium-magnesium alloys have reported good general corrosion resistance, suitable for structural parts as sheets, plates and profiles. Magnesium oxide combines with the

alumina ( $\text{Al}_2\text{O}_3$ ) to enhance the protective properties of the natural oxide film, accounting for a notable corrosion performance of aluminium alloys. The 5000 and 6000 series will be preferred in this application for their resistance to corrosion, their weldability and their level of mechanical characteristics<sup>94</sup>.

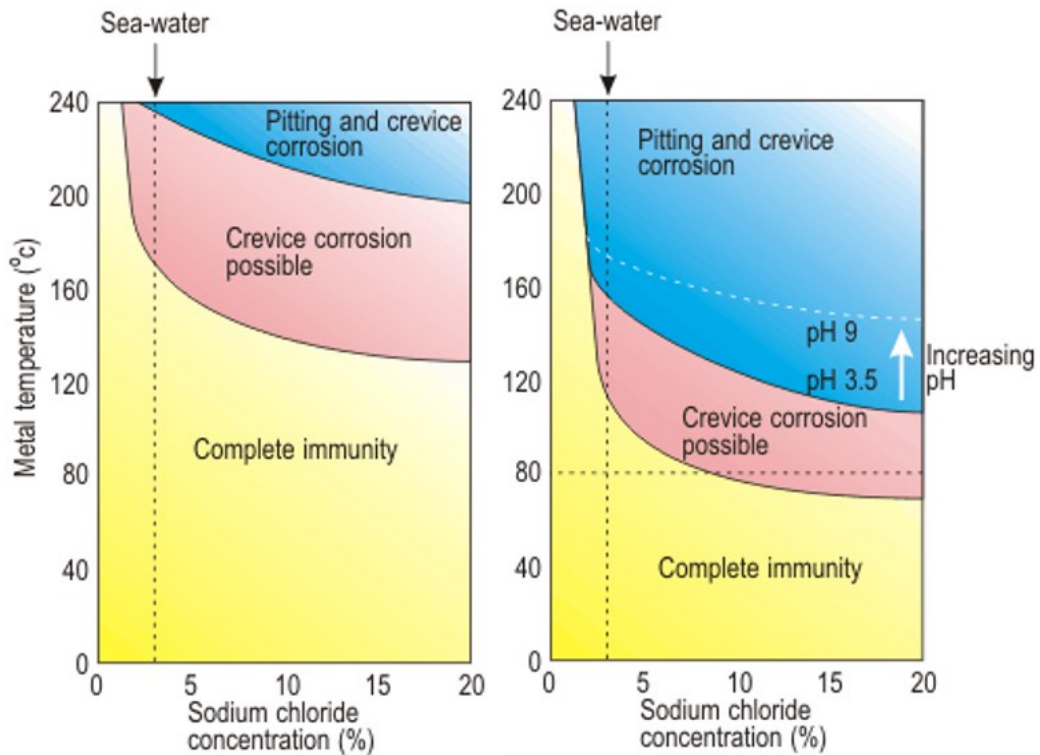


Figure 4-15. Corrosion resistance for titanium/palladium alloy (left) compared to pure titanium (right) and the influence of temperature, concentration and pH on crevice and pitting corrosion in seawater and sodium chloride brines. Source: Azom.com.

## Bibliography

---

1. Singh, R. Coating for Corrosion Prevention. in *Corrosion Control for Offshore Structures* 115–129 (Gulf Professional Publishing, 2014). doi:10.1016/b978-0-12-404615-3.00008-5.
2. Momber, A. W. & Marquardt, T. Protective coatings for offshore wind energy devices (OWEAs): a review. *J. Coatings Technol. Res.* **15**, 13–40 (2018).
3. Bleile, H. & Rodgers S. D. Marine Coatings. in *Encyclopedia of Materials: Science and Technology* (eds. Buschow, J. K. H. & Flemings, M. C.) 5174–5185 (Pergamon Press, 2001).
4. Knudsen, O. O. & Forsgren, A. Protection Mechanisms of Organic Coatings. in *Corrosion Control Through Organic Coatings* 5 (CRC Press, 2017).
5. Roberge, P. R. Protective Coatings. in *Handbook of Corrosion Engineering* (eds. Esposito, R. & Fogarty, D. E.) 781 (McGraw-Hill, 2000).
6. Taylor, S. R. Coatings for Corrosion Protection: Inorganic. in *Encyclopedia of Materials: Science and Technology* (ed. Buschow, K. H. J.) 1263–1269 (Pergamon Press, 2001). doi:10.1016/b0-08-043152-6/00238-2.
7. Olajire, A. A. Recent advances on organic coating system technologies for corrosion protection of offshore metallic structures. *J. Mol. Liq. Molliq.* (2018).
8. Momber, A. W., Irmer, M. & Glück, N. Performance characteristics of protective coatings under low-temperature offshore conditions. Part 2: Surface status, hoarfrost accretion and mechanical properties. *Cold Reg. Sci. Technol.* **127**, 109–114 (2016).
9. Hodgkin, J. Thermosets: Epoxies and Polyesters. in *Encyclopedia of Materials: Science and Technology* (eds. Buschow, J. K. H. & Flemings, M. C.) 9215–9221 (Pergamon Press, 2001).
10. HEMPEL'S COAL TAR. *hempel.com*.
11. *The Chemistry of Polyurethane Coatings.* (2005).
12. Davies, P. & Evrard, G. Accelerated ageing of polyurethanes for marine applications. *Polym. Degrad. Stab.* **92**, 1455–1464 (2007).
13. Smith, L. M. Introduction to Generic Coating Types. *J. Prot. Coatings Linings* **73**, (1995).
14. Chattopadhyay, D. K. & Raju, K. V. S. N. Structural engineering of polyurethane coatings for high performance applications. *Prog. Polym. Sci.* **32**, 352–418 (2007).
15. Thota, V., Nage, D. D. & Suresh, M. High performance coatings: Moisture cured urethanes. *Trans. Inst. Met. Finish.* **91**, 237–240 (2013).
16. Primeaux, D. J. Polyurea vs Polyurethane & Polyurethane / Polyurea: What ' s the Difference? in *PDA Annual Conference* (ed. Primeaux Associates LLC) (2004).
17. Primeaux, D. J. *Polyurea elastomer technology: history, chemistry & basic formulating techniques.* <http://www.hansonco.net/PUAHistChemFormulate> by Dudley.pdf (2004).
18. Knudsen, O. O. & Forsgren, A. Powder Coating. in *Corrosion Control Through Organic Coatings* 71–87 (CRC Press, 2017).
19. Masi, G., Metteucci, F. & Tacq, J. *State of the Art Study on Materials and Solutions against Corrosion in Offshore Structures North Sea Solutions for Innovation in Corrosion for Energy.* <http://www.nessieproject.com/library/reports-and-researches/nessie-report-2-1-study-on-materials-and-solutions-in-corrosion.pdf> (2018).
20. Powder Coating Offshore. *coating.co.uk* [coating.co.uk/powder-coating-offshore/](http://coating.co.uk/powder-coating-offshore/).
21. Bezborodov, V. P. & Saraev, Y. N. Use of coatings for protection of welded joints of steels, their structure and properties. *J. Phys. Conf. Ser.* **857**, 012005 (2017).
22. Fay, F. *et al.* Booster biocides and microfouling. *Biofouling* **26**, 787–798 (2010).
23. Yebra, D. M., Kiil, S. & Dam-Johansen, K. Antifouling technology — past , present and future steps towards efficient and environmentally friendly antifouling coatings. *Prog. Org. Coatings* **50**, 75–104 (2004).
24. Thomas, K. V. The Environmental Fate and Behaviour of Antifouling Paint Booster Biocides: a Review. *Biofouling* **17**, 73–86 (2001).
25. Gittens, J. E., Smith, T. J., Suleiman, R. & Akid, R. Current and emerging environmentally-friendly systems for fouling control in the marine environment. *Biotechnol. Adv.* **31**, 1738–1753 (2013).
26. Callow, J. A. & Callow, M. E. Trends in the development of environmentally friendly fouling-resistant marine coatings. *Nat. Commun.* **2**, 244 (2011).
27. Higaki, Y., Kobayashi, M., Murakami, D. & Takahara, A. Anti-fouling behavior of polymer brush immobilized

- surfaces. *Polym. J.* **48**, 325–331 (2016).
28. Ciriminna, R., Bright, F. V. & Pagliaro, M. Ecofriendly antifouling marine coatings. *ACS Sustain. Chem. Eng.* **3**, 559–565 (2015).
  29. de Rincón, O. *et al.* Evaluating Zn, Al and Al-Zn coatings on carbon steel in a special atmosphere. *Constr. Build. Mater.* **23**, 1465–1471 (2009).
  30. Metallic Coatings. in *Van Nostrand's Scientific Encyclopedia* (eds. Considine, G. D. & Kulik, P. H.) (John Wiley & Sons, Inc., 2006). doi:10.1016/b978-0-408-01175-4.50016-7.
  31. Bondareva, O. S. & Melkinov, A. A. Effect of the silicon content in steel on the hot-dip zinc coating microstructure formation. *IOP Conf. Ser. Mater. Sci. Eng.* **156**, 012015 (2016).
  32. Sepper, S., Peetsalu, P., Kulu, P., Saarna, M. & Mikli, V. The role of silicon in the hot dip galvanizing process. *Proc. Est. Acad. Sci.* **65**, 159–165 (2016).
  33. Corrosion protection of offshore structures. *Anti-Corrosion Methods Mater.* **32**, 6 (1985).
  34. Schulz, W. -D. & Thiele, M. Hot - dip Galvanizing and Layer - formation Technology. in *Handbook of Hot-Dip Galvanization* (eds. Maab, P. & Peibker, P.) (Wiley-VCH, 2011).
  35. Warnecke, W., Angeli, G., Koll, T. & Nabbefeld-Arnold, E. Performance of modern zinc-magnesium hot dip metal coatings. *Stahl und Eisen* **129**, 53–59 (2009).
  36. Tachibana, K., Morinaga, Y. & Mayuzumi, M. Hot dip fine Zn and Zn-Al alloy double coating for corrosion resistance at coastal area. *Corros. Sci.* **49**, 149–157 (2007).
  37. Dutta, M., Halder, A. K. & Singh, S. B. Morphology and properties of hot dip Zn-Mg and Zn-Mg-Al alloy coatings on steel sheet. *Surf. Coatings Technol.* **205**, 2578–2584 (2010).
  38. Duchoslav, J. *et al.* Evolution of the surface chemistry of hot dip galvanized Zn-Mg-Al and Zn coatings on steel during short term exposure to sodium chloride containing environments. *Corros. Sci.* **91**, 311–320 (2015).
  39. Schuerz, S. *et al.* Corrosion behaviour of Zn-Al-Mg coated steel sheet in sodium chloride-containing environment. *Corros. Sci.* **51**, 2355–2363 (2009).
  40. Metallizing vs. Galvanizing. [regalindustrial.com](http://www.regalindustrial.com/regalindustrial.com)  
[http://www.regalindustrial.com/metallizing\\_vs\\_galvanizing.html](http://www.regalindustrial.com/metallizing_vs_galvanizing.html).
  41. He, D., Dong, N. & Jiang, J. Corrosion Behavior of Arc Sprayed Nickel-Base Coatings. *J. Therm. Spray Technol.* **16**, 850–856 (2007).
  42. Vuoristo, P. Thermal Spray Coating Processes. in *Comprehensive Materials Processing* (ed. Cameron, D.) vol. 4 229–276 (Elsevier, 2014).
  43. Melchers, R. E., Moan, T. & Gao, Z. Corrosion of working chains continuously immersed in seawater. *J. Mar. Sci. Technol.* **12**, 102–110 (2007).
  44. Bonner, P. E. & Stanners, J. F. Protection of steel by metal spraying: A review. *Br. Corros. J.* **1**, 339–343 (1966).
  45. Wood, R. J. K. Tribo-corrosion of coatings: a review. *J. Phys. D Appl. Physics.* **40**, 5502–5521 (2007).
  46. Hou, B. R., Zhang, J., Duan, J. Z., Li, Y. & Zhang, J. L. Corrosion of thermally sprayed zinc and aluminium coatings in simulated splash and tidal zone conditions. *Corros. Eng. Sci. Technol.* **38**, 157–160 (2003).
  47. Chaliampalias, D. *et al.* High temperature oxidation and corrosion in marine environments of thermal spray deposited coatings. *Appl. Surf. Sci.* **255**, 3104–3111 (2008).
  48. Hardy, K. Anodizing Aluminium for Underwater Applications. *Ocean Eng.* **101** **15**, 54–56 (2009).
  49. Pokorny, P., Tej, P. & Szelag, P. Chromate conversion coatings and their current application. *Metalurgija* **55**, 253–256 (2016).
  50. Basu, A., Majumdar, J. D., Alphonsa, J., Mukherjee, S. & Manna, I. Corrosion resistance improvement of high carbon low alloy steel by plasma nitriding. *Mater. Lett.* **62**, 3117–3120 (2008).
  51. Somers, M. A. J. Nitriding and nitrocarburizing: Status and future challenges. *Heat Treat. Surf. Eng. - Proc. Heat Treat. Surf. Eng. HTSE 2013* 69–84 (2013).
  52. Rolinski, E. & Woods, M. The Benefits of Nitriding and Nitrocarburizing. *Machine Design* <https://www.machinedesign.com/materials/article/21836791/the-benefits-of-nitriding-and-nitrocarburizing> (2018).
  53. Verkholtantsev, V. V. Chemically active coatings. *Eur. Coatings J.* **49**, 32–37 (2003).
  54. Chilingar, G. V., Mourhatch, R. & Al-Qahtani, G. D. Corrosion Control and Detection. in *The Fundamentals of Corrosion and Scaling for Petroleum and Environmental Engineers* (Gulf Publishing Company, 2008).
  55. Askari, M., Aliofkhaezai, M., Ghaffari, S. & Hajizadeh, A. Film former corrosion inhibitors for oil and gas

- pipelines - A technical review. *J. Nat. Gas Sci. Eng.* (2018) doi:10.1016/j.jngse.2018.07.025.
56. Prochaska, S. & Tordonato, D. *Review of Corrosion Inhibiting Mechanisms in Coatings.* (2017).
  57. Taghavikish, M., Dutta, N. K. & Choudhury, N. R. Emerging corrosion inhibitors for interfacial coating. *Coatings* **7**, 1–28 (2017).
  58. Brycki, B. E., Kowalczyk, I. H., Szulc, A., Kaczerewska, O. & Pakiet, M. Organic Corrosion Inhibitors. in *Corrosion Inhibitors, Principles and Recent Applications* (ed. Aliofkhaezaei, M.) (IntechOpen, 2017). doi:10.5772/intechopen.72943.
  59. Zheludkevich, M. L., Serra, R., Montemor, M. F. & Ferreira, M. G. S. Oxide nanoparticle reservoirs for storage and prolonged release of the corrosion inhibitors. *Electrochem. commun.* **7**, 836–840 (2005).
  60. Zheludkevich, M. L., Tedim, J. & Ferreira, M. G. S. "Smart" coatings for active corrosion protection based on multi-functional micro and nanocontainers. *Electrochim. Acta* **82**, 314–323 (2012).
  61. Prasai, D. *et al.* Graphene: Corrosion-Inhibiting Coating. *ACS Nano* **6**, 1102–1108 (2012).
  62. Yasakau, K. A. *et al.* Novel and self-healing anticorrosion coatings using rare earth compounds. in *Rare Earth-Based Corrosion Inhibitors* (eds. Forsyth, M. & Hinton, B.) 233–266 (Woodhead Publishing Limited, 2014). doi:10.1533/9780857093585.233.
  63. Hughes, A. E. Self-healing coatings. in *Recent Advances in Smart Self-healing Polymers and Composites* (eds. Meng, H. & Li, G.) 211–241 (Woodhead Publishing Limited, 2015). doi:10.1016/B978-1-78242-280-8.00008-X.
  64. Self-Healing Academy. *Croda Coatings and Polymers* [croda coatings and polymers.com/en-gb/discovery-zone/self-healing-academy](http://croda coatings and polymers.com/en-gb/discovery-zone/self-healing-academy) (2020).
  65. Hu, Z. *et al.* Multistimuli-Responsive Intrinsic Self-Healing Epoxy Resin Constructed by Host-Guest Interactions. *Macromolecules* **51**, 5294–5303 (2018).
  66. Gould, P. Self-help for ailing structures. *Mater. Today* **6**, 44–49 (2003).
  67. Refait, P., Jeannin, M., Sabot, R., Antony, H. & Pineau, S. Corrosion and cathodic protection of carbon steel in the tidal zone: Products, mechanisms and kinetics. *Corros. Sci.* **90**, 375–382 (2015).
  68. Roberge, P. R. *Corrosion Engineering: Principles and Practice.* (McGraw-Hill, 2008). doi:10.1177/0340035206070163.
  69. Francis, P. E. *Cathodic Protection.* (2014).
  70. Huang, Y. Protection technology of material corrosion. in *Materials Corrosion and Protection* (eds. Huang, Y. & Zhang, J.) 425–482 (De Gruyter and Shanghai Jiao Tong University Press, 2018).
  71. Loto, C. A. Calcareous Deposits and Effects on Steels Surfaces in Seawater – (A Review and Experimental study). *Orient. J. Chem.* **34**, 2332–2341 (2018).
  72. Singh, R. Offshore Structures. in *Corrosion Control for Offshore Structures.* (ed. Singh, R.) 57–88 (Gulf Professional Publishing, 2014).
  73. Dodson, J. & Robinson, M. J. Hydrogen embrittlement of cathodically protected high strength steel in sea water and seabed sediment. *Br. Corros. J.* **37**, 194–198 (2002).
  74. Davies, K. G. & Kean, R. L. *Cathodic Protection.*
  75. Williams, G., Birbilis, N. & McMurray, H. N. The source of hydrogen evolved from a magnesium anode. *Electrochem. commun.* **36**, 1–5 (2013).
  76. Broesder, E. Coatings and Cathodic Disbondment - The True Story. in *Pipelines* 1604–1611 (ASCE, 2013).
  77. Priyotomo, G. & Nuraini, L. The Selection of Magnesium alloys as Sacrificial Anode for the Cathodic Protection of Underground Steel Structure. *Int. J. Eng. Trends Technol.* **51**, 78–82 (2017).
  78. DNV-GL-AS. Corrosion protection for wind turbines. *DNVGL-RP-0416 Standard* (2016).
  79. Ting, O. S., Potty, N. S. & Liew, M. S. Prediction of Corrosion Rates in Marine and Offshore Structures. in *National Postgraduate Conference* 1–6 (2011).
  80. *NORSOK STANDARD M-001.* (2002).
  81. Sridhar, N., Thodla, R., Gui, F., Cao, L. & Anderko, A. Corrosion-resistant alloy testing and selection for oil and gas production. *Corros. Eng. Sci. Technol.* **53**, 75–89 (2018).
  82. Iannuzzi, M., Barnoush, A. & Johnsen, R. Materials and corrosion trends in offshore and subsea oil and gas production. *npj Mater. Degrad.* **1**, 1–11 (2017).
  83. Igwemezie, V., Mehmanparast, A. & Kolios, A. Materials selection for XL wind turbine support structures: A corrosion-fatigue perspective. *Mar. Struct.* **61**, 381–397 (2018).
  84. Singh, R. Stresses, Shrinkage, and Distortion in Weldments. in *Applied Welding Engineering.* (eds. Guerin, B. & Jarm, P.) 201–238 (Butterworth-Heinemann, 2016). doi:10.1016/b978-0-12-804176-5.00017-7.

85. Garrison Jr, W. M. *Steels: Classifications. Encyclopedia of Materials: Science and Technology* (Pergamon, 2001). doi:10.1016/b0-08-043152-6/01587-4.
86. Compere, C. & Le Bozec, N. Behaviour of stainless steel in natural seawater. in *The First Stainless Steel Congress in Thailand* (1997).
87. Xiong, J., Manjaiah, G., Fabijanac, D., Forsyth, M. & Tan, M. Y. Enhancing the localised corrosion resistance of 316L stainless steel via FBR-CVD chromising treatment. *Corros. Eng. Sci. Technol.* **53**, 114–121 (2017).
88. Company, S. S. Specification Sheet: Alloy 904L. (2014).
89. Pitting Corrosion & PRE Numbers. *British Stainless Steel Association (BSSA)* <https://www.bssa.org.uk/topics.php?article=111> (2018).
90. Mudali, U. K. Materials for Hostile Corrosive Environments. in *Materials Under Extreme Conditions* (eds. Tyagi, A. K. & Banerjee, S.) 91–128 (Elsevier Inc., 2017). doi:10.1016/B978-0-12-801300-7.00003-6.
91. MICROBIOLOGICALLY INFLUENCED CORROSION (MIC). *Sandvik* <https://www.materials.sandvik/es-es/materials-center/corrosion-knowledge/wet-corrosion/microbiologically-influenced-corrosion-mic/>.
92. Lunde, L. & Seiersten, M. Offshore Applications for Titanium Alloys. in *Titanium and Titanium Alloys. Fundamentals and Applications* (eds. Leyens, C. & Peters, M.) vol. 2 483–497 (Wiley-VCH, 2003).
93. *Corrosion Resistance of Titanium*.
94. Alcan Marine. *Corrosion Behaviour of Aluminium in Marine Environments. Aluminium users' guide* (2017).

Los capítulos 5, 6, 7, 8 y 9 están sujetos a  
confidencialidad por el autor